Distribution and causes of high fluoride groundwater in the western Bushveld area of South Africa

by

Lewis Peter McCaffrey

Submitted in fulfilment of the requirements
for the degree of Doctor of Philosophy,
Department of Geological Sciences,
Faculty of Science,
University of Cape Town.

Supervisor: Professor J.P. Willis
March 1998

ABSTRACT

Dental fluorosis is endemic in the western Bushveld of South Africa. This study investigated the occurrence of fluoride (F^-) in groundwater in the area. It was hypothesised that fluoride in groundwater originated from the dissolution of fluorine-bearing minerals, principally fluorite, mica, amphibole and apatite, and that high F^- groundwater would be hosted in rocks with a high fluorine (F) content. It was further hypothesised that groundwater residence time, rare F-bearing minerals, ion exchange reactions and evaporation affected the F^- concentration of groundwater. These hypotheses were investigated by analysing data on F^- concentrations in groundwater, paired rock and soil samples, and selected minerals.

Three hundred and thirty eight samples of groundwater from the field area were analysed for F^- by both Fluoride Ion Selective Electrode and High Pressure Ion Chromatography. The results were added to a database of three thousand water samples covering the western Bushveld and together provide the first complete picture of the distribution of high F^- groundwater in the area. Twenty percent of boreholes contained groundwater with an F^- concentration greater than 1.5 mg/ℓ, the maximum recommended limit for South African drinking water. Given that 150 to 200 people are supplied by each borehole, over one hundred thousand people are exposed to drinking water with enough F^- to induce moderate dental fluorosis.

Forty two rock and soil pairs were analysed by X-ray fluorescence spectrometry. High concentrations of F (>2000 ppm) were found in rocks from the Pilanesberg and Lebowa intrusives. Soils have about 1 order of magnitude less total F than their underlying rocks. Leaching experiments show that most soils have very little soluble F (<4 mg/ℓ, <0.1% of total F), whereas some rocks yield leachate with very high F^- (>30 mg/ℓ). Leachate from some Pilanesberg and Lebowa Granite samples is supersaturated with respect to fluorite. A soluble fluorine-bearing mineral, such as villiaumite (NaF), is postulated to exist in these rocks. Analysis of minerals by electron microprobe shows that most micas have F concentrations below the detection limit (0.17 wt%), whilst F in amphibole minerals ranges from <0.17 to 2.69 wt%. Apatites with high F (up to 3.35 wt%) and Sr (up to 6.78 wt%) were found in fluorite-bearing ore associated with the Pilanesberg Complex. This ore was also shown to contain carbonate minerals, probably of igneous origin, and this is the first description of carbonate minerals from the Pilanesberg nepheline syenite complex.

The distribution of high F^- groundwater is coincidental with the outcrop area of those rock types found to have high F contents. Modelling of groundwater analytical data using the MINTEQA2 and JESS aqueous speciation modelling programmes has shown that many groundwaters with high F^- content are saturated with respect to fluorite. The computer modelling also indicates that most F in high F groundwater occurs as the fluoride ion, F^-.

CONTENTS

LIST OF TABLES

LIST OF FIGURES

ACKNOWLEDGMENTS

This study has been funded by the South African Water Research Commission. My mother, Mrs Valerie McCaffrey, and the United Kingdom Department of Health and Social Security provided funding assistance. I would like to thank my supervisor, James Willis, for his assistance and patience. I wish to thank all the people who helped me logistically in the field, including Paramount Chiefs Makapan and Mamogale, headmen, tribal policemen and officials, my interpreter Lillian Phiri, Bruce Brockett, Kate Parr, Johnson Maoke, Sam Otto and family, the staff of Agricor, Xu Yong Xin, Farouk Mangera, and Mr Damaneyt of the Tswaaing Crater Museum. Andras Bartha of the Bophuthatswana Geological Survey kindly carried out trace element analyses and is thanked for his enthusiasm and patience. 'Jim' Djiembowski of the South African (S.A.) Department of Water Affairs is thanked for providing access to the S.A. National Groundwater Database. John Kalk of the University of the Witwatersrand Medical School organised and paid for the analysis of water samples for iodide, for which he is gratefully acknowledged. The sampling trip to Northam Platinum Mine was arranged by Dr Ed Kable and conducted by Richard Viring. Dan Wilson assisted and instructed me on the use of GIS. Peter Wade of the CSIR is thanked for performing equilibrium speciation modelling using JESS. Thanks to Rob and Paul of PRo Publications International Limited for the use of their offices, heat, light, water and generosity. Thanks to Gavin Andrews for page checking and other menial-but-vital errands. The manuscript was improved by criticism from 3 anonymous examiners, James Willis, Hendrik Schloemann, Ron Watkins, Anton Le Roux, Steve Richardson and Heather Jameson.

The staff of the Department of Geological Sciences at UCT are thanked, specifically Chris Harris for his time and patience whilst training me on the preparation of samples and their analysis for stable isotopes; Martin Fey for instruction on the use of MINTEQA2; Dave Reid for help with references on the Bushveld; Nicky Grant for showing me the ropes around the XRF prep labs; Dick Rickard for the Probe sessions; Patrick Sieas for his able assistance in the IC lab, and the general helpfulness of Leon Myburg, Chalky and Neville Buchanan. I would also like to thank my colleagues, especially Ruth Lanyon, Andreas Späth, Jefferson 'Chubby Bunny' Chaumba and Hendrik Schloemann. Finally, thanks to Jessica Conway-Physic, for her absolute disbelief in various dotty theories; Robert McCaffrey and Kevin Hannavy, for general 'doctoral' advice (especially to Rob for the 'law of diminishing returns'); and to Robyn for her patience over such a prolonged period.

ABBREVIATIONS AND DEFINITIONS

α	(alpha) Fractionation factor for a particular isotope between two phases.
AG	Archaean Granite.
atm	Atmosphere.
BOP	Bophuthatswana.
Ca	Carbonatites.
Ch	Chuniespoort Sequence.
Cl	Clarens Formation.
CDTA	Cyclohexylene dinitrilo tetraacetic acid.
C_o	Initial ^{14}C activity.
C_s	Measured ^{14}C activity of a sample.
δ	(delta) Defined (for *e.g.* ^{18}O) as $$\delta\ ^{18}O = \frac{R_{sample} - R_{standard}}{R_{standard}} \times 1000$$
DWA	Department of Water Affairs (of Bophuthatswana).
DWAF	Department of Water Affairs and Forestry (of South Africa).
Ec	Ecca Formation.
G yrs	Giga years, 10^9 years.
Gr	Granophyre.
Ion balance	Calculated using the equation $$\%\ difference\ = 100 \times \frac{(\Sigma_{cations} - \Sigma_{anions})}{(\Sigma_{cations} + \Sigma_{anions})}$$
Ir	Irrigasie Formation.
kg	Kilogram.
$K_{25°C}$	Solubility product, specifically at 25°C.
K_{sp}	Solubility product.
K yrs	Kilo years, one thousand years or one millennium.
λ	(lambda) the decay constant of a radioactive substance.
Lb	Lebowa Granite.
Lt	Letaba Formation.
LLD	Lower limit of detection.
LOI	Loss on ignition.
ℓ	Litre.
M	Molar.

MWL	Meteoric water line.
μg	Microgram (0.000001 g).
meq	Milli equivalent
mg	Milligram (0.001 g).
ng	Nanogram (0.000000001 g).
Nb	Nebo Granite.
PDB	Peedee belemnite.
*p*K	Solubility product of a mineral, expressed as -log K.
Pl	Pilanesberg Complex.
pm	Picometer (one million millionth of a metre).
pmc	Percent modern carbon, measured relative to wood grown in 1850 and related to 1950. The standard is taken to be 100 pmc.
ppb	Parts per billion, solid equivalent of 1 μg/ℓ.
ppm	Parts per million, solid equivalent of 1 mg/ℓ.
Qu	Quaternary Formations.
Pr	Pretoria Sequence.
R	Ratio of atomic abundances of heavy isotope to light isotope.
RL or RLS	Rustenburg Layered Suite.
Rb	Rooiberg Suite.
$\Sigma_{cations, anions}$	(sigma) Sum of cations or anions, as molar equivalents.
SMOW	Standard mean ocean water.
T	Temperature, in °C.
T_h	Half life of a radioactive substance.
TISAB	Total ionic strength adjustment buffer.
$V_{A,B}$	Volumes of mixing groundwaters A and B.
Wt	Waterberg Group.
wt%	Weight percentage.
X	Mole fraction.

Note: In the following text, where fluorine occurs specifically in its elemental state, or when it occurs in an unknown form, it is referred to as "F". Where it occurs specifically in an ionic state, it is referred to as "F^-" or as "fluoride".

1 INTRODUCTION

1.1 Purpose of this study

The concentration of fluoride in groundwater has adversely affected the lives of millions of South Africans. This happens through the action of the fluoride ion (F^-) on teeth (causing dental fluorosis) and bones (causing skeletal fluorosis). The main source of F^- in the human diet is drinking water. Numerous studies have shown that ingestion of drinking water with elevated concentrations of F^- causes dental fluorosis (e.g. Driscoll *et al.*, 1983; Senewiratne *et al.*, 1973). Examples of African studies include those of Van Wyk *et al.* (1983); Ng'ang'a and Valderhaug (1993); Tobayiwa *et al.* (1991); Manji *et al.* (1986); McInnes *et al.* (1982). Very high concentrations of F^- in drinking water have been shown to cause skeletal fluorosis (e.g. Boyle and Chagnon, 1995; Felsenfeld and Roberts, 1991). Excess F^- in the diet has been implicated as one of the causes of goitre (Day and Powell-Jackson, 1972). One of the areas in South Africa where high F^- concentrations in drinking water has caused dental and skeletal fluorosis in humans is the western Bushveld, which is the subject area of this study.

Although the prevalence of dental and skeletal fluorosis in the area was recognised much earlier this century (Ockerse, 1941; Ockerse and Meyer, 1941), the implementation of the 'apartheid' system of government, starting in 1947, ensured that scant research was undertaken on the mainly black sufferers. Sporadic and small scale studies were undertaken by independent medical researchers (e.g. Zietsman, 1991; Rudolph *et al.*, 1995). Whilst a Government enquiry investigated fluoridation of drinking water supplies (McKenzie *et al.*, 1966), it was concerned only with urban (mainly white residents) water supplies. The majority of dental fluorosis sufferers (mainly black) live in rural areas. At the time of writing, no comprehensive survey of dental and skeletal fluorosis has been undertaken or is planned in the region.

Epidemiological studies around the world have tended to concentrate on the prevalence and severity of fluorosis, rather than study the distribution of high F^- groundwater, the main etiological factor. Without exception, previous studies of the distribution of high F^- groundwater in the Bushveld have relied on very few sampling sites. Zietsman (1991) evaluated the greatest number of boreholes (120) in one study, but her study covered only 7 villages. The data which these researchers needed did exist: routine

sampling and analysis of groundwater has been undertaken for decades by Government bodies. However, the area had been fragmented politically by the formation of the nominally independent homeland of Bophuthatswana in 1977. Exchange of data between Bophuthatswana and South Africa seldom took place, and the political boundaries limited and compromised studies which excluded one or other of the countries. The amalgamation of Bophuthatswana back into South Africa, beginning in practice in 1993, has allowed the present study to use the combined hydrochemical data set for the first time. The change of government in South Africa in 1994 has given impetus to calls for the introduction of fluoridation in the country (Moola, 1996), and the present study is of importance in determining areas which do not require further fluoridation.

The study has had two main objectives: to delineate F^- concentrations in groundwater in the study area, so that regions of high F^- concentration may be identified; and to investigate the cause(s) of high F^- groundwater. The study area covers all of the endemic fluorosis areas in the region, and is not constrained by artificial political boundaries. The study also aimed to investigate the following hypotheses: that groundwater F^- concentration is correlated to aquifer composition, especially the content of fluorine-bearing minerals and is controlled by the solubility of these minerals; that F^- concentration is also correlated to the residence time of groundwater; and that very high levels of F^- in groundwater are caused by processes in addition to simple dissolution of fluorine-bearing rock, for instance ion exchange and evaporation.

In this study the distribution of high F^- groundwater has been investigated by collection and analysis of groundwater samples, and the integration of this new data with pre-existing databases. Groundwater has been analysed for the major anions and cations as well as trace metals so that correlations between those elements and F^- can be evaluated, and so that full speciation calculations can be performed on the analyses. Groundwater-mineral equilibria were modelled using a computer program to clarify the mineral controls on water composition and possibly the extent of water-rock interaction. A limited number of water samples were analysed for iodide, as parts of the study area are afflicted with endemic goitre and it has been suggested that F interferes with thyroid function. Iodide in groundwater was analysed to determine whether goitre was likely to be caused by low iodide or high F concentrations in groundwaters. The causes of high F^- groundwater have been investigated by using chemical and mineralogical analyses of rocks, soils and minerals to ascertain the F^- content of these materials. Studies of the stable and radioactive isotopes present in groundwater were used to try to define the origin, environmental history and residence time of the groundwater.

The completion of this study will yield numerous benefits. It will increase knowledge about one of the world's largest areas of endemic fluorosis, and the processes which enrich F^- in groundwaters. For the first time in South Africa, areas of fluorosis risk will be accurately delineated. The study will also estimate for the first time the number of people likely to be affected by fluorosis in the region, highlighting the serious health consequences of high F^- groundwaters. Health authorities and water supply planners will now be able to take action to guard against dental fluorosis in these areas. The study will add to the knowledge of the concentration and distribution of health-related trace elements in Bushveld groundwaters. The increased knowledge of geohydrological and geohydrochemical systems at work in the area will be of use in the planning of water supplies to a previously neglected region, and will be of use in the exploration for low-F^- groundwater supplies. The study will contribute to knowledge of the stable and radioactive isotope systems at work in groundwaters of the Bushveld area. It will show for the first time that the usefulness of strontium isotope studies of groundwater may be limited by the natural variability of the source minerals, and that radiocarbon studies of Bushveld groundwaters may provide information on mineral reaction rates.

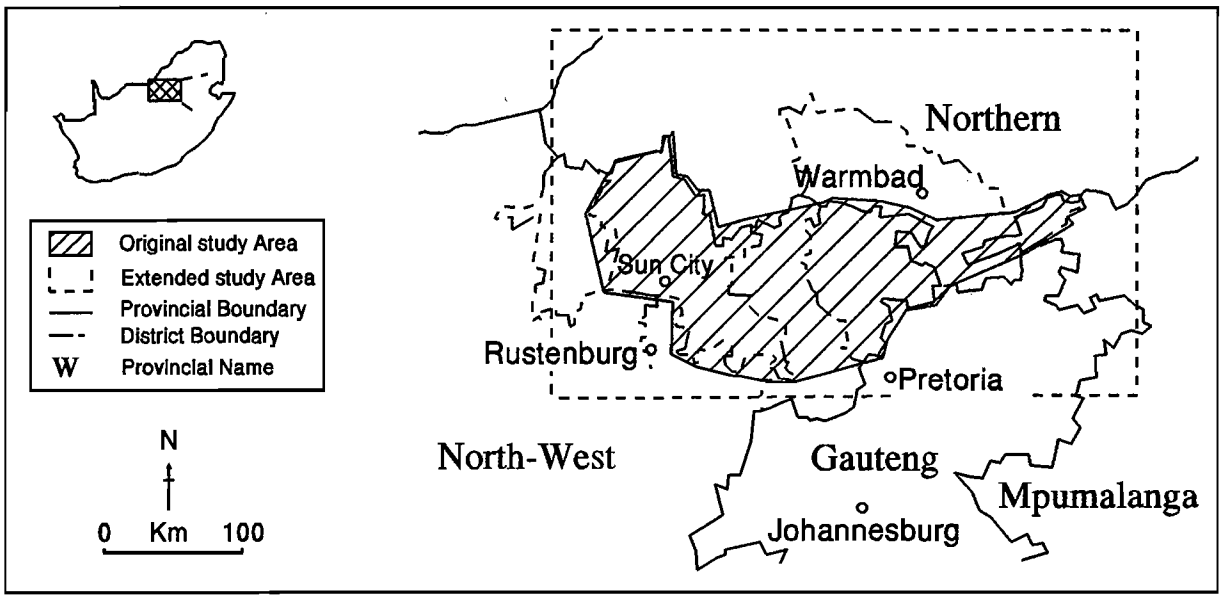

Figure 1.1 Location and extent of the field area.

1.2 Structure of this thesis

The thesis is divided into 7 chapters. This introductory chapter contains an outline of the study; the reasons for, and benefits of, undertaking it; the social and human context in which it was undertaken; and a review of previous work on the geology of the field area and

its physical characteristics. Chapter 1 also contains a review of the behaviour of the isotope systems used. Chapter 2 comprises a review of the geochemistry of fluorine, and the effect that F has on human health. Chapter 3 is a description of the methods used in the collection and analysis of materials. Chapters 4 and 5 contain descriptions of the results of these analyses on rocks, soils and minerals, and groundwater, respectively. Chapter 6 is a discussion of the data and puts the results into a human health and geochemical perspective. Chapter 7 summarises the thesis and proposes further areas of research.

1.3 Field area

1.3.1 Extent

The field area was defined initially in relation to the now defunct homeland of Bophuthatswana (Figure 1.1), and then redefined in terms of district boundaries after 27th April 1994 (the date when Bophuthatswana officially ceased to exist). Data covering an oblong area was provided by various Government departments and this area (shown in Figure 1.1) is termed the extended field area. It has an areal extent of approximately 47000 km^2, similar to that of the Netherlands.

1.3.2 Geography

A map of the principal physical features in the field area is shown in Figure 1.2. Much of the area is above 1000 meters in elevation, with several notable mountain ranges and blocks. In the south, the Magaliesberg range runs almost continuously from west of Rustenburg to the north of Pretoria. This is in effect the southern boundary of the field area. North of these hills are the flat plains of the Bushveld, occasionally broken by isolated hillocks ('koppies'). A prominent line of koppies 10 km north of the Magaliesberg, and running parallel to them, belongs to the Pyramid Gabbro-Norite member. Further to the north are the rolling plains and subdued hills of the Nebo Granite. Prominent mountain blocks include the circular ring-complex of the Pilanesberg Complex and the oblong Crocodile River Fragment. Koppies occurring to the west of the Pilanesberg are subdued versions of the Magaliesberg and are not as coherent in structure. The rolling landscape of the granites gives way in the east to the featureless plains of the Springbok Flats, which are broken occasionally by small sandstone knolls, seldom higher than 50 meters.

1.3.3 Geology

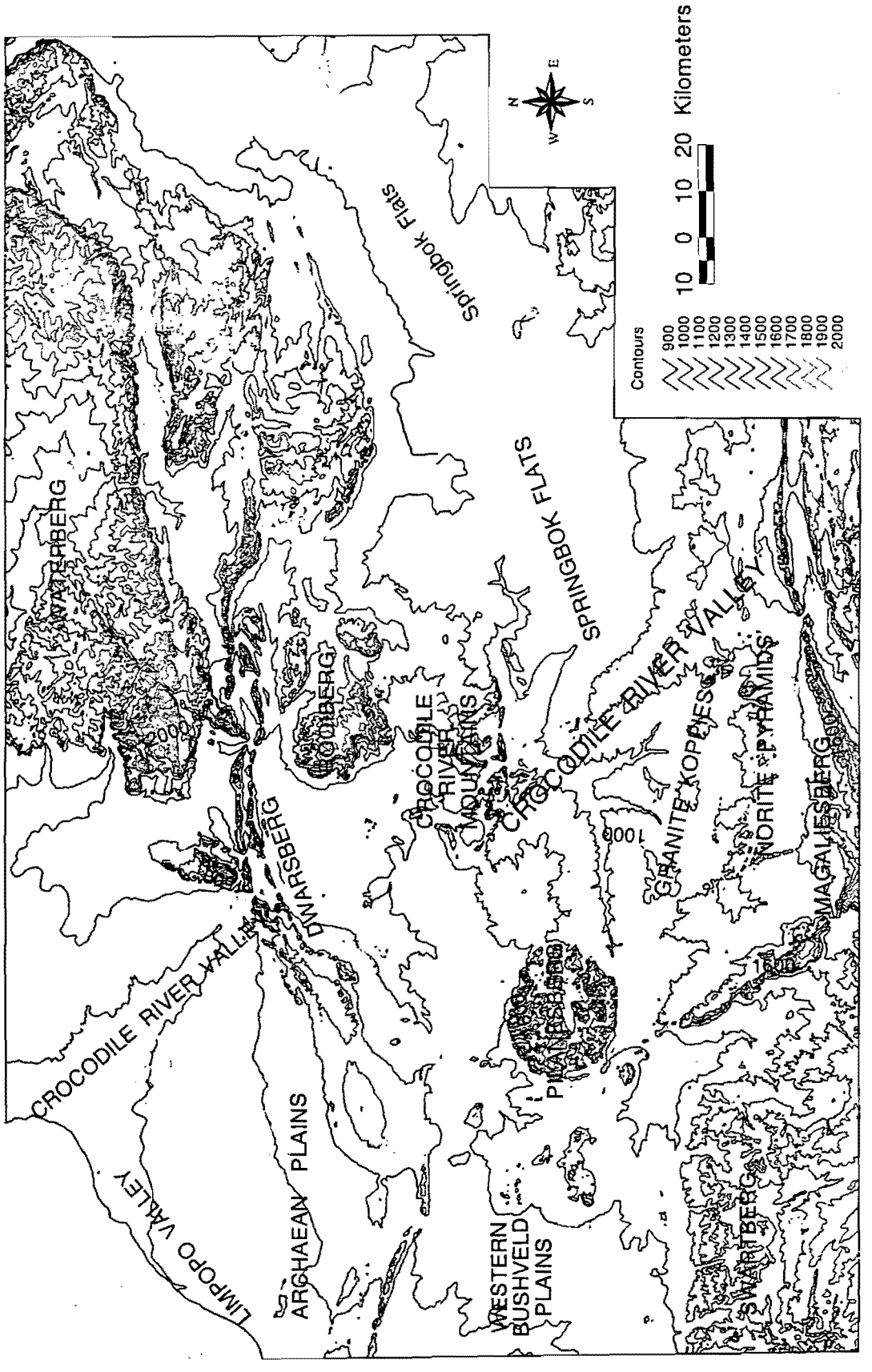

Figure 1.2 Physical features of the field area. Contours are in metres above mean sea level.

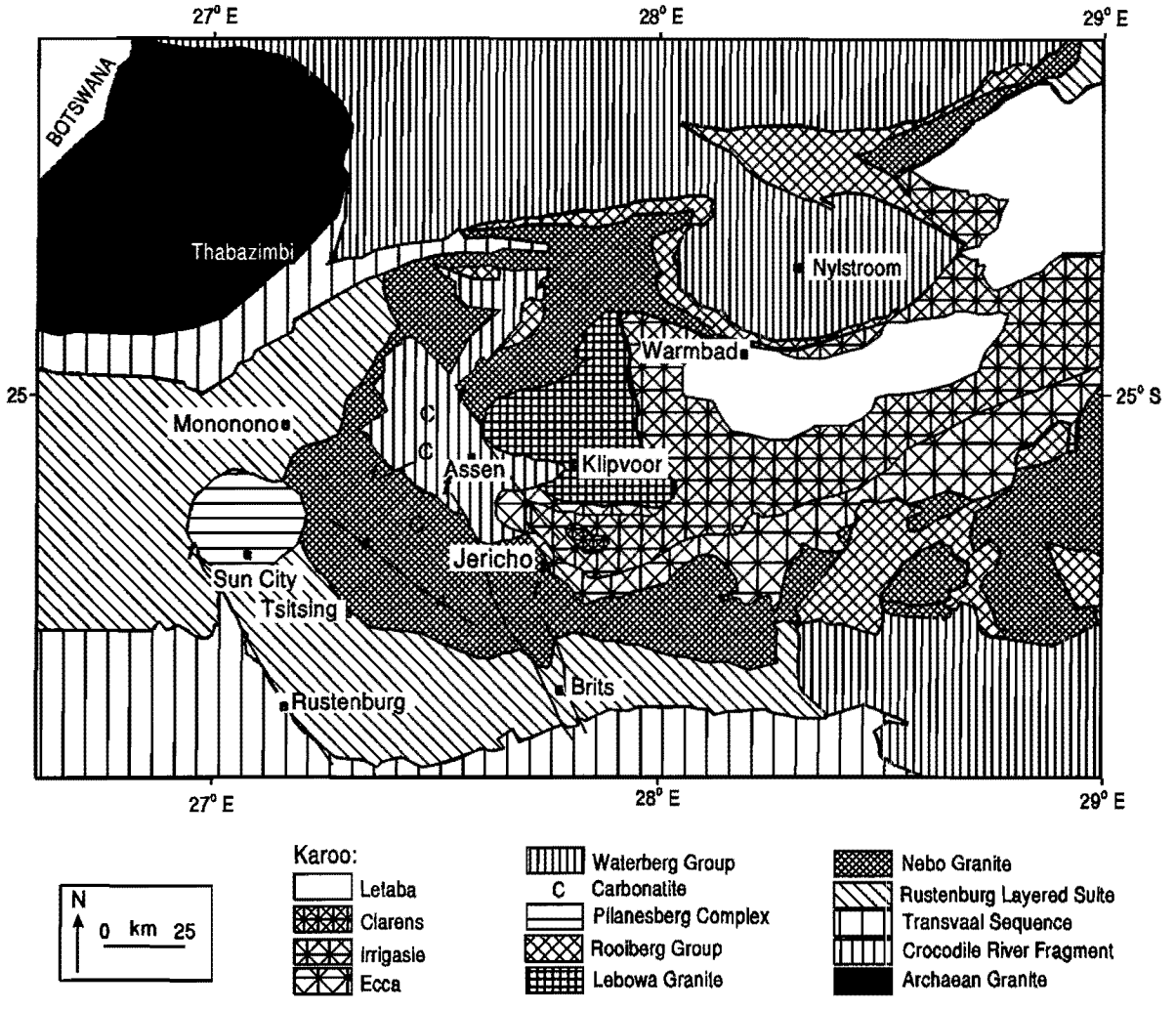

Figure 1.3 Sketch map of the geology of the extended field area.

An outline of the geology of the field area is contained in the guides to the 1:250000 geological maps covering the area, most importantly the 2526 Rustenburg map (Walraven, 1981). Rocks of the Transvaal Sequence and Bushveld Complex comprise much of the field area and the geology of these formations have recently been reviewed by Eriksson *et al.* (1995). The main geological features of the field area are shown in Figure 1.3. The stratigraphic names used here are generally in accordance with the South African Committee on Stratigraphy (SACS, 1980).

Lithology. The geology of the area is complex and is covered in detail in many publications (e.g. Eriksson *et al.*, 1995). A simple summary is provided here, starting from the oldest rocks. Archaean Granite occurs in the northwest and south of the area, overlain by dolomites of the Chuniespoort Group and clastic sediments of the Pretoria Group, both of the Transvaal Sequence.

Much of the area is underlain by rocks of the Bushveld Igneous Complex (BIC), which in this area was emplaced into the Pretoria Group, most prominently the Magaliesburg

Quartzite Formation. The BIC is divided into the mafic rocks of the Rustenburg Layered Suite (RLS), comprising pyroxenites, anorthosites, norites and gabbros; the Rashoop Granophyre Suite; and the Lebowa Granite Suite (LGS). The LGS has most recently been reviewed by Hill *et al.* (1996). The LGS has two principal components in the field area - the Nebo Granite and the Lebowa Granite, the latter being more mineralogically variable and mineralised. The Lebowa Granite is also known as the Bobbejaankop Granite. Sedimentary rocks of the Crocodile River Fragment (CRF), dominantly carbonates, shales and ironstones, are located near Assen. The Rooiberg Group make up the roof rocks of the BIC. They are predominantly siliciclastic volcanic rocks and are often highly mineralised with Zn, Sn and F (Rozendaal *et al.*, 1986; Schweitzer *et al.*, 1995). Clastic and carbonate sediments of Karoo age overlie the eastern parts of the BIC in the field area.

Several alkaline intrusions occur, including the Pilanesberg Complex nepheline syenite (Molengraaff, 1905; Humphrey, 1913; Shand, 1928; Retief, 1962 and 1963; Ferguson, 1973; Lurie, 1974), the associated Pilanesberg Dyke Swarm and several carbonatite complexes, such as Kruidfontein, Bulhoek and Tweerivier (Verwoerd, 1967 and 1993). Two kimberlite pipes have been found in and around the Pilanesberg Complex (Cawthorn, 1988). Ferguson (1973) proposed the Pilanesberg alkaline province. It consists of dykes, small plutonic bodies and the large Pilanesberg Complex nepheline syenite pluton. Several intrusions belonging to the province are carbonatites or are carbonatitic, e.g. those at Spitskop, Kruidfontein and Bulhoek (Harmer, 1992), yet the Pilanesberg Complex has so far been described as being devoid of carbonatite (Verwoerd, 1993). Given the large volume of undersaturated alkaline rocks (probably in excess of 500 km^3), the highly evolved nature of the Pilanesberg Complex, and the occurrence of carbonatite associated with many other southern African nepheline syenites, e.g. those at Schiel, Lofdal and Okorusu (Verwoerd, 1993), it is unusual that no carbonate rocks of igneous origin have been found in close association with the Pilanesberg.

Structure. The BIC occurs as a series of lobes of large dimensions, fed by postulated 'abyssal fractures' (Ferguson, 1973). Hamilton (1970) suggested that the BIC was formed by meteorite impact, although this has now been shown to be unlikely because of the absence of shock metamorphic effects in the rocks underlying the Bushveld (French, 1990). Intrusion of the complex has resulted in deformation of the Transvaal Sequence country rocks, so that dips of around 30° towards the centre of the complex occur in the underlying sediments. An extension of the main BIC body is found to the west of the Pilanesberg and is termed the 'western lobe'. The stratigraphy of the BIC is essentially conformable, with local unconformities. Granite overlies granophyre, which in turn overlies the RLS. Meyer and de Beer (1987) used deep resistivity methods to model the structure of the BIC. They confirmed earlier models that the BIC is not one single lopolith, but is instead comprised

of separate lobes. They concluded that the RLS directly overlies Transvaal Sequence rocks in the eastern and western Transvaal, but rests on Archaean Granite in the centre of the complex. Walraven (1976) showed that long-wavelength folding of the complex has occurred, with fold hinges trending northwest-southeast in the area around Tsitsing. Faulted contacts of BIC and Pretoria Group sediments occur occasionally, such as the large Rustenburg Fault and the Brits Graben. The contact of the Lebowa and Nebo Granites is obscured by younger Karoo rocks and the nature and location of the contact is uncertain.

The Crocodile River Fragment, correlated in part with the Transvaal Sequence, occurs within the body of the BIC and is variously interpreted as a mega-xenolith, as upfaulted floor rocks or as a roof pendant (Walraven, 1981). An extension of the Brits Graben to the northeast has been traced and appears to link up with the western edge of the Crocodile River Fragment (R. Holdsworth, Council for Geoscience, *pers. comm.*). The Karoo sediments in the area have their deepest extent near the village of Sephai, where they are approximately 430 m thick. The sediments are characterised by a lack of outcrop and flat topography and there is a marked decrease in altitude across the Lebowa Granite/Karoo contact. The Saltpan Crater 40 km northwest of Pretoria had previously been ascribed a volcanic origin (Wagner, 1920, 1922; Feuchtwanger, 1973; Fudali *et al.*, 1973), before a borehole penetrating the structure gave unambiguous evidence for a meteoritic origin (Reimold *et al.*, 1991, 1992). Brandt and Reimold (1995) showed that the fracture patterns in the Nebo Granite around the Pretoria Saltpan impact structure were not significantly different from regional lineations. This indicates that the cratering process has not significantly overprinted the regional fracture system, one of the most important of which has a horizontal to sub-horizontal orientation.

1.3.4 Meteorology

The area is semi-arid, with mean annual potential evaporation (2135 mm) far exceeding mean annual precipitation (MAP) of 622 mm. Figure 1.4 illustrates the variation in MAP over the field area. It will be seen that MAP increases from approximately 500 mm/yr in the west to almost 900 mm/yr in the east. MAP increases towards the southeastern corner (in the vicinity of Pretoria and the Magaliesberg Mountains) and towards the northeast (in the Waterberg Mountains). Increased rainfall station density around Pretoria is apparent, as well as a paucity of stations in the central Bushveld. Figure 1.5 shows the correlation of MAP with elevation - an indication that rainfall has an orographic component. This may explain high MAP values in the Magaliesberg and Waterberg.

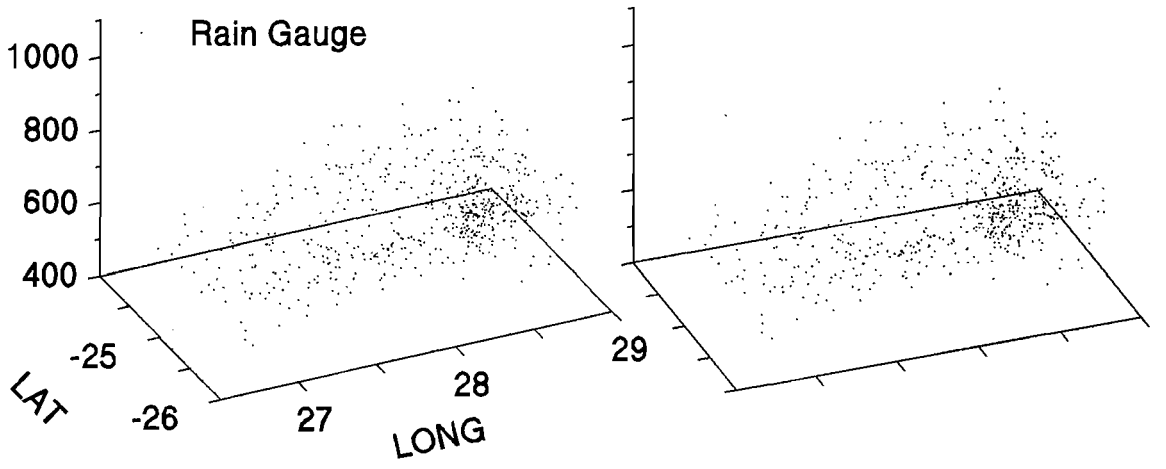

Figure 1.4 *Stereographic* representation of mean annual precipitation (MAP) in the study area.

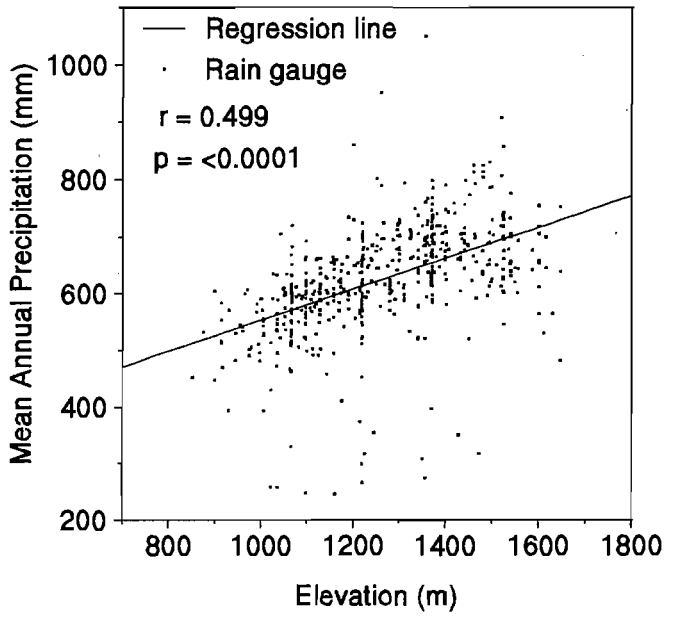

Figure 1.5 Correlation of mean annual precipitation with elevation, indicating an orographic influence.

Mean maximum temperature (MMT) has been found to be of importance in the epidemiology of fluorosis, as water is consumed in greater quantities in warmer climates. MMT is highly correlated with elevation, and this is shown graphically in Figure 1.6. Also shown in Figure 1.6 is the variation of MMT with latitude south. It is apparent that the correlation with latitude is poor, and so in the field area MMT is dominated by the effect of elevation.

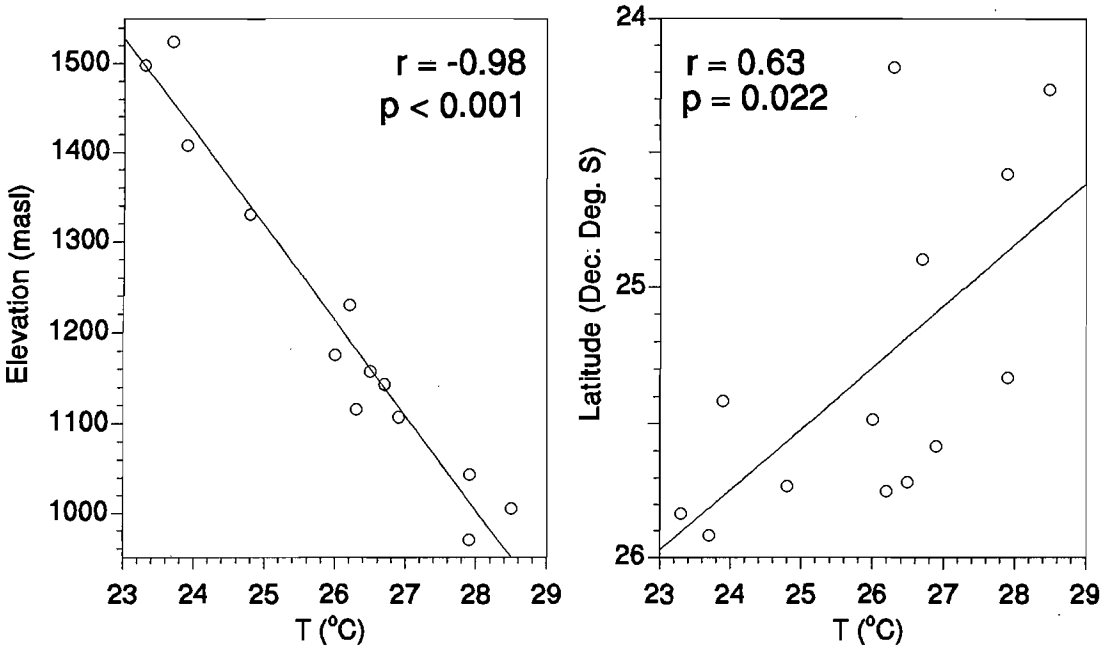

Figure 1.6 Correlation of mean maximum temperature (T) with elevation (in metres above sea level: masl) and latitude (in decimal degrees South). Raw data obtained from the Weather Bureau, Pretoria.

1.3.5 Hydrology

The river system is shown in Figure 1.7. Several perennial rivers cross the area, the Crocodile River being the largest, flowing south to north and eventually joining the Molopo river. Major tributaries of the Crocodile River include the Elands and Tolwane rivers. Many non-perennial streams occur.

1.3.6 Geohydrology

The geohydrology of the field area as a whole has been the subject of few academic studies, although a wealth of unpublished raw data of mixed quality exists in government drilling records. Historically the area had a higher water table than at present, as many of the farms are named after springs which are long since dry. Frommurze (1937) analysed drilling records from the area and drew a series of water yield - water depth curves for each lithology, but these curves are meaningless because of the small number of boreholes which were studied for each lithology. McCaffrey (1993) described the geohydrology of the Pilanesberg Complex as being characterised by surface weathering, fractures and faults in igneous rock, permeable tuff aquifers and lava aquitards. The water table had steep gradients because of the very low transmissivity of the rock mass as a whole.

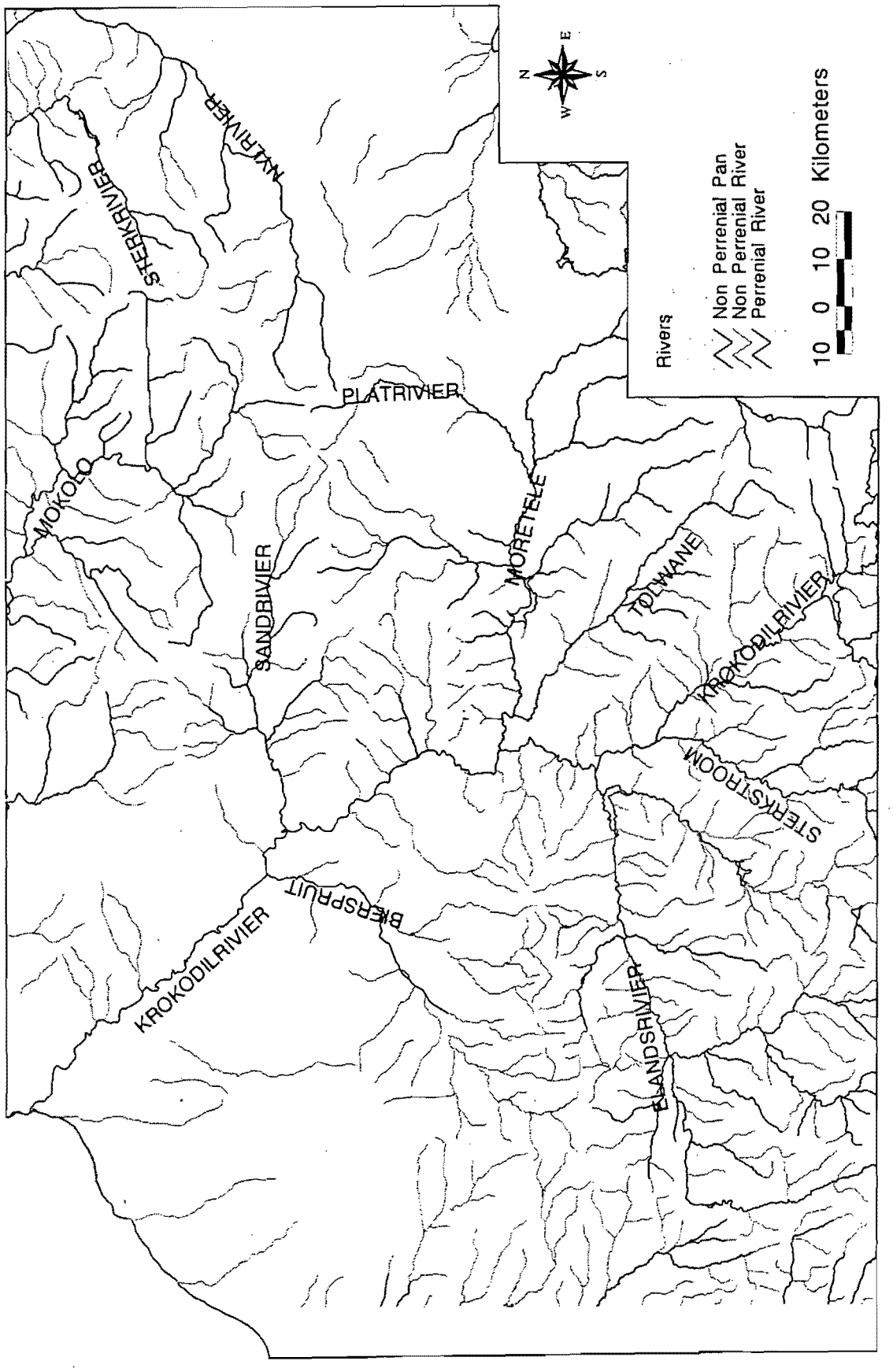

Figure 1.7 Hydrology of the field area. Data supplied by DWAF.

The review of continental-scale groundwater flow processes by Garven (1995) is of interest. Although based primarily on sedimentary basins, the review is applicable at times to large areas of basement rock. He notes that topographic relief is the dominant mechanism of groundwater flow, with a water table that is a subdued replica of the landscape. Convection cells may operate, driven by temperature and salinity gradients. Garven quotes a maximum flow rate in these cells of 1 m/yr, and this seems feasible for large fractures and faults in the Bushveld and Pilanesberg Complexes. The Bushveld Igneous Complex is probably closest to Garven's 'pressure compartments' model, where there is little or no flow between compartments (Figure 1.8).

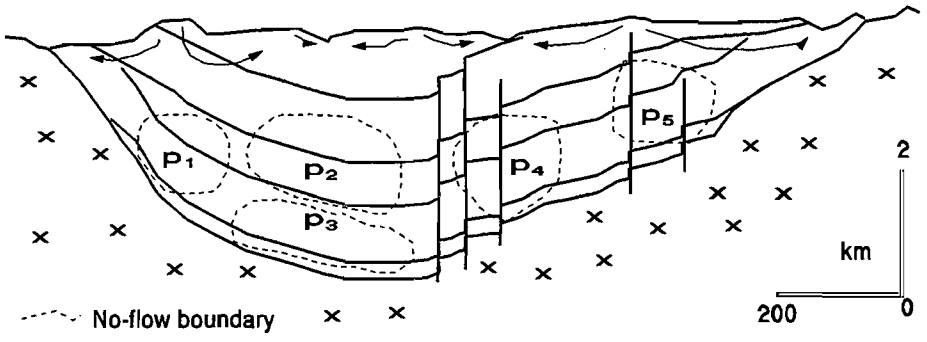

Figure 1.8 Compartmentalisation of a basin with no deep flow. $P_{1\text{-}5}$ refer to hydrogeological compartments. After Garven (1995).

A conceptual model of groundwater occurrence and flow in the Bushveld area is shown in Figure 1.9. Porosity, permeability and transmissivity is likely to be very low in the rocks of the Bushveld Igneous Complex. Groundwater is generally confined to the upper 150m and is hosted in shallow weathering zones, fractures and faults. Fractures are scarce and the system has a very high rock/water ratio. At greater depths virtually impermeable rocks are encountered. For instance, the platinum mines at Rustenburg, hosted in the southern subcrop of the RLS, are completely dry at 700m and below.

Water-bearing fractures do occur occasionally at great depths: Northam Platinum Mine on the northern subcrop of the RLS has serious development difficulties because of water ingress at depth. The water is contained in three types of features: type I fractures, type II fractures and dyke margins. Type I fractures contain salty water which flows very strongly (10 ℓ/s) when first intersected, but quickly run dry. Type II fractures cause the most disruption, as they continue to flow strongly (25 ℓ/s) for long periods after intersection. The temperature of the water at 1450m depth (approximately sea level) was 55°C when first intersected, but decreased in temperature steadily over several months. Water has also been

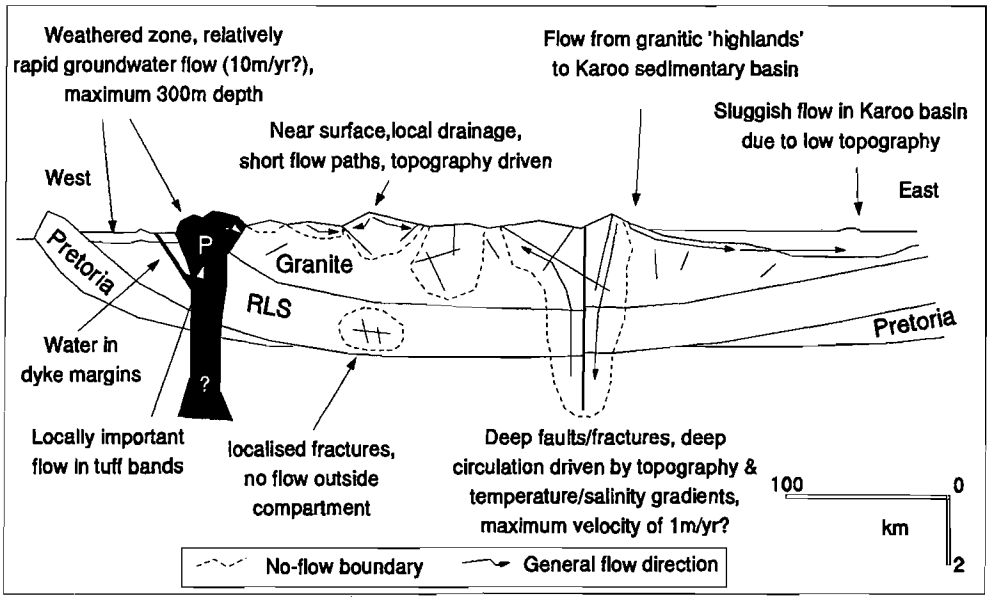

Figure 1.9 Schematic diagram of geohydrological conditions in the Bushveld area. 'P' is the Pilanesberg Complex.

encountered around a dyke belonging to the Pilanesberg Dyke Swarm. The mine has intersected all of these aquifer types down to 2000m below the surface, with water temperatures up to 60°C. A geohydrological interpretation of the type I and II fractures could be that type I fractures are relatively limited in size and do not tap into surface groundwater reservoirs. They are effectively closed fractures; the 'saltiness' of the water (not analysed in this study) suggests they may be remnant igneous fluids. Type II fractures probably continue to the surface, allowing them to drain the 'perched' water table within the first 300m of the surface. Decreasing temperatures with continuous flow suggest that the fractures are supplied from higher, large scale sources.

1.4 Isotope Hydrogeochemistry

Introduction. Although the principal subject of this thesis is fluoride, it is crucial to understand the behaviour of the groundwaters in which it occurs. Isotope studies in other areas have provided information on the origin of groundwater, the degree to which it has been evaporated, exchanged chemically with carbonates and sulphates, and in some cases its residence time and the identity of the main aquifers through which it has flowed.

Naturally occurring and anthropogenic isotopes provide valuable insights into geohydrological processes (*e.g.* Verhagen *et al.*, 1991, 1974; Blavoux and Letolle, 1995).

Determinations of ^{18}O and ^{2}H (also known as Deuterium, D) have been used in conjunction with hydrological modelling and radiogenic isotopes (^{14}C) to estimate palaeoclimates (Heaton *et al.*, 1986), for the location of recharge areas and for modelling water-rock interaction both terrestrially and extraterrestrially (Jakosky and Jones, 1994). McCaffrey (1993) used the isotopes of oxygen and hydrogen to investigate the origin and behaviour of the groundwaters of the Pilanesberg. Other radiogenic isotopes studies, principally ^{3}H, ^{14}C and ^{36}Cl, have concentrated on the estimation of recharge rates in sedimentary basins (e.g. Verhagen *et al.*, 1974) and continental scale groundwater flow. Measurements of $^{87}Sr/^{86}Sr$ ratios have been used for several purposes in the earth sciences, chiefly in dating rocks. Increasing use is being made of Sr isotopes for environmental geological purposes, such as dating glacial influences on landscapes (Blum *et al.*, 1994), investigation of water/rock interaction (Collerson *et al.*, 1988; Dia *et al.*, 1995), nuclear waste safety studies (Stuckless, *et al.*, 1991) and for groundwater provenance studies (Verdoux *et al.*, 1995; Banner *et al.*, 1994). No references to strontium isotope studies of groundwaters from the Bushveld could be found in the literature.

The use of ^{3}H as a recharge rate indicator is now limited, due to the decrease in ^{3}H activities, resulting from radioactive decay, to below natural background levels after the ending of atmospheric thermonuclear weapons testing in the 1960's. Blavoux and Letolle (1995) predict that anthropogenic ^{36}Cl, produced during thermonuclear tests in atolls of the Pacific between the years of 1952 and 1958, will supersede tritium as the tracer of choice. This will be due mainly to the large amounts of ^{36}Cl produced in these tests and the longevity of its half life (≈300 kyrs). Although the analysis of ^{36}Cl may have proved useful, no arrangements exist for its determination in South Africa at present.

Stable Isotopes of oxygen and hydrogen. The constituent elements of water, hydrogen and oxygen, each have several naturally occurring isotopes. They are used in this thesis as indicators of processes which have acted on surface and ground water. Analyses of ^{18}O and ^{2}H analyses are expressed in terms of an international standard known as Standard Mean Ocean Water (SMOW), as a δ value in parts per thousand. For instance, for ^{18}O:

$$\delta^{18}O = \frac{R_{sample} - R_{standard}}{R_{standard}} \times 1000 \qquad \textit{(eq. 1.1)}$$

where R is the ratio of atomic abundances of ^{18}O to ^{16}O. Most water molecules have a relative atomic mass of 18, composed of $^{1}H_2{}^{16}O$. The isotopes ^{18}O and ^{2}H have significant natural abundances (0.2% and 0.015%, respectively; Verhagen *et al.*, 1991) and so molecules of $^{2}H^{1}H^{16}O$ and $^{1}H_2{}^{18}O$ also occur. Since these molecules have differing vapour pressures, enrichment of the lighter isotope will occur in the most volatile phase during evaporation,

condensation or sublimation. This fractionation effect depends strongly on temperature, which gives rise to seasonal, altitudinal and latitudinal variations in ^{18}O and ^{2}H content of precipitation. For ^{18}O, the effect has been estimated to be between 0.28‰/°C and 0.70‰/°C (Suzuki and Endo, 1995; Yurtsever and Gat, 1981; Heaton *et al.*, 1986; Broecker, 1995). Global $\delta^{18}O$ and $\delta^{2}H$ values are linearly related in continental precipitation, as described by the equation

$$\delta^2 H = s\ \delta^{18} O + d \qquad \textit{(eq. 1.2)}$$

where s is the slope of the line (with a value of 8 for continental rain) and d is the deuterium excess, defined as the measured $\delta^{2}H$ value minus $8\times\delta^{18}O$ and calculated to be between 10‰ and 5‰ (Craig, 1961; Taylor, 1974). The line describing average isotopic content of continental precipitation is known as the meteoric water line (MWL). Most meteoric water has negative δ values, since water vapour is enriched in the lighter isotopes upon evaporation from the ocean surface. Upon evaporation from continental surface water bodies, isotope fractionation increases the proportion of heavier isotopes in the residuum, producing an evaporation line with a slope as low as 2. During the last glacial period, when temperatures were lower on average than they are at present, precipitation was isotopically lighter (Heaton *et al.*, 1986). Because temperature generally decreases with increasing elevation, $\delta^{18}O$ gradients occur in rainfall of between -0.15 to -0.40 ‰ per 100 m elevation. The temperature and elevation effects in isotope hydrology are well known (Craig, 1961; Dansgaard, 1964). More recently, Thorsden *et al.* (1992) found $\delta^{18}O$ to be well correlated with elevation, being between 0.3 and 0.35 ‰/100 m, and for elevation to be the dominant factor in determining $\delta^{18}O$. No correlation coefficient for their regression is quoted. Chemical effects, such as exchange of ^{18}O with $C^{16}O_2$ and $CaC^{16}O_3$, and exchange of ^{2}H with $^{1}H_2S$, alter the position of the sample on a $\delta^{18}O/\delta^{2}H$ diagram, Figure 1.10.

Few studies have linked the study of high F^- and stable isotopes in groundwater. However, the study by Datta *et al.* (1996) showed that ^{18}O and F^- were positively correlated in some groundwaters in the region of Delhi, India. It was theorised that soil moisture with a long residence time dissolved F^- salts in the soil and, at the same time, underwent partial evaporation, before infiltrating to the water table.

Strontium isotopes. It is hypothesised in this thesis that Sr isotopes can be used to characterise a groundwater body, and can thus be used to trace the movement of groundwater from one aquifer to another. It is necessary, therefore, to review the geochemistry of Sr and its geochemical analogue Ca, as well as the element which gives rise to radiogenic Sr, namely Rb. Ionic radii values are from Ahrens (1952). The ionic radius of Sr^{2+} (112 pm) is only slightly larger than that of Ca^{2+} (99 pm), and both are divalent

cations, thus allowing Sr to replace Ca in many minerals. Strontium is therefore present in many Ca-bearing minerals such as plagioclase, apatite and calcite. Strontium has four

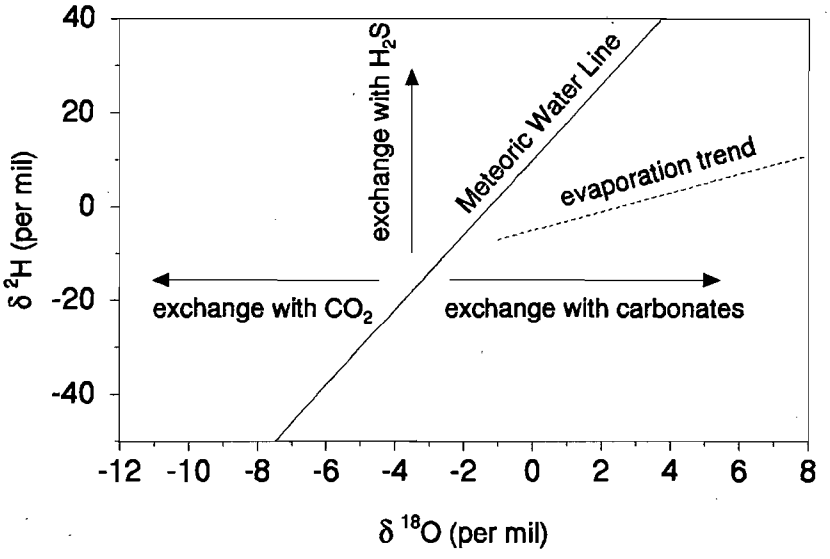

Figure 1.10 $\delta^{18}O/\delta^{2}H$ diagram for continental precipitation. The meteoric water line is that of Craig (1961). The evaporation trend is hypothetical. ^{18}O is displaced upon interaction with carbonates and volcanic CO_2, whilst ^{2}H values shift upon exchange with H_2S. After Verhagen *et al.*, 1991.

naturally occurring isotopes, all stable, namely ^{88}Sr, ^{87}Sr, ^{86}Sr and ^{84}Sr, but Sr isotope abundances are variable due to the decay of the naturally occurring radioactive ^{87}Rb to ^{87}Sr. The accepted decay constant for ^{87}Rb is $1.42\times10^{-11}yr^{-1}$, equivalent to a half life ($T_{½}$) of 4.88×10^{10} years (Faure, 1987). The Rb^+ ion has similar ionic radius (147 pm) to K^+ (133 pm) so that Rb can substitute for K in all K-bearing minerals, such as the micas and K-feldspar. Since Sr will partition into plagioclase and Rb will stay in the melt during fractional crystallization of plagioclase from a silicate magma, late stage differentiates tend to have high Rb/Sr ratios. Rocks and minerals with high Rb/Sr ratios will acquire progressively higher $^{87}Sr/^{86}Sr$ ratios over geological time. High $^{87}Sr/^{86}Sr$ ratios are said to be 'radiogenic' (Faure, 1987).

In groundwater, Sr actively participates in carbonate-water reactions in substitution for Ca and is not a conservative tracer. However, several characteristics of Sr can be useful in groundwater studies: different rocks can have very different Sr isotope ratios; Sr is relatively abundant in groundwater; and its isotopic composition can be measured accurately and precisely. For these latter reasons Sr isotopes have been used extensively as tracers of groundwater flow (e.g. Collerson *et al.*, 1988; Stuckless *et al.*, 1991; Banner *et al.*, 1994; Dia

et al., 1995; Verdoux *et al.*, 1995). The isotope ratio of dissolved Sr is attained in flowing groundwaters by dissolution of, or exchange with, aquifer materials. The resulting $^{87}Sr/^{86}Sr$ ratio is an integration of all ratios sampled along the flow path. It has been noted that for many water-rock pairs, groundwater Sr is not as radiogenic as its host (McNutt *et al.*, 1990). These differences between Sr ratios in groundwater and bulk aquifer can result from the preferential dissolution of minerals with differing $^{87}Sr/^{86}Sr$ ratios. For instance, mica and K-feldspar both have high Rb/Sr ratios (so that in Bushveld minerals the $^{87}Sr/^{86}Sr$ will be high) and dissolution of these minerals will result in groundwater with a high $^{87}Sr/^{86}Sr$ ratio. Conversely, anorthite has a low Rb content and low $^{87}Sr/^{86}Sr$ ratios: dissolution of anorthite will result in groundwater with low $^{87}Sr/^{86}Sr$ ratios. Of importance to this study is that fluorite and apatite are Sr-rich and Rb-poor (McNutt *et al.*, 1990), are common accessory minerals and are relatively abundant in the fractionated rocks of the study area. Dissolution of these mineral phases will result in a groundwater with a low $^{87}Sr/^{86}Sr$ ratio. No significant fractionation of Sr isotopes occurs during precipitation of minerals, such that the $^{87}Sr/^{86}Sr$ ratios of water and precipitate are virtually identical.

For very young groundwater, mineral dissolution rates will be an important factor in determining $^{87}Sr/^{86}Sr$ ratios, since readily soluble minerals will contribute their Sr first, regardless of Sr content. Table 1.1 shows that Ca-rich feldspar (anorthite) is quickly dissolved, followed by Na-feldspar (albite), K-feldspar and muscovite. Because of the relatively high Sr concentration and rapid dissolution of feldspar, especially anorthite, Sr isotope ratios in groundwater with a short residence time in contact with rock containing anorthite should be low. With time the Sr isotope ratio will increase, due to the dissolution of K-feldspar and mica.

Table 1.1 Dissolution time and typical $^{87}Sr/^{86}Sr$ ratios for 2.05×10^9 yrs old minerals. Weathering rates are for dissolution of a 1 mm crystal at T = 298 K and pH = 5.0, from Lasaga (1984). Sr isotope ratios for muscovite, K-feldspar and diopside from McNutt *et al.* (1990); for biotite and unspecified 'plagioclase' from Hamilton (1977) from the Main Zone of the RLS.

Mineral	Dissolution Time yrs $\times 10^3$	Relative Concentration Rb	Sr	$^{87}Sr/^{86}Sr$
Biotite	*n/a*	very high	very low	1.6067
Muscovite	2,700	very high	very low	>>1.0
K-Feldspar	520	moderate	moderate	0.730-0.800
Albite	80	low	moderate	0.706
Anorthite	0.11	very low	high	
Diopside	6.8	low	low	0.701-0.703

Radiocarbon. Libby and others in the 1950's showed that radiocarbon (^{14}C) is present in natural samples in sufficient quantities to allow relatively easy analysis (Libby, 1955). Today the dating of objects by measurement of radiocarbon is now a routine procedure. Analysis of the radiocarbon activity of groundwater has been used extensively to model groundwater residence time and has been reviewed by Mook (1980). The relative simplicity of dating a solid, carbon-bearing object is in contrast to the corrections and assumptions needed when attempting to date groundwaters. As Mook (1980) put it, *"there are many geohydrologists who feel that ^{14}C will never provide us with.. accurate groundwater ages"*. Nevertheless, dating of groundwater is frequently attempted and the basic assumptions are summarised here.

The activity of the sample, *a*, is expressed in pmc (percent modern carbon) calculated by comparing the activity of the sample to that of an oxalic acid standard:

$$a = \frac{A}{A_{ox}} \times 100 \qquad \textit{(eq. 1.3)}$$

where A is the measured activity of the sample in disintegrations per minute per gram (dpm/g) and where A_{ox} is 0.95 times the specific activity of NBS oxalic acid (0.95 × 13.56 dpm/g carbon in the year 1950).

Radiocarbon is produced naturally in the atmosphere at a rate of approximately 2.5 atoms/cm^2/s by the reaction of slow cosmic ray neutrons with stable ^{14}N. The variation of the cosmic ray flux over long time periods (Sonnet and Finney, 1990) means that radiocarbon production has not been entirely constant. For geohydrological studies, this variation is swamped by other uncertainties and can safely be ignored. Anthropogenic alteration of atmospheric radiocarbon activities has occurred. Firstly, combustion of fossil fuels has reduced tropospheric ^{14}C levels by about 10%. Secondly, since the 1960's, atmospheric thermonuclear weapons testing has radically increased the radiocarbon activity of the world's atmosphere. Groundwater samples with greater than 100 pmc are now quite possible.

2 FLUORINE GEOCHEMISTRY AND HEALTH

This chapter will review previous work on the geochemical behaviour of fluoride, the distribution and causes of high fluoride groundwater, fluorosis, and some aspects of hydrochemistry. These topics are of relevance to arguments advanced later in the thesis.

2.1 Geochemical behaviour of Fluorine

Fluorine is the lightest element in the Halogen group and is the 14th most abundant element in the lithosphere. It is the most electronegative and reactive element known. Fluorine is rarely found in the elemental state; usually it forms ionic bonds. Bonding with anions of groups VA, VIA and VIIA (apart from P, As, Sb and Bi) does not occur because of the high electronegativity of F.

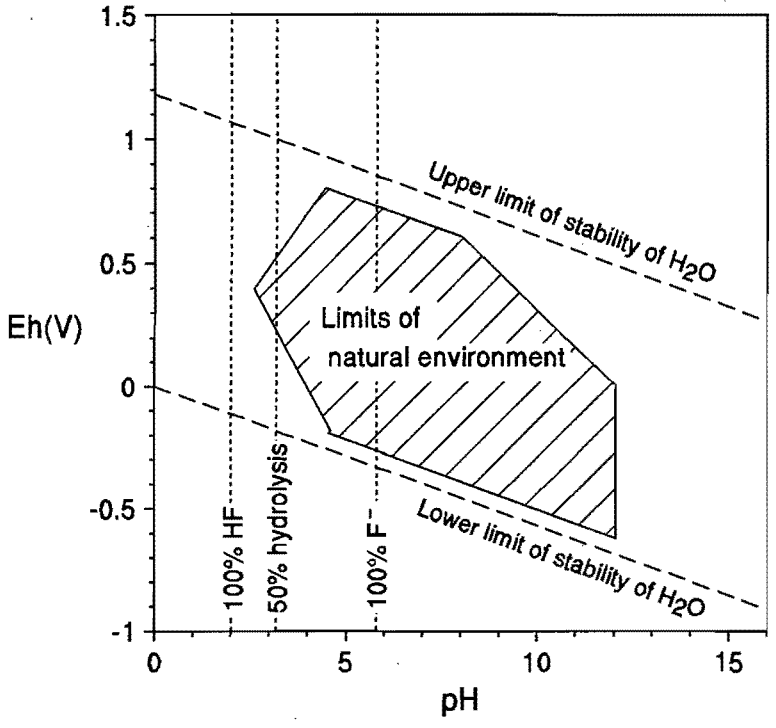

Figure 2.1 Eh-pH equilibrium diagram for the system F-H_2O at 25°C, and for total F concentration less than 2000 mg/ℓ. After Boyle (1976).

2.1.1 Natural Waters

Most simple compounds of F are readily soluble in water. The Eh and pH conditions of F speciation are shown in Figure 2.1. It is noted that under conditions in which water is stable, F usually exists as the monovalent anion, F^-. At a pH below 3.5, F in solution may occur in the HF° form. The close similarity in size and the equivalence of charge of hydroxide and fluoride ions causes interference when a fluoride ion selective electrode is used for water analysis. F can also occur as a complex, such as $(AlF_6)^{3-}$ or AlF^{2+}. Formation of these complexes takes place rapidly (in the order of minutes) at the pH and temperature of typical temperate groundwaters, and their formation can be regarded in the hydrogeological context as an equilibrium process (Plankey and Patterson, 1986).

2.1.2 Fluorine in minerals

Fluorine is not an essential element in any of the common rock-forming minerals. Topaz ($Al_2[SiO_4](OH,F)_2$) and fluorite (CaF_2) are the only two common accessory minerals in which F is an essential element. Just under 150 fluorine-bearing accessory minerals are known, and many others contain small amounts of F^- replacing OH^- and O^{2-} (Koritnig, 1974). Table 2.1 shows a comparison of the ionic radius of F^-, with the other members of the halide group and the geochemical analogues of F^-, OH^- and O^{2-}. It is apparent that the F^-, OH^- and O^{2-} ions have similar ionic radii, with OH^- having the same charge as F^-; Cl^-, Br^- and I^- have the same charge but much larger ionic radii. This leads to very different partitioning behaviour between F^- and the rest of the halides in silicate melts.

Table 2.1 Relative atomic mass (RAM) and ionic radius of halogen group ions and geochemical analogues. Ionic radii are in picometres and are for coordination number VI. *Source:* Ahrens (1952), quoted in Henderson (1986).

Ion	Symbol	RAM	Ionic Radius	Ion	Symbol	RAM	Ionic Radius
FLUORIDE	F^-	**19**	**133**	Chloride	Cl^-	35.5	181
Hydroxide	OH^-	17	140-160	Bromide	Br^-	79.9	196
Oxide	O^{2-}	16	132	Iodide	I^-	126.9	220

Because of the similarity in ionic radius to OH^-, F^- can isomorphously replace OH^- in minerals such as topaz, micas, [e.g. muscovite, $K_2Al_6Si_6O_{20}(F,OH)_4$], and amphiboles, [e.g. tremolite-ferroactinolites, $Ca_2(Mg,Fe^{2+})_5Si_8O_{22}(F,OH)_2$] (Deer *et al.*, 1977). A higher thermal stability has been reported for pure fluormica (phlogopite) compared to hydroxy phlogopite,

and this is the case with many minerals with solid solutions of F and OH. The ability of F^- to substitute for OH^- or O^{2-} depends mainly on the coordination and kind of ligand that the OH^- or O^{2-} ions form within the lattice of a given mineral (Boyle, 1976). The amount of F in a magmatic system is the primary control of F concentration in minerals, but O fugacity affects the F concentration of micas and amphiboles (Koritnig, 1974). According to Koritnig coexisting amphibole and biotite have F contents of about the same magnitude.

2.1.3 Magmatic systems

Koritnig (1974) summarised the geochemical behaviour of F in igneous rocks in general, whilst Bailey (1977) reviewed the geochemistry of F in granitic rocks and melts. Boyle (1976) discussed the F concentrations for many rock types and his values are shown here in Tables 2.2, 2.3 and 2.4. Fluorine concentrations within similar lithologies are subject to large variations, for instance in granites ranging from tens of ppm to several percent (Bailey, 1977). However, in general the concentration trend in igneous rocks follows ultramafic < intermediate < granitic < alkaline. The mean concentrations are approximately 100, 400, 800 and 1000 ppm, respectively (Koritnig, 1974; Bailey, 1977), although Boyle (1976) gives slightly different mean values (Table 2.2).

In granitic melts F^- replaces O^{2-}, breaking the Si-O chains and forming Si-F bonds instead, in effect depolymerizing the melt. With decreasing SiO_2/alkali ratios F becomes linked to Na and Ca, although the exact proportions are not clear (Kogarko *et al.*, 1968). Fluorine has been found to depress the temperature of the liquidus by up to 110°C, delays the onset of crystallization, and promotes quartz, topaz and feldspar above biotite in the order of crystallization in granitic magmas (Bailey, 1977). The main rock forming minerals are unable to accept F into their structure and so F is enriched in fractionating magmatic systems. Boyle (1976) stated that F is enriched in the residual, aqueous and vapour phases of a magma, and is often associated with pegmatites and hydrothermal alteration.

F-rich melts may immiscibly separate into a fluoridic alkaline melt and a polymerized silicate melt. It has been found that large amounts of F (8%) are needed to maintain carbonatite magmas in the liquid state at the low eruption temperatures (500-590°C) seen at the carbonatite volcano Oldoinyo Lengai in Tanzania (Jago and Gittins, 1991). In alkaline magmas the separation of F into a separate gaseous phase is suppressed, F is trapped by NaF and F therefore becomes enriched in the magma.

Between 30 and 90% of F in calc-alkaline granites is found in biotite, with the remainder in hornblende, muscovite and accessory minerals such as fluorite. The concentration of F in these biotites is a function of the H_2O-HF composition and

Table 2.2 Fluorine in intrusive and extrusive igneous rocks. After the compilation by Boyle (1976). 'Tr.' is trace. All concentrations in ppm.

Rock Type	Range		Mean	Number
	Minumum	Maximum		
Intrusive				
Ultramafic	Tr.	2000	130	37
Gabbros	50	11000	430	47
Diorites	300	1300	665	20
Granites and Granodiroties	20	30000	810	182
Syenite and monzonite	200	4000	1360	26
Alkaline ultramafic	Tr.	3800	1400	41
Alkali syenite	100	25800	1800	249
Alkali granite	670	12400	5500	20
Carbonatites	200	24000	8100	96
Kimberlites	520	2500	1310	42
Dolerites	198	500	420	14
Pegmatites	800	9000	4320	6
Extrusive				
Basalts	20	2400	375	317
Andesites	Tr.	1200	250	97
Rhyolites	Tr.	6850	610	151
Trachyte and Latite	200	2250	750	9

temperature of the fluid which last re-equilibrated with the mica, and the composition of the mica (Mg rich biotites can contain much more F than those rich in Fe) (Speer, 1984).

In F-rich granites and metasomatic roof zones, accessory minerals such as fluorite, apatite, sphene, microlite, pyrochlore, topaz, tourmaline and bastnäsite can host more than 50% of the total F. Fluorine is also found in solid and fluid inclusions (e.g. micas in feldspar and fluid inclusions in quartz), and as glasses (Bailey, 1977; Correns, 1956). Fluorine concentrations in granitic fluid inclusions are usually less than those of H_2O, CO_2 and Cl (Roedder, 1972). Near-surface degassing causes the F content of extrusive rocks to be generally lower than that for the equivalent intrusive rock (although it should be noted that the inclusion of some alkali basalts in the mean for basalts in table 2.2 has increased the basalt mean beyond that for andesites). The HF content of volcanic gases is generally below 0.03 vol% (White and Waring, 1963).

After solidification of silicic magmas (between 600 and 450°C), F probably forms highly soluble complexes with a variety of elements, e.g. $[AlF_2(H_2O)_4]^+$, $(SiF_6)^{2-}$ and $NaAlF_4$. These early complexes decompose with decreasing temperature and pressure, releasing F as a true gas phase. Greisenization takes place in these conditions. Between 400 and 200°C F combines with Al and Ca to form topaz and fluorite in hydrothermal quartz veins (Shcherba, 1970). Fluorine-metasomatism during greisenization is associated with deposition of W, Sn, Be and Li.

2.1.4 Metamorphic rocks

Fluorine concentration in metamorphic rocks is highly variable (Table 2.3), as the F content is related to the amount present in the pre-metamorphic protolith. Fluorine is remobilised during regional metamorphism to zones of low pressure, temperature or F concentration or to reactive rocks such as limestone. Regional metamorphic rocks are generally low in F, as shown, for instance, by the mean values for schists (250 ppm) and shales (790 ppm, Table 2.4). Fluorine substitutions for O^{2-} tend to occur at high temperatures and pressures, resulting in the minerals sphene and pyrochlore. Fluorine is lost from biotite at low tempertaures but gained at higher grades. Biotite has 0.65% F in granulite facies compared to 0.24-0.38% F in amphibolite facies and <0.2% F in low grade rocks (Filippov *et al.*, 1974; Guidotti, 1984). Muscovite has F up to 0.25%, but usually around 0.1%. Guidotti (1984) proposed that as metamorphic grade increases, hydrous minerals are lost and F becomes enriched in the remaining hydrous phases.

Metasomatised rocks may have high F contents because, along with CO_2, HCl and H_2O, HF can be a major component of metasomatising fluids. Skarns can contain a wide range of F-bearing minerals such as fluorite, apatite, hornblende, mica, topaz and sphene.

2.1.5 Sedimentary rocks

Fluorine becomes a component of sedimentary rocks through several processes. Fluorine may be present in resistant minerals such as topaz, tourmaline and apatite, and to a lesser extent fluorite and the micas. It may be absorbed onto an anion receptor such as a clay particle, or it may be transported into the sediment as an aqeous ion or complex. In marine sediments it may co-precipitate from seawater with $CaCO_3$ and phosphate. In clastic sediments F is highest in clay-bearing rocks such as shales and mudstones (Table 2.4), although some sandstones have become cemented by fluorite. In limestones some CaF_2 and MgF_2 coprecipitate with $CaCO_3$, but most F is found as fluorapatite in the skeletal remains of marine organisms. In anhydrite and gypsum, F co-precipitates with $CaSO_4$ as CaF_2, but

Table 2.3 Fluorine in metamorphic rocks. After the compilation by Boyle (1976). 'Tr.' is trace. All concentrations in ppm.

Rock Type	Range		Mean	Number
	Minumum	Maximum		
Regional				
Metagabbro	99	140	120	2
Schists	60	580	250	48
Amhpibolite	140	1400	740	10
Gneiss	240	2800	1030	14
Metasomatic				
Hornfels	26	7800	1630	57
Contact Skarns	700	43500	9780	28
Greissens	1600	20400	9800	26
Kaolinized Granite	800	7400	2800	26
Fenite	Tr.	600	400	3

Table 2.4 Fluorine in sedimentary rocks. After the compilation by Boyle (1976). 'Tr.' is trace. All concentrations in ppm.

Rock Type	Range		Mean	Number
	Minumum	Maximum		
Clastic				
Shales, siltstones and mudstones	10	11660	790	141
Sandstones and Greywackes	10	880	180	49
Oceanic sediments	100	1600	640	151
Biogenic/Chemical				
Limestone	Tr.	1210	220	98
Dolomite	110	400	260	14
Phosphate Rock	10400	42000	30500	74
Anhydrite and Gyppsum	130	890	600	6
Rock salt	2	6	5	4

the inability of F to precipitate as Na or K compounds is reflected in the very low concentrations in rock salt.

2.1.6 Fluorine in Soils

Fluorine is richest in soils with high contents of phosphates, clay minerals and colloids and at its lowest concentration in light, sandy soils (Boyle, 1976; Robinson, 1978), and is generally depleted in soils relative to the parent fresh rock (Koritnig, 1974). Micas and amphiboles have F leached from them without dissolution of the mineral, with the process presumably taking place more efficiently at tropical temperatures, low F concentration of the leaching water and high water-mineral ratios. In general, F^- can be absorbed onto mineral surfaces in place of hydroxide, but the element is displaced by the hydroxide ion with increasing pH (Matthess, 1982; Hübner (1969) quoted in Koritnig, 1974). Fluorine is boosted artificially by the addition of superphosphate fertilisers.

Mobility in soils. Soils adsorb F^- from dilute and concentrated solutions (Fluhler *et al.*, 1982; Gupta *et al.*, 1982) and this process is being used industrially (e.g. Ginster and Fey, 1995). Pickering (1985) noted that F^- mobility depends on soil type, the pH of the system and F^- concentrations. Retention of F^- in the soil system was favoured in acidic sediments containing clays and poorly ordered hydrous oxides of aluminium. Jinadasa *et al.* (1993) investigated F^- adsorption onto the surface of goethite (FeO.OH). They found that adsorption was minimal above pH 7, and increased with decreasing pH, being greatest at pH 4. Meeussen *et al.* (1994) assumed that the behaviour of F^- in a soil profile was mainly determined by adsorption onto metal oxide and hydroxide surfaces, specifically goethite and gibbsite.

2.1.7 Biosphere

In plants fluorine is mostly stored in the leaves, after translocation from the root system or directly from absorption from the atmosphere. The availability of F to the root system is decreased by increases in the pH, phosphate, Ca, clay and organic matter content of the soil. Typical F concentrations in non-accumulator plants are below 20 ppm dry weight. Notable amongst plants which accumulate F is *camellia sinensis*, the tea bush. In Chinese varieties the concentrations in dried leaves reach 178 ppm, and in Indian varieties up to 115 ppm (Robinson, 1978). Fluorine usually accumulates as microscopic crystals of fluorapatite, but some plants accumulate it as fluoracetate, fluor-oleic acid or fluor-palmitic acid. These compounds are extremely toxic to mammals. In F intolerant plants increased F concentration disturbs photosynthesis, carbohydrate metabolism and water management

causing intense respiration, growth retardation, inhibition of pigment synthesis, chlorosis, wilting, plasmolysis and collapse of cells followed by necrosis. Susceptibility varies greatly between species, and even between varieties (Robinson, 1978).

2.1.8 Mineral - aqueous fluoride interaction

Ionic compounds of F dissolve congruently and can be modelled using simple equations. Those compounds where F is adsorbed onto the surface or where F replaces OH are more complex, as they often dissolve incongruently.

Ionic compounds of F. The congruent dissolution of ionic compounds of F^- is well known and behaves according to the equation

$$cCnF \rightleftharpoons cB + nF^- \quad (1)$$

where C is a cation such as sodium or calcium, B is the aqueous species of that cation and c and n are the molar proportions. The equilibrium dissolution of the compound then follows the equation

$$K_{cCnF} = \frac{(a_C)^c \cdot (a_F)^n}{a_{cCnF}} \quad (2)$$

where K is the equilibrium constant (also known as the solubility product) for that reaction and a is the activity (at low ionic strength equivalent to concentration). For instance, simple dissolution of CaF_2 produces activities of Ca^{2+} and F^- in solution according to the equation

$$K_{CaF_2} = \frac{a_{Ca^{2+}} \cdot (a_{F^-})^2}{X_{CaF_2}} \quad (3)$$

The mole fraction (X) of pure CaF_2 is one, and so the equation is simplified to

$$K_{CaF_2} = a_{Ca^{2+}} \cdot (a_{F^-})^2 \quad (4)$$

The value of K_{CaF_2} is 4.26×10^{-11} (Gill, 1996), or in logarithmic form,

$$\log_{10} K_{CaF_2} = -10.4 \quad (5)$$

By analogy with pH, $pK_{CaF_2} = 10.4$. Table 2.5 shows the solubility products of fluoride minerals.

Table 2.5 Solubility products of fluoride minerals, expressed as *p*K (-log *K*) at 25°C. First two values from Gill (1996). Final four values recalculated from solubility data in Handbook of Chemistry and Physics (Weast, 1975).

Compound	*p*K
CaF_2	10.4
BaF_2	5.8
SrF_2	8.57
KF	-2.4
MgF_2	8.14
NaF	0.0044

Dissolution of F-bearing alumino-silicates. The dissolution of F-bearing alumino-silicate minerals has been little researched, and few references to the leaching of F from alumino-silicates are found in the literature. Nagy (1995) reviewed the dissolution kinetics of sheet silicates, and summarised that most sheet silicates have a dissolution rate of approximately 10^{-17} mol/cm^2/sec at 25°C and a pH of 5. The rate for biotite dissolution under these conditions is 6×10^{-17} mol/cm^2/sec (Stumm *et al.*, 1987), and for muscovite 10^{-17} mol/cm^2/sec (Acker and Bricker, 1992). Trotignon and Turpault (1992) studied the dissolution of biotite, using F-free specimens. They showed that dissolution of biotite is strongly dependant on the pH of the solution. Acker and Bricker noted that biotite dissolved incongruently between pH 3 and 7, with preferential release of Mg and Fe over Si. Most dissolution takes place on the edge of biotite crystals, which are altered to vermiculite. Fanning and Keramidas (1977) stated that high F concentrations in micas retard the release of cations and thus the weathering process.

Sverdrup (1990) was of the opinion that "weathering rates and mechanisms of dissolution of inosilicates [pyroxenes and amphiboles] are poorly understood, and that for augite and hornblende are particularly deficient". Inosilicates often weather non-stoichiometrically (incongruently), with rapid release of Ca and Mg (Brantley and Chen, 1995). However, they found that hornblende approached stoichiometric dissolution after experimental weathering of longer than 115 days duration. For hornblende in a solution at 25°C and ph 4.0, Zhang *et al.* (1993) calculated a dissolution rate of 1.3×10^{-8} mol/cm^2/sec, whilst Sverdrup (1990) calculated a rate of 3×10^{-8} mol/cm^2/sec under the same conditions. These rates are remarkably fast. Sverdrup stated that solution chemistry made little difference to dissolution rates, apart from high Al and P_{CO_2}. To summarise, alumino-silicates dissolve incongruently and slowly in near surface conditions, and little is known of the

behaviour of F during dissolution of these minerals. No solubility constants were found for these minerals.

2.1.9 Review of the base exchange process

It will become evident that ion exchange processes may be important in influencing several groundwater compositions, and so a review of this process is provided (Freeze and Cherry, 1979; Lloyd and Heathcote, 1985). Aqueous cations are preferentially absorbed onto exchange media in the following order:

$$Cs^+ > K^+ > Na^+ > Li^+$$

$$Ba^{2+} > Sr^{2+} > Ca^{2+} > Mg^{2+}$$

In other words, in order of increasing hydrated ionic radius, and with divalent ions more strongly adsorbed than monovalent ions. The exchange of cations can be described by equilibrium reactions, e.g.

$$2NaR + Ca^{2+} \rightleftharpoons CaR_2 + 2Na^2 \quad (6)$$

where R is the exchange medium. The equilibrium is described by

$$Q_{(Na \rightarrow Ca)} \rightleftharpoons \frac{X_{Ca}}{X^2_{Na}} \cdot \frac{(Na^+)^2}{(Ca^{2+})} \quad (7)$$

where X is the equivalent fraction of the ion on the exchanger R, e.g.

$$X_{Ca} = \frac{2[CaR_2]}{2[CaR_2] + [NaR]} \quad (8)$$

Q is the selectivity coefficient which, as it varies with the ionic strength of the solution, is only semiquantitative. Q decreases with increasing ionic strength, as shown by the values in Table 2.6. Cation exchange capacity varies with pH (Freeze and Cherry, 1979).

Table 2.6 Ion exchange on clays with solutions containing Ca^{2+} and K^+ at equivalent concentrations.

Clay	Exchange capacity (meq/g)	Variation of Ca^{2+}/K^+ ratio (Q) on clay, with concentration of solution (meq/ℓ)			
		100	10	1	0.1
Kaolinite	0.023	-	1.8	5.0	11.1
Illite	0.162	1.1	3.4	8.1	12.3
Montmorillonite	0.810	1.5	-	22.1	38.8

2.1.10 Distribution and causes of high F^- concentration in groundwater

Global. Many countries of the world have significant areas where groundwater contains elevated concentrations of F^-. The United States of America, Canada, China and India are amongst countries in the northern hemisphere that experience high F^- groundwater (e.g. Corbett and Manner, 1984; Yong and Hua, 1991; Gupta and Sharma, 1995; Boyle and Chagnon, 1995; Hitchon, 1995). Yong and Hua (1991) attributed high F^- groundwater to several separate causes: high F content of aquifers; low groundwater flow rates; arid and semi-arid climate increasing potential evaporation; and water with high pH.

In a detailed study in the Alberta basin of Canada, Hitchon (1995) found formation waters with up to 22 mg/ℓ F^-. He noted a trend of increasing fluorite saturation from shallow, cool, low Ca, fresher waters to deeper, hotter (73°C), more saline and Ca-rich water. He noted the importance of the MgF^+ complex, and that the complexes NaF^0, VO_2F^0 and AlF_2^+ were of minor importance. He stated that the F concentration in groundwater is controlled by an intricate relation between saturation with respect to fluorite and the concentration of ions which form F complexes, all of which are controlled by ionic strength and temperature. It was calculated that many possible F complexes were not in fact of quantitative importance, e.g. aluminium complexes from AlF^{2+} to AlF_6^{3-}, vanadium complexes VOF^+ and VOF_2, FeF^{2+} and SiF_6^{2-}.

Kraynov *et al.* (1969) found that waters with up to 15 g/ℓ F^- had been in contact with villiaumite (NaF), an abundant accessory mineral in the deep zones of the Lovozero Massif. The massif is composed of alkalic rocks, similar to those of the Pilanesberg Complex. The author noted that evaporation had increased the F^- concentration in the groundwaters. The waters are highly alkaline (pH > 12) and are characterised by very high concentrations of Na (up to 26 g/ℓ), Si (up to 13 g/ℓ) and virtual absence of Ca.

Africa. In Africa, high F^- groundwaters have been studied in some detail in Kenya (Gaciri and Davies, 1993; Davies, 1994), Ethiopia (Ashley and Burley, 1994; Gizaw, 1996) and Tanzania (Smet, 1992). The abundance of F^- in Rift Valley groundwater has been attributed to weathering of alkaline volcanic rocks rich in F and the interaction of groundwater with volcanic HF exhalations (Gaciri and Davies, 1993); outgassing of CO_2, geothermal heating and low groundwater Ca and salinity (Gizaw, 1996) and ion exchange processes (Ashley and Burley, 1994). Botchway *et al.* (1996) attributed high F^- concentrations in the groundwater of Accra in Ghana to the decay of plant material. Other countries which have F^- enriched groundwaters include Sudan (Ibrahim *et al.*, 1995), Nigeria, Senegal, Algeria, Egypt, Zimbabwe, Morocco, Uganda and Somalia (Smet, 1992).

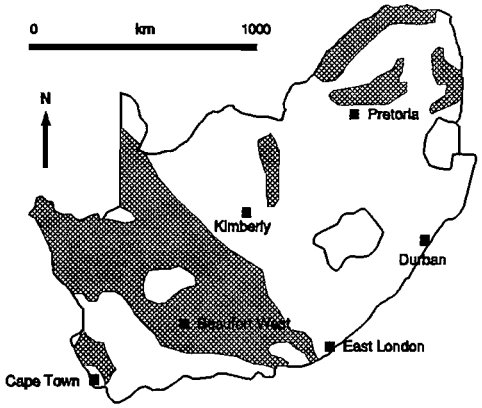

Figure 2.2 South African groundwater with F^- concentration greater than 1.5 mg/l.

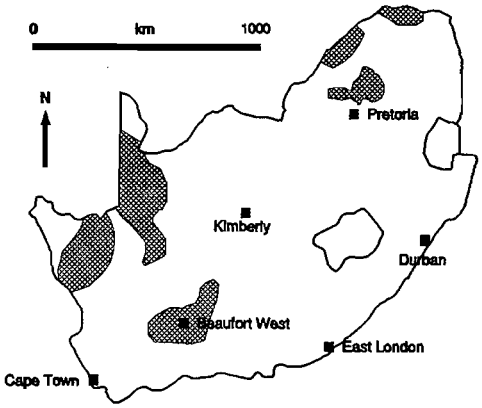

Figure 2.3 South African groundwater with F^- concentration greater than 3.0 mg/l.

South Africa. Several researchers have noted the high F^- content of certain groundwaters in South Africa, especially in the Pilanesberg and Bushveld Complexes. Shand (1928) gave a description of the hydrology of the Pilanesberg Complex and commented on spring water composition: 'high level' springs being pure, 'low level' springs being 'high in soda'. Ockerse (1943) measured rock, soil and groundwater concentrations of F^- in an attempt to understand the causes of endemic dental fluorosis. His study covered the whole of South Africa but unfortunately gave the western Bushveld only superficial attention. He did, however, single out the Pilanesberg, Warmbaths and Pretoria Saltpan as areas with endemic dental fluorosis deserving greater investigation. He suggested F^- in groundwater of the Springbok flats came from the Ecca formation, and suggested detrital fluorapatite as the source. Grobler and Dreyer (1988) determined F^- concentrations in drinking water from surface waters and groundwaters for 162 towns and cities across South Africa. Forty percent of the groundwaters had F^- below 0.1 mg/ℓ, and less than 7% had F^- greater than 1.0 mg/ℓ. Of the groundwaters, 84% had significantly lower concentrations of F^- when water

levels increased, which Grobler and Dreyer ascribed to dilution. They also showed that groundwaters had significantly higher F^- concentrations that surface waters. Raubenheimer *et al.* (1990) determined F^- concentrations in rivers flowing through the Kruger National Park. Their main conclusion was that all 5 rivers (the Olifants, Luvuhu, Letaba, Sabie and Crocodile Rivers) had higher concentrations of F^- during the latter part of the dry winter season. The Olifants River had differences of up to 2 mg/ℓ F^- between wet and dry season flows. Changes in mean F^- concentration in each of the 5 rivers over 5 years was very slight, and not significant. Fayazi (1995) suggested that the Karoo sedimentary strata contained fluorite derived from the surrounding Bushveld Granites during episodes of arid erosion. He suggested that F^- concentrations in groundwater hosted by the Karoo formations is strongly controlled by the geochemistry of the rock.

McKenzie *et al.* (1966) published a map of groundwater with a F^- concentration above 1.5 mg/ℓ, prepared by the Soil Research Institute. The map was based on unspecified data sources and is at variance with the current known distribution, as presented in Figures 2.2 and 2.3. These figures are based on unpublished distribution maps calculated from the SA National Groundwater Database. It can be seen that large areas of the country are subject to F^- concentrations in groundwater greater than 1.5 mg/ℓ, especially in the arid western and south-western Cape.

Bushveld area. Bond (1947) was the first worker to extensively discuss chemical analyses of ground water from the Pilanesberg Complex. He noted the 'high soda alkalinity and the consistently high fluoride content'. He stated that the highest recorded concentration of fluorides in ground water 'so far discovered in the Union' of South Africa was 67.2 ppm in spring water from the farm Doornhoek, although the exact location was not given. Retief (1963) published 9 analyses of ground water, which were only analyzed for F^- and Cl^-. Fluoride was consistently high in his analyses. Lurie (1974) gave a full chemical analysis of water from an artesian borehole in tuffs, which showed a F^- concentration of 2.4 mg/ℓ. Bond (1947) described groundwaters occurring in other lithologies in the field area, based on a fairly limited sample set. He stated that Pilanesberg groundwater was similar in chemical composition to those of the 'Red Granites' (Lebowa Granite Suite) which are also characterised by high F^- concentrations. The 'Old Granite' (Archaean Granite) occasionally has 'an appreciable F^- content', whilst in some samples it is absent. Both Bond (1947) and Ockerse (1943) stated that fluoride was present in solution as "sodium fluoride".

2.2 Fluorine and Health

As Paracelsus, a philosopher from Ancient Greece put it,'*All substances are poisons; there is none which is not a poison. The right dose differentiates a poison and a remedy.*' Fluorine is an excellent example of this principle. It is one of a group of trace elements which are beneficial at low dosages, but which at higher doses are harmful and even fatal. Fluorine not only affects humans. The first recorded outbreak of recognisable fluorosis in farm animals took place after the eruption of the volcano Hekla in the eighteenth century. Mass mortality of livestock due to acute F^- poisoning caused starvation and a 25% reduction in the human population of Iceland (Fridriksson, 1983). Chronic fluorosis in animals is manifested by severe dental lesions, lameness and exostoses. Fluorosis in animals has been recorded from just north of the field area (Botha *et al.* , 1993). Also affected are wildlife (Fourie *et al.*, 1996) and plants (see earlier in this chapter). However, this section addresses the affect of F^- on human health only.

2.2.1 Metabolism of fluoride

Fluoride passes into the blood plasma by absorption through the lungs or gastrointestinal tract. In contrast to the other halogens, F^- is rapidly absorbed from the stomach; plasma F^- concentrations peak approximately 1 hour after ingestion. The free F^- ion is converted to HF in the stomach (Jenkins, 1990). In the blood three quarters of the total F^- is found in the blood plasma, with the balance taken up by red blood cells. Fluorine in plasma exists primarily as the free F^- ion, whilst the rest is present as lipid-soluble organic fluorocompounds. The kidneys rapidly remove F^- from the blood, so that a typical background level is only 0.02 mg/ℓ (Jenkins, 1990). Approximately 50% of absorbed F is eliminated from the body within 24 hours, primarily in urine. The residue becomes associated with calcified tissue, where 99% of the total F in the body is found. Whilst Jenkins (1990) states that F is firmly bound to the bone, Whitford (1996) states that F is not irreversibly bound to the surface bone crystallites, so that F concentration in bone can eventually reflect changes in the amounts of F ingested chronically. The fluoride half life in bone is approximately 8 years (Schlatter, 1978). Fluoride is not accumulated in the thyroid gland and is eliminated many times faster than the other halogens. Urinary pH affects the efficiency with which the kidneys remove F^- from the body, so chronic acid-base disturbances are important in F metabolism. Acid-base status is influenced primarily by diet, as well as certain drugs, metabolic and respiratory disorders, physical activity and altitude

(Whitford, 1996). Fluoride freely passes through the placenta, so that foetal F^- plasma levels are directly proportional to those of the mother.

The cariostatic effect of F^- is probably due to its ability to promote enamel remineralisation and to inhibit acid production by plaque bacteria - F is a potent inhibitor of many enzymes. Fluoride has the ability at low levels to *inhibit* soft tissue calcification and may decrease the chances of death due to cardiovascular disease, particularly ischemic heart disease.

2.2.2 Dental Fluorosis

Human beings throughout history have suffered from dental fluorosis, but until this century the aetiology of the condition was unknown. Given the common incidence of high F^- groundwaters in the East African Rift Valley (Gaciri and Davies, 1993; Smet, 1992), it is quite possible that ancient ancestors of humanity could have had dental fluorosis. The victims of the volcanic eruption at Pompeii in *A.D.* 79 suffered from dental fluorosis, probably due to high F^- concentrations in their drinking water (Torino *et al.*, 1995). The eruption of the Icelandic volcano Hekla in the eighteenth century produced severe fluorosis in the surrounding human populations (Fridriksson, 1983) and recent eruptions continue to release F^- into the hydrosphere (Gíslason *et al.*, 1992). Early studies of stained tooth enamel in communities in Colorado showed that such staining did not render the tooth more susceptible to dental caries (McKay and Black, 1916). However, the inverse relationship between dental caries and mottled enamel was only established by Bunting and co-workers in 1928 and by McKay in 1929 (Dean, 1954). This led to the search for the causative agent of mottled enamel, which was found to be the high F^- concentrations in drinking water supplies of the affected communities. Since then it has been widely shown that high concentrations of F^- in drinking water can cause deleterious effects in human dentition (e.g. Senewiratne *et al.*, 1973; Driscoll *et al.*, 1983; Dissanayake, 1996). It has also been shown that a moderate intake of F^-, often facilitated by fluoridation of drinking water, is beneficial to dental health by causing a reduction in dental caries (Arnold *et al.*, 1953; Newbrun, 1989). Fluoride deficiency is marked by an increased incidence of dental caries.

The incidence and severity of dental and skeletal fluorosis are influenced by other factors apart from the concentration of F^- in drinking water. A diet deficient in vegetables and fruit has been suggested as a factor (Dodd *et al.*, 1960). The increase in the availability of fluoridated toothpaste and fluoride supplements has caused an upsurge in dental fluorosis in communities with optimally fluoridated water (Pendrys, 1995). The increases in dental fluorosis with increasing altitude (observed by Shortt *et al.*, 1937) and average temperature

(Galagan and Lamson, 1953; Brouwer *et al.*, 1988) are due to increased water consumption, thus increasing total F^- intake. Whitford (1996) attributes increasing fluorosis at higher altitudes to the alteration of kidney function, which affects the excretion of F^-. Unusual causes of fluorosis has been described from Spain (Franke *et al.*, 1978), where NaF was added to wine to avoid abnormal fermentation, resulting a form of skeletal fluorosis ("wine fluorosis"), and China, where high F in tea has caused skeletal fluorosis in immigrant Tibetans (Cao *et al.*, 1996). Other effects of F^- are discussed in section 2.2.3.

Symptoms. Mottled tooth enamel is a common sight in many rural parts of the world. Until 1931 the term 'mottled tooth enamel' was common, but since the source of the condition has been traced to excess ingestion of F^-, the term 'dental fluorosis' has been adopted. The following descriptions of the clinical manifestations of dental fluorosis are summarised from Fejerskov *et al.* (1988). Normal tooth enamel is a microporous solid comprised of highly ordered, tightly packed hydroxyapatite crystals. The surface of the enamel in normal teeth is translucent, smooth and glossy even when dry, with a pale creamy white colour. Dental fluorosis is a developmental disturbance which increases with time. Therefore primary teeth are less severely affected than the permanent teeth, and those teeth which erupt first (the incisors and first permanent molars) are less affected than those erupting later (the premolars and other permanent molars).

The first signs of dental fluorosis (*moderate dental fluorosis*) are thin white lines running across the entire enamel surface and which can only be seen after drying of the tooth surface. This phenomenon is caused by air replacing saliva in enamel porosities, increasing opacity in the more porous areas. The porosity occurs at crystal boundaries and is caused by impairment of the final growth of the hydroxyapatite crystals. With more fluorosis these thin lines become broader, merge and may be clear without the need for drying. At slightly greater severity the tooth surface shows distinct, irregular, opaque or cloudy white areas, caused by increasing porosity of the tooth enamel. The patches may take up brown stains from food particles. Rarely, minute pits may occur in the cloudy areas.

Moderate dental fluorosis is characterised by the entire tooth surface becoming chalky white. Such teeth can be damaged by mechanical wear in the mouth and by the probing of dentists. In *severe dental fluorosis* pits occur in the now completely opaque enamel. The pits, of varying diameter, are scattered over the tooth surface to begin with, but merge to form a band across the tooth, often coincidental with the position of the top or bottom lip. The pits are caused by hypomineralized enamel breaking off, revealing normal enamel underneath. At no time is dentine exposed. Severely fluorotic teeth have an almost total loss of surface enamel, and become misshapen and are often stained brown or black. The

staining, although common, depends entirely on the post-eruptive oral environment and is not an intrinsic feature of dental fluorosis.

Dental clinicians originally used the classification of dental fluorosis proposed by Dean *et al.* (1942), which used the descriptions *normal, questionable, very mild, mild, moderate* and *severe*. More recently, dentists have turned to the TF index, proposed by Thylstrup and Fejerskov (1978) which arranged the severity of dental fluorosis into 10 classes, from 0 (equivalent to *normal*) to 9 (*severe*). Unfortunately, the precise levels of F^- dietary intake at which each level of fluorosis becomes apparent are not well established (Brouwer *et al.*, 1988; Leung, 1988; White, 1988; Du Plessis, 1995).

Dental fluorosis in the field area. Investigations of dental fluorosis in the field area are confined to village-based studies only. No full scale census or survey has been carried out. Ockerse (1941 and 1943) and Ockerse and Meyer (1941) were the first workers to report on the occurrence of endemic dental and skeletal fluorosis in South Africa. In the field area Ockerse (1943) found evidence of the condition in the Pilanesberg, Warmbaths, Kalkheuvel and Pretoria Saltpan areas. Not all occurrences were large; only 3 cases were located around the Saltpan, and the cases at Kalkheuvel were found only in the workers of a certain quarry. However, he stated that the Pilanesberg was '*one of the worst affected endemic fluorosis areas in the Transvaal*', and that '*some of the worst cases of mottled enamel are found among school children who were born and grew up in Warmbaths*'. He stated that 144 endemic areas had been identified in the Transvaal, mostly in areas underlain by the Bushveld Igneous Complex.

The studies of Zietsman (1985, 1989 and 1991) have been methodical and illuminating, with surprising and controversial conclusions. Her small study area encompassed several villages, in the centre of the current author's field area. Most of the villages were situated on Nebo Granite and granophyre, whilst one was situated on the edge of the Ecca Formation outcrop. Zietsman (1989) discussed the spatial variation of dental fluorosis in 7 villages, and attempted to correlate the variation to underlying geological causes and to the variation of F^- concentrations in groundwaters. She sampled 120 boreholes, and found much spatial variation of F^- concentrations, ranging from 0.1 to 5.5 mg/ℓ. Importantly, she found that 33% of children drinking groundwater with a F^- content of <0.5 mg/ℓ had dental fluorosis. Furthermore, she found the occurrence of different rock types did not *fully* explain the spatial variation in groundwaters F^- concentration. Her conclusions are somewhat compromised in that, in her discussion of the geological setting of the village of Rietgat, whilst correctly stating that the village is within the outcrop area of the Ecca Formation, she ignores the fact that the village is on the very edge of the Karoo basin. Boreholes in the

village in all likelihood penetrate through the Ecca formation, into the underlying Nebo Granite. Geological logs of the boreholes would be needed to confirm this contention.

Zietsman (1991) further developed her ideas on spatial variation and fluorosis in the same study area. Each of the 3103 school pupils which were examined for dental fluorosis were linked to individual drinking water sources, usually boreholes. The history of each source was known for up to 30 years before the study, and from this Zietsman based her conclusions. The positive correlation between F^- concentration in the drinking water and the *severity* of dental fluorosis was statistically significant at 95% confidence limits, but the spatial variation in fluorosis was not fully explained by the variation in F^- concentration. She could recommend no safe 'threshold level', as the severity of fluorosis formed a continuum at any F^- concentration. She also found only 4% of the groundwaters exhibited variation in the F^- concentration from dry to wet season, and that this variation was always less than 30% of the mean value. If any criticism had to be levelled at this excellent paper, it would be that children (with an ungauged and questionable sense of direction) were responsible for pointing out the location of their principal source of water.

Rudolph *et al.* (1995) have investigated dental fluorosis in four villages near the Pilanesberg Complex. Two of the villages had high F^- groundwater, whilst the two control villages had low F^- groundwater. They found that severe dental fluorosis occurred in 28% of subjects drinking groundwater with a F^- concentration of 7 to 8 mg/ℓ, whilst 41% had moderate dental fluorosis. Every person in the two villages with high F^- groundwaters showed some evidence of dental fluorosis. Three people from the two villages with low F^- also had dental fluorosis. In 1991, 95% of the inhabitants of Bophuthatswana received their drinking water from groundwater (Pelpola *et al.*, 1992).

Dental fluorosis has been studied in several other part of South Africa. The study by Lewis and Chikte (1995) of school children in KwaNdebele showed that even at a drinking water F^- concentration of between 0.6 - 1.6 mg/ℓ, 90% of the subjects had some sign of dental fluorosis, bringing into question the recommendations of the WHO (1984). Furthermore, Carstens *et al.* (1995) showed that children in the North Western Cape who drank water with a F^- concentration below the WHO recommendations still had a high incidence of dental fluorosis. They recommended a drinking water F^- concentration of only 0.4 mg/ℓ. According to du Plessis *et al.* (1995), race was found to be a factor in the severity of dental fluorosis. They found that 39% of white school children in the Bloemfontein area had evidence of dental fluorosis on the maxillary central incisors, compared to 16% of black schoolchildren drinking water of the same F^- concentration (0.54 mg/ℓ). Retief *et al.* (1979) showed that a positive association existed between F^- concentration in tooth enamel and

the degree of fluorosis in the individuals of the town of Kenhardt in the northern Cape, supplied with high F^- drinking water (3.2 mg/ℓ). The study of van der Merwe *et al.* (1977) reached similar conclusions.

2.2.3 Other effects of F^- on the human body

Skeletal fluorosis. Fluorapatite is an order of magnitude less soluble than hydroxyapatite, the principal mineral constituent of bone. The F^- ion aggressively substitutes for the OH^- ion, leading to a build up of F in bone tissue with increasing age. A typical 55 year old human is expected to have between 2000 and 2500 ppm F in their bones, although up to 6000 ppm F has been recorded with no pathological change (Jenkins, 1990). Skeletal fluorosis often occurs in endemic dental fluorosis areas; generally, only villages with higher than average F^- will also have cases of skeletal fluorosis. Asymptomatic skeletal fluorosis can be diagnosed most securely with X-Rays. This is due to the increased bone density, especially in vertebrae (Meunier *et al.*, 1989). Several studies, such as Riggs *et al.* (1990) on women with postmenopausal osteoporosis, showed that with very high F^- consumption, bone mass increases but skeletal fragility also increases.

The first symptoms of skeletal fluorosis are aching joints and muscles. Increasing severity produces stiffness of the lumbar, thoracic and cervical regions of the spine and restriction of head movement, caused by thickening of the joints and mineralisation of the tendons. In extreme cases the vertebrae of the back become rigid, giving rise to a condition known as 'poker back' or 'bamboo spine'. The patient is unable to stand erect, the rib-cage becomes rigid and all breathing is performed abdominally, whilst bony outgrowths form at the end of ribs and along the long bones (Shortt *et al.*, 1937; Ockerse, 1941). Paraplegia, quadriplegia, wasting of the muscles and neurological disorder (radiculomyopathy) may finally ensue (Boyle and Chagnon, 1995; Goldman *et al.*, 1971).

Artificial skeletal fluorosis was first described in Danish workers, who ingested large amounts of F by accidental inhalation of cryolite dust (Na_3AlF_6; Moller and Gudjonsson, 1932). In parts of India, notably Madras, where ingestion of water with a F concentration greater than 8 mg/ℓ has occurred for more than 40 years, skeletal fluorosis is endemic (Shortt *et al.*, 1937). Endemic skeletal fluorosis has been reported in many countries (Lyth, 1946; Kilborn *et al.*, 1950; Hamamoto, 1957; Zipkin *et al.*, 1958; Odenthal and Wieneke, 1959; Felsenfeld and Roberts, 1991; Boyle and Chagnon, 1995).

Skeletal fluorosis has been reported from several areas of South Africa. Ockerse (1941) reported 6 cases of confirmed skeletal fluorosis in workers at a cement factory north of Pretoria. The occurrence in Kenhardt in the Northern Cape Province (Dodd *et al.*, 1960)

is unusual in that children have been affected; in other parts of the world skeletal fluorosis usually manifests itself after 20 to 40 years. The groundwater of the area is only moderately enriched in F, at 4.8 ppm. The symptoms are also unusual in that softening of the long bones occurred, causing bending. Fluoride in this case is probably only one of several aeteological factors in the condition, another being malnutrition. Pettifor *et al.* (1989) suggested that low dietary calcium intakes may exacerbate the severity of bone lesions in children living in areas of endemic fluorosis.

Goitre. It has been noted that endemic goitre is often found in the same area as high F^- concentrations in groundwaters, although it is unlikely that F^- is directly goitrogenic (Day and Powell-Jackson, 1972). Yang *et al.* (1994) investigated the effects of high iodine and F on children's intelligence. Although they found intelligence quotient was lowered in children with high F and iodine intakes, Yang *et al.* did not investigate which element was responsible. Parts of the current field area are iodine deficient (Kalk *et al.*, 1997).

Cancer. Childhood osteosarcomas occur most frequently in the knees, ankles, shoulders and wrists, areas showing a high response (osteoblast proliferation and bone formation) to F^- (Schulz *et al.*, 1984). High F^- drinking water was initially implicated in higher rates of osteosarcoma (Kinlen, 1975). However, more recent research (Oldham and Newell, 1977; Hrudey *et al.*, 1990; Anderson, 1991; Mahoney *et al.*, 1991; US Dept of Health and Human Services, 1991; Freni and Gaylor, 1992; Gelberg *et al.*, 1995) has shown that F^- is not osteocarcinogenic in humans.

Acute fluoride poisoning. Gessner *et al.* (1994) reported acute F^- poisoning in a small community in Alaska. The incident followed an accidental NaF overdose at a water treatment works. Initial symptoms include nausea, epigastric distress and vomiting. Excessive salivation, mucous discharge from the nose and mouth, headaches, sweating, diarrhoea and general weakness are sometimes present. Spasm of the extremities, tetany and convulsions develop in lethal doses, as well as failure of the cardiovascular system indicated by a weak pulse and cardiac arrhythmias. Renal function and respiration is depressed causing respiratory and metabolic acidosis. Extreme disorientation is followed by unconsciousness and death.

Large amounts of F^- must be ingested to induce acute F^- poisoning, far more than is possible from the ingestion of almost all naturally fluoridated drinking water. Gessner *et al.* (1994) reported death after ingestion of 18 mg/kg body weight, although other workers have quoted an LD_{100} (the dose which is 100% lethal to a specified group of subject, in this case human males of 70kg mass) of a quarter of this value.

2.2.4 Risk levels and optimal fluoride concentration in drinking water

There is uncertainty as to the precise concentrations of F^- in drinking water which are optimal for human health. Table 2.7 shows that the F^- concentration limits for drinking water suggested by national and international bodies vary considerably. It is apparent that the upper limit for avoiding widespread dental fluorosis is approximately 2.0 mg/ℓ, although this value is reduced in tropical climates because of increased water ingestion (see below). The upper limits for skeltal fluorosis and crippling skeltal fluorosis show no such agreement between countries. This may be because of the smaller amount of epidemiological evidence on which to base guidelines. The high guideline value for Tanzania is a result of widespread very high F^- concentrations in that country, and the resulting economic and humanitarian consequences of imposing a more realistic value. Similar arguments have resulted in the double standard in Argentina.

Table 2.7 Guidelines for F^- concentration in drinking water, based on the affects of drinking such water. After Smet (1992).

	Proposed effects/ mg/ℓ F in drinking water		
	Objectionable dental fluorosis	Skeletal fluorosis	Crippling skeletal fluorosis
WHO (1984)	> 1.5	3.0 - 6.0	> 10.0
US EPA	> 2.0		> 4.0
Tanzania		>8.0	
Argentina - urban - rural	> 1.5 > 2.2		
Brouwer *et al.* (1988) - tropics	> 0.6		> 7.0
South African Drinking Water Guidelines (DWAF, 1996)	>1.5	>3.5	

It has been noted that as water ingestion is proportional to air temperature, the optimal F^- concentration in groundwater used for drinking purposes should be dependant on the mean maximum temperatures experienced in any particular area. This led Foss and Pittman (1986) to propose an empirical equation for optimal F^- concentration, equivalent to:

$$optimal\,F^- = \frac{0.34}{0.2364 + \frac{9T}{5}\,0.0062} \quad (9)$$

where T is temperature in °C. The resulting calculated optimal F^- concentration in drinking water for large towns in the field area is shown in Table 2.8. There is a small variation of 0.07 mg/ℓ F^- about the mean of 0.65 mg/ℓ F^-, over the range of mean maximum temperatures experienced in the study area. All of the values are similar to the maximum safe concentration of 0.7 mg/ℓ F^- calculated by Du Plessis (1995) for the Orange Free State gold fields.

Table 2.8 Optimal F^- concentration in groundwater, calculated using the equation of Foss and Pittman (1986). Raw data obtained from the Weather Bureau, Pretoria. Latitude and longitude are in decimal degrees. 'mamsl' = meters above mean sea level.

Location	Lat. S.	long. E.	Elevation (mamsl)	Mean Maximum temp. (°C)	Optimum F^- level (mg/ℓ)
Rustenburg	25.72	27.30	1157	26.5	0.64
Buffelspoort	25.75	27.48	1230	26.2	0.64
Brits	25.58	27.77	1107	26.9	0.63
Pretoria	25.73	28.18	1330	24.8	0.66
Waterkloof	25.83	28.22	1498	23.3	0.68
Irene	25.92	28.27	1524	23.7	0.68
Lindleyspoort	25.48	26.70	1175	26.0	0.65
Pilanesberg	25.33	27.17	1043	27.9	0.62
Funda Muni	25.42	28.87	1407	23.9	0.68
Thabazimbi	24.58	27.42	970	27.9	0.62
Warmbaths	24.90	28.33	1143	26.7	0.64
Sentrum	24.27	27.35	1005	28.5	0.61
Potgietersrus	24.18	29.02	1116	26.3	0.64
			Mean:	26.0	0.65

3 METHODOLOGY

This chapter describes the methods used in sampling, preparation and analysis of water, rock and soil samples.

3.1 Groundwater

This section described the methodology used for sampling of groundwater, analysis in the field, preparation for analysis in the laboratory and analysis for major ions and isotopes.

3.1.1 Sampling and field tests

Groundwater sampling took place during July and September 1993 and in October 1994. Sample locations were selected primarily to give an even distribution over the field area and secondly to fill in spatial gaps in the existing Bophuthatswana groundwater database. This effectively meant sampling took place in agricultural areas rather than villages.

Sampling protocol. A protocol for water sampling was formulated before fieldwork commenced and was adhered to as much as possible. The sampling protocol comprised the following steps:

1) Check that water can be obtained from the borehole (wind is blowing, machinery in working order and permission has been obtained from farmer, owner or local chief).
2) Note the date, time, type and state of equipment, size and state of the borehole apron, possible sources of contamination (e.g. kraals, pit latrines, industries, dams, oil soaks), topographic setting, surrounding rocks/soil type and (if available) depth of borehole and water level.
3) If the borehole has been frequently used recently (i.e. wind has been blowing for several days or a frequently used village handpump) take the samples immediately. If it is not frequently used, pump until no change in emerging water temperature and colour occurs.
4) Carry out the field tests (see below).
5) Rinse the 'trace metal' and 'major ion' sample bottles with groundwater. Filter approximately 400 ml of groundwater, using 0.45 μm Teflon filter papers. Although

Teflon is a fluorinated compound, its extreme inertness ensured that no contamination of the samples took place. Fill 2×100 ml 'major ion' bottles with unfiltered sample and 2×100 ml 'trace element' bottles with filtered sample. Where bacterial contamination is suspected, or when cloudy or coloured samples are obtained, filter the sample for the 'major ion' bottles.

6) Add 5 drops of 1 M nitric acid to the 'trace element' bottles. Check with universal indicator paper that the pH is below 2; if not add another 5 drops of acid and repeat. Seal the tops tightly.
7) Mark the site and sample number with an indelible marking pen on the top and the sides of the bottles. Note in the field notebook the sample and site number, whilst marking the site number on the 1:50000 map.
8) Pack all equipment securely. Scan the site for any equipment and rubbish.

The samples were stored in the dark and at approximately 4°C whenever possible, but the large number of samples and duplicates meant that not all bottles could be accommodated in refrigerated storage. Visual inspection at the time of major ion analysis at the University of Cape Town showed that almost all of the samples were identical in appearance to the original: no precipitation of minerals or growth of bacteria or algae had taken place. Sample site details are shown in Appendix A1.

Radiocarbon sampling. Radiocarbon sampling entailed directing 150 to 200 ℓ of groundwater sample into a stout plastic bag. With phenolphthalein solution as an indicator, a pH greater than 9 was maintained using sodium hydroxide solution. The dissolved carbonate (and in some cases, sulphate) species were precipitated by adding 500 mℓ barium chloride solution. This amount generally ensures complete precipitation of dissolved carbonate and sulphate. The precipitate was harvested from the plastic bag into 2ℓ plastic containers with tightly sealed tops (McCaffrey, 1993).

Field tests. Groundwater was analysed in the field for pH, electrical conductivity (EC) and dissolved oxygen (DO) by means of a Corning 'general purpose combination electrode', 'conductivity/TDS sensor' and 'DO sensor' probes, respectively, connected to a Ciba-Corning 'Checkmate 90' portable millivoltmeter. Standards used were Ciba-Corning pH buffers at 4.00, 7.00 and 10.01; Corning 12.88 ms conductivity standard; and Ciba-Corning zero oxygen solution. Each day the pH probe was recalibrated using a 2 point calibration, the DO meter was calibrated whenever near fresh water, and the EC probe was recalibrated each morning.

To measure pH, EC and DO, a 50 ml beaker was rinsed first with deionised water, rinsed with groundwater, then filled with 50 ml of groundwater. The analysis of pH was indicated to the nearest 0.01 by the digital meter, and drift in the analysis of standards was less than 0.1 per day, making the measurement of pH reproducible and accurate. Groundwater was prepared for temperature measurement by filling a 50 ml glass beaker full of fresh, unfiltered ground water, allowing the glass of the beaker and thermometer to equilibrate to the water temperature, then refilling with fresh groundwater and quickly measuring temperature, all out of direct sunlight. To measure total alkalinity, two drops of screened methyl orange indicator were added to 50 ml of groundwater in a conical flask. The mixture was then titrated to the green/purple colour change using an automatic levelling pipette filled with 0.1 M HCL. Fluoride in each of the water samples was measured each evening at the field base (see next section).

3.1.2 Sample preparation and analysis

Major Ions. High pressure ion chromatography (HPIC) was used to determine the concentration of major ions in the groundwater samples. Samples with a high EC, as determined from field measurements, were diluted so that the EC was reduced to less than 200 mS/m. This prevented overloading of the separator column and conductivity detector. Highly coloured samples were passed through a Dionex® 'Onguard P' filter to remove organic acids which might degrade the column.

Tables 3.1 and 3.2 show the experimental conditions used for anion and cation analysis, respectively. A Dionex® DX300 ion chromatography system controlled by AI-450 software was used. The analytical column used for the majority of anion analyses was the Dionex® AS4A separator column, replaced on occasion by an AS11 column and finally replaced by an AS4AC column.

Fluoride ion selective electrode. A Total Ionic Strength Adjustment Buffer (TISAB) was used to bring all samples to approximately the same ionic strength and pH (Frant and Ross, 1966; Harwood, 1969; Campbell, 1987; APHA, 1995). The TISAB used in the field contained 1 g/ℓ CDTA (1,2,Cyclohexylene Dinitrilo Tetraacetic Acid, known commercially as Titriplex IV) as a chelating agent to break up aluminium fluoride complexes (Harwood, 1969). In later experiments CDTA was omitted from the TISAB in order to gauge its effect (discussed in a later section). The other components of the TISAB were 58.5 g NaCl, 15 mℓ glacial acetic acid and 66 g sodium acetate, made up to 1 ℓ with distilled water.

Table 3.1 Experimental conditions used in the determination of anions (F^-, Cl^-, NO_3^-, PO_4^{3-} and SO_4^{2-}). ASRS = Anion Self Regenerating Suppressor. Waters HPLC instrumentation was used by the South African Institute of Medical Research.

Instrument	Dionex® DX300 HPIC			Waters HPLC
Experimental conditions\Method	Sodium Tetraborate	Sodium carbonate/ bicarbonate	Sodium Hydroxide	
Eluent 1 (and 3 for sodium tetraborate method)	5.0 mM $Na_2B_4O_7$ 2 minutes, 5 minutes	1.7 mM $NaCO_3$ 1.8 Mm $NaHCO_3$	21 Mm NaOH	4 Mm potassium hydrogen phthalate
Eluent 2	50 mM $Na_2B_4O_7$ 3 minutes	none	none	none
Column	AS4A	AS4A*	AS11	IC-pak A
Flow rate (ml/min)	1.0	2.0	1.0	2.0
Detector	Conductivity	Conductivity	Conductivity	Electrochemical
Suppressor	ASRS	ASRS	ASRS	none
Run Time (mins)	10	7	7	15
Sample Loop Volume (µl)	50	50	50	100
Best For:	Accurate fluoride analysis	Routine analysis of major anions	fast analysis of major anions in low carbonate samples	Analysis for iodide

* Replaced in later analyses by an AS4A-SC column

Groundwater F^- concentrations were measured every evening at the base camp, where a rudimentary laboratory was established. A Corning fluoride ion selective electrode (FISE) was used (Frant and Ross, 1966), connected to a Corning 'Ion Analyser 255' digital millivoltmeter. Fluoride was subsequently remeasured at UCT using TISAB with and without CDTA.

Trace elements. Trace element analysis was performed by Dr. A Bartha at the Geological Survey of Bophuthatswana using a Varian Liberty 200 inductively coupled plasma - atomic emission spectrometer (ICP-AES). Standards with concentrations of 0.2, 0.5 and 1.0 mg/ℓ were used for all elements analysed (Ni, Li, Mo, Al, Zn, Ba, V, Cr, Cu, Pb, Co, Cd and Sr). The results were processed by the WATERTRACE programme.

Iodide. A 5 ml subsample of the acidified water sample was put into sample-rinsed plastic 5 ml phials and sent to the South African Institute for Medical Research (SAIMR) for analysis. Analysis for iodide was conducted using a Waters High Performance Liquid

Chromatograph with a Ag electrode detector. A standard stock solution of 1000 ppm I^- was prepared by dissolving 0.118 ±0.001 g NaI in 100 ml >18MΩ Milli-Q water.

Table 3.2 Experimental conditions used in the determination of cations (Ca^{2+}, Na^+, Mg^{2+} and K^+). CSRS = Cation Self Regenerating Suppressor, MSA = Methyl Sulphonic Acid.

Experimental conditions	Method A	Method B
Eluent	20 mM MSA	22 mM MSA
Column	CS12	CS12A
Flow rate (ml/min)	1	1
Detector	Conductivity	Conductivity
Suppressor	CSRS	CSRS
Run time (mins)	15	14
Sample loop volume (µl)	25	25

Stable isotopes. Preparation took place in the stable isotope laboratory at UCT, supervised by Dr. Chris Harris. The preparation technique used for O was that of Socki *et al.* (1992). Approximately 1.5 ml of sample was frozen into a pre-evacuated glass phial and the phial was re-evacuated. The phial was then filled with 0.5 atmospheres of CO_2 and put into a water bath at 25°C for 4 hours to allow equilibration between O in the CO_2 and H_2O. The CO_2 was then sub-sampled into a break-seal glass tube. Hydrogen was obtained by reduction of 1 µl of water sample by Zn at 450°C for 30 minutes, and the resulting H_2 sealed in a break-seal glass tube.

Analysis took place on a VG 602E gas-source mass spectrometer. The external standards used in the analysis were provided by Dr T. Venneman of the University of Michigan, and were deionised water and snow from Michigan.

Radiocarbon. Preparation took place in the Schonland Nuclear Research Centre at the University of the Witwatersrand under the supervision of Professor Balt Verhagen. The precipitate collected in the field had to be converted to ethane, which is easily ionised in the detectors. The $BaCO_3$ in the precipitate was first converted to CO_2 using orthophosphoric acid. The gas was then converted to acetylene using lithium at 600°C. Acetylene was catalysed to ethane by palladium metal and stored in large glass bulbs for analysis.

A gas-proportional scintillation detector was used to analyse for radiocarbon. Measurement of each sample took place on three occasions separated by approximately a

week, to differentiate between disintegrations due to radiocarbon and those due to radon, which have the same energies. Since radon has a much shorter half life than radiocarbon, the radon content is that part of the scintillation count which measurably reduces over a month or two and can therefore be corrected for. Standards were radiocarbon-free groundwater from dolomites in the Pretoria area.

Strontium isotopes. All preparation took place in the clean laboratory of the Radiogenic Isotope Facility at the University of Cape Town, and was performed by Justin Underwood. The cations in the samples were converted to chloride salts by repeated drying and dilution with 5 ml of 6.2N HCl. The dry residue was dissolved in 0.7 ml of 2.5N HCl and centrifuged to remove insoluble matter. Strontium was separated from other cations by ion chromatography. The separation of Sr from other cations had been calibrated using chloride salts. The resulting Sr chloride solution was converted to a nitrate solution by repeated drying and addition of 7M nitric acid. The solution was finally diluted with 0.5N phosphoric acid and 2% nitric acid and evaporated onto a tantalum filament.

The isotopes of strontium were analysed using a VG Sector solid-source mass spectrometer run in dynamic multi-collector mode. The standard used was NBS 987 strontium carbonate, normalised to 0.71022. The measured $^{87}Sr/^{86}Sr$ values were normalised to $^{88}Sr/^{86}Sr = 0.1194$ to correct for mass fractionation.

3.2 Rock and soil

This section deals with the solid materials studied during the project. It describes the methodology used for the sampling of rock and soil and the preparation of these samples. It describes the analysis of major and trace elements; the methods used for mineral identification and analysis of mineral composition; and the analysis of stable and radioactive isotopes in solid samples.

3.2.1 Sampling

Rock and soil sampling took place during June 1994. The objective was to obtain at least three samples of each major rock type and associated soil in the area to provide an indication of the variability of the lithology and geochemistry of each rock and soil type. Rock and soil samples were taken in pairs, with the samples usually located not more than 10 m from each other. Whenever possible, sampling was performed at road-cut profiles, so that soil directly overlying fresh rock could be taken. More often the soil sample was taken

in the vicinity of a fresh rock outcrop. At least 1 kg of rock sample was taken, and up to 5 kg when the rock was coarse grained. The rocks were broken into pieces with their long axes not greater than 20 cm and with all weathered surfaces trimmed off.

Soils were sampled from the top 20 cm either by spade or hand-held auger. No attempt was made to sample vertically. The rationale for taking a sample from the surface was that it would be the most easily accessible and the driest part of the soil. The disadvantage of taking a topsoil sample was that it is this part of the soil which is often subjected to transport and input of anthropogenic and aeolian material (Schloemann, 1995). Forty two rock samples and 40 soil samples were obtained by this method. Difficulties were encountered in sampling Karoo Sequence rocks, since they produce a flat relief with few rock outcrops. Only two samples were collected from the Karoo Sequence. Sample site details are shown in Appendix A2.

3.2.2 Sample preparation

Drying. The samples were taken in the middle of the Transvaal winter (the dry season), in the heat of the day, and were therefore thoroughly dry; no artificial drying took place before crushing. Samples were kept tightly sealed in plastic bags in Cape Town to prevent contamination by airborne salt particles.

Crushing and milling. Rock samples were first split into sub 2 cm chips using a hydraulic splitter, then crushed to sub 5 mm chips in a jaw crusher (Mn-steel ribbed plates). Soil samples were generally fine grained and when pebbles were present, they were broken into sub 5 mm pieces using a geological hammer. Both rock and soil samples were then milled for 3 minutes at high speed in either a carbon steel or Ni-Cr alloy Seibtechnik® swing mill. This should have reduced all grains to less than 50 μm diameter. Problems were experienced with the milling of soil from sites 7 and 9, both of which are examples of 'black turf', the local name for the black soil derived from the weathering of pyroxenite and norite. The plastic nature of these soils caused the mill to smear the material onto the side wall, rather than to disaggregate it. The samples were therefore disaggregated manually with a geological hammer, left to dry further for two years and then milled.

XRF briquettes. For trace element analysis using X-ray fluorescence spectrometry, 6 g of the powdered sample were pressed into a 30 mm diameter granular-H_3BO_3-backed briquette using a hydraulic ram. For sandy samples, which tended to disintegrate under vacuum, 5 drops of a 2% Mowiol solution were added as a binder. The mowiol was mixed thoroughly with the sample powder using an agate mortar and pestle. All briquettes were placed under vacuum for at least an hour to both degas them and to induce failure in a bell

jar rather than inside the XRF spectrometer. The soil briquettes were observed to be generally more water absorbent than the rock briquettes, as shown by the longer times taken for the vacuum in the spectrometer to reach the specified level.

XRF fusion disks. Fusion disks were prepared according to the method of Norrish and Hutton (1969). Two grammes of the sample powder were weighed out accurately to 5 decimal places into a clean platinum crucible. To determine loss of water (H_2O^-), the sample was dried at 110°C for at least 4 hours, cooled and then reweighed. To determine the combined water, CO_2 and organic material loss on ignition (LOI), the crucible was then put into a furnace at 850°C overnight, cooled and the mass recorded. Other preparation schemes undertake the latter step at 950°C or 1000°C, but because several samples were syenitic with large amounts of fluorine, it was decided to roast all samples at temperatures below the melting point of these rocks.

Duplicate fusion disks were made by mixing 0.28 g (±0.002 g) of sample with 1.5 g (±0.02 g) Johnson Matthey 105 flux and 0.02 g $NaNO_3$. The mixture was fused for approximately 10 minutes and thoroughly mixed in a platinum crucible before being poured onto a heated graphite mould and stamped flat with an aluminium plunger heated to the same temperature as the mould. Only sample RO19 required an extra long period of fusion.

XRD. An excess of the −50 μm powdered sample was loaded onto an indented aluminium holder and pressed into place with a spatula. The excess was removed using the edge of the spatula, so that the powder surface was level with that of the holder.

Electron microprobe. The rock was cut into slices and polished thin sections prepared, then washed in soapy water, deionised water, and acetone, and air dried. Minerals of interest were identified using a petrographic microscope and were circled with a technical drawing pen. A sketch of each section was made, identifying mineral locations. The section was then coated with carbon in an electric arc coater and mounted in a conducting frame for analysis.

Stable isotopes. Carbon and oxygen isotope ratio analyses of the bulk carbonate were made using the method of McCrea (1950). Powdered samples were reacted with orthophosphoric acid at 50°C overnight and a value of $\alpha_{CO_2\text{-calcite}}$ of 1.009 was assumed (Al-Aasm *et al.*, 1990). The value of $\alpha_{CO_2\text{-strontianite}}$ would be expected to be similar to that for $\alpha_{CO_2\text{-calcite}}$, given the closeness of the $10^3 \ln\alpha$ *vs.* temperature curves for the two minerals in equilibrium with water (Friedman and O'Neil, 1977: Figure 13). An internal standard (Namaqualand Marble) was used to normalise the data to the V-SMOW and V-PDB scales (Coplen, 1995).

3.2.3 Analysis

X-Ray Fluorescence Spectrometry (XRFS). Major (SiO_2, TiO_2, Al_2O_3, Fe_2O_3, MnO, MgO, CaO, K_2O, P_2O_5 on fusion disks) and Na_2O, F and trace (Mo, Nb, Zr, Y, Sr, U, Rb, Th and Pb on powder briquettes) element concentrations were measured using a Siemens SRS303AS XRF spectrometer. Standard instrumental conditions (Duncan *et al.*, 1984; Willis, 1995) and in-house and certified reference materials were used for calibration. A special fusion disk with 6% SrO was prepared, using $SrCO_3$, NIM-G and the method outline above, for the analysis of the high Sr samples.

X-Ray Diffraction (XRD). Mineral phases were qualitatively determined using a Philips PW1130/90 X-ray diffractometer using CuKα radiation, a LiF (200) monochromator, a NaI scintillation counter, pulse height selector and generator settings at 25 kV and 40 mA. The JCPDS PDF-2 computer database was used to identify mineral phases based on d-values and relative peak intensities.

Carbonate "Bombe". The equivalent CO_2 content of several samples was determined using the "Karbonat Bombe" method of Birch (1981). Concentrated hydrochloric acid was added to a powdered rock sample in an airtight container, liberating CO_2 from the carbonate minerals. The resultant CO_2 pressure, measured within 1 minute of the addition of acid, is proportional to the $CaCO_3$ and $SrCO_3$ content of the sample. Dolomite, $(Ca,Mg)CO_3$, reacts more slowly and does not contribute significantly to the initial pressure increase.

Gas-source Mass Spectrometer. Two different mass spectrometers were used for stable isotope analysis: a VG602E mass spectrometer with dual inlet and double collectors; and a Finnigan Mat 252 multi-collector instrument.

Solid-Source Mass Spectrometer. The instrumentation used for Sr isotope analysis was a VG Sector 7-collector thermal-ionisation mass spectrometer, at the Radiogenic Isotope Facility at the University of Cape Town, operated by Dr Steve Richardson and Justin Underwood. Two hundred ratios were measured per bead (*i.e.* per sample) and approximately 170 ratios were accepted for calculating final Sr isotope ratios.

Electron microprobe. Analysis of mineral phases was undertaken using a Cameca Camebax Microbeam electron microprobe. Carbonate minerals were analysed according to the parameters of Lane and Dalton (1994), with an accelerating voltage of 15 kV and a final beam current of 14 nA and a beam diameter of 10 μm. Silicate minerals were analysed using the same accelerating voltage, but with a beam current of 40 nA and a beam diameter of 1-2 μm. Data from both mineral types were reduced using ZAF correction.

3.3 Leaching experiments

The solubility of fluoride bearing phases in rock and soil samples from the field area was investigated using leaching experiments. Many different methods for leaching soil have been proposed and there is no widely accepted standard method. Various soil leaching techniques were evaluated by Schloemann (1995); all techniques have advantages and disadvantages associated with them and it is apparent that no technique is universally optimal (Table 3.3). For this reason it was decided not to mimic previous experimental conditions, but rather to optimise the conditions for the current set of sample compositions, methods of analysis and detection limits.

Table 3.3 Comparison of sample preparation techniques prior to the extraction of elements from soil samples (modified after Schloemann, 1995).

	Method 1 Sieved soil, coarse fraction discarded	**Method 2** Sieved soil, coarse fraction crushed to -2 mm	**Method 3** Untreated soil	**Method 4** Powdered soil (this study)
Comparison with literature	good	reasonable	impossible	impossible
Comparison with whole-soil analysis	limited	good	good	good
Pretreatment time	little	long	none	none for this study
Representative sub-sampling	possible	difficult to possible	difficult to impossible	easy
Increases relative surface area	limited	yes	no	yes
Simulation of *in situ* conditions	limited	reasonable to limited	reasonable	limited

The *maximum* concentration of fluoride soluble by natural water from rock and soil was of prime interest. Powders of rock and soil had already been prepared for XRF analysis and so it was decided to use these powders as the raw material for the experiment. Because the powders have been milled to nominally the same grain size (-50 microns), it was possible to add constant volumes of leachate and be able to assume a constant surface-area to leachate-volume ratio. This is the assumption in 'saturated paste' leaching experiments. A suitable mass of sample (10 g ±0.1 g) was chosen to fit into the 125 ml plastic bottles in

which the experiment was carried out. It was decided that a 1:2 ratio of sample to leachate was optimal. A lesser ratio would mean that although fluoride concentrations might be higher, lengthy vacuum filtering of the sample would be needed to achieve conveniently sized samples for analysis. A higher ratio would entail lower concentrations of fluoride and more samples below the detection limit. The volume of leachate (20 ml ±0.05 ml) was added to the sample using a digital burette. This volume of leachate gave a convenient volume (between 5 and 15 ml) for analysis after filtration.

Selection of the leachate composition was of importance. Since the leaching experiment was an attempt to *broadly* simulate natural conditions, an 'artificial rainwater' leachate was used. Two litres of deionised water were left to equilibrate with the atmosphere for 24 hours at approximately 20°C in a beaker covered with perforated polyethylene film on a shaking-table, becoming weak carbonic acid through the dissolution of atmospheric carbon dioxide. The duration of the leaching experiment was set at 96 hours, which, although not allowing for full equilibrium dissolution (Brown and Robertson, 1977), would allow the dissolution of soluble and sparingly soluble phases.

The sample containers were shaken continuously along their long axes on a shaking table to facilitate mixing of solid and leachate. The experiment was performed at room temperature (approximately 22°C). After 96 hours the samples were allowed to settle for 2 hours, the supernatant liquid was filtered through 'Whatman qualitative medium crystalline' filter paper, then centrifuged for 20 minutes at 3000 revolutions per minute, corked and stored upright. Analysis for fluoride using a FISE took place within 4 hours of the end of the leaching period.

A pilot experiment was undertaken with a variety of soils with high- to low-fluorine concentrations as determined by XRFS. The experimental conditions were as detailed above, apart from the sample to leachate ratio, which was 1:1, and the duration of leaching, which was 48 hours. The results are shown in Table 3.4 and indicated that even samples with very low total fluorine concentrations would yield a fluoride concentration in leachate above the detection limit when using the experimental conditions detailed above.

Table 3.4 Results of a pilot experiment showing feasibility of the experimental conditions for rock and soil leaching experiments. The blank was conducted under identical conditions but used pure crushed quartz.

Sample No.	SO3	SO8	SO20	SO2	Blank
Lithology	Foyaite	Granophyre	Granite	Norite	Quartz
Total F (ppm)	2340	1130	177	<62	<62
Leachate pH	6.67	7.32	7.28	7.24	6.23
Leachate F^- (mg/ℓ)	0.51	1.03	0.15	0.07	0.06

3.4 Data quality

This section contains a discussion of the quality of the analytical data for groundwater, rock and soils, and of the spatial quality of the data.

3.4.1 Groundwater data quality

Fluoride Ion Selective Electrode. Frant and Ross (1966) proposed the use of an ion selective electrode to measure fluoride activity in solution. The use of a total ionic strength adjustment buffer (TISAB) brings all solutions to approximately the same ionic strength and pH (≈5.5) and is intended to break up aluminium-fluoride complexes which might otherwise reduce the fluoride activity. The addition of CDTA to TISAB was proposed by Harwood (1969) as an effective de-complexing agent. Warner (1971) demonstrated the use of FISE in a variety of natural waters, some with high concentrations of metals. Nicholson and Pasquier (1993) and Pakalns and Farrar (1976) have studied the effects of organic acids, iron and surfactants on the effectiveness of the FISE method. These substances are fortunately not present in significant quantities in the groundwater of the area.

When using standards of 1.0 and 0.5 mg/ℓ, the accuracy at a nominal concentration of 0.25 mg/ℓ is 0.4% relative, whilst at 0.1 mg/ℓ it is about 20% relative (Figure 3.1). Precision is approximately 1%, and the error bars are too small to be shown in Figure 3.1. In the field the lowest routinely used standard was 0.1 mg/ℓ, implying that the detection limit in the field was in the vicinity of 0.05 mg/ℓ. Other studies (Barnard and Nordstrom, 1982a) have shown that under ideal circumstances the lower limit of detection (LLD) for the FISE is between 0.3 and 1 µg/ℓ. Such low LLDs have little relevance in this study.

Fluoride was measured in fifty acid-preserved samples using FISE with CDTA in the TISAB and without. The results are shown in Figure 3.2. It can be seen that the results are

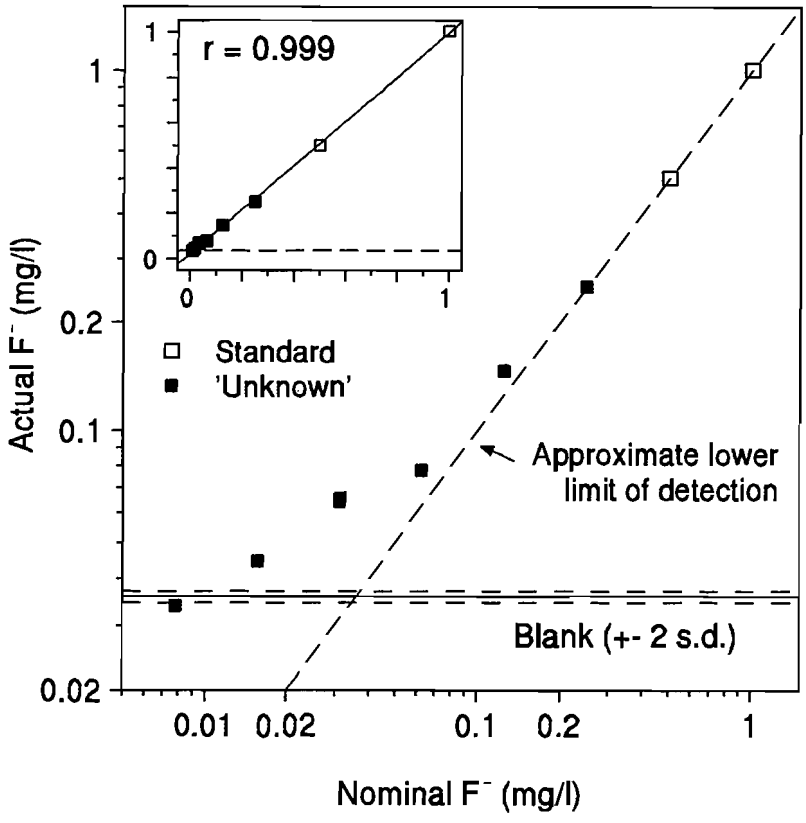

Figure 3.1 Accuracy and precision of FISE using standards at 1.0 and 0.5 mg/l. Instrumental precision error bars are smaller than the markers.

in excellent agreement, although at higher concentrations (~>0.3 mg/ℓ) a consistently higher value of F^- was obtained using CDTA. When the differences between the two analyses are plotted against Al concentrations, however, many of the samples with significant differences have very low Al concentrations (Figure 3.3). There is no correlation between Al concentration and F^- difference. The difference in F determination can therefore not be attributed to differing Al concentrations in these samples.

Al solubility increases at high and low pH levels, and is lowest near pH 5 and 8 (Mason and Moore, 1966). Since this subset of samples was acidified *after* filtration, Al concentration could not have been increased by solution of suspended aluminium-containing sediment. Groundwaters in the field area have a near-neutral pH and so are unlikely to have high Al concentrations. This implies that Al complexation is unimportant in the determination of unacidified samples with an original pH close to 7.

High pressure ion-chromatography. High pressure ion-chromatography (HPIC) has been used extensively in this project for the routine determination of major anions and cations. A sample chromatograph for anions is shown in Figure 3.4, using an AS4A analytical column. It can be seen that when a sodium carbonate-bicarbonate eluent is used, the chloride peak is invariably well defined and chloride concentration is easily determined.

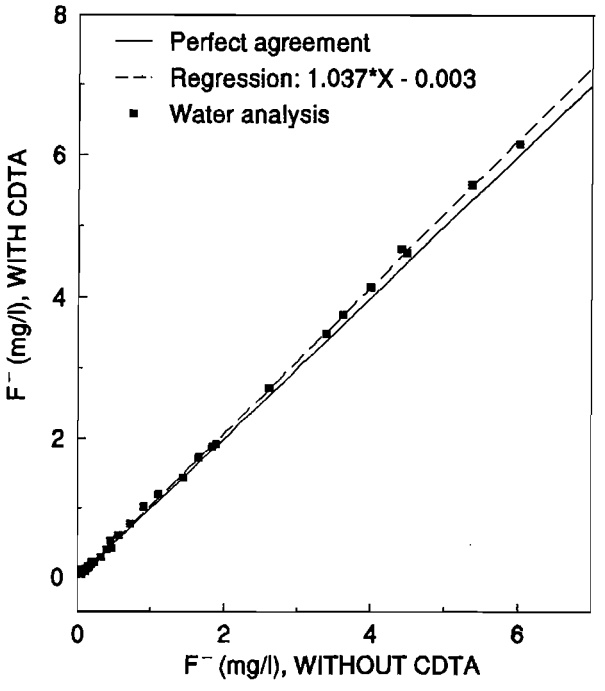

Figure 3.2 Fluoride concentration determined by ion selective electrode, using TISAB with and without CDTA.

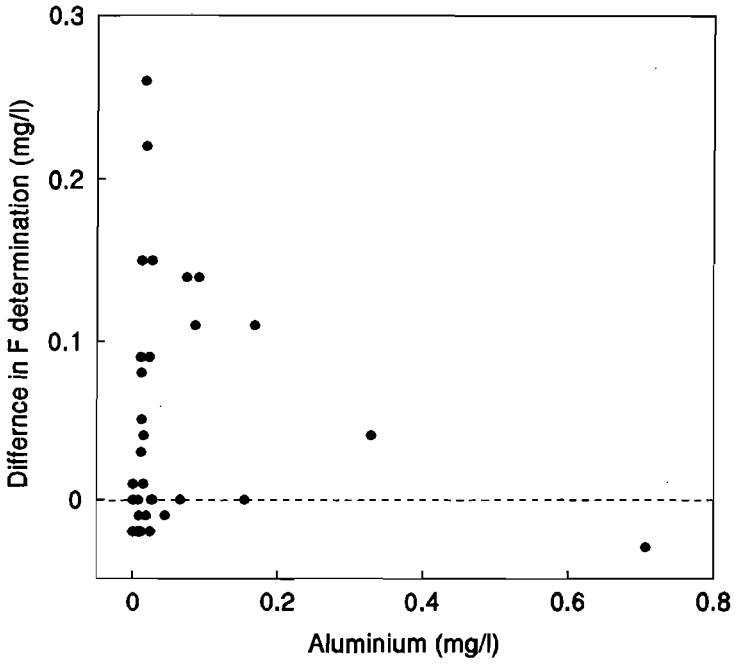

Figure 3.3 Difference in fluoride determination when using a buffer with and without CDTA on samples with differing Al concentrations.

Nitrate and nitrite are also resolved with sharp peaks. Phosphate occurred in concentrations generally lower than the detection limit. Sulphate was very well resolved, but suffered somewhat from peak broadening. Iodide and bromide occur at very low levels in most of

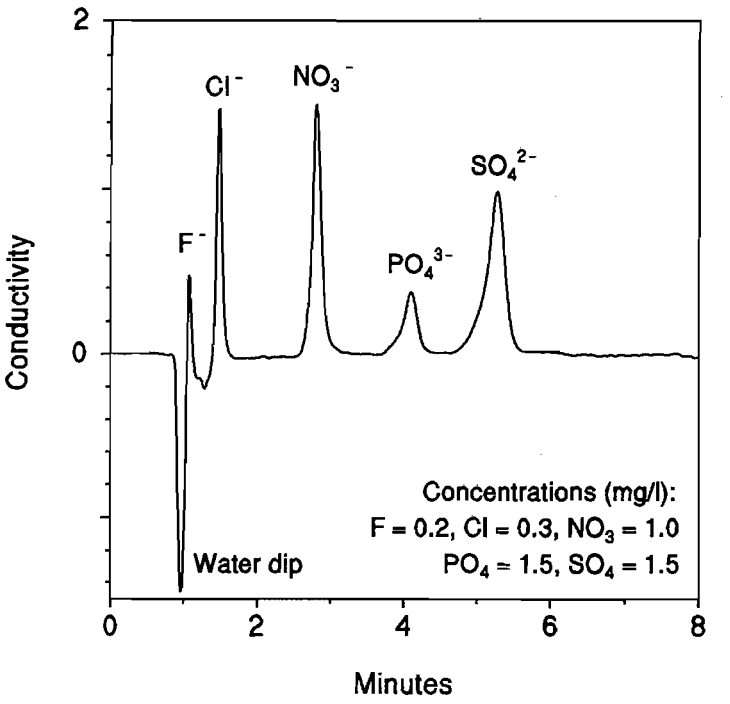

Figure 3.4 A sample chromatograph using sodium carbonate and bicarbonate eluent and the AS4A separator column, showing excellent resolution. However, note the proximity of the water dip to the fluoride peak.

the samples. The bromide peak was generally sharp and eluted just before NO_3^-. Iodine elutes as a broad peak after sulphate and was generally below the background variation of the baseline. It was found that, under the operating conditions recommended by the manufacturers, the AS11 separator column suffered from bunching of analytes, reduced peak definition, as well as a severe interference from carbonate.

Consistent differences in the determination of fluoride in groundwater from HPIC and FISE have been reported by some laboratories and so an investigation was undertaken to compare the results of the two methods (McCaffrey, 1994). The results of the two techniques for all water samples collected in this study are shown in Figure 3.5. It can be seen that HPIC using a carbonate/bicarbonate eluent often over-estimates the concentration of fluoride relative to FISE.

Different standards were used for HPIC and FISE. However, when the HPIC standard was analysed by FISE, the measured value was identical to the given value to within 1% relative. No normalisation has therefore been applied. The presence of a water dip in the carbonate/bicarbonate chromatogram generally complicates the process of determining a baseline for the fluoride peak and is the probable cause of the overestimation of F^-.

The use of sodium tetraborate eluent greatly improves the relationship of HPIC to the FISE determination of F^- (Figure 3.6), and so samples with inaccurate results using the

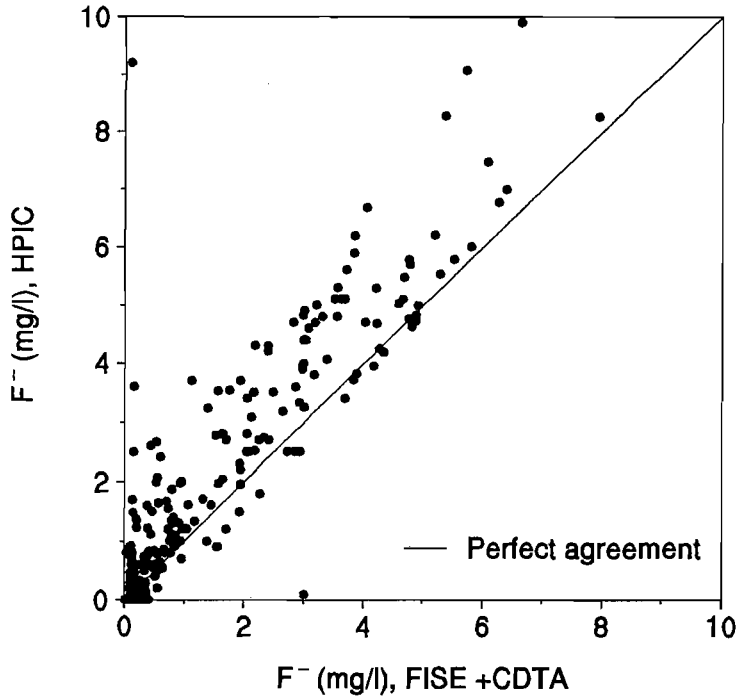

Figure 3.5 Fluoride determinations on the same samples by high pressure ion chromatography and ion selective electrode. HPIC determinations generally yield high F^- concentrations.

carbonate/bicarbonate eluent were reanalysed using sodium tetraborate as the eluent. Fluoride elutes well away from the water dip and all other major anions (Figure 3.7). The baseline is even and easy to determine either manually or automatically. Acetate does give a minor interference, but its concentration in natural waters is very low and it is therefore not considered a serious problem (Figure 3.8). The use of sodium tetraborate as an eluent gives an accurate and precise determination of fluoride in solution but is rather slow and other anions cannot be determined in the same run.

Towards the end of this project, an alternative analytical column became available, namely the 'Star-Ion' column supplied by Phenomenex™. Although the column does not separate Cl^- from the later anions as successfully as the Dionex AS4A column, it has a greater separation between the water dip and the fluoride peak (Figure 3.9), allowing better quantification of the fluoride peak. Running parameters are identical to the AS4A column.

Overall quality of water analyses. Since water samples are electrically neutral, total charges on cations and anions should be equivalent. The ion balance error for all samples

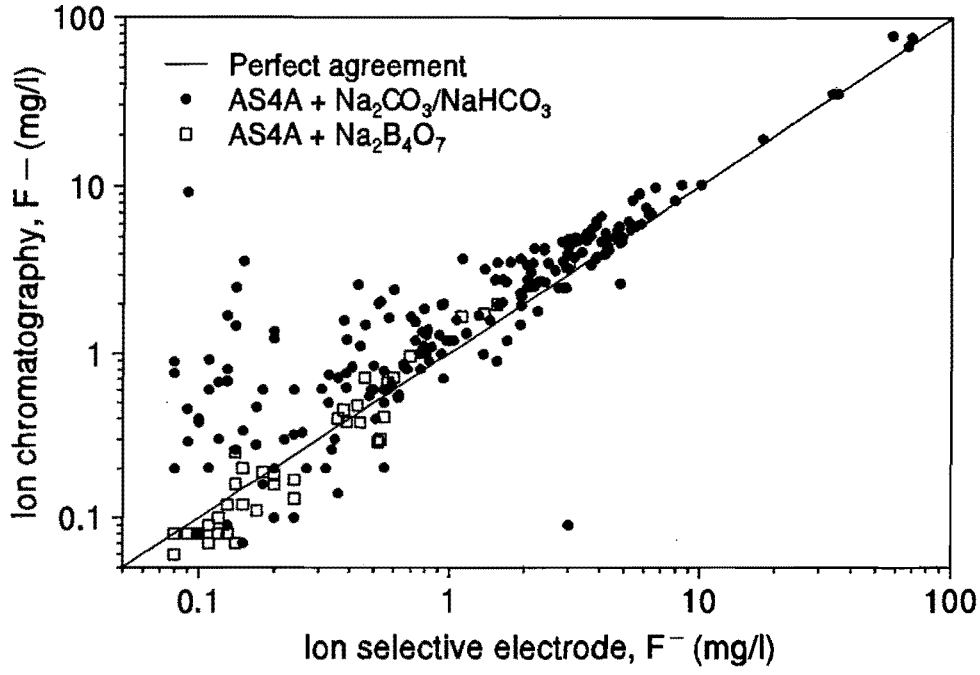

Figure 3.6 Improvement in fluoride determination when using $Na_2B_4O_7$ as an eluent.

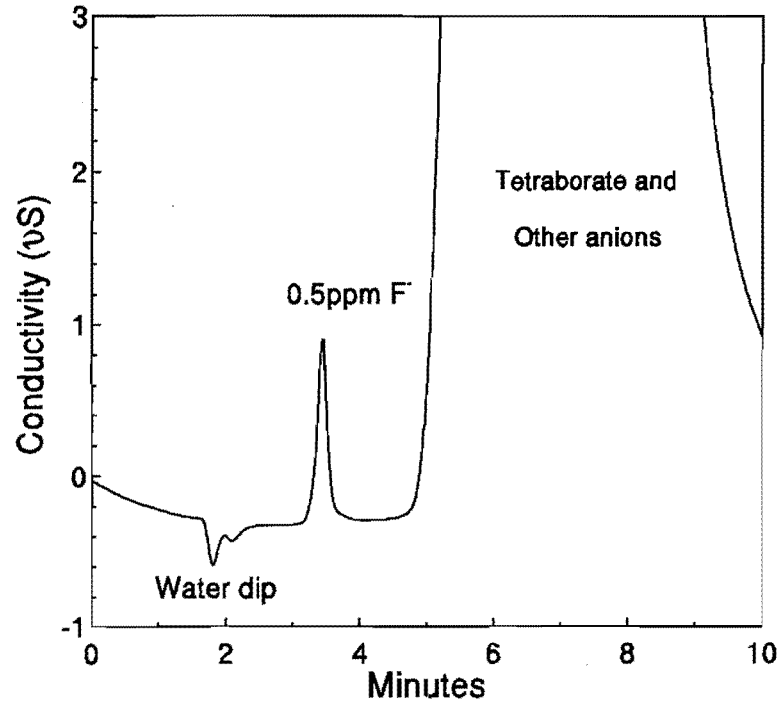

Figure 3.7 Determination of fluoride using sodium tetraborate as the eluent and the AS4A separator column. Note that the water dip and fluoride peak are well separated. Experimental conditions are shown in Table 2.1.

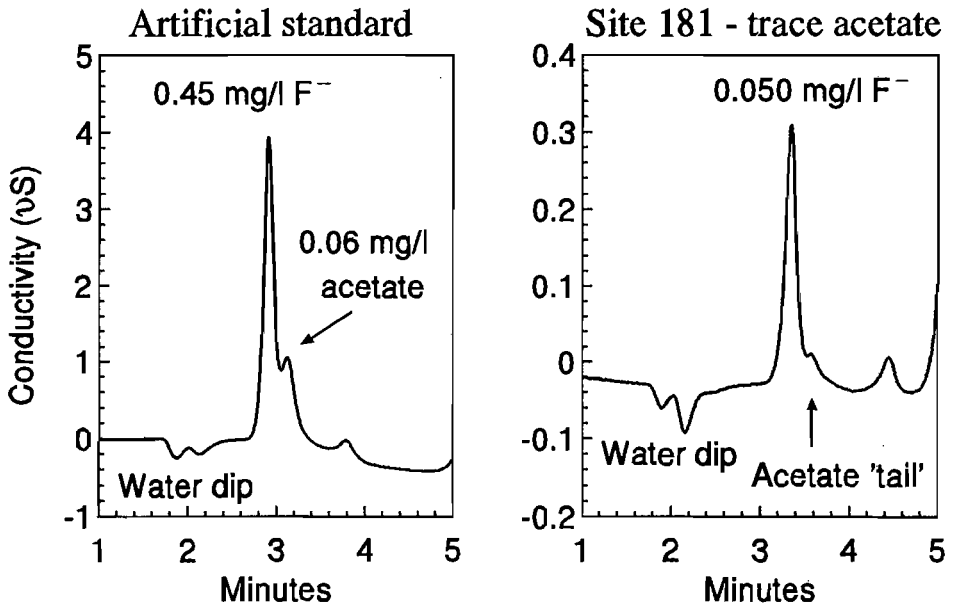

Figure 3.8 Chromatograms showing interference with the fluoride peak by acetate in an artificial solution and an actual sample. Experimental conditions are given in Table 2.1.

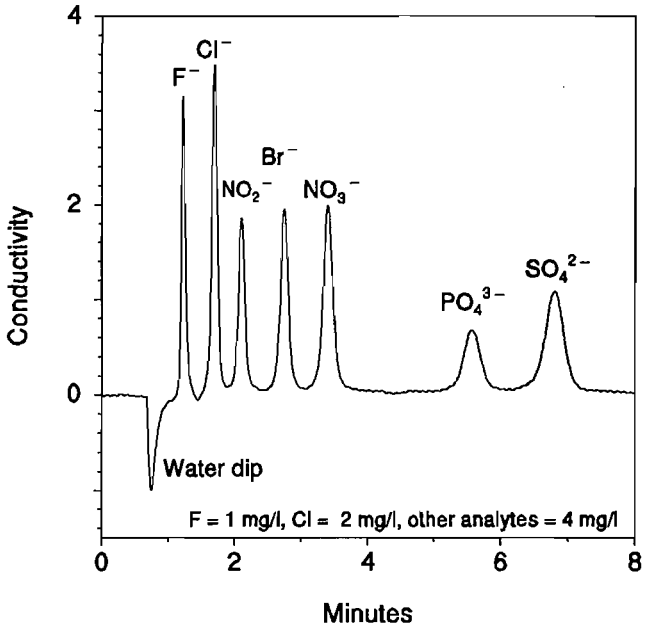

Figure 3.9 Sample chromatogram using a Star-ion analytical column and operating conditions identical to those used for the Dionex AS4A. Note the separation of the water dip and fluoride peak. Compare with Figure 3.4.

used in this study has been calculated using the equation of Lloyd and Heathcote (1985):

$$Ion\ balance = \frac{\Sigma cations - \Sigma anions}{\Sigma cations + \Sigma anions} \times 100\ per\ cent$$

where cations and anions are expressed as milliequivalents. Since all major ions have been determined for the majority of samples, ion balance error cannot be attributed to missing analytes. The practice of calculating a concentration for an unanalysed ion by reducing the ion balance error to zero has generally not been employed in this thesis. However, samples 230 and 231 do not have a measured total alkalinity due to difficulties in the field, and a zero ion balance error has been used to estimate total alkalinity in these samples.

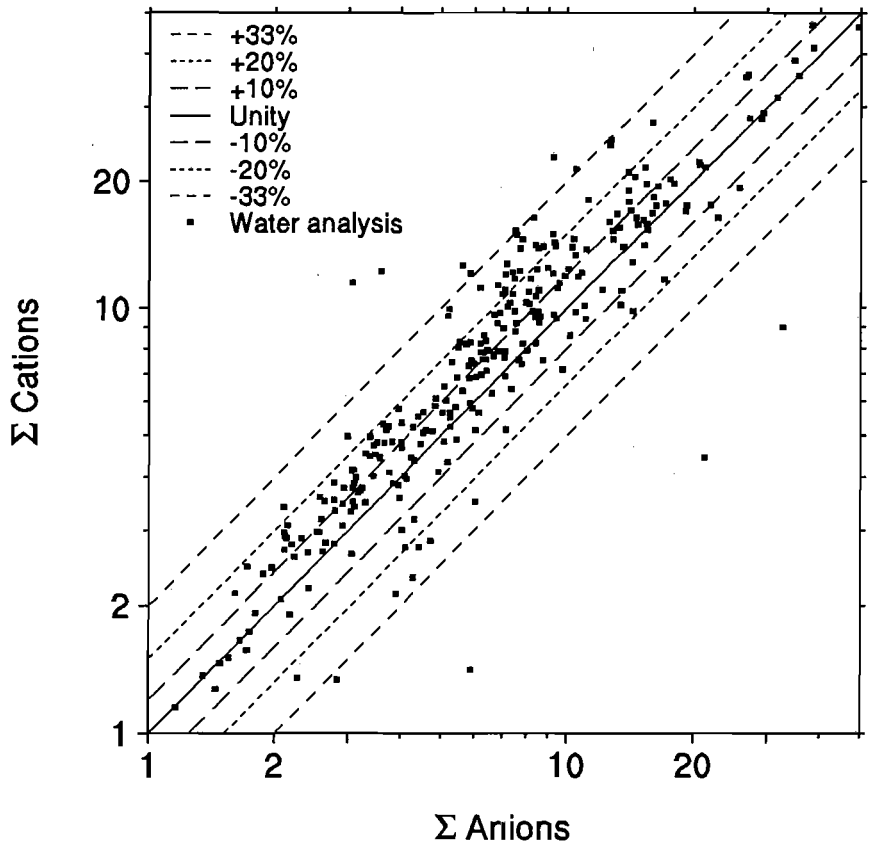

Figure 3.10 Ion balance graph for water analyses performed during this project.

Figure 3.10 shows an ion balance plot for the samples analysed during this project. It can be seen that the ion balance is generally good, although there is a significant bias towards a cation excess or anion deficiency. An ion imbalance of >10% is generally unacceptable, but it should be noted that analyses with an ion balance error >10% have been used in this thesis, introducing considerable 'noise' to the data. This was considered

to be acceptable, but not ideal, for a study interested primarily in fluoride. Conclusions based on the cation and anion data have, therefore, to be treated with caution.

Figures 3.11 and 3.12 show ion balance graphs for raw data received from the Departments of Water Affairs of South Africa and the former Bophuthatswana, respectively. Distinct differences in ion balance error are present. South African data is tightly clustered with few analyses outside the acceptable limits, but it has a bias towards anion excess. The Bophuthatswana data has two distributions: one group is widely scattered, whilst the other is seen to lie on or very close to the 0% ion balance error line.

Spatial distribution of water samples. Several factors affect the spatial distribution of the samples, which is variable. In rural areas the data is often clustered, since boreholes are most common in villages. In game parks such as Pilanesberg and Borakalalo, data is more evenly distributed because of the need for game to have evenly distributed watering points. The availability of groundwater and river water has also modified the sample distribution. Certain parts of the study area have a low sample density because of the absence of boreholes, such as the granite areas to the northeast of the Pilanesberg and north of Brits (see Figure 1.3). Boreholes in these areas have low success rates and low yields - they are either abandoned after drilling or fall into disrepair after being equipped, so that samples are unavailable from these areas. Conversely, few boreholes exist in the vicinity of the perennial rivers, since water is usually available from the river all year round. A third factor influencing sample distribution is groundwater quality. Boreholes with good quality water are maintained and more boreholes are drilled in the area. However, boreholes with poor quality water tend to be abandoned after drilling, or are equipped but fall into disrepair, and naturally act as a disincentive for further drilling in the area.

Any data concerning groundwater chemistry collected from rural areas, anywhere in the world, might be affected in these ways. The current data set is, therefore, biased towards clustered boreholes with high yields and good water quality. The results from this study are therefore unlikely to be truly representative of the overall groundwater quality, being biased towards better quality water. Nevertheless, the current data are entirely suitable in terms of relating F^- concentrations in drinking water to human health, as, self-evidently, the samples taken represent the waters ingested by the inhabitants of the area.

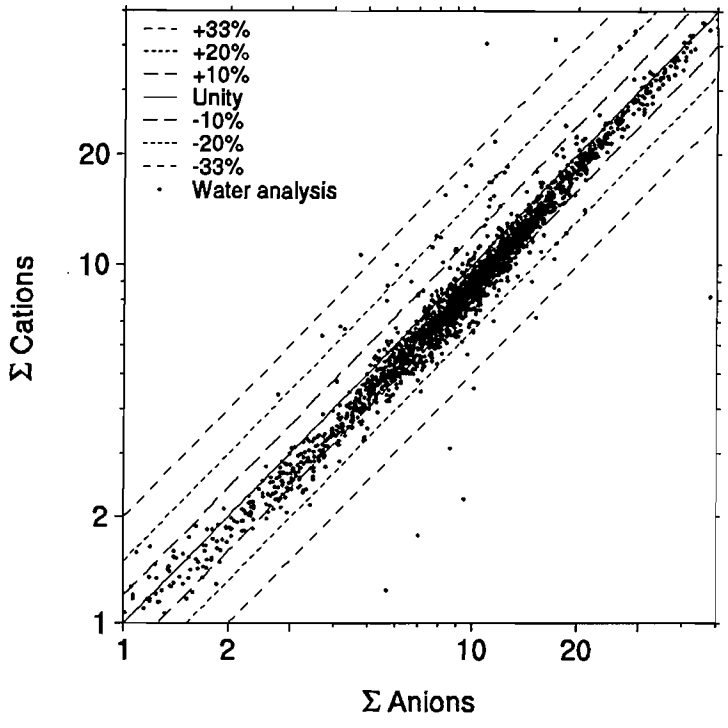

Figure 3.11 An ion balance graph for groundwater analyses provided by South African Department of Water Affairs and Forestry. The data has a consistent anion excess or cation deficiency.

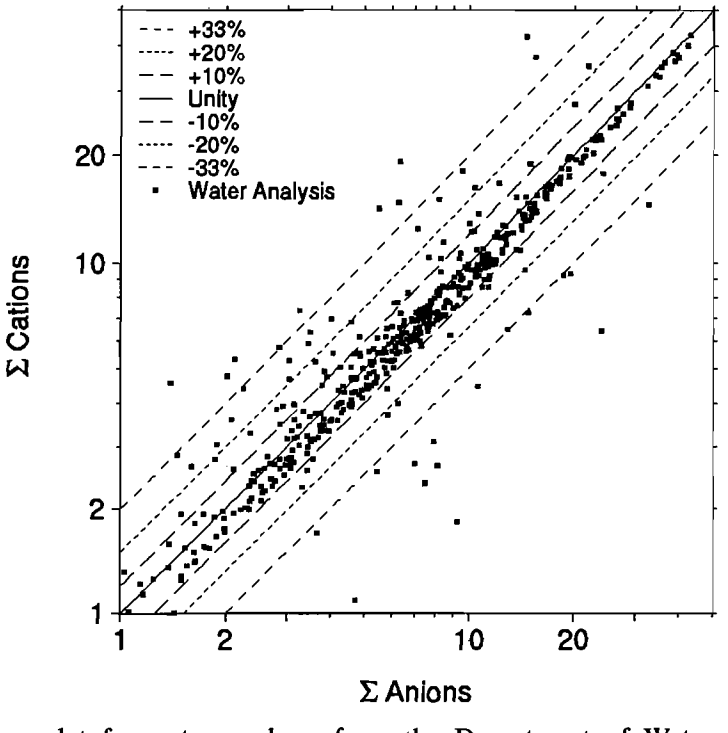

Figure 3.12 Ion balance plot for water analyses from the Department of Water Affairs of the former Bophuthatswana.

3.4.2 Rock and soil data quality

Elemental analysis. Figure 3.13 shows a calibration graph for fluorine in rocks and soils by XRF spectroscopy, produced for this project. The agreement is excellent, despite the very shallow x-ray penetration depths into the powder briquette and the potentially large mineralogical effects. The extended counting times for fluorine resulted in an acceptable detection limit of approximately 60 ppm.

Spatial distribution. With a study area of 75000 km^2 and only 42 rock and soil samples, data density over the area is low. No meaningful spatial distribution maps can be drawn for such a small data set. However, evaluation of the Regional Geochemical Survey maps of the study area produced by the Council for Geoscience show that the stream sediments and soil samples derived from a lithological unit have similar geochemical characteristics over their areal extent. For instance, a distribution map of Rb mirrors lithological boundaries very clearly, because of the contrasting Rb contents of the different rock types. It is inferred from this that a small number of samples can satisfactorily discriminate between, if not entirely represent, the different lithologies. The main rock types were sampled at least three times, and the rock types with high F concentrations (Pilanesberg Foyaites and Lebowa Granite) were sampled at least 4 times.

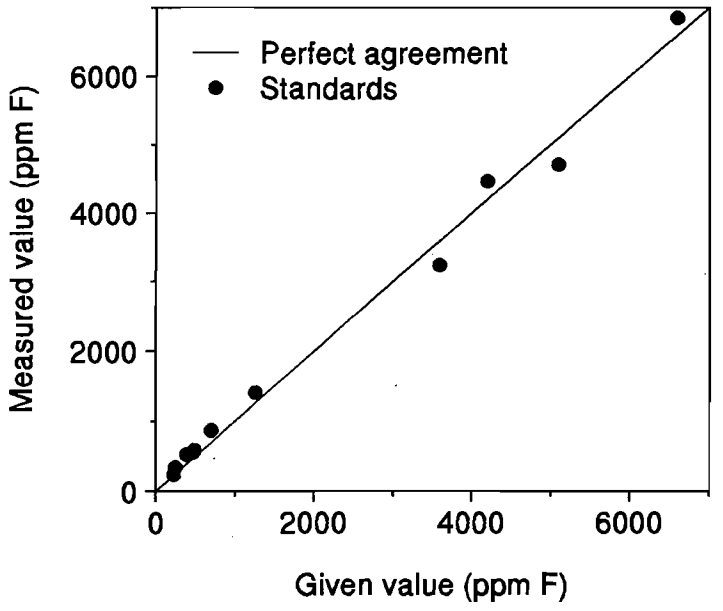

Figure 3.13 Calibration graph for fluorine in rock standards using XRF spectroscopy.

3.5 Computer manipulation of data

This section contains a description of the computer programmes used to manipulate and store the data.

3.5.1 General computer programs

Information on attributes of the sampling sites were stored using a DBASE based program called HYDROCOM, provided by Professor Hodgson of the Institute for Groundwater Studies at the University of the Orange Free State, South Africa. The program allowed for storage of all relevant information about each sampling site, including geochemical information. The program was compatible with the databases of Bophuthatswana and South Africa, allowing easy integration of their databases with the author's.

A QuattroPro spreadsheet programme was used to calculate ion balance errors for the major ion data and to estimate residence times using radiocarbon data. CoStat was used to calculate regression equations and graphs were produced using CoPlot and CoDraw.

3.5.2 Analysis of spatial data

Analysis of data with a spatial component took place using a Geographical Information System (GIS) software package called ARC/INFO. Lithological boundaries were digitised from the 1:250,000 scale geological maps sheets for Rustenburg, Pretoria and Thabazimbi. The Nelspruit map was unavailable at the time of digitising and so this section of the map was obtained from the 1:1,000,000 scale geological map of South Africa. Digital data on topographic contours, roads, major settlements and rivers were provided by the Department of Water Affairs and Forestry. In order to initially classify groundwater analyses in terms of surface geology, a 'spatial join' was performed between the analyses and the digitised geology. This is a rapid and accurate method of performing such a classification, given the large number of data points. With fewer data points, classification by hand plotting each borehole on a geologic map sheet would be more efficient, and GIS would not be needed.

To produce a 'fluorosis risk map', groundwater samples were classified into 4 groups on the basis of their F^- concentration: <0.7, 0.7-1.5, 1.5-3.0 and >3.0 mg/ℓ. These are designated no risk, medium risk, high risk and very high risk, respectively. For the origin of these divisions, see Chapter 2. Theissen polygons were generated for each sample point, resulting in approximately 3000 polygons. Where adjacent polygons had the same classification, they were merged. In this way 300 areas have been delineated where there is

a medium risk of fluorosis or higher. Theissen polygons admirably mirror human behaviour, in that people generally fetch water from the nearest borehole: points within a given theissen polygon are closer to the central point (the borehole) than any other borehole. Accordingly, one of the advantages of this method is that people living within the area of the polygon will probably receive their water from the boreholes within the polygon. A further advantage to this method is that it avoids a visually confusing clutter of points, which results if the original 3500 data points are not reduced in this way. A disadvantage is that geographically isolated boreholes result in very large polygons, which have a disproportionate visual impact relative to their importance.

3.5.3 Speciation modelling

The programs MINTEQA2 (Metal Speciation Equilibrium Model for Surface and Ground Water) and PRODEFA2 (Problem Definition Program for MINTEQA2) were used to model mineral-groundwater interaction. MINTEQA2 is a geochemical model capable of calculating equilibrium aqueous speciation, adsorption, gas phase partitioning, solid phase saturation states, and precipitation-dissolution of metals. Not all of these facilities were used. The model contains a large thermodynamic data base. To describe information for use in MINTEQA2, the program PRODEFA2 was used. It is an interactive program that assists the user in developing and building an input data file for the MINTEQA2 model. Version 3.11 of MINTEQA2 was used, provided by the Computing Centre for Water resources of Natal University.

4 ROCKS, MINERALS AND SOILS

4.1 Introduction

The western Bushveld is the main site of South Africa's platinum mining industry, and because of this the economic geology of the area has been intensively studied. The majority of studies of Bushveld rocks are concerned with elements of economic significance, such as the platinum group elements (e.g. Von Gruenewaldt *et al.*, 1986; Campbell *et al.*, 1983) and chromium (e.g. Cameron, 1980). Tools in the investigation of the distribution of these elements have included Sr isotopes (e.g. Davies *et al.*, 1970; Sharpe, 1985) and more recently, the study of hydrogen isotopes (Mathez *et al.*, 1994; Chaumba, *in prep.*). Data has been published on the halogen content of Bushveld minerals (e.g. Boudreau *et al.*, 1986), principally for use in gauging the temperature and chlorinity of mineralising hydrothermal fluids. The Bushveld granites have been well studied in terms of whole rock geochemistry (e.g. Kleeman and Twist, 1989). Comparatively few studies of the RLS have been concerned with major element variation, probably as a result of the early and continuing reliance on modal mineralogy for the classification criteria for RLS stratigraphy (e.g. Eales *et al.*, 1993). No published analyses of whole rock F in the RLS could be found in the literature. Despite the health implications of fluorine-rich aquifers, comparatively little work has been undertaken on the whole rock F concentration in the area.

The primary intention of this chapter will be to present baseline data on the fluorine concentration of rocks, soil and minerals from the field area. It is not intended to discuss the geochemistry of the rocks, or the causes of variation of F in the different rock types. The mineralogy of an aquifer is of crucial importance in controlling water-rock interaction. The petrography of rocks from the sample set is described briefly and discussed in terms of reactions which may affect F^- concentration in groundwater. The composition of selected minerals, with reference to F, is described. The results of the leaching experiments are described.

Isotope ratios of strontium are used in Chapter 6 to characterise groundwater types. Strontium in groundwater originates principally from dissolution of aquifer rocks and for this reason the strontium isotope composition of selected rock samples will also be discussed.

4.2 Petrography

Sample locations are shown in Figure 4.1 in relation to the regional geology and are detailed in Appendix A2. Microscopic examination generally confirmed the classification made in the field from hand specimens, apart from the reclassification of several of the granite specimens to alkali granites, based on the modal proportion of plagioclase to alkali feldspar. Descriptions of the thin sections can be found in Appendix B1. The sample set includes 3 examples of syenite from the Pilanesberg Complex, 4 norites from the RLS (all from the Upper Zone), 7 alkali granites and 7 granites. Also represented are banded ironstones, sandstone, limestone and dolomite. The sample set can be regarded as a representative selection of lithologies present in the western Bushveld. Several unusual rock types are included in the sample set, namely:

RO2	a quartz-biotite monzonite;
RO6	a carbonatitic fluorite ore;
RO17	a garnet-biotite hornfels of similar occurrence to RO2;
RO24, RO31	alkali granites with conspicuous granophyric textures;
RO34	felsite from the Rooiberg Group; and
RO36	greenschist facies metagabbro.

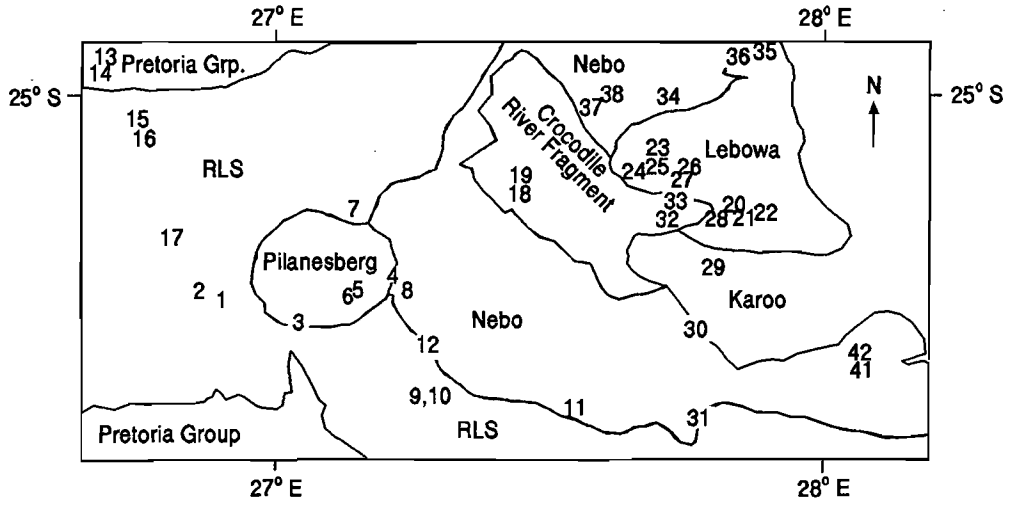

Figure 4.1 Position and sample number of rock and soil samples taken for analysis during this study. Lithological boundaries are shown as lines. The area is part of that shown in Figure 1.3.

Occurrence of F-bearing minerals. The rocks of the RLS and the Pretoria Sequence generally contain no major F-bearing minerals. The Rashoop Granophyre, Nebo and Lebowa granites and the Pilanesberg alkaline complex all contain fluorite (CaF_2), and the

estimated volume percentages from this study are shown in Appendix B2. Apart from one sample (RO6), fluorite is an accessory mineral, but it can have a controlling effect on groundwater F^- concentrations even at low percentages because of its moderate solubility (Chapter 6). Micas and amphiboles may contain F^-, substituting for OH^-, and both mineral types occur in the rocks of the area. Fluorapatite is a common accessory mineral in granitic rocks (Deer *et al.*, 1977), but microscopic examination failed to reveal its presence (but see section 4.4.3).

It will be argued in Chapter 6 that the highly soluble mineral villiaumite, NaF, probably occurs in Pilanesberg and Lebowa rocks. The amount of villiaumite required to produce the concentrations of fluoride detected in the leaching experiments is in the order of 0.005 wt% (assuming total dissolution of the mineral). This percentage is much less than can easily be detected by either optical or electron microscopy or by XRD. This assertion is especially true if villiaumite is disseminated in fine grains throughout the rock. The modelling of leaching experiment data is, therefore, the only evidence for the presence of villiaumite in these rocks.

4.3 Chemical composition of rock and soil samples

This section will discuss the results of analyses of rock and soil samples undertaken during the study using the XRF facilities at UCT (Chapter 3).

4.3.1 Previous work

Kleeman and Twist (1989) provided a key work on the geochemistry of the Bushveld granites, summarising analytical and mineralogical studies of 133 samples. They state that the Nebo Granite is a sill-like body, between 2.5 and 3.5 km thick, extending over an area of 30,000 km and is chemically and mineralogically zoned. From the base to the top of the body, Si, K and Rb increase, whilst Fe, Ti, Ca, P, Ba, Sr and Zr decrease. The overlying granites (the Lebowa, Bobbejaankop and Klipkloof granites, for instance) have no such systematic variation and have less variation overall. An example is the SiO_2 content, which varies from 74-77 wt% in the Klipkloof Granite, compared to 69-76 wt% in the Nebo Granite: the composition of the overlying Klipkloof Granite is similar to the most evolved Nebo granite composition. The concentration of Na is similar (3.2-4.9 wt%) throughout the Nebo Granite and overlying granites. Regrettably, no F concentration data were presented by Kleeman and Twist (1989).

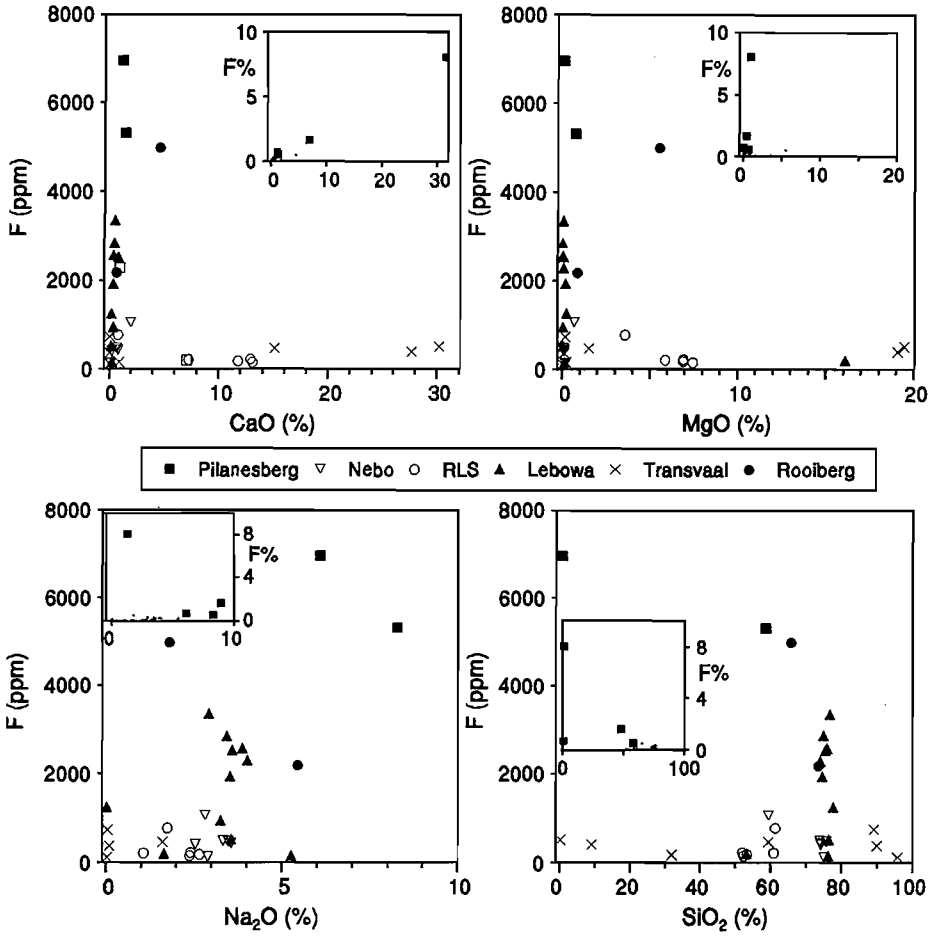

Figure 4.2 Relationship of CaO, MgO, Na_2O and SiO_2 to F in rock samples.

4.3.2 Whole rock fluorine concentration

Analyses of whole-rock powders by XRF are detailed in Appendix C. Since the sample set is so heterogenous, bivariate diagrams of major and trace elements are virtually meaningless. Even plots of F against major elements (Figure 4.2) show no clear trend. This section is therefore confined to a description of the F concentrations found in rocks from the field area, with a brief discussion on whole rock chemistry to put them into some geochemical context. Figure 4.3 shows the F concentration in the lithologies of the field area. The plot will be discussed in conjunction with the analyses of the rock types in the following sections.

Norite. Few recent whole rock analyses of norite from the study area have been published, probably because the interest of igneous petrologists is directed at the platiniferous pyroxenites instead. The F content of ultramafic rocks is rarely analysed or reported. The F concentrations of the norite samples from this study are all low, ranging from 221 ppm to below the detection limit of 60 ppm, within the range given by Boyle (1976; this volume, Chapter 2). The major element data for norite samples shown in Table

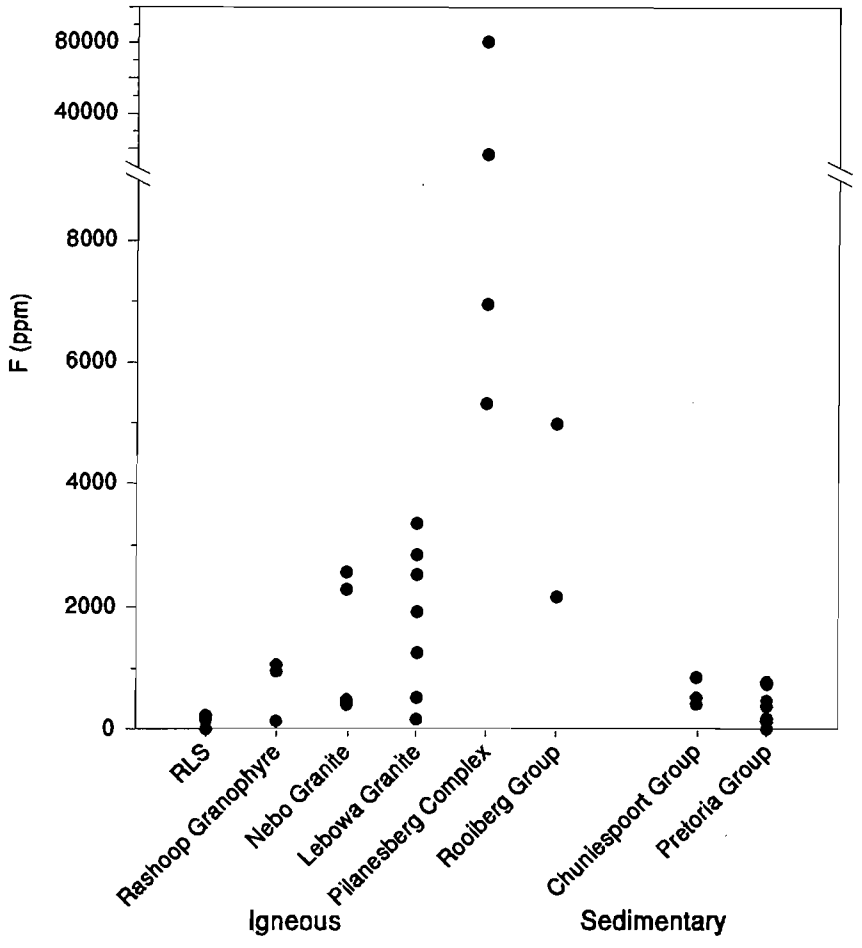

Figure 4.3 Concentrations of F in igneous and sedimentary formations in the field area. 'RLS' is the Rustenburg Layered Suite.

4.1 are in general agreement with previous published analyses of norite (Lombaard, 1932) and hypersthene gabbro (Wager and Brown, 1968). It is notable that sample RO16 has a low Al_2O_3 and CaO content and high MgO content.

Granitic rocks. Representative analyses of Nebo and Lebowa Granite samples are shown in Table 4.2, together with comparative data (Kleeman and Twist, 1989). Good agreement is found between the analyses (Appendices B1 and C). The six Nebo Granite samples have a range of F concentrations from 410 to 2570 ppm, and three samples have similar F concentrations, at approximately 450 ppm. The Lebowa Granite also has a wide range of F concentrations, from 163 ppm to 3350 ppm, but with no clustering of values. Fluorine concentrations in the Rashoop Granophyre range from 127 to 1060 ppm. The analyses which Koritnig (1974) used to calculate his mean F concentration of 800 ppm for granitic rocks is based on a similarly large range of concentrations, from 200 to 2950 ppm.

Table 4.1 XRF analyses of norite samples from the Rustenburg Layered Suite of the field area and a comparative sample (A), a norite from Bon Accord Quarry, north of Pretoria (Lombaard, 1932). In this and the following tables, concentrations are expressed as weight %, apart from F which is in parts per million. *'n/r'* is not reported. For this table, correction of the total due to F substitution of O is not significant. Total Fe expressed as Fe_2O_3.

Sample No.	RO16	RO7	RO9	A
Site Name	Rampapaanspoort	North of Pilanesberg	Lesung	Bon Accord
SiO_2	53.12	53.34	52.43	52.48
TiO_2	0.32	0.15	0.22	0.56
Al_2O_3	10.62	18.58	17.24	16.95
Fe_2O_3	11.30	7.55	7.65	9.04
MnO	0.18	0.15	0.16	0.22
MgO	16.13	6.91	7.45	7.50
CaO	7.11	11.79	13.10	11.06
Na_2O	1.65	2.67	2.38	2.50
K_2O	0.41	0.22	0.23	0.30
P_2O_5	0.05	0.00	0.01	0.10
H_2O^-	0.05	0.05	0.08	0.37
LOI	0.00	0.11	0.08	*n/r*
F (ppm)	205	183	153	*n/r*
Total	100.96	101.54	101.05	101.08

Table 4.2 XRF analyses of some selected Nebo and Lebowa Granite samples from the field area and comparative samples. Abbreviations: 'Alk G' = Alkali granite; 'G' = granite; 'A G' = albitized granite; 'L' = Lebowa Granite; 'N' = Nebo Granite; '(L)' = Klipkloof Granite, equivalent to Lebowa Granite; *'n/r'* = not reported. Final three samples from Kleeman and Twist (1989). Concentrations are expressed as weight %, apart from F which is in parts per million. Total Fe expressed as Fe_2O_3.

Sample No.	RO20	RO30	RO37	RO42	RO11	GGr-175	GN-8	GGr-255
Type, Source	G, L	G, N	Alk G, N	G, N	Alk G, N	A G, (L)	G, N	G, N
SiO_2	76.21	75.81	75.78	73.99	73.88	76.70	74.13	73.74
TiO_2	0.12	0.21	0.21	0.22	0.18	0.07	0.20	0.23
Al_2O_3	11.85	11.35	12.19	12.05	12.25	11.98	11.72	11.69
Fe_2O_3	3.43	3.29	1.54	3.58	3.33	1.34	3.04	3.32
MnO	0.02	0.04	0.01	0.05	0.04	0.02	0.05	0.05
MgO	0.14	0.1	0.05	0.13	0.07	0.00	0.00	0.00
CaO	0.24	0.72	0.38	0.78	0.62	0.52	0.81	0.92
Na_2O	5.27	3.49	3.88	3.56	3.33	4.62	3.97	3.65
K_2O	1.92	4.95	5.62	5.3	5.54	4.28	5.12	5.15
P_2O	0.07	0.02	0.02	0.03	0.04	0.01	0.01	0.02
H_2O^-	0.22	0.16	0.29	0.11	0.18	0.13	0.30	0.22
LOI	0.94	0.32	0.39	0.48	0.36	0.35	0.33	0.47
F (ppm)	163	480	2570	437	489	*n/r*	*n/r*	*n/r*
subtotal	100.45	100.51	100.62	100.32	99.87	100.02	99.68	99.46
O≡F	0.01	0.02	0.11	0.02	0.02	-	-	-
Total	100.44	100.49	100.51	100.30	99.85	100.02	99.68	99.46

Syenite. The Pilanesberg syenite samples have variable compositions, with SiO_2 ranging from 48 to 58 wt%, and F from 5310 to 16400 ppm (Table 4.3). The mean F concentration of the unaltered syenites (~6100 ppm; n=2) is very much in excess of the mean for alkalic rocks of 1000 ppm suggested by Koritnig (1974). The major element analyses are in general agreement with those of Retief (1963). Sample RO4 can be expected to differ somewhat from his analyses, since it was taken from a zone of known hydrothermal alteration.

Sedimentary rocks. The Chuniespoort and Pretoria Group sediments have a range of F concentrations from below 60 ppm (the detection limit) to 900 ppm. The means for dolomite (454 ppm; n=2) and sandstone (340 ppm; n=4) are almost twice the value of the means for these rocks presented in Koritnig (1974). The F concentration of 858 ppm in the

limestone sample RO29, of Karoo age, is very high compared to the mean for limestones of 220 ppm in Koritnig (1974). Full analyses are presented in Appendix C.

Table 4.3 XRF analyses of syenite from the Pilanesberg complex, and comparative sample (A) of Pilanesberg syenite (Retief, 1963). (a) $H_2O^+ + H_2O^-$. (b) includes 0.14 wt% Cl. Total Fe expressed as Fe_2O_3.

Sample No.	RO3	RO4	RO5	A
Site Name	Green Tweed	Thabayadiotsa	Kubu Drive	Koedoesfontein
SiO_2	58.44	47.76	57.31	54.58
TiO_2	1.09	0.77	0.22	0.64
Al_2O_3	17.17	15.79	16.72	19.13
Fe_2O_3	5.42	6.25	10.38	4.45
MnO	0.31	0.8	0.47	0.72
MgO	0.73	0.44	0.1	1.12
CaO	1.37	7.03	1.15	2.49
Na_2O	8.28	8.9	6.08	7.10
K_2O	5.52	5.06	4.59	3.65
P_2O_5	0.1	0.06	0.04	0.08
H_2O^-	0.25	0.18	0.64	1.80[a]
LOI	1.36	4.35	1.36	1.69
F (ppm)	5310	16400	6960	3300
subtotal	100.57	99.03	99.76	100.65[b]
O≡F,Cl	0.22	0.69	0.29	0.17
Total	100.35	98.34	99.47	100.48

4.3.3 Fluorine in paired rock and soil samples

Fluorine was determined in soil samples taken from the vicinity of each rock sample (see Chapter 3). Figure 4.4 shows a comparison of the concentrations found in the whole rock and whole soil samples. It is seen that the soil fluorine concentration is generally lower than the corresponding rock fluorine concentration. Several gaps are seen in the trend, where F concentration increases in abrupt jumps along the series of rock samples; the gaps do not correspond to a change in rock type. No significance is attached to these gaps, which probably result by chance and from the small number of samples. Many of the soil concentrations are up to an order of magnitude less than that for the corresponding rock. One soil sample has a very high fluorine concentration compared to its paired rock sample;

this comes from the Kwarriekraal fluorite mine and probably results from contamination of the soil by mine tailings.

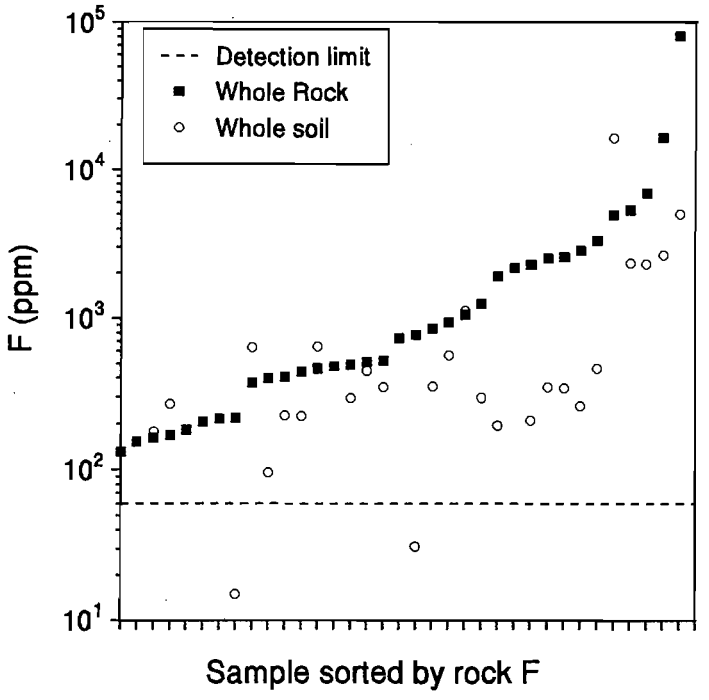

Figure 4.4 Fluorine concentration in paired rock and soil samples. Soil generally has a lower F concentration than the associated fresh rock, indicating that F is leached away during soil formation.

The leaching of F from rock during the soil forming process is a well known and global phenomenon (Koritnig, 1974). Fluorine concentration would be expected to be at a minimum at the soil surface, increasing downwards towards the fresh rock boundary, as found by Koritnig (1951) in the weathering profile of a soil. Elrashidi and Lindsay (1986) modelled the equilibria which control fluorine solubility in soils. They found that the solubility of most fluoride minerals (including KF, NaF, CdF_2, ZnF_2 and PbF_2) is very high and that they are not likely to remain in soils (e.g. NaF in Figure 4.6). Under typical soil conditions, AlF_2, FeF_3, MgF_2 and CaF_2 are more insoluble, with the latter, fluorite, being the most stable above pH 5.0. At a pH of less than 4.5, however, AlF_3 can be the most stable mineral. The fluorapatite/hydroxyapatite system is more stable than fluorite at higher values of pH (Figure 4.5). Figure 4.5 is constructed assuming a CO_2 partial pressure of 0.003 atmospheres; Na^+, K^+ and Cl^- activity is fixed at 10^{-3} M; and Al^{3+} activity is controlled by gibbsite equilibria.

Spatial distribution of F in rock and soil. Figure 4.6 shows the spatial distribution of F in rock and soil samples discussed in the previous section and shown in Figure 4.4. It is clear that high F occurs in the Lebowa Granite and Pilanesberg Complex, whilst the Nebo

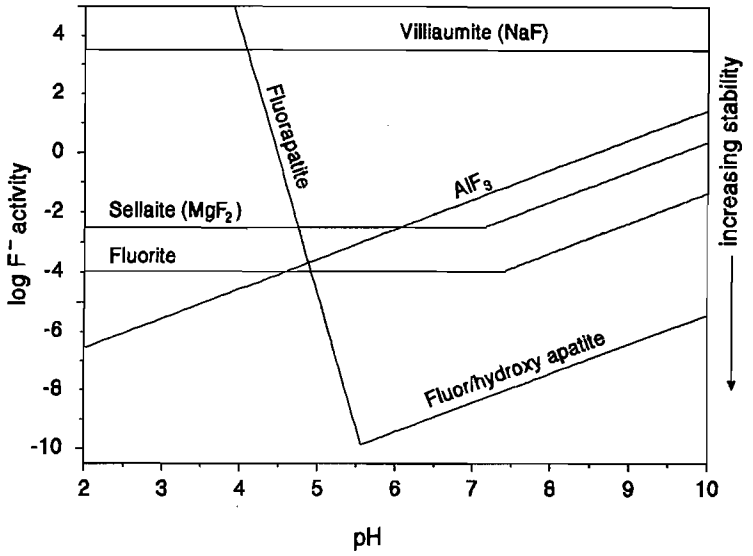

Figure 4.5 Stability of important fluorine-bearing minerals in typical soil conditions. After Elrashidi and Lindsay (1986). See text for assumptions used in construction of diagram.

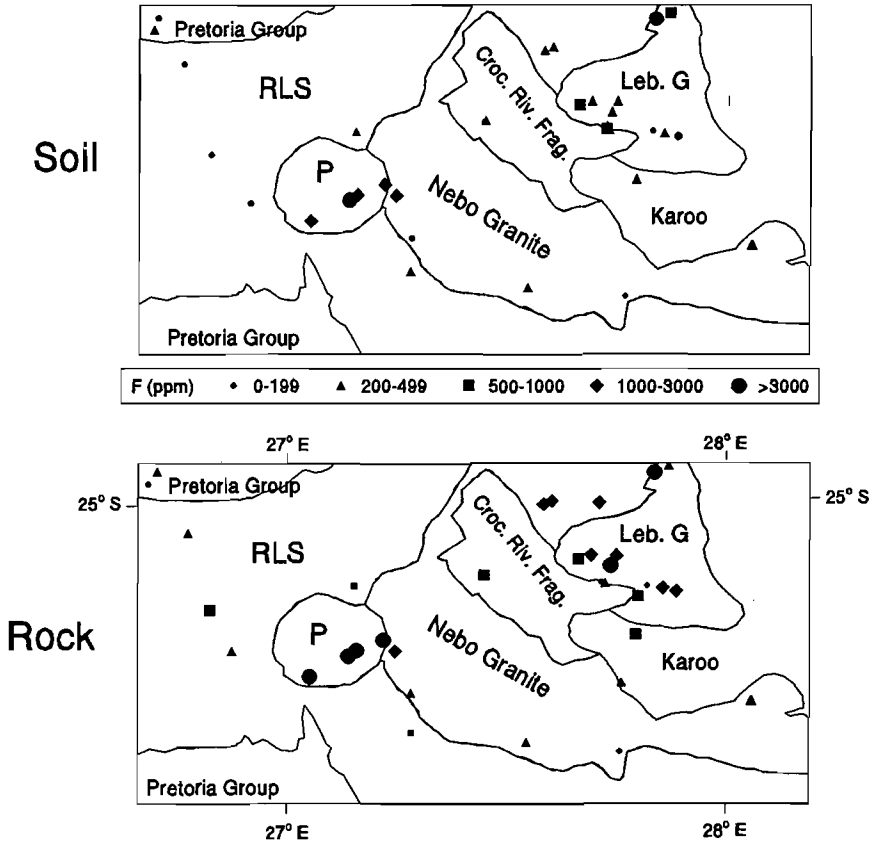

Figure 4.6 Distribution of F in soil and rock samples in the western Bushveld. Lines represent lithological boundaries (see Figure 1.3). The Pilanesberg and Lebowa Granites both have high rock and soil F.

Granite has scattered high values and the RLS is uniformly low. Fluorine in soil has a similar relative distribution, but the absolute concentrations are lower. Of note is the distribution of F in rock and soil, which is very similar to the distribution of high F concentrations in groundwater (see Chapter 5).

4.4 Mineral chemistry

Isomorphous replacement of OH^- by F^- occurs in rock-forming minerals such as micas, amphiboles and apatites. A knowledge of the F concentration in these minerals is important in understanding the processes which give rise to high fluoride groundwater in contact with these minerals. Mica, amphibole and apatite from 10 rock samples were analysed by electron microprobe (Chapter 3) and the results are discussed in this and the following section. The full analyses are reproduced in Appendix B3.

4.4.1 Mica

The expected mean F concentration in biotite from granite is 0.24 wt% (n=168; from the compilation of Koritnig, 1974). Only one mica, a biotite from the garnet-biotite hornfels RO17, had detectable F, at 0.35 wt%. Fluorine concentrations in micas from the Lebowa and Nebo granite were below the detection limit (0.17 wt%), and so they are presumably hydroxy-micas.

That these micas had low F concentrations is an unusual result, since mica should be an efficient trap for F in F-rich magmas (Koritnig, 1974; Nash, 1976) and these micas come from magmas rich in F. However, Nash (1976) also showed that biotites in the Skaergaard intrusion of Greenland lost F during interaction with meteoric water. Nash (1976) calculated that meteoric fluids exchanging with the Skaergaard intrusion would have low F concentrations. He used oxygen isotope values in co-existing plagioclase to gauge exchange with groundwater in the intrusion and found an inverse correlation between the degree of exchange and the F content of biotite. The F concentration of apatites from the same samples was unaffected. In contrast, Munoz and Ludington (1974) showed that biotite acts as an effective scavenger of F in F-bearing fluids. The low F content of the micas from the Nebo and Lebowa granites, which have high whole-rock F (section 4.3.2), would therefore be interpreted as resulting from the reaction of these micas with low F-fugacity fluids. Alternatively, the high FeO content of these biotites may have resulted in the exclusion of F from the octahedral and hydroxyl sublattices, due to the reciprocal mixing properties of (Mg, Fe^{II},Al^{VI}) and (F,Cl,OH) in biotite (Zhu, 1991; Zhu and Sverjensky, 1992). Table 4.4 shows analyses of selected micas.

Table 4.4 Analyses of mica from rock types in the field area. Concentrations expressed as wt%, "*n/d*" is not detected, "*n/r*" is not reported. Total Fe as FeO. H_2O calculated on the basis of F+OH = 2.0 in the structural formula. RO11 is an alkali granite, RO17 is a garnet biotite hornfels and RO30 is a granite. Comparative sample: A) Phlogopite from magnetite gabbro, BIC (Boudreau, *et al.*, 1986).

Element	RO11	RO17	RO30	A
SiO_2	32.76	35.25	34.03	37.90
TiO_2	3.35	4.32	1.44	3.44
Al_2O_3	13.24	18.66	11.43	14.43
FeO	36.59	21.70	39.53	12.99
MnO	0.21	*n/d*	*n/d*	*n/r*
MgO	0.20	7.98	0.83	16.22
CaO	0.06	*n/d*	*n/d*	*n/r*
Na_2O	0.07	0.08	*n/d*	0.22
K_2O	8.04	9.53	7.95	9.43
F	*n/d*	0.35	*n/d*	0.42
Cl	*n/d*	0.16	*n/d*	0.35
subtotal	94.52	98.04	95.21	95.40
O=F,Cl	0.00	0.22	0.00	0.26
H_2O	3.55	3.77	3.53	3.74
Total	98.07	101.59	98.74	98.88

4.4.2 Amphibole

Fluorine concentrations in amphibole analysed for this study ranges from below the detection limit of 0.17 wt% to 2.69 wt% in sample RO3. Pilanesberg amphiboles (n = 4) had a mean F concentration of 1.26 wt%, Nebo Granite amphiboles (n = 3) 0.61 wt% F and Lebowa Granite amphiboles (n = 2) <0.17 wt%. These results are somewhat unusual, since the whole rock F concentration of the Lebowa Granite samples are at least double the mean F concentration of 500 ppm for the Nebo Granite samples. It is obvious, therefore, that total F concentration in the Lebowa Granite is not controlled by the F concentration in the amphiboles. The abundance of fluorite is probably the controlling factor in this case. Table 4.5 shows selected amphibole analyses.

Table 4.5 Analyses of amphibole from samples RO3 and RO4 (syenites) and RO11 (alkali granite). H_2O calculated on basis of F+OH = 2.0 in the structural formula. Concentrations in wt%, "*n/d*" is not detected.

Element	RO3	RO4	RO11
SiO_2	45.39	47.67	39.27
TiO_2	2.79	0.58	1.69
Al_2O_3	6.46	1.35	8.80
FeO	14.04	25.67	33.63
MnO	1.02	1.71	0.58
MgO	12.82	2.05	0.55
CaO	10.10	16.61	10.61
Na_2O	4.11	3.92	2.01
K_2O	1.32	*n/d*	1.45
F	2.69	*n/d*	0.65
subtotal	100.74	99.56	99.24
O≡F	1.13	0.00	0.27
H_2O	0.73	1.90	1.52
Total	100.34	101.46	100.49

4.4.3 Apatite

Apatites from sample RO6 (a fluorite ore) were suspected to be fluorapatites because of the high F content of the rock (8 wt%), and they were analysed to confirm this. All contained appreciable F and no detectable Cl (Table 4.6). Of note is the high concentration of SrO, which reached 6.78 wt% in one analysis. Although the apatites are not saamitic (where SrO almost entirely replaces CaO and reaches 46 wt%; Elfimov *et al.*, 1962), the Sr content is higher than most igneous apatites (Edgar, 1989 and references contained therein). Edgar (1989) noted that high-Sr apatites had high F concentrations, and these analyses confirm that observation. He also noted that apatite composition closely reflects the composition of the magma from which it is derived. The analysis of the host rock (Appendices B4 and C)) shows that it has a high carbonate content, which suggests that the low analytical totals of these apatites may be due to the presence of CO_2 in the apatite structure. A high rare earth element content is also feasible.

Table 4.6 Typical analysis of apatite from sample RO6 (fluorite ore; Pilanesberg), and a comparative analysis. Concentrations expressed as wt%, *n/d* is not detected, *n/r* is not reported. H_2O calculated on the basis of F + Cl + OH = 1.0 in structural formula. A) chlorapatite from the Merensky Reef, BIC (Boudreau *et al.*, 1986). [a]Includes 0.07 wt% Y_2O_3, 0.27 wt% La_2O_3 and 0.56 wt% Ce_2O_3.

Element	RO6	RO6	RO6	RO6	A
P_2O_5	39.21	39.89	40.02	40.07	40.43
CaO	49.70	51.47	49.64	51.61	53.34
SrO	6.78	3.94	6.76	2.59	0.04
FeO	*n/d*	*n/d*	*n/d*	*n/d*	0.28
MnO	*n/d*	*n/d*	*n/d*	*n/d*	*n/r*
MgO	*n/d*	*n/d*	*n/d*	*n/d*	*n/r*
SiO_2	*n/d*	*n/d*	*n/d*	*n/d*	0.49
F	3.60	2.60	2.64	3.55	0.12
Cl	*n/d*	*n/d*	*n/d*	*n/d*	6.85
subtotal	99.29	97.90	99.06	97.02	102.45[a]
H_2O	0.00	0.47	0.45	0.01	0.00
O≡F,Cl	1.52	1.09	1.11	1.49	1.60
Total	99.29	97.28	98.40	96.34	100.85

4.5 Leaching experiments on rocks and soils

Leaching experiments were performed on all soil and rock samples (Section 3.3). The highest concentrations of fluoride in the leachate came from rocks and soils with the highest fluorine concentrations. Figure 4.7 shows the relationship of total F to soluble F in rock and soil samples. In the rock experiment, many of the samples had leachate with very high fluoride concentrations (up to 100 mg/ℓ), and in general the leachate had a concentration approximately 2 orders of magnitude less than the whole rock concentration, *i.e.* soluble F was approximately 1% of the total F. In the soil experiment, the leachate was found to contain very low concentrations of F. Leachable F is generally 3 orders of magnitude less than total F, *i.e.* approximately 0.1% of the total F. Most of the fluoride concentrations in the leachate derived from soil samples were below ≈4 mg/ℓ, which is approximately the concentration of F^- in solution from the stoichiometric dissolution of CaF_2 (see Chapter 6).

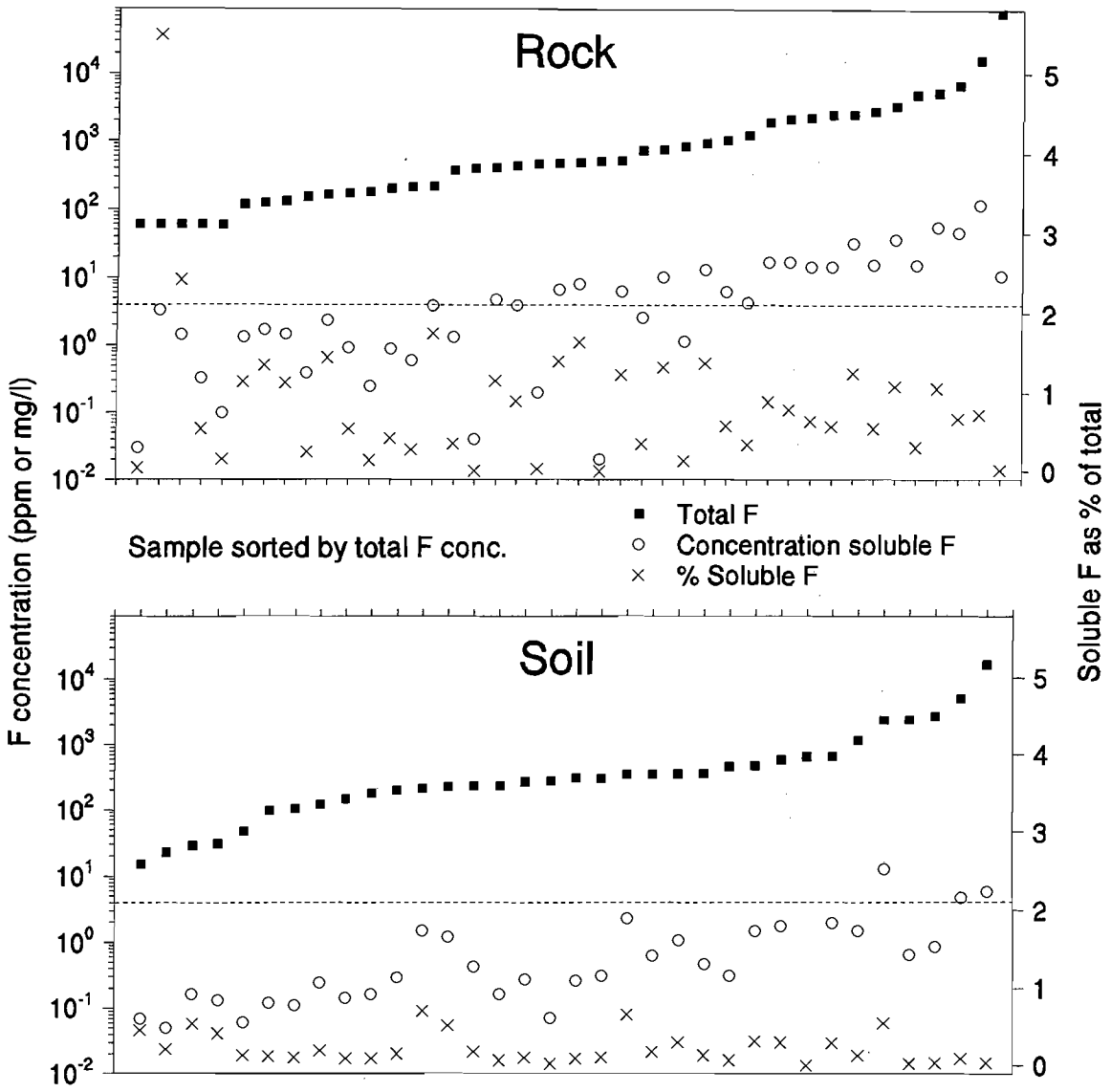

Figure 4.7 Results of leaching experiments on rock and soil samples. The dotted line represents the concentration of F^- from stoichiometric dissolution of fluorite. See text for discussion.

4.6 $^{87}Sr/^{86}Sr$ composition of rocks in the field area

Strontium isotope ratios are used in Chapter 6 in an attempt to characterise groundwaters and the aquifers from which the groundwaters originated. It has been reasoned that groundwaters acquire a distinctive Sr isotope ratio from their host rocks, and that this value may be maintained after the groundwater has migrated some distance. Whilst this method has been used successfully in carbonate terrains (see Chapter 1), it is the first use of the method in the Bushveld area. Since it was planned to match groundwater Sr isotope ratios with those from rock, of importance to this study is the availability of whole rock Sr isotope ratios for most of the major rock types in the study area.

4.6.1 Previous Work

Many rock and mineral samples from the area have been analysed by previous workers for the isotopes of Sr and Rb, almost exclusively to be used as a means of dating igneous rocks, but also as a method of gauging crustal contamination in ascending magmas (e.g. Schreiner (1958); Hunter and Hamilton (1978); Davies *et al.* (1970); Harmer and Farrow (1995)) and subsequent fluid-rock interactions (Walraven, 1987). Many of the studies were summarised by Walraven and Hattingh (1993). The relevant results are shown in Table 4.7. It can be seen that Bushveld Granite has by far the largest value and range of Sr isotope ratios of any of the rocks in the field area. The rocks of the RLS have a very small range, whilst diorites in the area have a range of ratios between that for the basic and acid rocks of the Bushveld.

Table 4.7 $^{87}Sr/^{86}Sr$ whole rock ratios for western Bushveld igneous rocks. [a]Initial ratio, but correction to the present ratio is small because of low Rb/Sr ratio.

Rock type	Location	Reference	$^{87}Sr/^{86}Sr$
Granite	Veerkraal	Davies *et al.*, 1970	0.8176-1.8989
Carbonatite	Tweerivier	Harmer, 1985	0.7027[a]
Norite	RLS	Davies *et al.*, 1970	0.7069-0.7070
Anorthosite	RLS	Davies *et al.*, 1970	0.7066-0.7076
Diorite	BIC	Davies *et al.*, 1970	0.7273-0.7308

4.6.2 Current Work

As shown in the previous section, Sr data exist for the igneous rocks of the field area, thus avoiding the necessity of analysing a large number of rock samples for background values. However, since the time of deposition of sedimentary rocks cannot be measured using the $^{87}Sr/^{86}Sr$ method, no such data for the Karoo sedimentary rocks were available. To provide a sample of the Sr isotope ratio for this potentially important aquifer, sample RO29 (a Karoo Sequence sandstone) was analysed (Chapter 3). The rock was found to have a whole rock $^{87}Sr/^{86}Sr$ ratio of 0.7244 ($\pm$0.0008), just below the values for diorite. This value is compared in the following chapter to the $^{87}Sr/^{86}Sr$ value of groundwater from the same formation.

5 GROUNDWATER CHEMISTRY

5.1 Introduction

This chapter discusses the hydrogeochemistry of groundwater of the western Bushveld, with the emphasis on fluoride. Previous work on the groundwater chemistry of the area is presented, followed by a discussion of the standards against which water quality can be judged. There then follows a discussion of the concentrations and occurrence of major ions in groundwaters from the field area. This discussion is based primarily on the chemical and isotope analyses performed on approximately 320 water samples taken from the primary field area (Appendix D); the sampling strategy for these groundwaters was discussed in Chapter 3. A large database of groundwater analyses exists for the Republic of South Africa, to which the author was granted access and these analyses are also considered. Sampling points for both data sets are shown in Figure 5.1. Although the distribution and concentration of fluoride is of primary significance in the study of fluorosis, the chemical characteristics of the groundwater are also of interest, and provide insight into the occurrence of high fluoride groundwater. It will be shown in this chapter that several chemical parameters are present in the groundwater of the western Bushveld at concentrations above recommended safe limits. It is well beyond the scope of this thesis to discuss remediation of groundwater; the reader is referred to Fejerskov *et al.* (1988) for a discussion of defluoridation techniques.

The trace element data, based on a subset of the samples collected for this study, is then presented and discussed, followed by a description of the stable and radioactive isotope results for groundwaters in the study area.

5.2 Previous work

Bond (1947) undertook a major survey of groundwater chemistry in the Union of South Africa, and generally described groundwaters based on their host lithology. He noted that groundwaters from the Bushveld granites and felsites and from the Pilanesberg Complex have similar chemical characteristics, although groundwater from the granites and felsites have appreciably higher Cl concentrations than that from the Pilanesberg. He presented 10

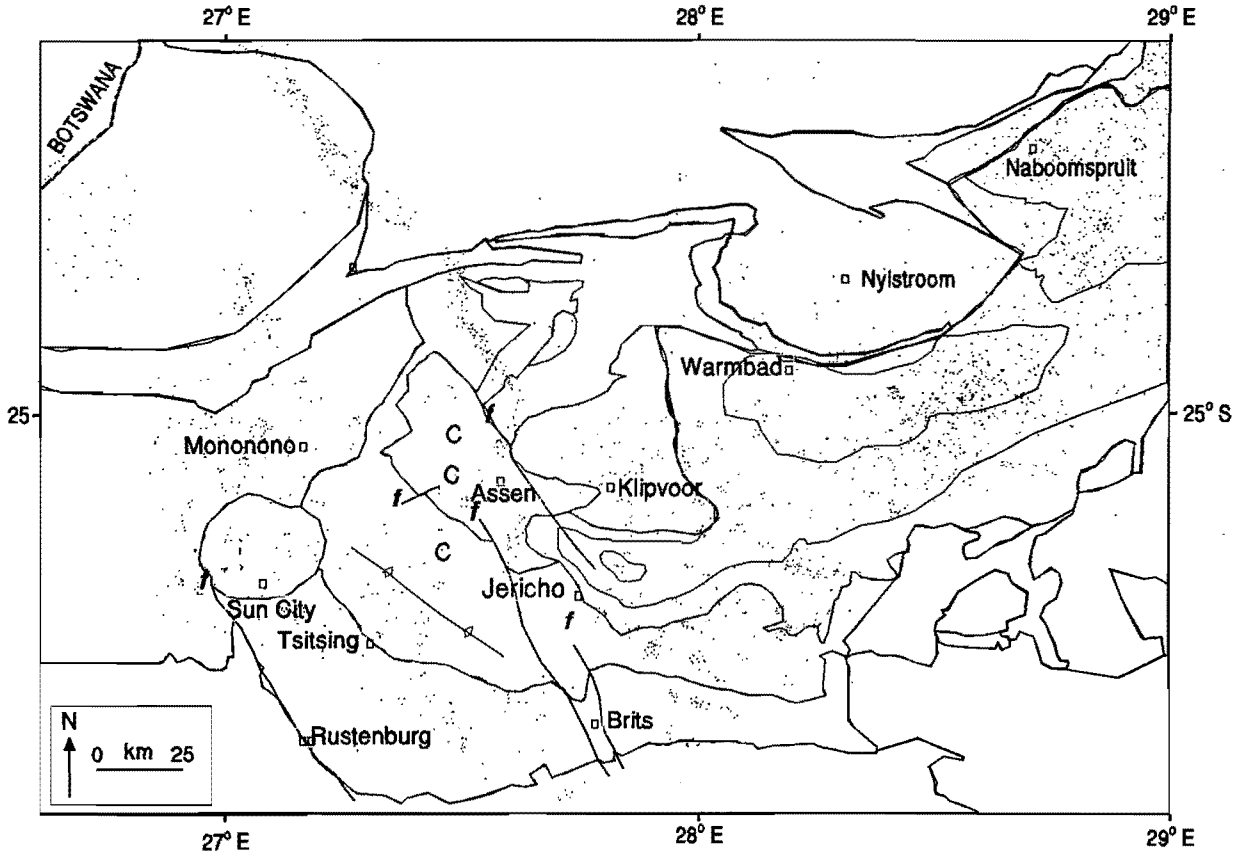

Figure 5.1 Sampling locations in the extended study area. Lines represent lithological boundaries (see Figure 1.3)

rock analyses and noted the high alkali content of the aforementioned lithologies. He asserted that high F is present in Pilanesberg groundwater as NaF. He conjectured that the water from the Warmbaths spring is magmatic in origin. He also compared the water of the Pretoria Saltpan (PSP) crater with that in the surrounding rocks. PSP water has similar ionic proportions to surrounding groundwater, apart from the readily precipitated Ca, Mg and Si. PSP water has a greatly increased concentration overall, which he ascribed to evaporation of inflowing groundwater from the Nebo Granite. Bond could find no fluorite in his rock samples and so ascribed F in groundwater to the dissolution of apatite.

McCaffrey (1993) studied the hydrochemistry of major, trace, lanthanide and actinide elements, as well as stable and radioactive environmental isotopes in the Pilanesberg Complex. It was postulated that two different water types exist in the complex, one with a long residence time and very high F^- concentrations, the other with a shorter residence time and moderately elevated F^- values.

5.3 Water quality standards

Standards for ions and physico-chemical parameters in drinking water have been published by various agencies for use internationally (WHO, 1993) and in South Africa (CSIR, 1991; DWAF, 1996). The recommendations of the CSIR (1991) are in the simple form of "no risk", "low risk" and "high risk" ranges. DWAF (1996) is a comprehensive summary of water quality and its associated effects, and its recommendations are in broad agreement with the recommendations of CSIR (1991). However, the recommendations are in the form of health and other effects associated with varying levels of concentration and cannot easily be summarised or converted into a graphical form. The standards used here are, therefore, those of the CSIR (1991) and are shown in Table 5.1.

5.4 Physico-chemical parameters

Although no borehole log is associated with samples taken in the field for this study, each sample has been classified according to presumed host rock by digitising the relevant 1:250000 geological maps and performing a spatial join using ARC/INFO. Sixteen host rocks were identified for initial groundwater classification purposes, which in decreasing age order are the Archaean Granite, Chuniespoort and Pretoria Group sediments of the Transvaal Sequence, Rustenburg Layered Suite basic rocks, Rashoop Granophyre, Nebo Granite, Lebowa Granite, Rooiberg Felsites, Pilanesberg Complex nepheline syenite,

Table 5.1 Recommended limits of chemical parameters in South African domestic drinking water, based on health effects. Source: CSIR (1991). All values in mg/ℓ, except EC and pH.

Parameter	Maximum limit of no risk	Low risk range	High risk limit
EC (mS/m, 25°C)	300	300-400	>400
pH low	5.5	5.5-4.0	<4.0
pH high	9.0	9.0-11.0	>11.0
Ca	200	200-400	>400
Mg	100	100-200	>200
Na	400	400-800	>800
K	400	400-800	>800
Cl	600	600-1200	>1200
SO_4	600	600-1200	>1200
F	1.5	1.5-3.0	>3.0
NO_3 as N	10.0	10-20	>20

Carbonatite, Letaba basalt, Ecca, Irrigasie and Clarens formations of Karoo age, Waterberg sandstone and Quaternary deposits. Figure 5.2 shows the abbreviations used to represent these lithologies in later figures. In these figures the lithologies, plotted on the X axis, have been ordered thus: age decreases to the right, and degree of fractionation of the igneous rocks increases to the right; igneous rocks on the left (AG-Lt), sedimentary rocks on the right (Ch-Qu). This allows the identification of age, fractionation and genetic trends.

The results are described for each element, with reference to the host lithology where features of significance exist. Histograms of the distribution of physico-chemical parameters in groundwater from 16 lithologies are presented in Appendices E1 to E11.

5.4.1 Electrical Conductivity (EC) and Total Dissolved Solids (TDS)

EC and TDS are highly correlated (Figure 5.3), as is to be expected from electrochemical theory. Groundwaters scatter around the trend, especially at higher ionic strengths. The scatter is probably due in part to the differences in ionic composition of each groundwater. This alters the proportion of ions with small hydrated ionic radii, modifying the electrolytic behaviour of the groundwater. The slope of the regression line is within the limits of 5.5 to 8.0, suggested as typical by Lloyd and Heathcote (1985). EC tends to increase disproportionately at TDS concentrations above 1000 mg/ℓ, possibly because the Na-Cl

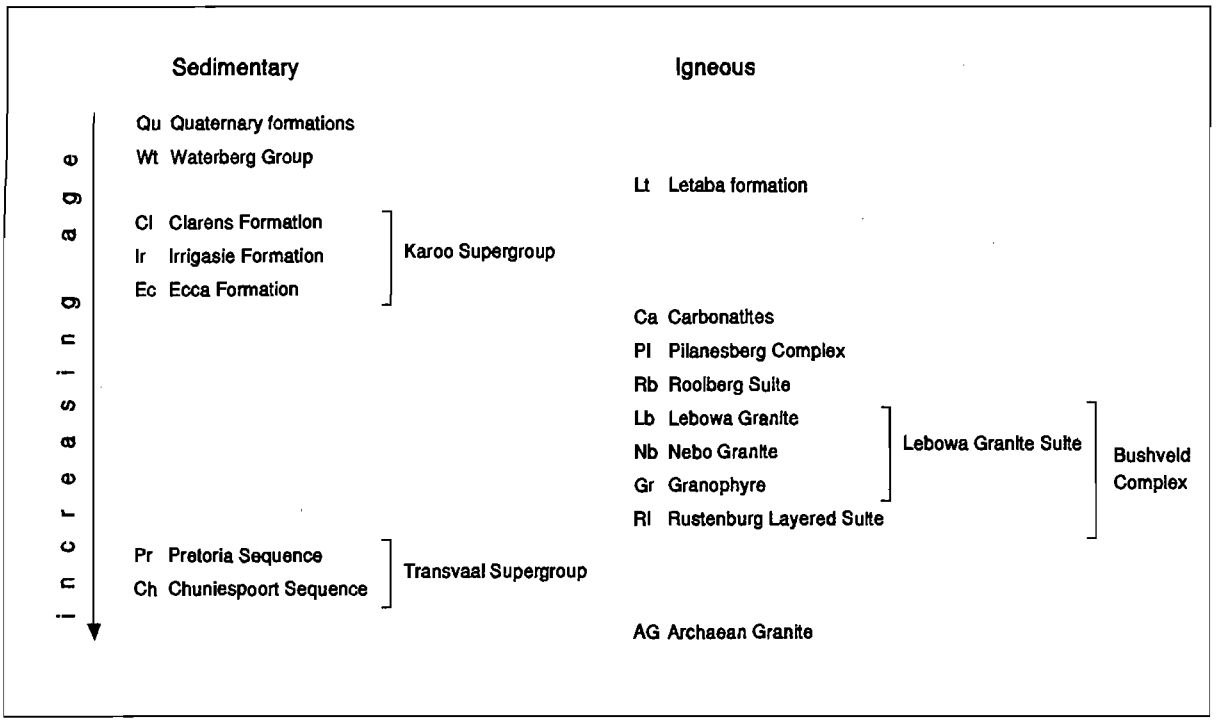

Figure 5.2 Key to abbreviations used in the following figures.

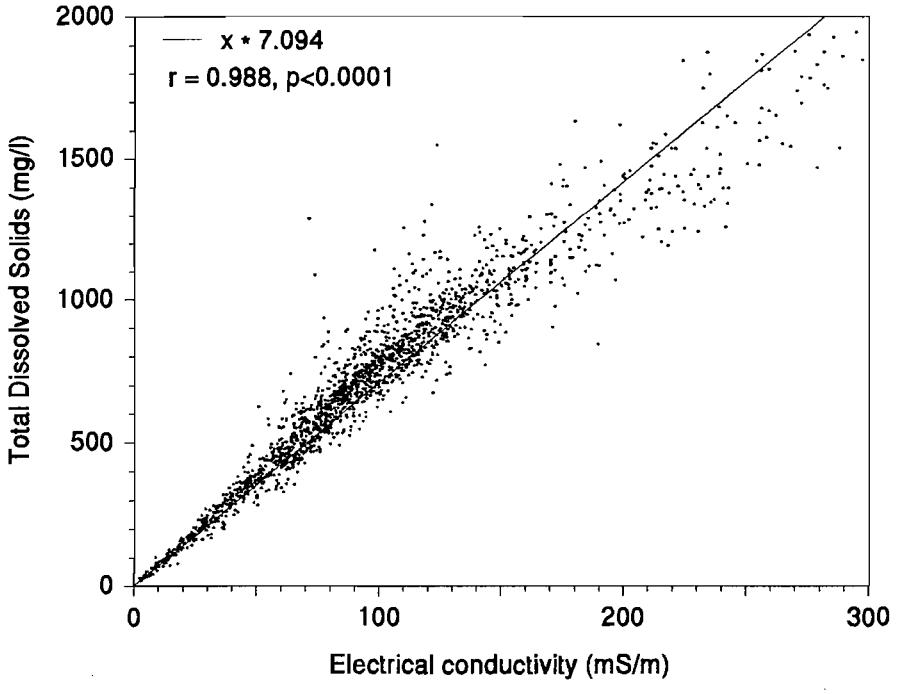

Figure 5.3 EC *vs.* TDS for RSA and Bophuthatswana analyses. An excellent correlation is evident.

compositions which dominate brackish and briney groundwater compositions are better electrolytes than the Ca-CO_3 compositions of fresher waters.

Groundwater from the carbonatites has the highest mean EC, whilst the Letaba Formation and Irrigasie formation groundwaters have very high maximum EC values. No lithology has a mean above the low risk maximum health limit, but many have maximum EC above this limit (Figure 5.4). Apart from a sample from the Pretoria Saltpan, no brines (TDS > 10g/ℓ) were sampled.

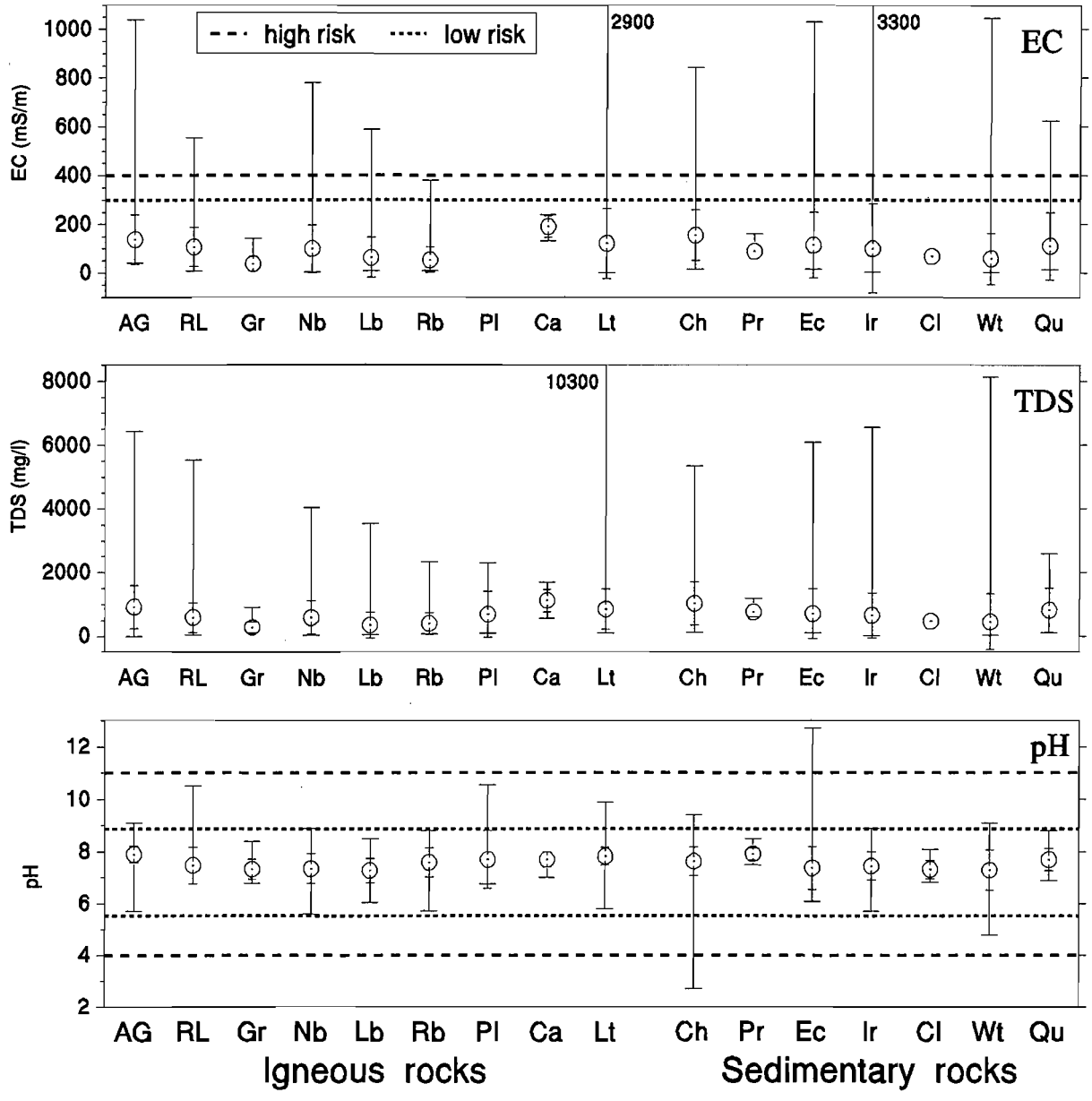

Figure 5.4 Summary statistics for EC, TDS and pH in groundwater from 16 lithologies. In this and following figures, circles mark the mean, small ticks show ±1 standard deviation, large ticks are minimum and maximum values.

5.4.2 pH

Only Pilanesberg groundwaters, which have a number of high pH values, deviate significantly from the normal distribution expected for pH (see Appendix E3). The Archaean Granite has the highest mean pH, at 7.9, whilst the Chuniespoort Group has a sample, from the RSA database, with a pH of 3.0 (Figure 5.4).

5.5 Major elements - Anions

The analytical results for cations and anions are presented in Appendix D1. Histograms of the distribution of anions in groundwater from 16 lithologies are presented in Appendices E1 to E11.

5.5.1 Fluoride

A histogram of F^- concentration in groundwater for the entire study area is plotted in Figure 5.5. The median concentration is 0.2 mg/ℓ, whilst the mean is 1.43 mg/ℓ; the population is strongly skewed towards high F^- concentrations. The distribution is not Gaussian even when transformed logarithmically. Although the tail of the histogram is irregular, there is an increased frequency of F^- values between 2.6 and 4.9 mg/ℓ. Figure 5.6 show histograms of F^- concentration in the 16 major lithologies of the study area, and Figure 5.7 presents summary statistics for each of these lithologies.

Fluoride is found at low concentrations in most samples from the Rustenburg Layered Suite, with a mean of 0.4 mg/ℓ F^-. High values occur in isolation and these may be due to Pilanesberg Dykes. Of interest are the histograms for the Lebowa Granite and the Pilanesberg Complex. Fluoride concentrations are high in the acid parts of the Bushveld Igneous Complex (BIC), but with the two granites showing very different levels of groundwater F^-. Nebo Granite groundwater has a mean concentration of 2.0 mg/ℓ F (Figure 5.7). Much higher values were determined for samples from the Lebowa Granite, reaching over 10 mg/ℓ and having a higher mean value (3.9 mg/ℓ). The Lebowa groundwater F^- histogram approximates a normal Gaussian distribution, whilst the Nebo does not. Groundwater around the Pretoria Salt Pan, which is hosted in Nebo granite, had F^- concentrations up to 20 mg/ℓ, and the brine in the pan had a F^- value of 195 mg/ℓ. This is in direct contradiction to the findings of Ashton and Schoeman, (1983), who found that F^- concentrations in the Pretoria Saltpan brine were generally below their detection limit. Although they did not specify a detection limit, they report a concentration of 0.14 mg/ℓ F^- in the springwater entering the pan, and it is assumed that their detection limit

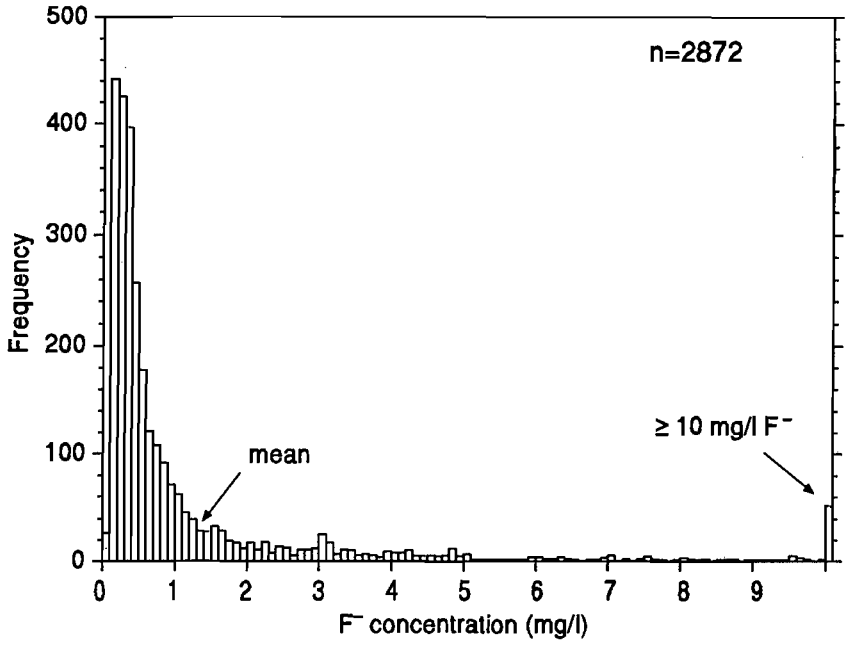

Figure 5.5 Groundwater fluoride histogram for all sites.

was below this value. The Rooiberg Group has a number of elevated F^- concentrations as well as a group of low concentrations. The two populations may reflect the heterogenous nature of the Rooiberg Group (see section 1.3.3). The Pilanesberg has two types of F^- enriched groundwater, a high F^- type occurring in the centre of the complex, and a much higher F^- type occurring on the perimeter of the complex (McCaffrey, 1993). The complex as a whole has the highest mean groundwater F^- concentration of any of the rock types in the study area, at 15.0 mg/ℓ. Concentrations on the perimeter of the complex reach 80 mg/ℓ F^- at the Quarantine Camp borehole, although values for the perimeter are in the range of 40 to 80 mg/ℓ F^-. Fluoride concentrations within the geographic boundaries of the Complex range from 2 to 7 mg/ℓ and approximate a normal gaussian distribution. No systematic variation in F^- values with the various foyaite bodies has been discerned.

Groundwater taken from boreholes in the outcrop area of the Ecca shales have a mean value of 2.3 mg/ℓ F^-. The majority of samples have less than 3 mg/ℓ F, but outliers occur at much higher values. The groundwater from boreholes in the outcrop areas of the Irrigasie and Clarens Formations, in the central part of the basin, have lower mean F^- concentrations, at 1.0 and 0.9 mg/ℓ F^- respectively, (Figure 5.7) and there are fewer high F^- outliers than in the Ecca.

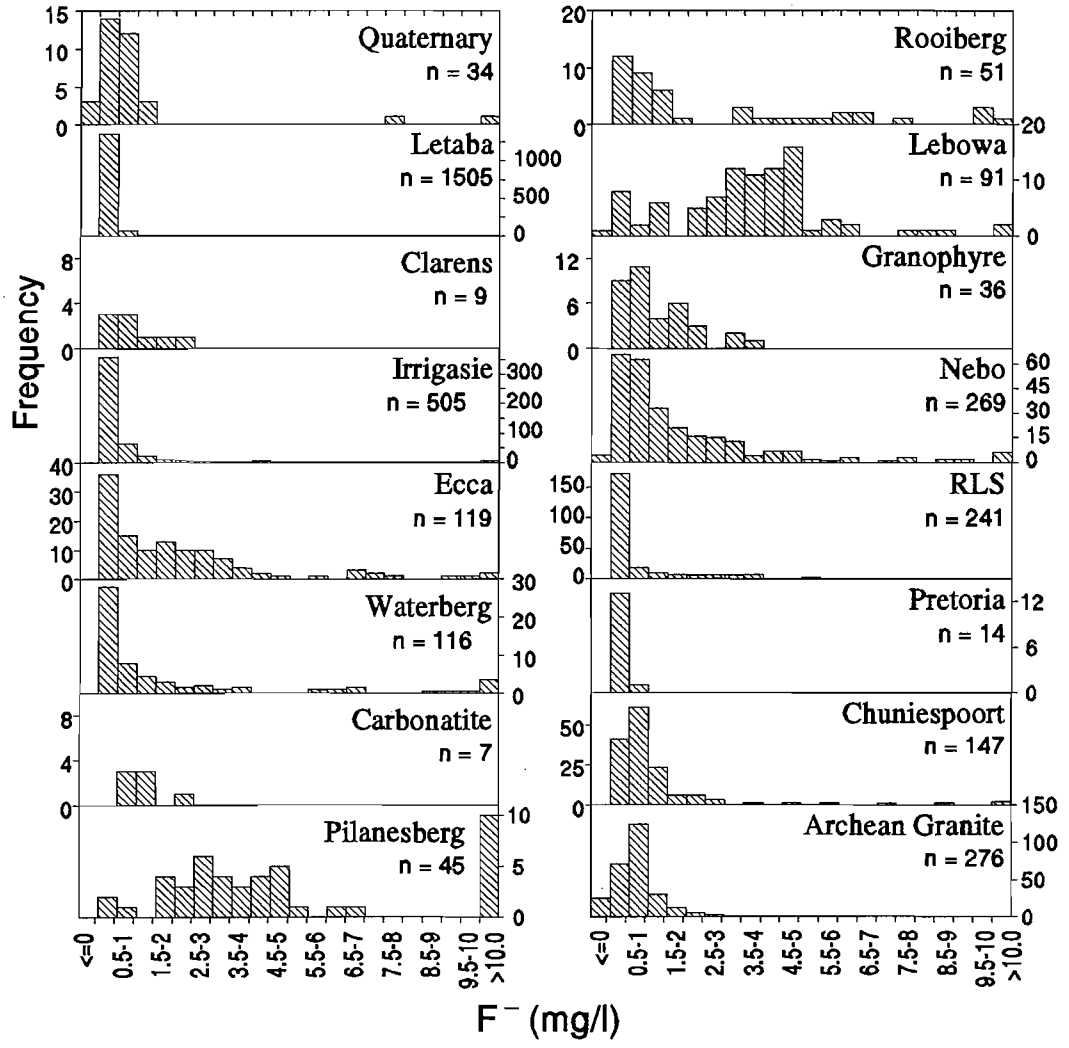

Figure 5.6 Summary statistics of F^- in 16 lithologies from the western Bushveld. Symbols as for figures 5.2 and 5.4.

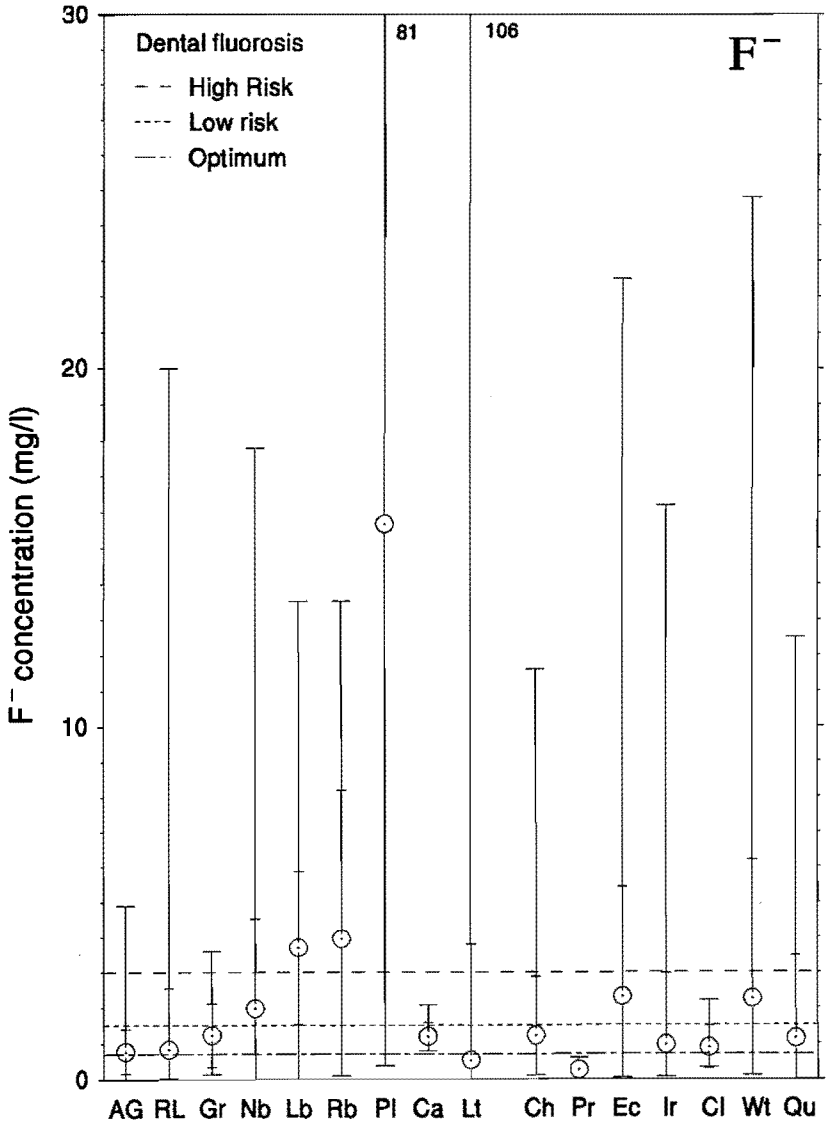

Figure 5.7 Summary statistics of F^- in 16 lithologies from the western Bushveld. Symbols as for figures 5.2 and 5.4.

5.5.2 Chloride

It is striking that the carbonatites have a very high mean concentration of Cl in groundwater (Figure 5.8), but because of the small number of samples (n=6), this may not be significant. No clear trend is apparent for either the igneous or the sedimentary rocks. None of the lithologies have a mean concentration even approaching the low risk health limit, but, as with EC and TDS, several have maximum values well above this range.

5.5.3 Nitrate

Mean nitrate concentrations exceed the high risk health limit in several of the lithologies, principally the RLS, Nebo Granite and Letaba formations (Figure 5.8). None of these lithologies contain significant amounts of N-bearing minerals, and so the high values are almost certainly of anthropogenic origin. McCaffrey (1993) showed that high NO_3 values in RLS groundwaters to the west of the Pilanesberg were spatially associated with villages.

5.5.4 Sulphate

High mean concentrations of sulphate (>100 mg/ℓ) are found in the carbonatites and the Chuniespoort Group, whilst elevated levels (>50 mg/ℓ) occur in the Archaean Granite, RLS, Ecca and Irrigasie formations. All of the mean sulphate concentrations are well below the low risk health limit. These levels are probably related to weathering of sulphide minerals which are known to occur in these rock types.

5.6 Major elements - Cations

Summary statistics for cations are presented in Figure 5.9.

5.6.1 Calcium

The highest mean Ca concentration in groundwater occurs in the carbonatite. The Letaba basalt and Chuniespoort Group also have elevated concentrations. The Granophyre and Pilanesberg have quite low mean Ca concentrations in groundwater. No clear trend is seen in the BIC, but the rocks of the Karoo sedimentary sequence host groundwater with a Ca concentration which decreases with increasing stratigraphic level.

5.6.2 Magnesium

Mean Mg concentrations in groundwater are all less than the low risk limit (CSIR, 1991). High mean concentrations are present in the RLS and Letaba formations (composed of

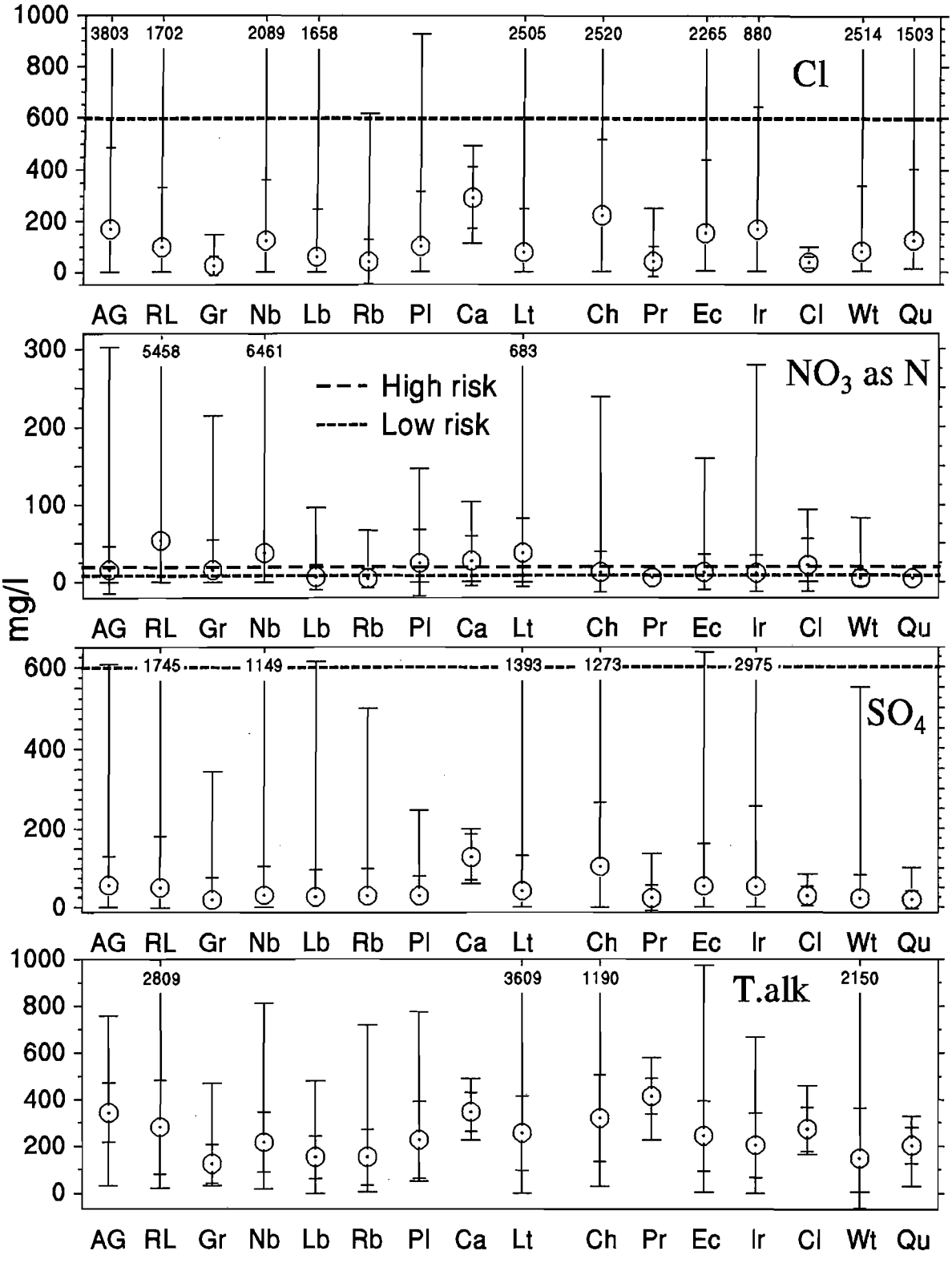

Figure 5.8 Summary statistics for Cl, NO_3 as N, SO_4 and total alkalinity from 16 major lithologies from the western Bushveld. Symbols as shown in figures 5.2 and 5.4.

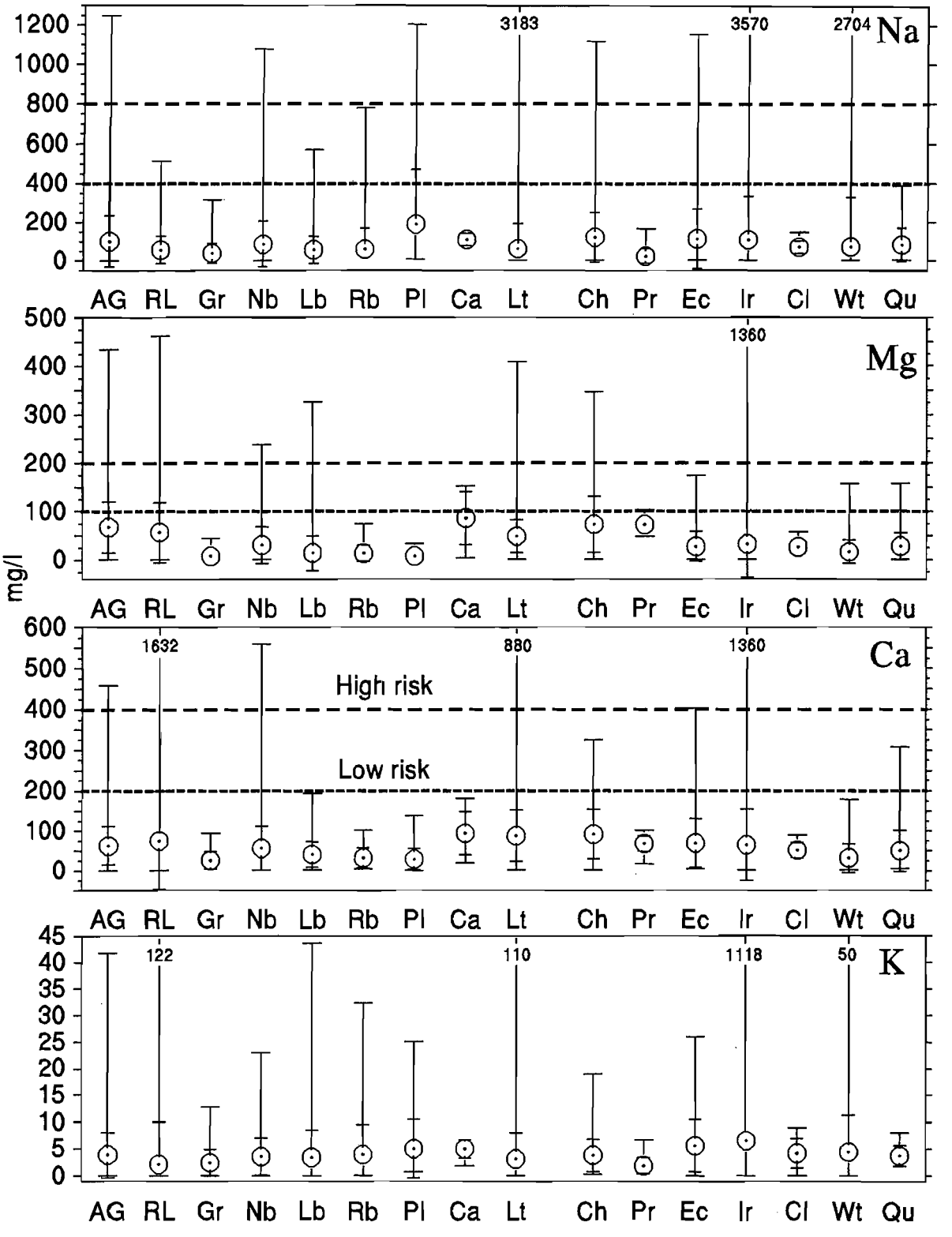

Figure 5.9 Summary statistics for cation analyses from 16 lithologies from the western Bushveld. Symbols as shown in Figures 5.2 and 5.4.

mafic minerals), the Chuniespoort Group (predominantly dolomite), the Archaean Granite and the carbonatites.

5.6.3 Sodium

Of the igneous rocks, the Pilanesberg groundwaters have the highest mean concentration of Na, whilst the concentration is similar in all the BIC lithologies. The relative concentrations of Na are very similar to those of Cl, apart from the Pilanesberg. Several of the lithologies, notably the Lebowa Granite, Rooiberg and Pilanesberg, have groundwater with maximum Na concentrations greater than the low risk limit.

5.6.4 Potassium

No clear trend of mean K concentration with rock type is evident. The Irrigasie Formation groundwaters are notably enriched in K. The vast majority of analyses are below the low risk health limit.

5.7 Covariation of elements

The variation of the major ions against each other is shown as a scattergram matrix in Figure 5.10. Also shown is the correlation coefficient (r) value of the regression equation for each element pair. Most of the values tend to be low, often as the result of outliers. Correlations are considered significant when r is above 0.5. Positive correlations are seen between F and K, F and Na, Na and K, Na and Cl, and Cl and K. A weak correlation exists between F and Cl. These covariances can be explained either by salinisation, evaporation or by ion exchange mechanisms. The covariance of Ca with F is discussed in detail in the following chapter.

5.8 Trace elements

5.8.1 Introduction

Groundwater samples from 8 of the 16 lithologies were analysed for trace elements (see Chapter 3). It is possible that these trace elements are important in the metabolism of F^- and therefore in the incidence of fluorosis. The formation of fluoro-complexes, such as those formed by Al and Zn, could conceivably prevent F^- from being metabolised in the human body, and complex formation could influence the total F concentration in

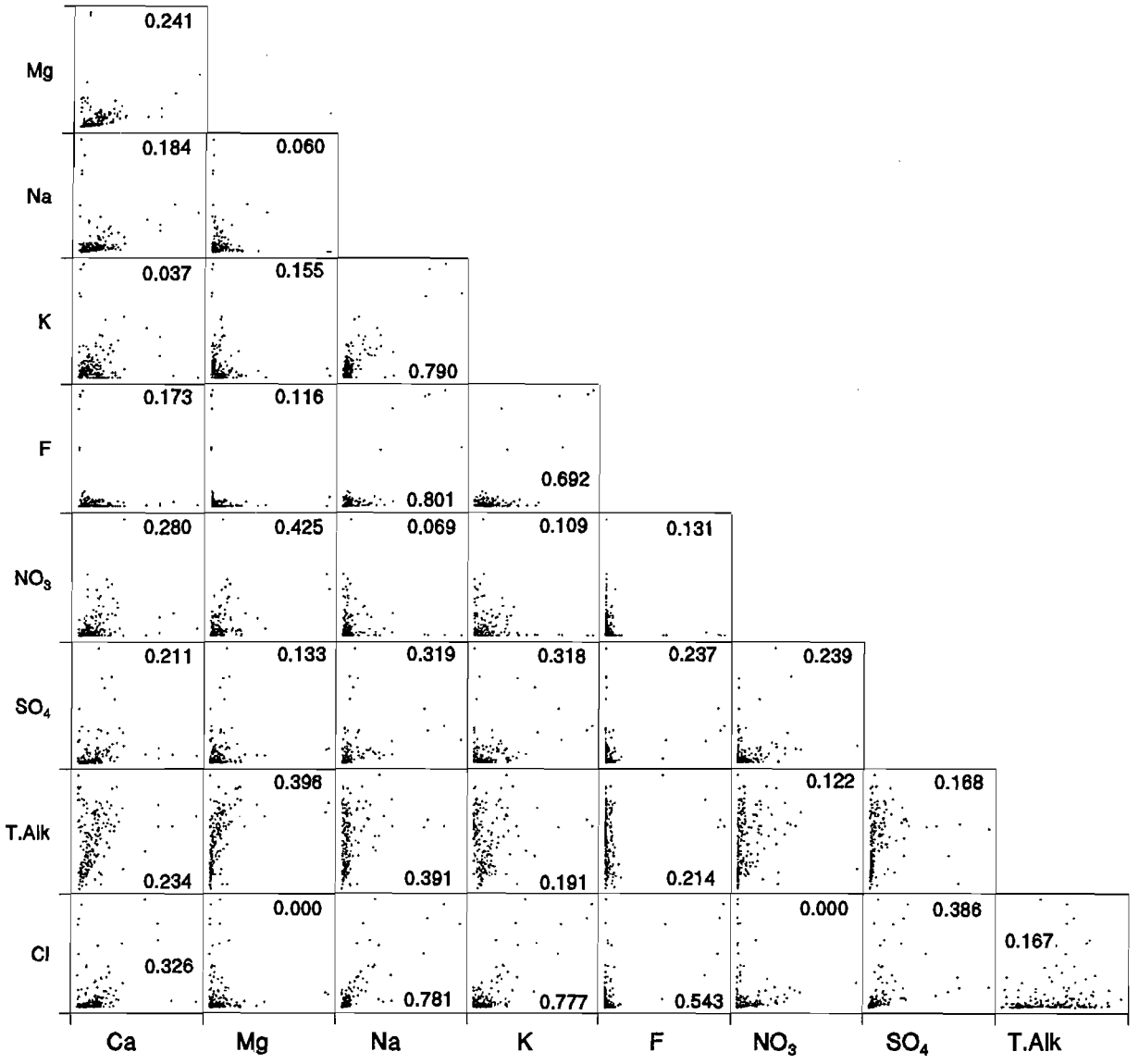

Figure 5.10 Scattergram matrix and correlation coefficients for major ions in groundwaters from the study area.

groundwater. Iodide was included in this study because it has been suggested that F^- competes with I^- in the thyroid gland (Day and Powell-Jackson, 1972). The results are discussed in descending order of mean concentration, apart from Sr, Al and I, which are discussed in more detail at the end of the section. Trace element patterns in groundwater are briefly discussed by rock type at the end of this section.

5.8.2 Results

Summary statistics (mean and standard deviation) are shown graphically in Figure 5.11 and figure 5.12 for 8 of the 16 lithologies. The method for calculating statistics in the following figures is detailed in Appendix F. The full analyses are listed in Appendix D2.

Maximum concentrations are shown in Figure 5.13. These figures follow the previous format, igneous rocks on the left (RL-Pl), sedimentary rocks on the right (Ec-Cl).

Zinc. Zinc occurs in appreciable quantities in groundwaters of the region, especially in the Pilanesberg Complex, where one sample is above the maximum safe limit (10 mg/ℓ: CSIR, 1991). No trend is seen in the BIC groundwaters, but Zn concentration increases in Karoo groundwaters from lower to higher stratigraphic units.

Molybdenum. Little variation is seen in Mo concentration, which is generally at very low levels, close to the detection limit. However, Lebowa Granite groundwater has a mean concentration above the maximum safe limit of 0.2 mg/ℓ. Molybdenum is an element frequently enriched in pegmatites and other highly fractionated rocks.

Barium. Interesting and very clear trends appear in the Ba concentration of these groundwaters. Barium concentrations are much lower in groundwaters of the BIC than those of the Karoo rocks, and decrease with increasing fractionation of the host rock. This is the opposite trend from that expected from a fractionating magma. Mean Ba concentration in groundwater from the Karoo sediments clearly decreases in higher stratigraphic units.

Lithium. There is no clear trend for Li concentration in BIC groundwaters, but Li concentrations in the Karoo groundwaters decrease markedly from lower to higher stratigraphic units. This trend is more pronounced than that for Ba.

Lead. Only the Lebowa Granite, Ecca and Clarens formations have groundwater with a mean Pb concentration above the detection limit.

Vanadium. Most of the analyses for vanadium are below the detection limit. Only groundwaters from the RLS, Nebo granite and Clarens formation have mean values above the LLD.

Copper. No trend in Cu concentrations can be identified in groundwater from the BIC, but in the groundwater of the Karoo sediments Cu decreases from the Ecca shales to the Clarens sandstone.

Arsenic. Most arsenic determinations were below the LLD. Nebo granite groundwater has elevated As concentrations, but the maximum is well below the low risk health limit.

Chromium. Most of the results are below the detection limit and the mean values cannot be used with confidence. The maximum Cr concentration in RLS groundwater is predictably higher than that of the more acidic lithologies.

Cobalt, Cadmium and Nickel. These three elements have concentrations generally below the detection limit and the identification of trends from the means is pointless. The maximum values, whenever above the LLD, show no meaningful trends.

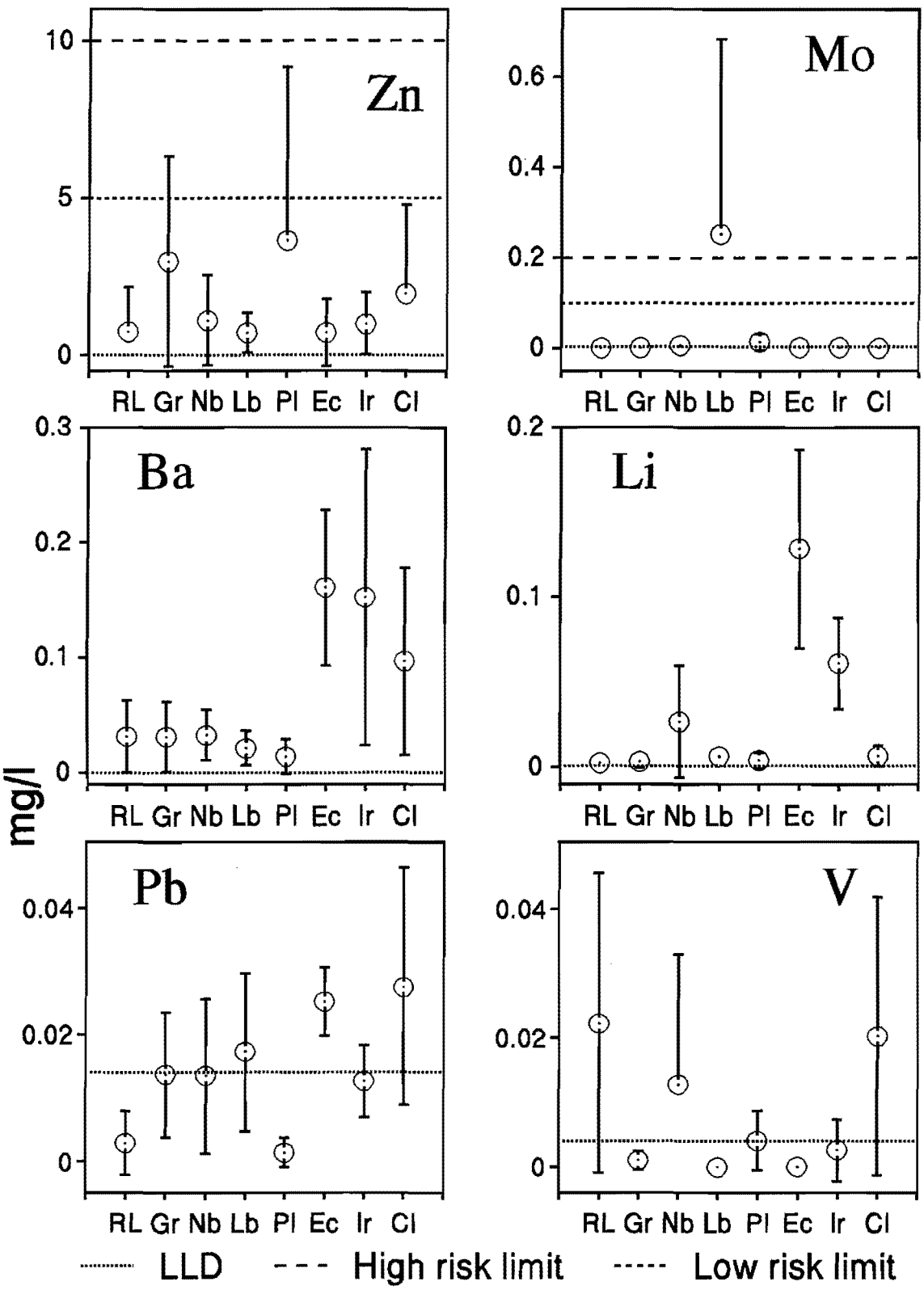

Figure 5.11 Mean concentrations of Zn, Mo, Ba, Li, Pb and V in groundwater from 8 major lithologies in the western Bushveld. Point in the circle represents the mean, bars represent one standard deviation.

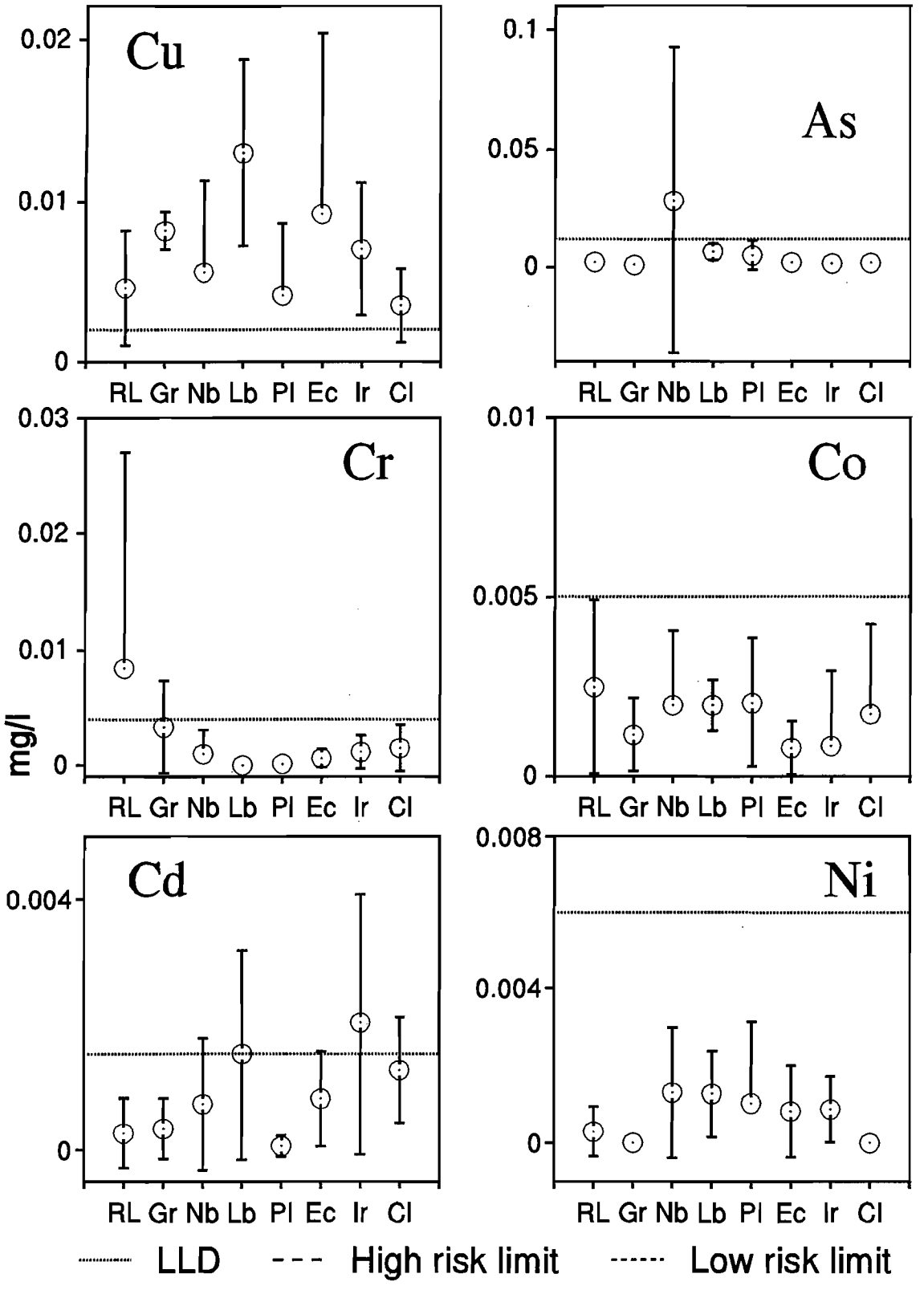

Figure 5.12 Mean concentrations of Cu, As, Cr, Co, Cd and Ni in groundwater from 8 major lithologies from the western Bushveld. Point in circle represents the mean, bars are one standard deviation.

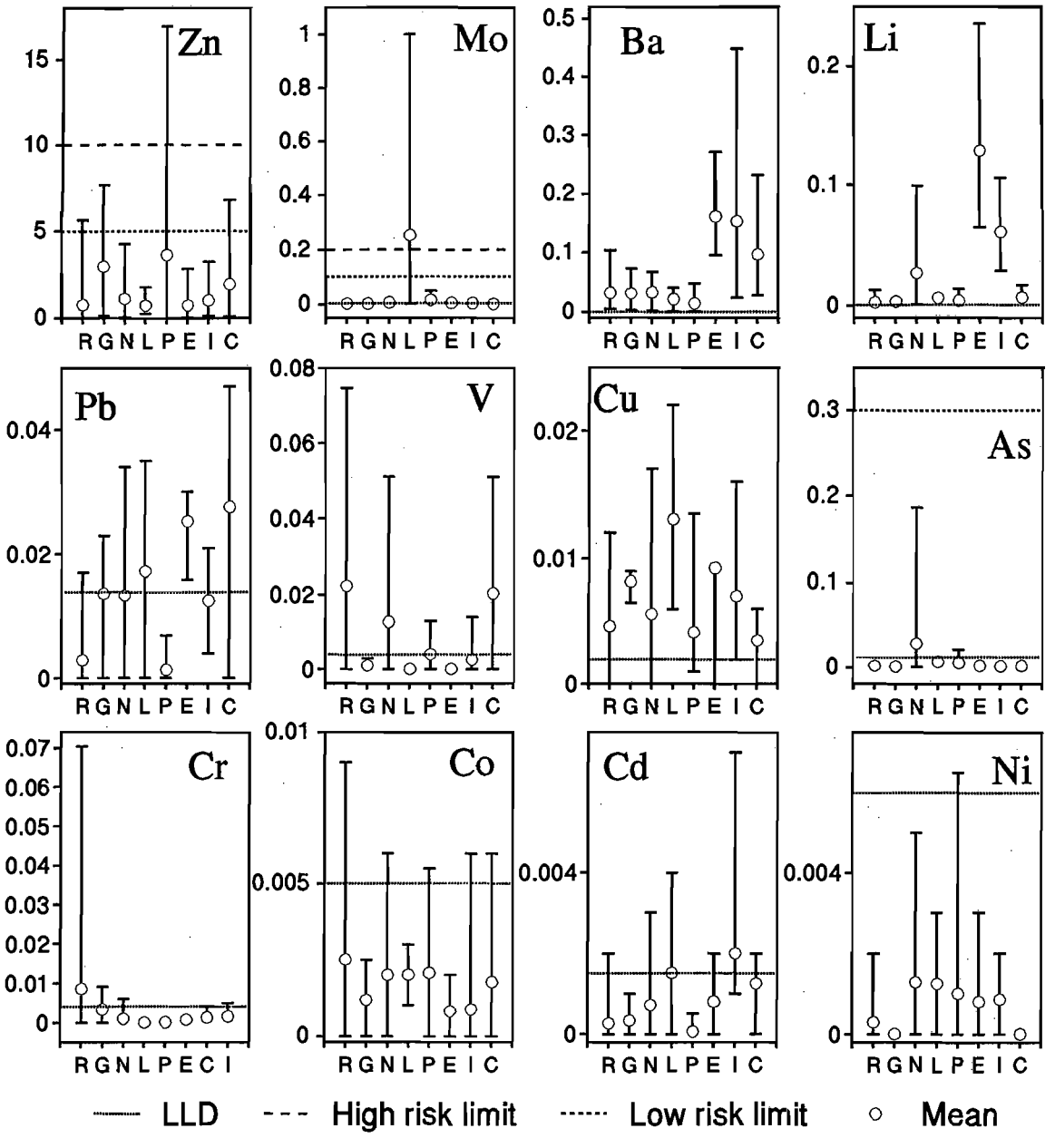

Figure 5.13 Minimum and maximum concentrations (bars) of trace elements in groundwater. Circles represent the mean.

5.8.3 Iodide

The iodine data, shown in full in Appendix D3 and summarised in Table 5.2, is for a sub-set of the acidified samples. The detection limit, calculated as 3 times the baseline noise, was 1 ppb (South African Institute for Medical Research, *pers. comm.*). Twenty-one of the samples had no detectable iodide, 11 had between 1 and 20 µg/ℓ, 16 had between 20 and 100 µg/ℓ and 4 had over 100 µg/ℓ. Notably, water from the Pretoria Saltpan lake had a very high iodide concentration, of 641 µg/ℓ.

Matthess (1982) stated that 'the iodide content in most fresh waters should lie below the detection limit', but did not put a value to that limit or detail the analytical method. Fuge (1989) stated that the mean for I in spring and well waters in the United Kingdom was 4.11 µg/ℓ. The World Health Organisation recommends an intake of 100 µg/ℓ per day (W.J. Kalk, Dept. Medicine, Div. Endocrinology, University of the Witwatersrand, *pers. comm.*).

Given that I^- is present in rainwater at concentrations generally less than 5 µg/ℓ (Fuge, 1988), and that the field area is over 1000 km from the nearest source of marine-derived I^- aerosol, the results, 39% of which exceed 20 µg/ℓ, would indicate that I^- in the groundwaters of the study area is derived from weathering of rocks. The very large variations in I^- concentration also suggest that atmospheric deposition is not a factor. The discussion of I^- levels in groundwaters around the world in Fuge (1989) indicates that those groundwaters of the western Bushveld with >20 µg/ℓ I^- are anomalously enriched. Summary statistics for I^- concentration from 8 lithologies are shown graphically in Figure 5.14. It is apparent that high concentrations occur in the Irrigasie formation, which is predominantly shaley (Section 1.3.3). The Ecca formation also shows elevated concentrations. The Pilanesberg has the highest I^- concentration in groundwater contained in the igneous rocks, but no clear trend is seen from basic through acid to undersaturated rocks. This is in accordance with the fact that I^- concentrations in most igneous rock types are similar, at approximately 0.25 ppm (Fuge,

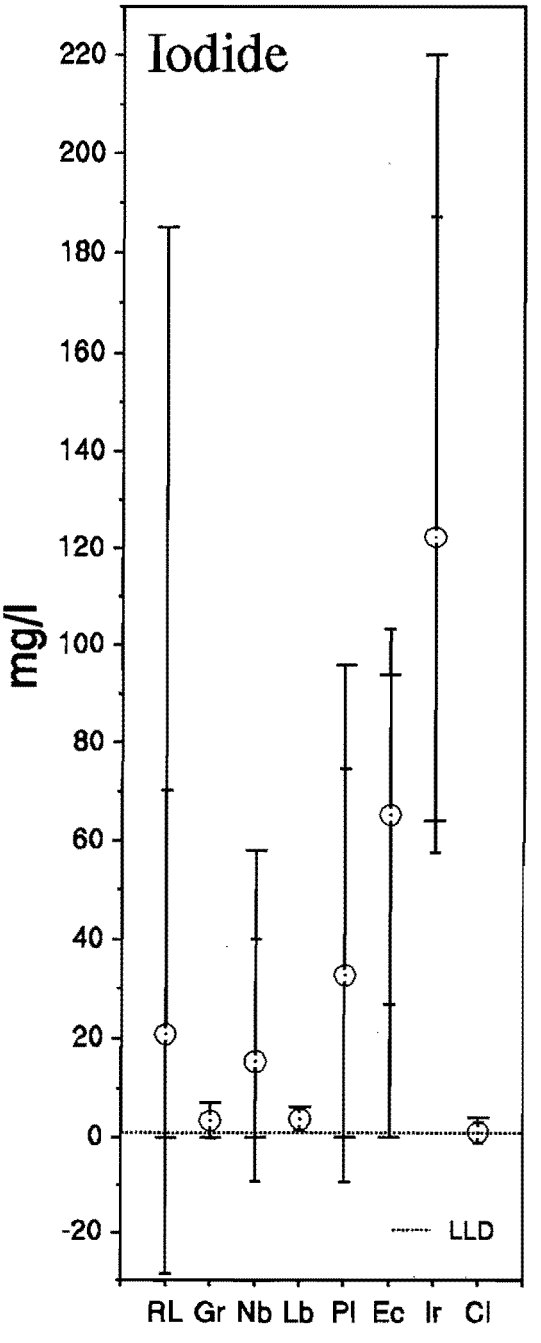

Figure 5.14 Summary statistics for iodide in groundwater from the field area. Abbreviations and symbols as in figures 5.2 and 5.4.

1996). It is of interest to note that F^- has been implicated as a goitrogen in areas of low groundwater I^- (Day and Powell-Jackson, 1972). It is further noted that the Lebowa Granite has some of the lowest I^- and highest F^- groundwater concentrations in the area. Goitre does occur in the western Bushveld (W.J. Kalk, Dept. Medicine, Div. Endocrinology, University of the Witwatersrand, *pers. comm.*), and F^- may play an important role in its occurrence.

Table 5.2 Summary statistics of iodide concentrations in groundwater from the BIC, Pilanesberg Complex and Karoo sediments. Concentrations in $\mu g/\ell$. See Appendix D3 for original analyses.

Lithology	Iodide, $\mu g/\ell$		
	mean	std. dev.	number
RLS	21	49	17
Granophyre	3	4	3
Nebo Granite	15	25	5
Lebowa Granite	4	2	3
Pilanesberg	33	42	7
Ecca	65	38	5
Irrigasie	122	65	6
Clarens	1	2	4

5.8.4 Strontium

Although present at very low concentrations, Sr is of importance when using Sr isotopes in the study of groundwater provenance. Sr should behave similarly to Ca in the geochemical environment (Section 1.3.7), and Figure 5.15 shows that in the more fractionated (Ca and Sr poor) rock types of the BIC, the groundwater becomes increasingly impoverished in Sr. The Pilanesberg, known for its high Sr content (Lurie, 1974) and which contains the mineral strontianite (see Appendix B4) has a mean groundwater Sr concentration similar to that of the RLS. The Karoo sediments show a decreasing trend from lower to higher stratigraphic units. The Ecca and Irrigasie formations both have groundwater with moderately high (>1 mg/ℓ) Sr concentrations.

5.8.5 Aluminium

Generally an element with low solubility at normal pH levels, Al concentrations peak in Pilanesberg groundwater (Figure 5.16), where pH values greater than 10 occur (Section 5.4.2). BIC and Karoo groundwaters show no clear trends in Al concentration.

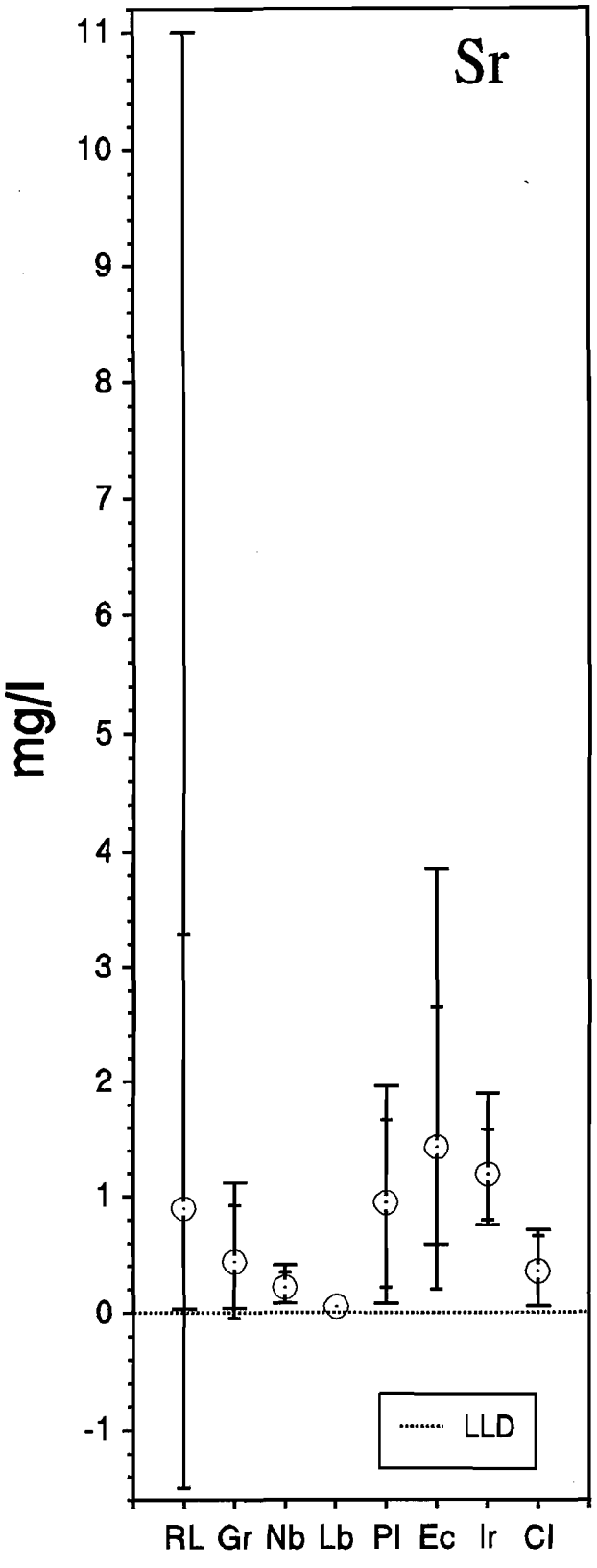

Figure 5.15 Summary statistics for Sr concentration in groundwater from the western Bushveld.

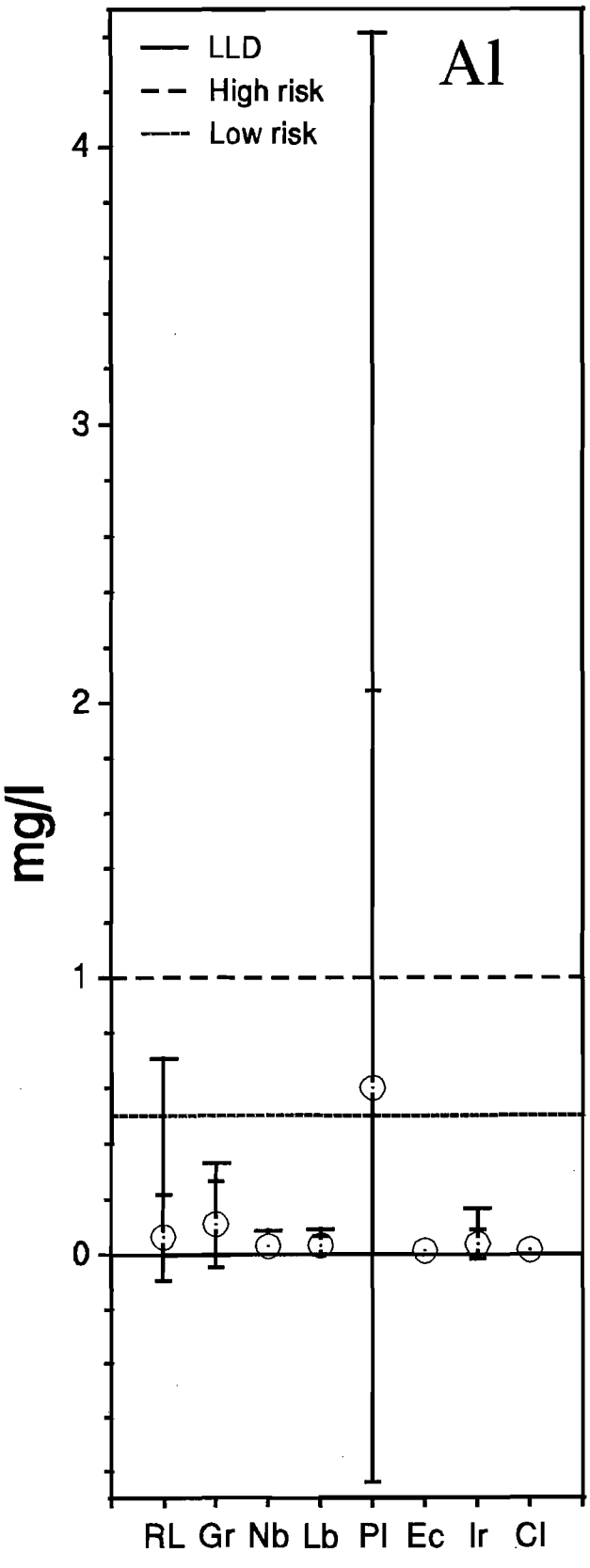

Figure 5.16 Summary statistics for Al concentration in groundwater from the western Bushveld.

5.8.6 A summary of trace element concentrations in groundwater by host rock type.

It is noted that groundwater from each rock type is characterised by typical high and low values of certain trace elements. It is also noted that the geochemical succession from basic to highly evolved acidic magma in the BIC is paralled by the concentration of certain of the trace elements in groundwaters contained within those rocks. The groundwaters contained within the Karoo rocks also show strong compositional trends.

Igneous Rocks. The groundwaters of the RLS are high in the chalcophile elements V and Cr. Indeed, only RLS groundwaters contain Cr above the detection limit. Granophyre groundwaters are high in Zn and Cu, whilst Nebo Granite groundwaters are high in Li and very high in As. The Lebowa Granite groundwaters have high concentrations of Pb, Mo, Cu and Cd, and are notably low in Zn, Ba and Sr. Groundwaters from the Pilanesberg complex are noted for their high Zn and Al concentrations, and low concentrations of Ba and Cu.

Sedimentary Rocks. Groundwaters from the Ecca formation, at the base of the local Karoo stratigraphy, are very high in Li, Ba, Cu and Sr. Those from the Irrigasie formation are high in Ba, Cd and I, whilst Clarens formation groundwaters are high in Zn, Pb and V, and low in Li, Cu, I and Sr. Trends can be seen in the mean groundwater concentrations from the Karoo rocks, with Zn and Sr increasing in concentration from the Ecca shales to the Clarens Sandstones, and Ba, Li and Cu decreasing in the same direction. No trend is shown by Mo, Pb, As, Cr, Cd, Ni or Al. Iodine is present at the highest mean concentration in groundwaters from the formation with the highest proportion of shales, the Irrigasie.

5.9 Temporal variation

A number of boreholes were resampled to determine possible temporal variation in chemical composition. Sites 298 and 299 were resampled at an interval of approximately 1 year, whilst the other sites were sampled after an interval closer to two years. The results are shown in Figure 5.17. There is a great deal of variation, especially in NO_3^- and SO_4^{2-}. To a lesser but still significant extent, the measured concentrations of the other major ions also vary with time. The anion concentrations vary most at site 34, just west of the Pilanesberg, where Cl^- has replaced NO_3^- and SO_4^{2-} as the dominant anion, and Ca^{2+} shows a marked increase over time. Site 298 has a significant decrease in its Ca^{2+} and Mg^{2+} concentrations, whilst the Na^+ and K^+ concentrations in the groundwater at site 233 have decreased over the sampling time.

Fluoride shows the least temporal variation (Figure 5.18). This may be because F^- is buffered by dissolution-precipitation reactions, where kinetic factors can be important,

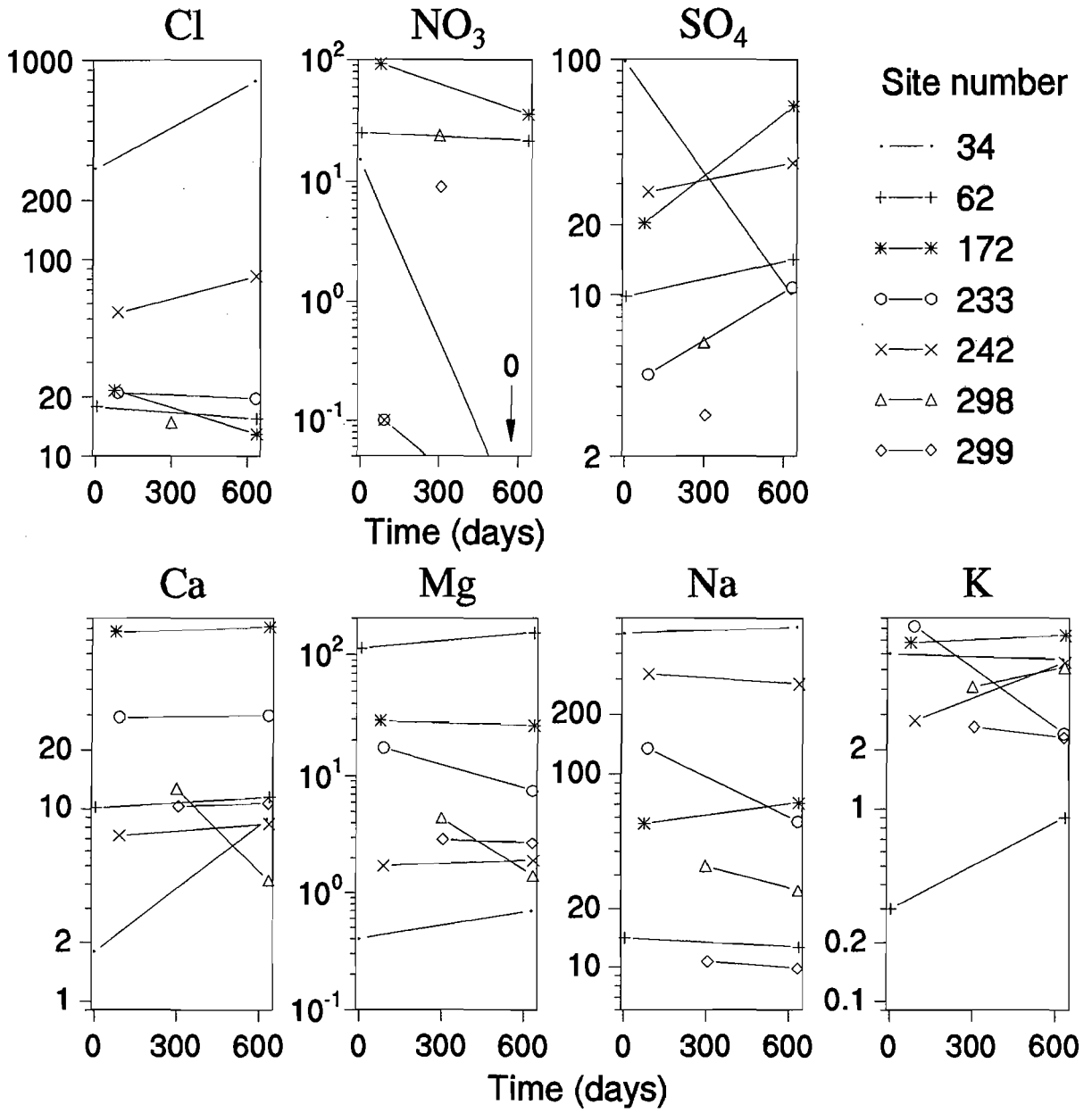

Figure 5.17 Variation in groundwater ionic determinations with time from resampled boreholes. Concentrations are expressed in mg/ℓ.

whereas the concentration of other major ions are controlled more by dilution and concentration. Chapter 6 contains a discussion of the kinetics of fluorite dissolution. Temporal variation in groundwater is not well documented in South Africa; the inauguration of a national groundwater chemistry monitoring network in 1996 should rectify this.

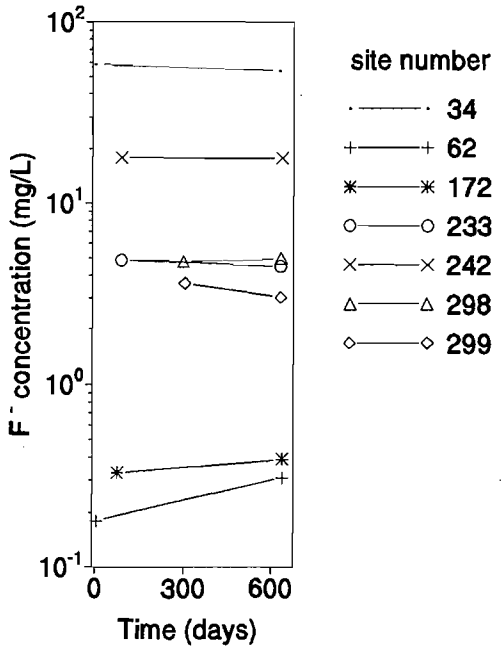

Figure 5.18 Temporal variation of fluoride concentration in groundwater from resampled boreholes.

5.10 Results of isotopic analyses

The isotope ^{14}C (radiocarbon) and the ratio of the isotopes $^{18}O/^{16}O$, $^{2}H/^{1}H$ and $^{87}Sr/^{86}Sr$ have been used in this study to provide information on the rate and nature of geohydrological processes which have a bearing on the concentration and location of high F^- groundwaters. Radiocarbon analyses haves been used to estimate the mean residence time (or 'age') of groundwaters, and thus allows an estimate of rates for hydrogeochemical reactions and the speed of natural processes. The study of the stable isotopes of hydrogen and oxygen allow an estimation of the degree of evaporation to which a groundwater has been subjected. Strontium isotope ratios may be used as natural tracers to indicate whether high F^- groundwaters found in one aquifer may have originated in another. The results are presented in Table 5.3 and discussed in the following sections. Figure 5.19 shows the sampling locations.

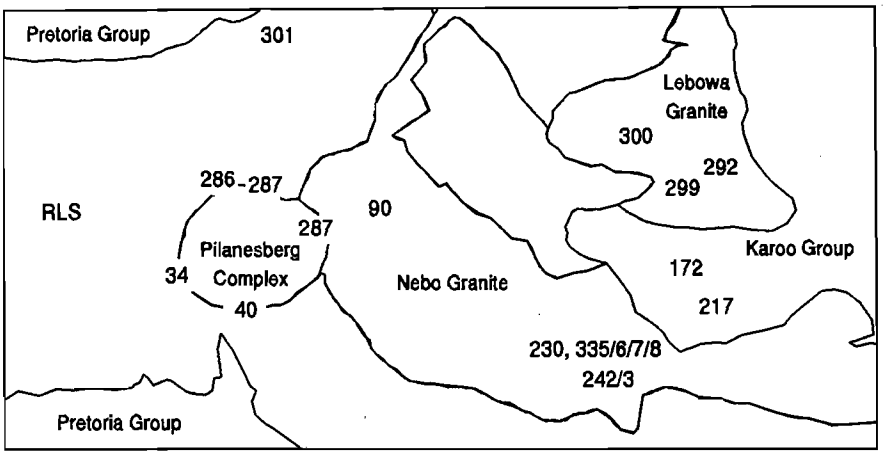

Figure 5.19 Location of samples taken for isotope analysis.

5.10.1 Environmental Isotopes

Oxygen and hydrogen isotopes. Marked differences in oxygen and hydrogen isotope ratios occur in the groundwater of the field area (Figure 5.20). The results for $\delta^{18}O$ in groundwater, range from -5.69 ‰ from the Quarantine Camp borehole to -2.03 ‰ from a borehole in the yard of Mr Mon's Trading store, 1 km from the Pretoria Saltpan. It is apparent that the $\delta^{18}O$ values of these groundwater samples vary according to the host lithology; Pilanesberg groundwater has a $\delta^{18}O$ of between -5.7 and -4.5 ‰ (between -6.4 and -3.8 ‰ according to McCaffrey (1993)), the Nebo Granite samples have around -4.5 ‰, except for the sample from Mr Mon's borehole. Groundwater samples from the Lebowa Granite are around -3.5 ‰. Groundwater becomes enriched in ^{18}O the further east the sample is taken. Notably, the $\delta^{18}O$ values for samples from the perimeter of the Pilanesberg are low, as predicted by McCaffrey (1993). The analysis of a groundwater sample from the Quarantine Camp borehole yielded a value of -5.69 ‰ in this study. Water from the same borehole was analysed and reported in McCaffrey (1993) as having a $\delta^{18}O$ of -6.4 ‰.

When $\delta^{2}H$ is plotted against $\delta^{18}O$ it is seen that most of the groundwaters plot along the meteoric water line of Craig (1961). Deviations from this line towards higher ratios of hydrogen and oxygen indicate that evaporation has taken place. Pilanesberg central groundwater shows a marked evaporation trend, as noted and discussed in McCaffrey (1993). Lebowa Granite groundwater has a wide range of $\delta^{2}H$ values, with little variation in $\delta^{18}O$. Such variation is difficult to explain.

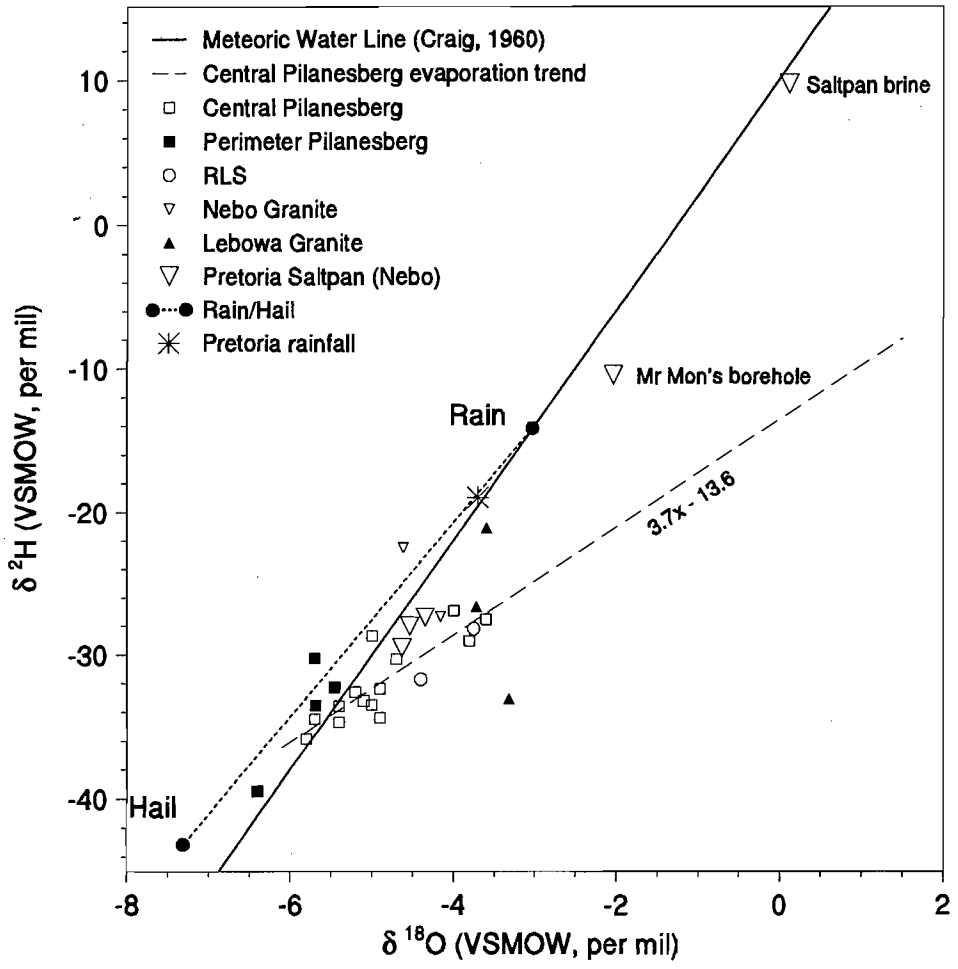

Figure 5.20 O and H isotope analyses for groundwaters from the field area. Extra data on Pilanesberg perimeter groundwater from McCaffrey (1993). Error bars are smaller than the symbols.

Table 5.3 Isotope analyses for groundwater, precipitation and pan water from the study area. See text for details of notation and analysis. 'P' is Pilanesberg, 'N' is Nebo Granite, 'L' is Lebowa Granite, 'RLS' is Rustenburg Layered Suite, 'PSP' is Pretoria Saltpan. Sample types are 'G', groundwater, and 'B', brine from the surface of the Pretoria Salt Pan. '*n/d*' is not determined.

Site no.	Location	Type	Lithology	^{14}C (pmc)	δ^2H ‰	$\delta^{18}O$ ‰	std. dev.
287	Quarantine Camp	G	P	4.0	-33.56	-5.69	*n/d*
286	Letswaaneng	G	P	55.0	-32.27	-5.46	0.01
-	Pilanesberg	Hail	-	*n/d*	-43.17	-7.31	0.07
-	Pilanesberg	Rain	-	*n/d*	-14.18	-3.03	0.02
242	Theledi's Farm	G	N	3.2	-22.49	-4.62	0.01
243	Stinkwater	G	N	63.3	-27.31	-4.16	*n/d*
292	Makoropeja	G	L	9.0	-33.06	-3.31	0.04
299	Klipvoor	G	L	87.5	-26.62	-3.72	0.02
300	Slipfontein	G	L	51.9	-21.08	-3.59	0.03
301	Northam Plat	G	RLS	*n/d*	-28.16	-3.75	0.02
230	PSP Surface	B	-	*n/d*	+9.68	+1.89	0.01
335	PSP, Old artesian	G	N	*n/d*	-27.34	-4.35	0.01
336	PSP, Strat	G	N	*n/d*	-28.00	-4.54	0.02
337	PSP, Museum	G	N	*n/d*	-29.52	-4.63	0.03
338	PSP, Mr Mons	G	N	*n/d*	-10.48	-2.03	0.02

Water from the first 5 cm of the surface of the Pretoria Saltpan had a $\delta^{18}O$ of +1.89 ‰ and δ^2H of +9.68 ‰, a very 'heavy' sample of potentially great significance to the regional geohydrology (see Chapter 6). Also sampled were rain and hail from the same thunderstorm, on the night of the 7th May 1995, which occurred over the Pilanesberg. Rain water was collected in a saucepan, whilst the hail was collected from the centre of drifts up to 50 cm thick found the next day. The difference between the two samples is large and may be influenced by several processes. As these results do not bear directly on the matter of high F^- groundwater, a discussion of their significance can be found in Appendix G.

5.10.2 Radiogenic Isotopes

Radiocarbon. A wide range of radiocarbon (^{14}C) activities has been shown to occur in groundwaters of the field area, from just 2 pmc in a Pilanesberg groundwater (at the

Quarantine Camp) to 98.5 pmc in groundwater at Mankwe Camp, also in the Pilanesberg (McCaffrey, 1993). The two analyses from the perimeter of the Pilanesberg reported here complement the data of McCaffrey (1993). The radiocarbon content of groundwater from Letswaaneng(Table 5.3), on the perimeter of the Pilanesberg, is not as low as predicted in McCaffrey (1993). This may have been caused by an admixture of recent groundwaters due to the difficulties of obtaining an undisturbed groundwater sample in the marshy ground of the sampling site. Groundwater derived from granites also have a wide range of radiocarbon contents, from 3.2 pmc at Theledi's Farm to 87.5 pmc at Klipvoor Dam.

The radiocarbon content of these samples has a marked correlation with F^- content (Figure 5.21), although this may be a function of a small sample set. The use of radiocarbon in the estimation of groundwater residence time and reaction rate is discussed in Chapter 6.

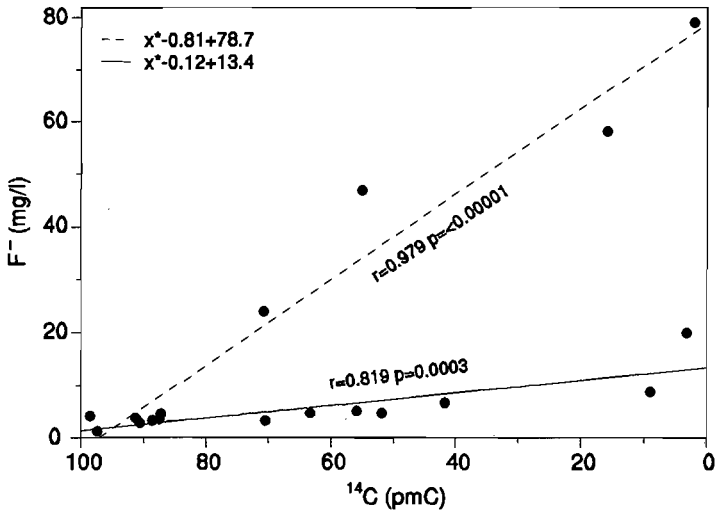

Figure 5.21 ^{14}C plotted against F^-, showing two possible correlations. See text for discussion.

Strontium isotope ratios. The $^{87}Sr/^{86}Sr$ ratios of groundwaters from lithologies of the field area show a wide range of values, from 0.70382 in the Pilanesberg to 0.80284 in the Lebowa granite. Where more than one sample has been taken from the same lithology at different locations, the $^{87}Sr/^{86}Sr$ values are generally similar (within 0.02). The results are shown in Table 5.4, where results have been grouped into lithologies. The results are shown graphically in Figure 5.22. Good discrimination is achieved between groundwaters hosted in different formations. Lebowa Granite groundwater has a significantly different Sr isotope ratio to the other formations. Figure 5.22 also shows the range of Sr isotopic ratios for the host rocks. General similarity between groundwater and host is apparent (i.e. groundwater

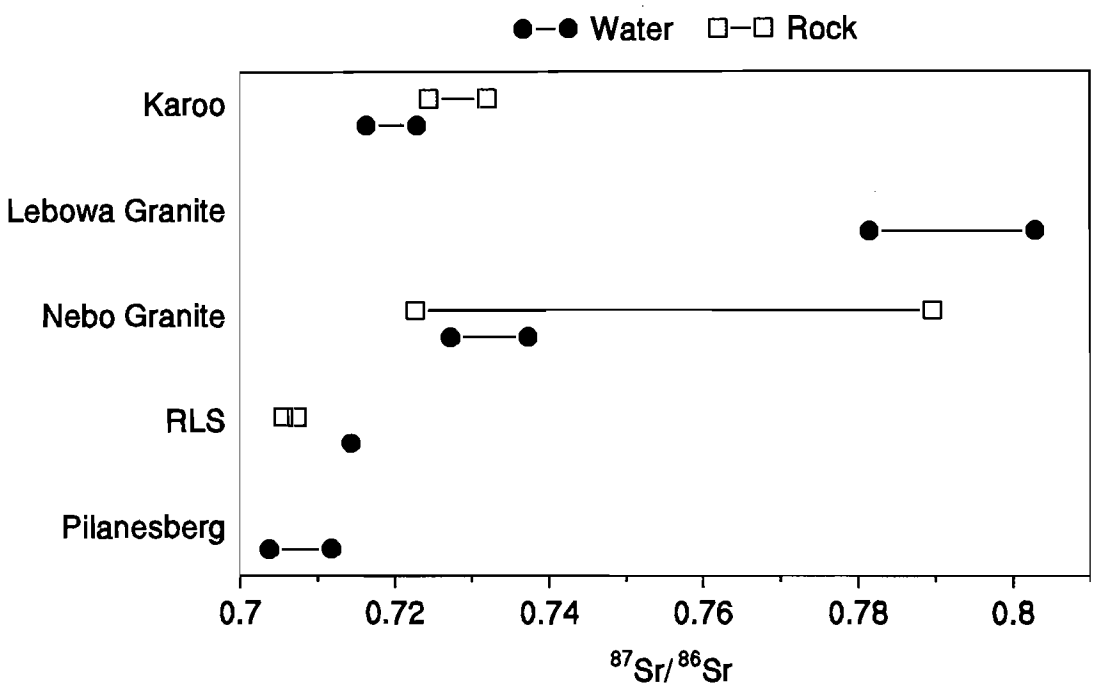

Figure 5.22 Sr isotope data for groundwater and host rocks from the Bushveld. All groundwater and Karoo rock Sr ratios from Radiogenic Isotope Facility, UCT. Values for RLS from Hamilton (1977), Nebo from Harmer (1992).

plots within or near the rock ratios), but no systematic offset is shown. No $^{87}Sr/^{86}Sr$ ratios could be found in the literature for the Pilanesberg Complex or Lebowa Granite.

Sr/Ca ratio and Sr concentration. The Sr/Ca ratios of these groundwater samples are up to two orders of magnitude higher than typical values suggested by Faure (1987) for river water. He found a Sr/Ca ratio of 1.5×10^{-3} for waters draining igneous and metamorphic terrains, and a ratio of 5.0×10^{-3} for waters draining carbonate terrains. Pilanesberg groundwater has a very high Sr/Ca ratio, probably resulting from the high Sr/Ca ratios in Pilanesberg rocks. The comparatively low Sr/Ca ratio found in the Quarantine Camp sample (compared to the other Pilanesberg sample) suggests that this groundwater has been subject to some process which disturbs Ca and Sr concentrations in solution. Of note is the rather large variation of Sr concentration in groundwaters from the same formation, e.g. the Lebowa Granite groundwater and the Karoo formation. These large ranges are not ideal for groundwater characterisation, as is demonstrated in Chapter 6.

Table 5.4 $^{87}Sr/^{86}Sr$ values for groundwater in various lithologies. Samples run by Justin Underwood and Dr Steve Richardson in the Radiogenic Isotope Facility (RIF) at the University of Cape Town. Ca and Sr concentrations in mg/ℓ, analyses performed by Caroline Iets, Department of Archaeology, University of Cape Town.

No.	Site Name	Lithology	Ca	±	Sr	±	Sr/Ca	$^{87}Sr/^{86}Sr$
40	Ledig	Pilanesberg	13.49	0.05	3.28	0.033	2.4×10^{-1}	0.70382
287	Quarantine Camp	Pilanesberg/ Nebo Granite	4.05	0.06	0.13	0.001	3.2×10^{-2}	0.71183
90	Rietspruit	Nebo Granite	35.20	2.36	0.35	0.002	9.9×10^{-3}	0.72728
242	Theledi's Farm	Nebo Granite	8.05	0.10	0.27	0.006	3.3×10^{-2}	0.73732
292	Makoropeja	Lebowa Granite	17.86	0.23	0.70	0.012	3.9×10^{-2}	0.78148
300	Slipfontein	Lebowa Granite	30.48	0.61	0.14	0.003	4.6×10^{-3}	0.80284
172	Sephai	Karoo, Clarens	10.28	0.13	0.10	0.0004	9.7×10^{-3}	0.72290
217	Botshabelo	Karoo, Irrigasie	67.88	1.92	2.98	0.071	4.4×10^{-2}	0.71637
301	Northam Mine	Rustenburg Layered Suite	55.18	0.61	0.24	0.003	4.0×10^{-3}	0.71436

6 DISCUSSION

6.1 Introduction

In this chapter the significance of the results presented in Chapters 4 and 5 will be discussed from several aspects: 1) the health related aspects of groundwater fluoride concentration and speciation; 2) geochemical controls of fluoride concentration and speciation; 3) the hydrochemical systems present in the western Bushveld.

6.2 Health related aspects of fluoride concentration

6.2.1 Fluoride concentration and fluorosis risk

Magnitude of the problem. The results presented in Chapter 5 show that much of the study area is underlain by groundwater having a F^- concentration above both the optimum (~0.7 mg/ℓ) and the recommended maximum concentrations (1.5 mg/ℓ). Spatial analysis by GIS shows that groundwater underlying approximately 17000 km^2 of the western Bushveld has a F^- concentration >0.7 mg/ℓ. Just over 540 of the 3000 groundwater samples have F^- concentrations >1.5 mg/ℓ. Since between 150 and 200 people are supplied by each borehole (BDWA, 1992), approximately 82 000 to 109 000 people are drinking groundwater which may induce dental or skeletal fluorosis.

Distribution of risk areas. It is essential to have a map of areas in the western Bushveld where F^- concentrations in groundwater are above optimum levels. Possible methods of representation include marker size and colour variation, contours and pseudotopographic perspective. Given the variability of F^- concentrations in some areas, such as the groundwater of the Nebo Granite and the Karoo basin, marker size, colour plots and contouring are visually confusing. A perspective view (Figure 6.1) gives a general impression of the distribution of high values, but is not a useful analytical or planning tool. Figure 6.2 shows the preferred method of representing areas of fluorosis risk. The F^- concentration

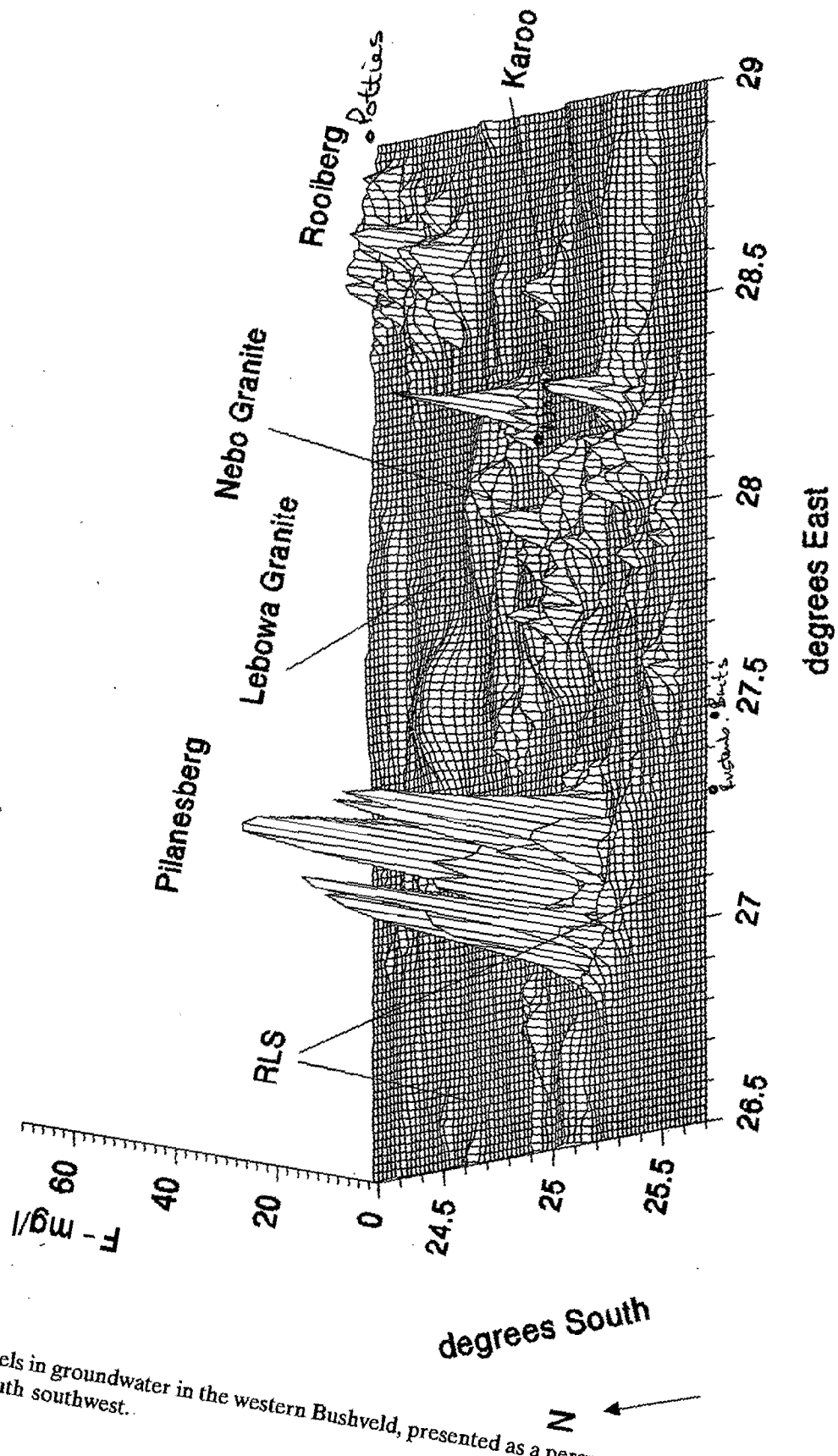

gure 6.1 Fluoride levels in groundwater in the western Bushveld, presented as a perspective topographic view from the south southwest.

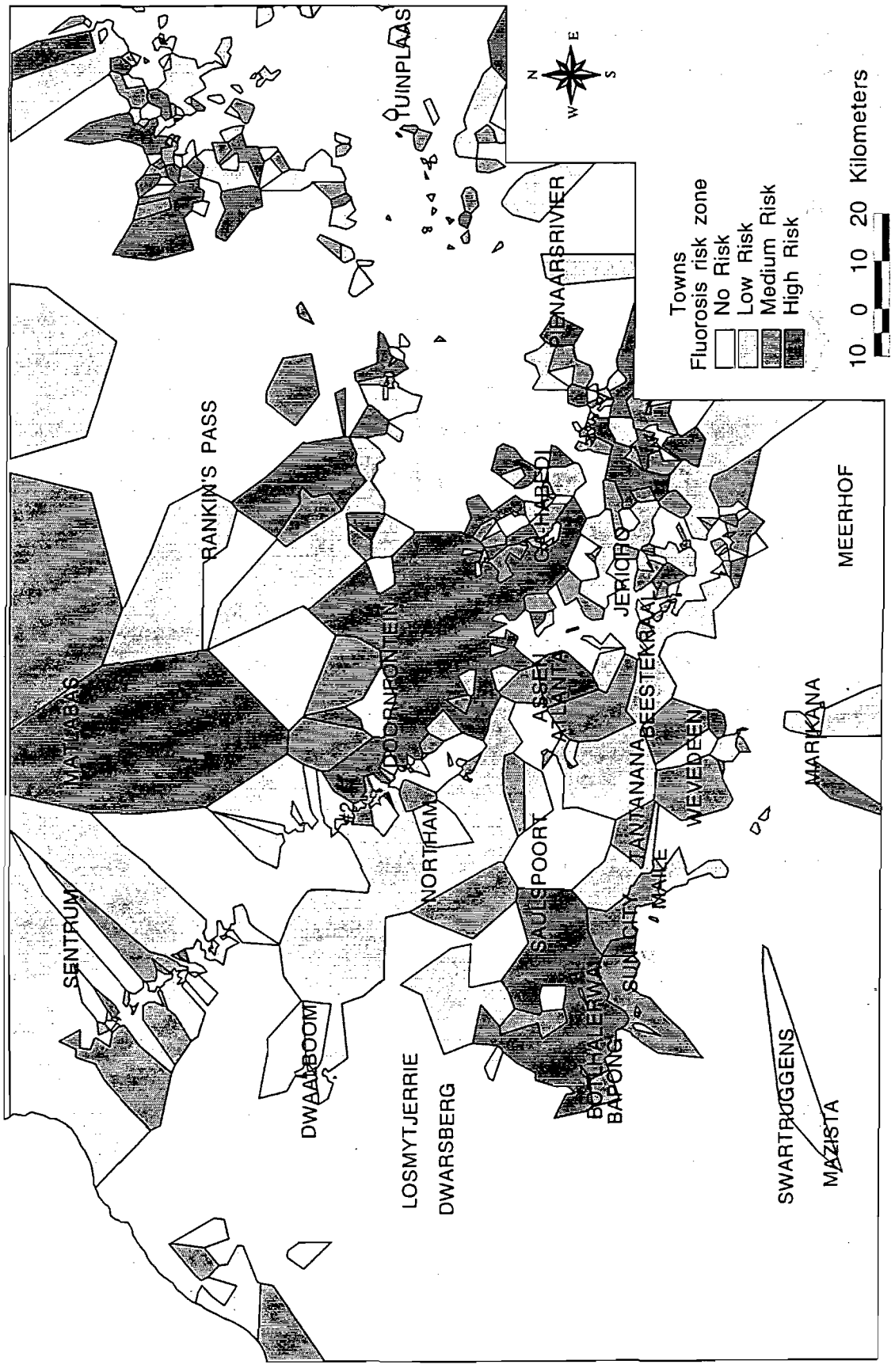

Figure 6.2 Fluorosis health risk zones in the western Bushveld, based on Theissen Polygons. See text for discussion.

of the groundwater was classified into **no risk** (<0.7 mg/ℓ), **low risk** (0.7 - 1.5 mg/ℓ), **medium risk** (>1.5 - 3.0 mg/ℓ) and **high risk** (>3.0 mg/ℓ). Thiessen polygons (Thiessen, 1911) were constructed around each sampling point (i.e. borehole) and classified into risk groups according to groundwater F^- concentration. Adjoining polygons with the same classification were merged. The resulting areas accurately reflect the accessibility of groundwater of different degrees of fluorosis risk. Even in areas of low borehole density this statement is likely to be valid, assuming that no unsampled boreholes exist within the polygon. However, the *size* of the Thiessen polygons *increases* with *decreasing* borehole density, giving them a disproportionate visual impact.

6.2.2 Bioavailability and speciation

It was shown in Chapter 3 that the FISE method using TISAB determines the *total* concentration of F^- in solution. However, F^- can be complexed by Al, Ca, Mg and H ions in solution. These complexes may not be as bioavailable as the free F^- ion but F-complexation may increase the total amount of F in solution, and so thermodynamic modelling of several samples was carried out to estimate the degree of F^- complexation. The computer programme MINTEQA2 (Allison *et al.*, 1991) was used to estimate the speciation of elements in solution, based upon the measured concentration of ions. The same programme also provides estimations of saturation indices for various minerals, and these are used later in the discussion.

MINTEQA2 is a public domain software package, notable for its relative ease of use. However, the thermodynamic database upon which calculations are based is not internally consistent (P. Wade, CSIR, *pers. comm.* 1995) and so the conclusions reached must be treated with caution. The copy of MINTEQA2 used here was implemented on a 386 personal computer running at 40 MHz, and was obtained from the Computing Centre for Water Research. Calculations for each water analysis generally took less than 60 seconds.

Table 6.1 shows the results of speciation calculations made by the programme MINTEQA2, based upon all water analyses with Al concentration >0.050 mg/ℓ. It is apparent that in five out of eight samples, less than 5% of F^- is complexed by Al, Mg or Ca, and that Mg is the strongest complexing ion in these samples. The majority of F exists in the form of the free fluoride ion, F^-. Only at site 109 does the groundwater have a high percentage of complexed F^-. This groundwater has very low F^- and high Ca^{2+}, Mg^{2+} and Al concentrations. In such cases where the amount of F^- is very low, the complexation of F^- by Al is of little biological or quantitative hydrochemical significance. It can be concluded that in almost all Bushveld area groundwaters the formation of Al-F complexes

will not significantly increase the amount of F in solution. However, in many waters the complexation of F^- by Mg is probably an important factor in controlling the F^- concentration. Complexation of Al by other aqueous species is discussed in the next section.

Table 6.1 Speciation calculations of F^- complexation in groundwaters with >0.050 mg/ℓ Al. Species which contribute less than 1 % of the total are ignored.

Site	Analysed (mg/ℓ)				Speciation calculated by MINTEQA2 (% of total F)					
	Al	Ca^{2+}	F	Mg^{2+}	F^-	MgF^+	CaF^+	$AlF_3°$	AlF^{2+}	AlF_2^+
27	0.118	49.7	3.54	12.1	94.3	2.0	-	2.2	-	-
37	4.416	11.2	2.05	2.8	97.2	-	-	1.4	-	-
74	0.162	14.9	69.4	4.5	99.1	-	-	-	-	-
103	0.154	101	0.08	59.1	91.2	7.7	1.0	-	-	-
108	0.064	6.35	0.12	1.73	93.6	5.7	-	-	-	-
109	0.707	1630	0.09	460	69.5	22.1	6.1	-	1.0	1.1
155	0.168	61.6	0.95	9.4	97.8	1.3	-	-	-	-
201	0.091	3.5	5.51	1.6	96.2	-	-	2.6	-	-

Speciation of F inside the human body. The speciation calculations above were made at the temperature and pH which was measured at the well head. It is of interest to determine the speciation of ions within a biological system, since such speciation may be significantly different from that found underground.

In order to model the speciation of ions in a typical groundwater under the conditions of the human stomach, the pH must be reduced to around 3, and the temperature increased to 37°C. Although the water would be mixed with the other stomach contents, and thus the ionic composition would change, for the purposes of this simulation the stomach is assumed to contain only stomach acid (HCl). It can be seen from Figure 6.3 that complexation of F^- by Al is only slightly affected by changing pH. With decreasing pH, the percentage of $AlF_3°$ increases at the expense of AlF_2^+ and MgF^+. This effect is swamped by the conversion of free F^- to HF°. The concentration of total F in groundwater, even at concentrations likely to cause fluorosis, is too low to allow the HF° to be dangerous as an acid. Residence time of F in an empty stomach is in any case very short, at approximately 30 minutes (Backer Dirks, 1992).

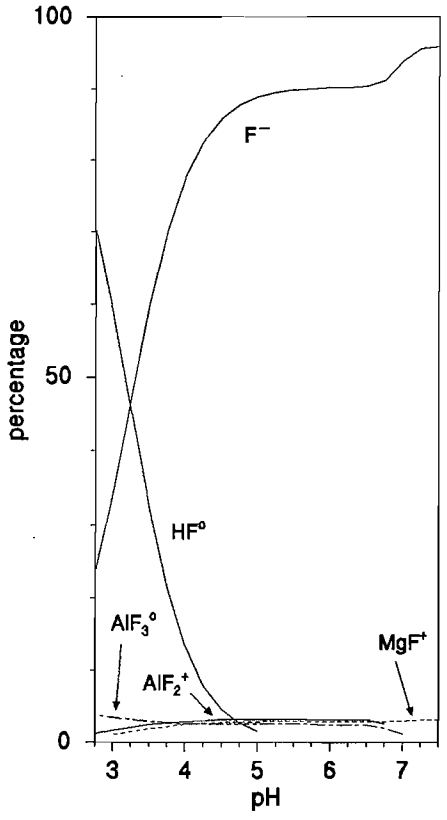

Figure 6.3 Speciation of F^- in water from site 27, down to a pH found in the human stomach and at 37°C, calculated using MINTEQA2 and assuming a stomach containing only stomach acid (HCl) and no food.

6.2.3 Other elements

Groundwaters from the field area often have concentrations of several trace elements in excess of South African health guidelines. These will be discussed briefly.

Aluminium. The solubility of Al^{3+} is very low at the pH usually found in groundwater, whilst it increases at very high (>10) and very low (<4) pH levels. A plot of pH against aluminium concentrations (Figure 6.4) for groundwaters of the western Bushveld shows that no clear trend exists. Water at near neutral pH usually has less than 0.02 mg/ℓ (Roberson and Hem, 1969).

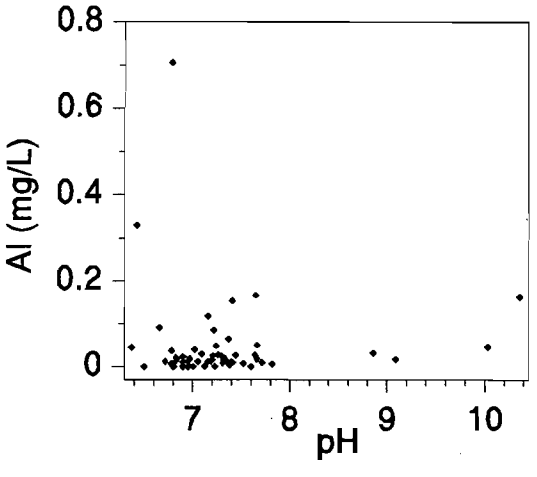

Figure 6.4 Aluminium concentration plotted against pH.

Speciation calculations performed using MINTEQA2 show that at high pH, Al is present in solution as $Al(OH)_4^-$, consistent with the findings of Pokrovskii and Helgeson (1995). The results of speciation modelling (shown graphically in Figure 6.5) also show that at pH < 7, neutral species such as $Al(OH)_3^\circ$ and AlF_3° can be more abundant than $Al(OH)_4^-$. The low pH, low Al and high concentration of F^- in groundwater from site 201 results in all the aluminium being complexed by F^-, and none is associated with OH^-. Also of interest is the speciation of Al in groundwater from site 74. Even though the F^- concentration is 69 mg/ℓ, the highly alkaline pH of 10.03 results in all Al occurring as one species, $Al(OH)_4^-$.

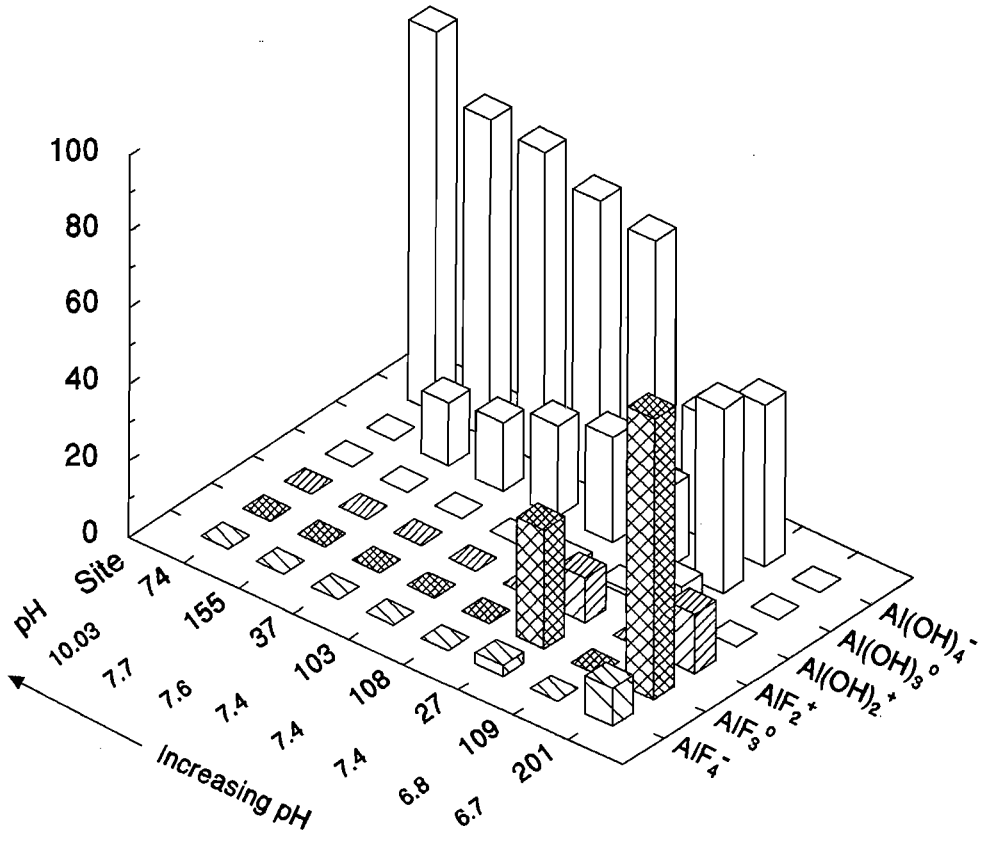

Figure 6.5 Aluminium speciation in groundwaters containing greater than 0.05 mg/ℓ Al. Modelled using MINTEQA2.

Molybdenum. One sample, site 192 from Doornfontein grazing camp situated on the Lebowa Granite, had an anomalously high molybdenum concentration of 1.0 mg/ℓ, above the high risk health limits for South African drinking water (0.20 mg/ℓ Mo; CSIR, 1991). Molybdenite, MoS_2, is sparingly soluble in water and late stage granites are often enriched in this mineral. Mo concentrations in natural waters are usually less than 0.05 mg/ℓ, but can reach 0.20 mg/ℓ around mining operations (Galvin, 1996).

Zinc. Zinc occurs in surprisingly high concentrations in groundwaters from the area. The highest concentrations are found in groundwater from the Pilanesberg Complex. No systematic variation of Zn concentration with pH is seen in this sample set (Figure 6.6). Zn speciation has been modelled in a similar manner to Al, and the results are presented in Figure 6.7. A greater variety of Zn species, compared to Al, are present, but this may be due to the abundance of thermodynamic data on these species. Much of the Zn is present either as Zn^{2+} or as a complex of carbonate, the form of which is determined by pH. At higher pH, $ZnCO_3^\circ$ and $Zn(CO_3)_2^{2-}$ are dominant. $ZnHCO_3^+$ is more abundant at a pH close to 7, whilst Zn^{2+} dominates in acidic samples. Where appreciable concentrations of other anions are present, such as SO_4^{2-} and Cl^-, these also form complexes with Zn but to a limited degree. Of interest is the predicted absence of Zn-F complexes, such as ZnF^+. At a pH of 3.0 and 37°C, all Zn is likely to be in the form Zn^{2+}, which is likely to be readily metabolised in the human gut.

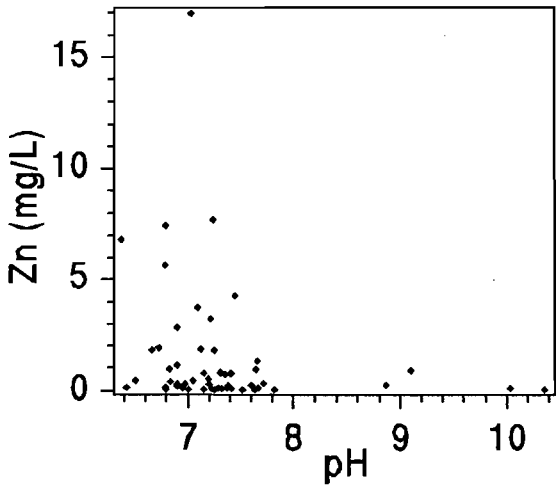

Figure 6.6 Zn plotted against pH.

6.3 Geochemical controls of groundwater fluoride concentration

6.3.1 Whole Rock composition

For most chemical elements in a rock, the most important factor controlling their interaction with water is not the total percentage of the element in the rock, but rather the minerals in which the element is located. For instance, Na in NaCl passes more readily into the hydrosphere than Na in nepheline ($NaAlSiO_4$). This is simply a function of the solubility constant of the mineral. That rock RO6 has 8% total F is less important to this study than the mineral forms in which the F is present. There are exceptions to this rule, however, e.g. iodine. Since I (and to a lesser extent, Br) is not readily accepted into crystal lattices of common rock forming minerals, it tends to be adsorbed onto crystal surfaces, as well as occurring in fluid inclusions (Fuge, 1988). However, iodine presumably binds more readily to some mineral surfaces than others, and so for iodine the mineralogy of the rock still exerts a certain control on elemental availability. For this reason the mineralogy, and not

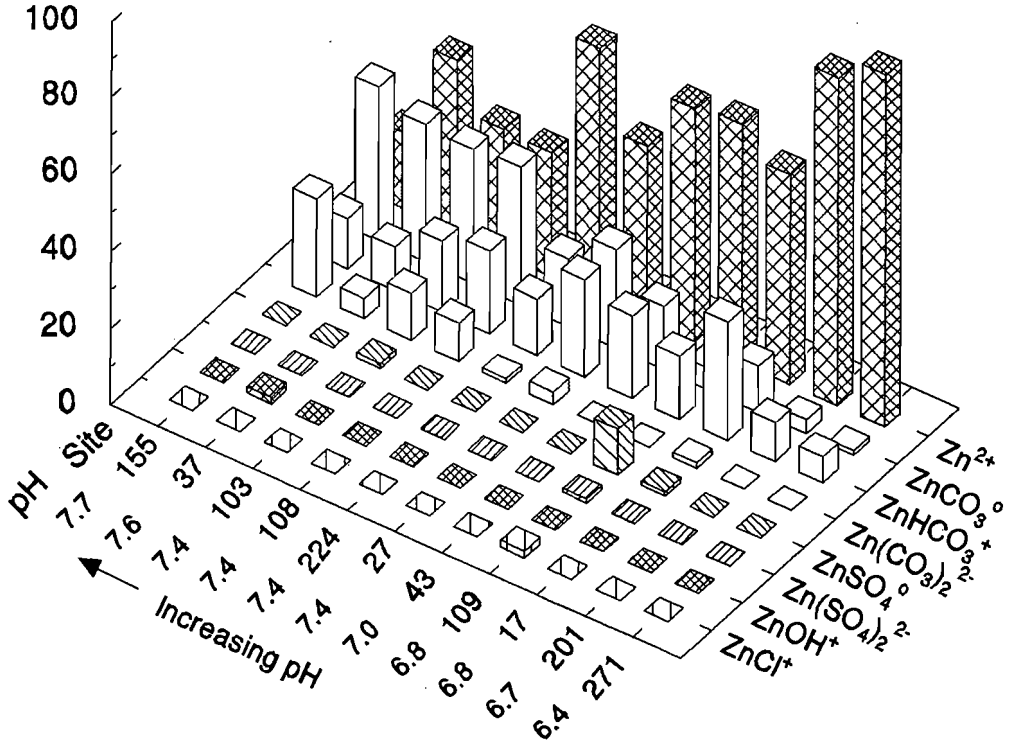

Figure 6.7 Speciation of Zn in several groundwaters from the field area, calculated using MINTEQA2.

the bulk chemical composition, is stressed in the following discussion.

6.3.2 Mineral solubility

Solubility products (pK or $pK_{25°}$ if specifically at 25°C) are available for most rock forming minerals, but there is often considerable uncertainty associated with these values. A discussion of the solubility of various minerals is warranted, especially of the main F-bearing minerals fluorite, fluorapatite, micas and amphiboles.

Fluorite. The solubility of fluorite has been investigated by many workers including Guntz (1884), Petersen (1889), Treadwell and Koch (1904), Seemann (1905), Kohlrausch (1908), Launay (1913), Auméras (1927), Charter (1928), Mougnard (1931), Kazakov and Sokolova (1950), Smyshlyaev and Edeleva (1962), Strübel (1965) and Nordstrom and Jenne (1977). The solubility of fluorite, expressed as the concentration of F^- in solution in mg/ℓ, calculated by some of these workers are shown in Figure 6.8. A great deal of variation exists in the calculated solubility of fluorite. Strübel (1965) reviewed the work of all previous workers and revised the solubility for fluorite at ambient and elevated temperatures and pressures, as well as in NaCl solution of varying molality. He found that fluorite exhibits

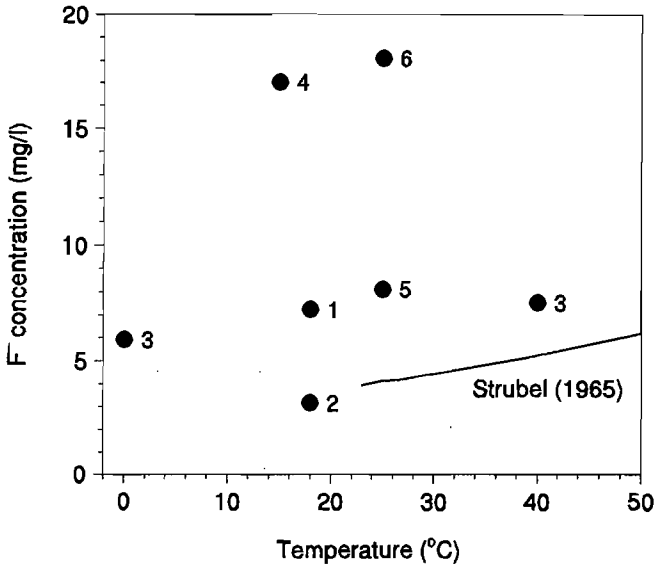

Figure 6.8 CaF_2 solubility, as the concentration of F^- in aqueous solution. Sources; 1: Treadwell & Koch (1904), 2: Seemann (1905), 3: Kohlrausch (1908), 4: Launay (1913), 5: Auméras (1927), 6: Charter (1928).

retrograde solubility at temperatures above 100°C. Supporting evidence for retrograde solubility in natural systems was found by Nordstrom and Jenne (1977). The solubility of fluorite (160 mg/ℓ) reported by Freeze and Cherry (1979) is seen to be incorrect.

Qi and Knaebel (1989) showed that, since natural fluorite is rarely pure and usually contains calcite and quartz inclusions, the solubility of fluorite in a system in equilibrium with the atmosphere, fluorite and calcite is controlled predominantly by the activities of F^-, HCO_3^- and Ca^{2+}. Fluorite is regarded as the mineral which most frequently controls F^- concentration in natural waters (e.g. Alberta (Hitchon, 1995), Yellowstone (Stauffer, 1982), Kenya (Gaciri and Davies, 1993), Ethiopia (Ashley and Burley, 1994) and New Zealand (Ellis and Mahon, 1977)). There are three main reasons for implicating fluorite as a major control of F^- distributions in natural waters: fluorite is the most ubiquitous and abundant F containing mineral; it is sparingly soluble; and Ca is generally always present in natural waters. These three factors also show why fluorapatite is less frequently cited as a controlling factor in F^- concentration: fluorapatites are relatively uncommon, they are markedly less soluble than fluorite, and phosphate is found at very low concentrations in natural waters.

Figure 6.9 shows the solubility of fluorite in the presence of Ca and F ions, plotted against the Ca and F analyses for groundwaters from the field area. It can be seen that most of the groundwaters fall in the field below the solubility of fluorite, suggesting simple dissolution. However, several of the groundwaters sampled from the Pilanesberg Complex,

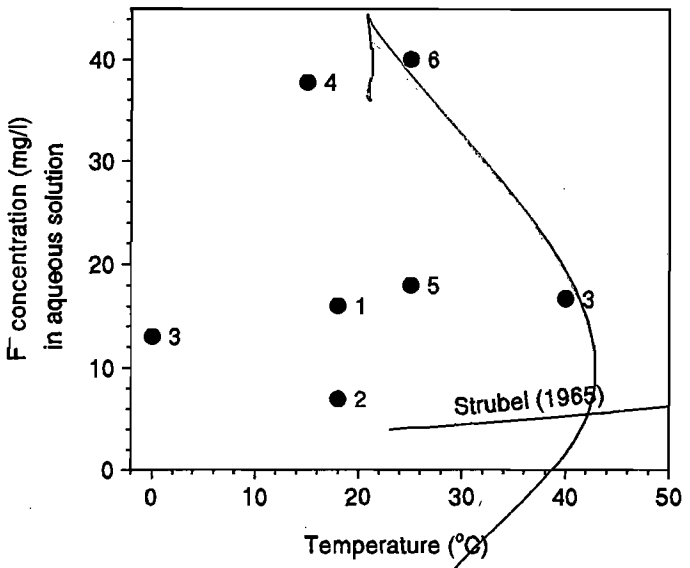

Figure 6.8 CaF_2 solubility, as the concentration of F^- in aqueous solution. Sources; 1: Treadwell & Koch (1904), 2: Seemann (1905), 3: Kohlrausch (1908), 4: Launay (1913), 5: Auméras (1927), 6: Charter (1928).

retrograde solubility at temperatures above 100°C. Supporting evidence for retrograde solubility in natural systems was found by Nordstrom and Jenne (1977). The solubility of fluorite (160 mg/ℓ) reported by Freeze and Cherry (1979) is seen to be incorrect.

Qi and Knaebel (1989) showed that, since natural fluorite is rarely pure and usually contains calcite and quartz inclusions, the solubility of fluorite in a system in equilibrium with the atmosphere, fluorite and calcite is controlled predominantly by the activities of F^-, HCO_3^- and Ca^{2+}. Fluorite is regarded as the mineral which most frequently controls F^- concentration in natural waters (e.g. Alberta (Hitchon, 1995), Yellowstone (Stauffer, 1982), Kenya (Gaciri and Davies, 1993), Ethiopia (Ashley and Burley, 1994) and New Zealand (Ellis and Mahon, 1977)). There are three main reasons for implicating fluorite as a major control of F^- distributions in natural waters: fluorite is the most ubiquitous and abundant F containing mineral; it is sparingly soluble; and Ca is generally always present in natural waters. These three factors also show why fluorapatite is less frequently cited as a controlling factor in F^- concentration: fluorapatites are relatively uncommon, they are markedly less soluble than fluorite, and phosphate is found at very low concentrations in natural waters.

Figure 6.9 shows the solubility of fluorite in the presence of Ca and F ions, plotted against the Ca and F analyses for groundwaters from the field area. It can be seen that most of the groundwaters fall in the field below the solubility of fluorite, suggesting simple dissolution. However, several of the groundwaters sampled from the Pilanesberg Complex,

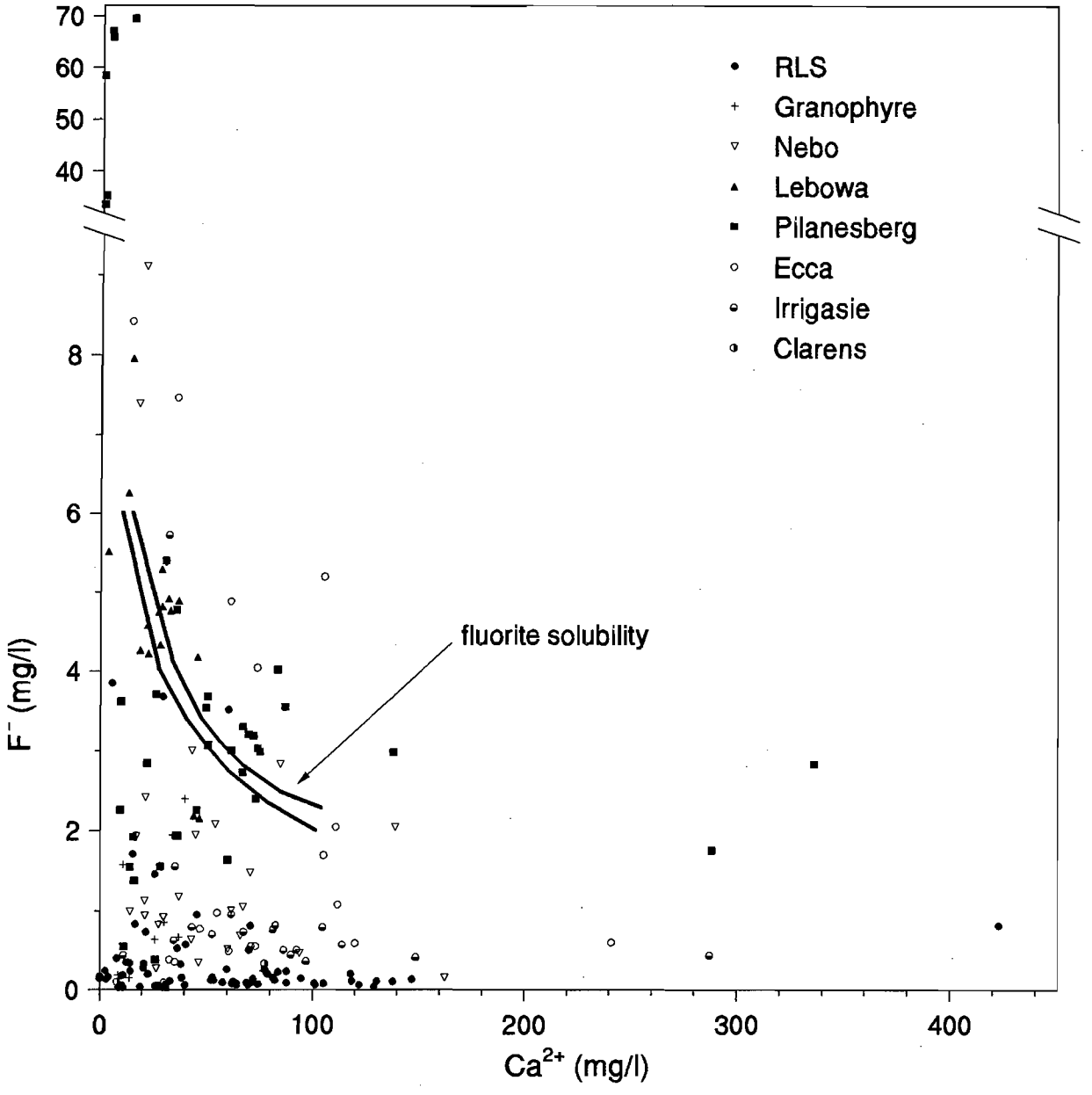

Figure 6.9 A plot of Ca^{2+} against F^- for groundwaters from the field area. Estimate of fluorite solubility plus experimental error, from Pekdeger *et al.* (1992).

Lebowa Granite and Karoo rocks have Ca and F above that which would be expected if Ca and F were controlled solely by fluorite solubility and several of the Pilanesberg groundwaters have large amounts of F^- and very little Ca (<5mg/ℓ): these groundwaters may have been subjected to base exchange softening (see following sections).

Fluorapatite and hydroxyapatite. Stauffer (1982) thoroughly reviewed the thermodynamic data pertaining to hydroxyapatite and fluorapatite. He found that the $pK_{25°}$ of hydroxyapatite ranged from -57.0 to -59.4, the wide variation resulting from ion substitutions in the natural crystals used in experiments. The $pK_{25°}$ of fluorapatite is even less well known, but is accepted to be less than that for hydroxyapatite. The values accepted

by Stauffer (1982) range from -59.8 to -62.3. In relation to dental health, fluorapatite is much less soluble than hydroxyapatite, and F^- aggressively substitutes for OH^- in hydroxyapatite, thereby hardening tooth enamel and reducing caries.

Micas and Amphiboles. Rates of dissolution and precipitation of micas and amphiboles are described in Chapter 2. No reference to solubility constants could be found for mica or hornblende in the literature, possibly as they frequently dissolve incongruously.

6.3.3 Fluorite dissolution kinetics

Brown and Roberson (1977) found that over a three year period fluorite did not fully reach equilibrium with dilute sodium perchlorate solutions, but had reached an approximation of equilibrium after 34 days. Hamza and Hamdona (1991) showed that the dissolution rate of fluorite was dependent on the relative degree of undersaturation with respect to fluorite (Figure 6.10). The data show that the dissolution rate decreases as the solution approaches saturation with respect to fluorite, and that dissolution of fluorite in very undersaturated solutions is rapid. In their experiments the surface area of the crystals presented to the solution seemed to have a negligible effect (Figure 6.11). The experiments of Hamza and Hamdona (1991) were inconclusive on the question of the effect of fluid flow across the crystals.

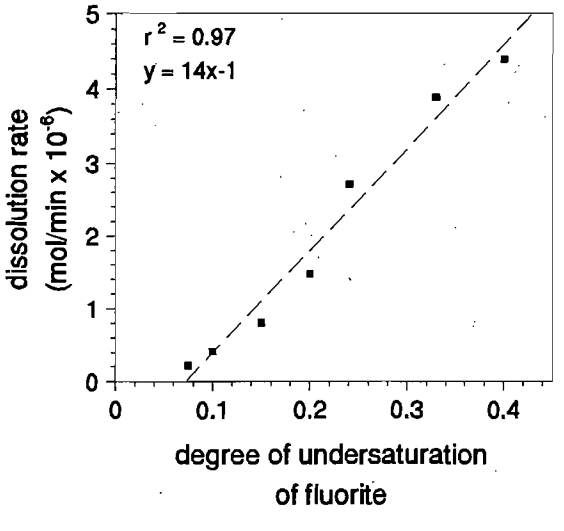

Figure 6.10 Effect of degree of undersaturation on dissolution rate of fluorite, for 16 crystals/g. Data from Hamza and Hamdona (1991).

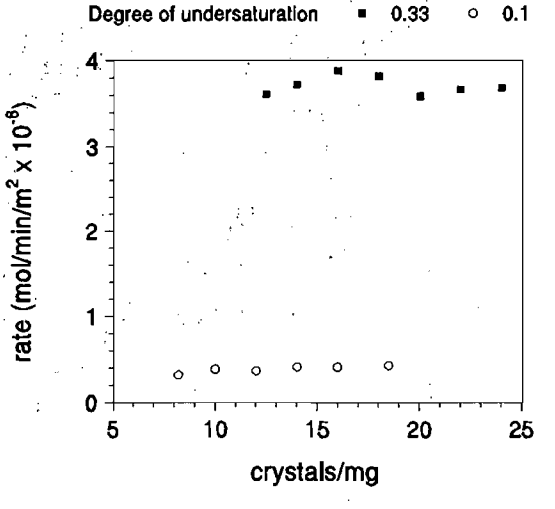

Figure 6.11 Effect of crystal size on dissolution rate of fluorite. Ionic strength 0.5 mol NaCl/ℓ, at 25°C. Ca=0.129x10^{-3} mol/ℓ, F=0.258.x10^{-3} mol/ℓ. Data from Hamza and Hamdona (1991).

Peng *et al.* (1996) showed that, since most natural fluorite contains solid inclusions of calcite, the kinetics of fluorite dissolution in nature ($4 > pH < 9$) are probably controlled by the activities of F^-, Ca^{2+} *and* HCO_3^-. In the ternary system CaF_2-H_2O-$CaCO_3$, complexation of F was not considered of significance in fluorite dissolution kinetics.

6.3.4 Thermodynamic modelling of mineral controls on groundwater composition

As shown in Chapter 4, the lithologies of the study area have a wide range of chemical and mineralogical compositions. The degree to which groundwater is saturated with respect to certain minerals with which it is in contact has been modelled using the computer programme MINTEQA2 (Allison *et al.*, 1991). Table 6.2 gives the chemical composition of minerals of importance in this study. A selection of the results is shown graphically in Figures 6.12 to 6.16. A negative saturation index for a particular mineral implies that it is undersaturated in the solution, whilst a positive index implies that the solution is supersaturated with respect to the mineral (As shown on Figure 6.12). A saturation index close to zero implies that the solution is saturated with a mineral. Langmuir (1971) in his study of carbonate waters states that an error of ± 0.05 pH units will result in a calculated

Table 6.2 Fluorine-bearing minerals and minerals involved in the thermodynamic modelling of mineral controls on groundwater composition. Solubility product (*p*K) from the MINTEQA2 thermodynamic database (Allison *et al.* , 1991).

Mineral	Chemical formula	*p*K
Calcite	$CaCO_3$	3.15
Strontianite	$SrCO_3$	9.25
Magnesite	$MgCO_3$	8.03
Dolomite	$CaMg(CO_3)_2$	17.03
Natron	$Na_2CO_3.10H_2O$	1.31
Trona	$NaHCO_3.Na_2CO_3.2H_2O$	not used
Halite	NaCl	-1.58
Sylvite	KCl	not used
Fluorite	CaF_2	10.96
Sellaite	MgF_2	not used
Villiaumite	NaF	-0.0044
Gypsum	$CaSO_4.2H_2O$	4.85

error of $\approx \pm 0.05$ saturation index units for e.g. calcite. With other uncertainties, such as in the analysis of cations, and the uncertainties in pK for calcite and dolomite, he put a total uncertainty on his saturation index calculations at ≈ 0.1 and he therefore assumed that all values within 0.1 of zero are saturated. The same is assumed to be so in this study.

In almost all cases, halite and natron are very undersaturated, in accordance with their high solubility and scarcity in the rocks of the field area. Although deposits of halite and natron are found only within the Pretoria Saltpan in the field area, estimations of the saturation index for these minerals give an impression of the salinity of the groundwaters.

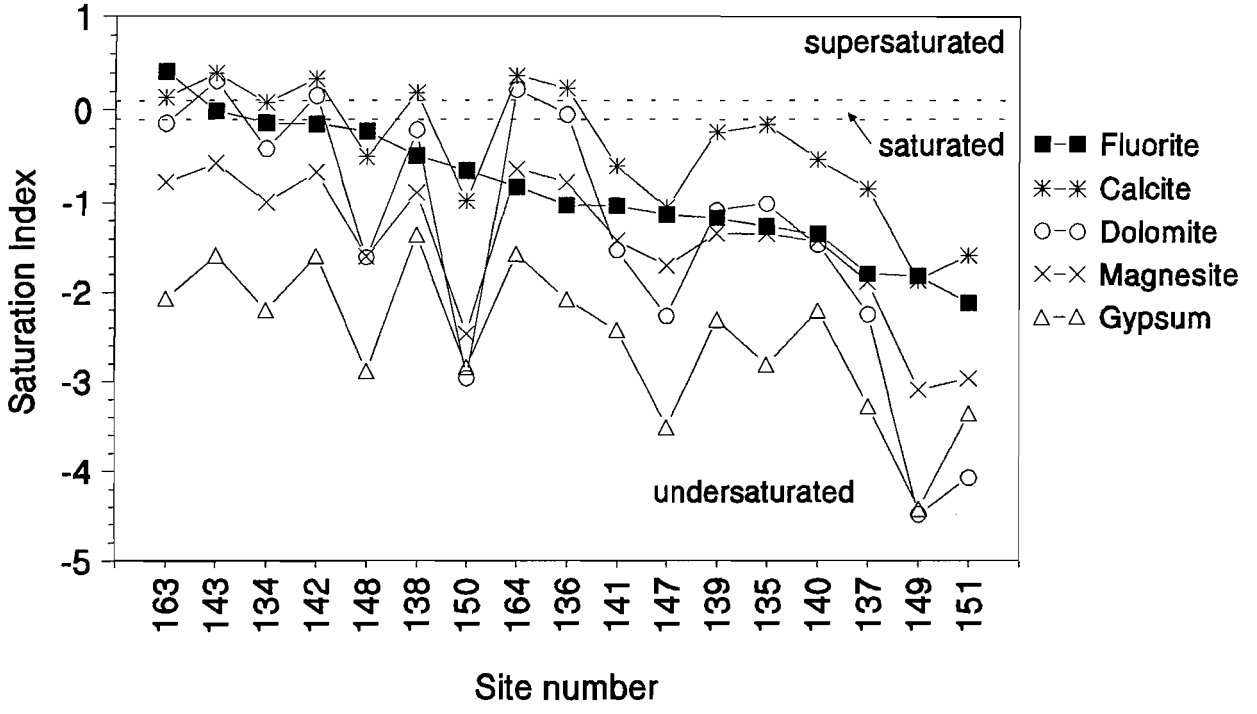

Figure 6.12 Saturation indices for selected minerals, calculated for groundwater analyses from the Nebo Granite. Limits of saturation are shown. In this and subsequent plots, groundwaters are ordered by saturation of fluorite.

Nebo Granite. Groundwater hosted in Nebo Granite is mostly undersaturated with respect to fluorite, whilst calcite is mainly saturated (Figure 6.12). Dolomite and magnesite are close to saturation or slightly undersaturated.

Lebowa Granite. In the Lebowa Granite, the groundwater is generally saturated with respect to fluorite and calcite, whilst Mg-containing minerals are just undersaturated (Figure 6.13). Sites 325, 299 and 328 are the most undersaturated with respect to all minerals, indicating either a shorter groundwater residence time, proximity to a recharge area or dilution with very fresh water.

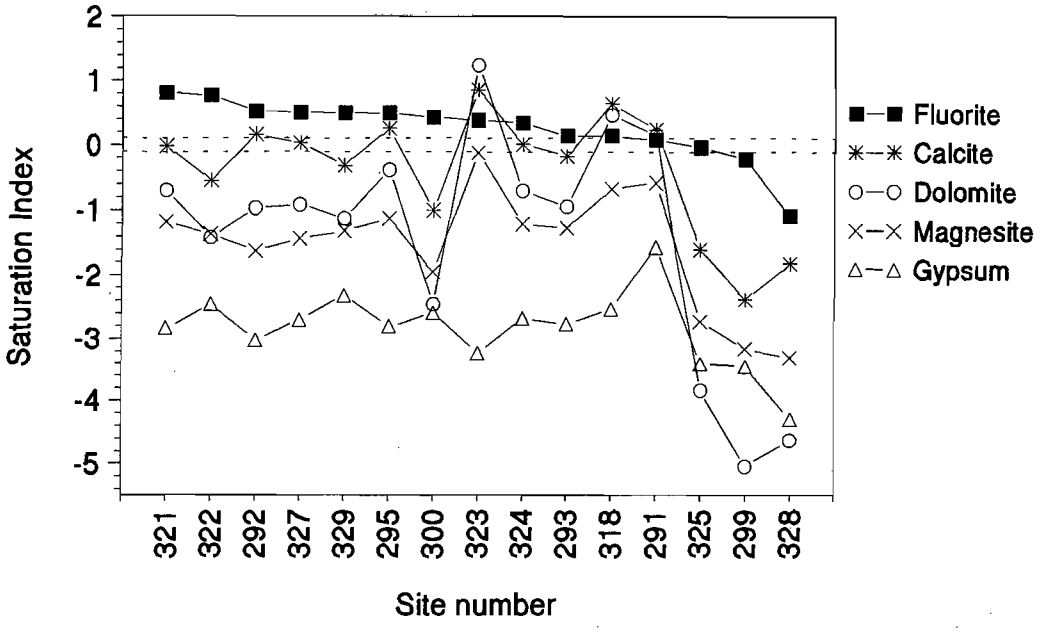

Figure 6.13 Saturation indices for selected minerals, calculated from groundwater analyses from the Lebowa granite, using MINTEQA2.

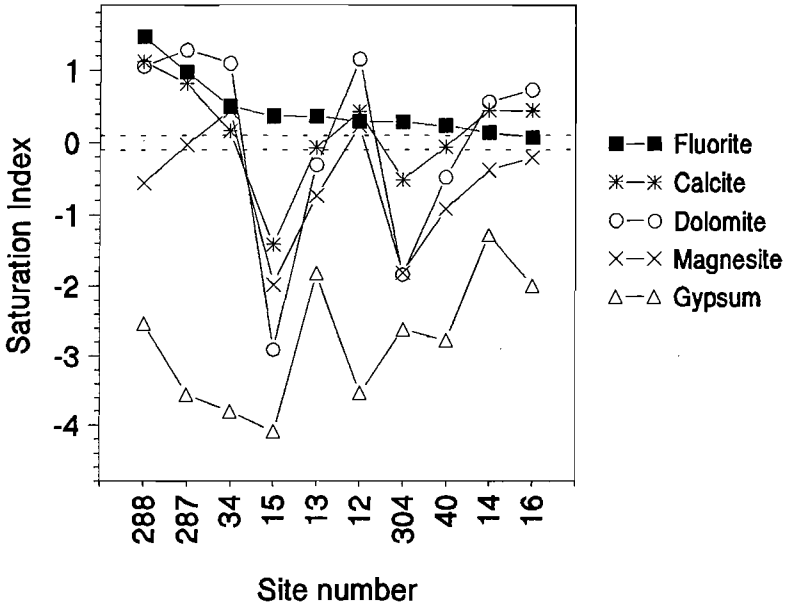

Figure 6.14 Saturation indices of common minerals for selected groundwater samples from the Pilanesberg Complex, calculated using MINTEQA2.

Pilanesberg. Pilanesberg groundwater F^- concentrations are likely to be controlled by fluorite solubility, since all samples are approximately saturated with respect to the mineral (Figure 6.14). Decreasing fluorite saturation is concurrent with an increase in gypsum saturation. Most groundwaters are close to saturation with respect to calcite, dolomite and magnesite. Site 15 and 12 are anomalous. Site 15 is unusual in that it is close to saturation

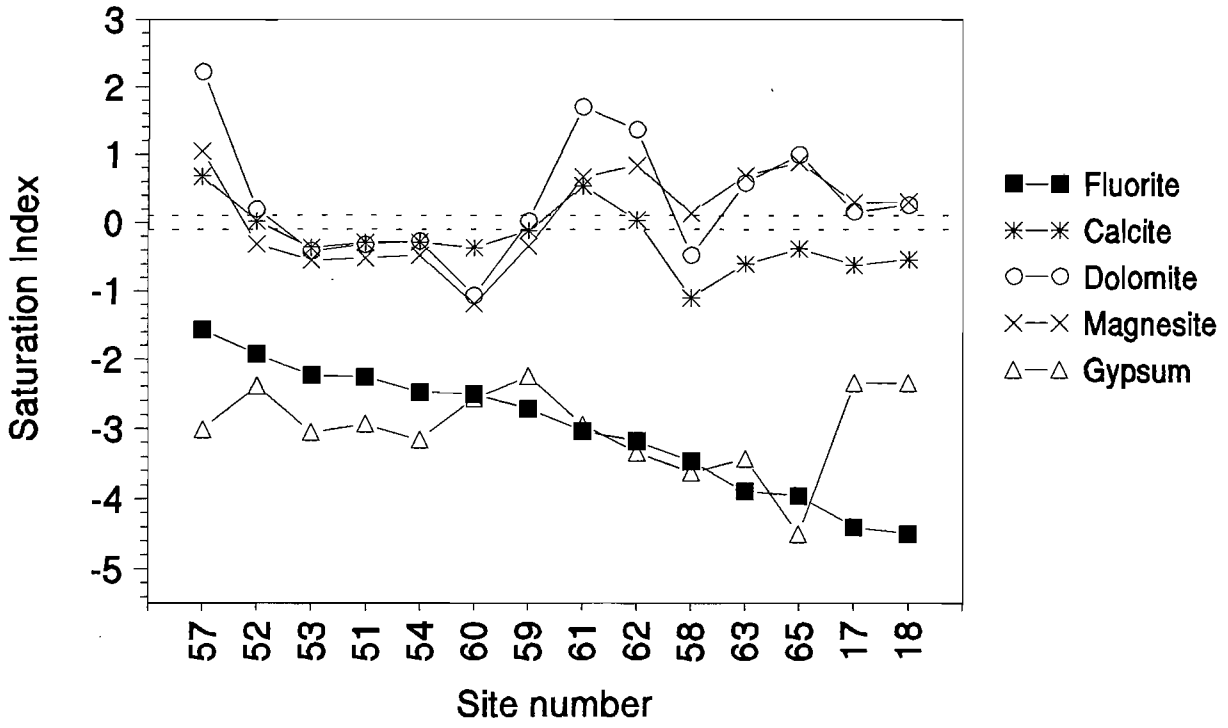

Figure 6.15 Saturation indices for selected minerals for selected samples from the Rustenburg Layered Suite, calculated using MINTEQA2.

with fluorite but undersaturated with respect to carbonate minerals, i.e. calcite, dolomite and magnesite. This may indicate that, in this instance, $CaCO_3$ precipitation, which should take place when the groundwaters are saturated with respect to $CaCO_3$, is not an active process in upsetting the Ca^{2+}-F^- equilibrium, thereby boosting F^- concentrations. Groundwater sample 12 is similar to groundwaters 288, 287 and 34, in that it has high saturation indices for natron and halite, and is oversaturated with dolomite.

Rustenburg Layered Suite. RLS groundwaters are all undersaturated with respect to fluorite but are generally close to saturation with respect to calcite and magnesite, and oversaturated with respect to dolomite (Figure 6.15). Fluorite is not found in the RLS, whilst the rocks have abundant Mg-bearing silicate minerals. Since Si was not determined, it is unfortunately not possible to calculate the saturation indices for silicate minerals.

Carbonatites. The Nooitgedacht Carbonatite, which is remarkable for the absence of fluorite, is the only carbonatite from which groundwater was collected in this project. All samples from the Nooitgedacht carbonatite are undersaturated with fluorite, with sample 334 showing the greatest degree of saturation (Figure 6.16). Natron is as undersaturated in groundwater from the Nooitgedacht carbonatite as with groundwater from other rock types. This may indicate that the Nooitgedacht Carbonatite is poor in soluble sodium minerals.

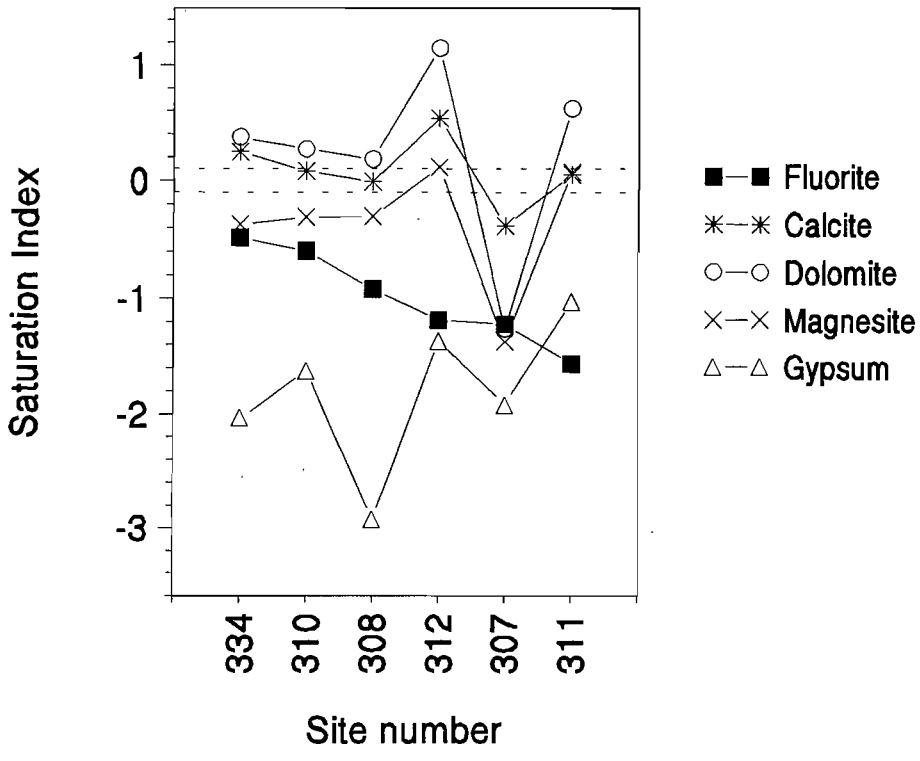

Figure 6.16 Saturation indices for 7 minerals for all groundwater samples from the Nooitgedacht carbonatite in the field area, calculated using MINTEQA2.

Groundwaters associated with the Kruidfontein carbonatite complex, which is notable for its abundance of fluorite, are expected to be fully saturated to oversaturated with respect to fluorite.

Groundwater in the Pretoria Saltpan area. The Nebo Granite groundwater in the vicinity of the Pretoria Saltpan has a variable series of saturation indices (Figure 6.17). The Saltpan brine, sample 230, is supersaturated with respect to fluorite, calcite and dolomite. The brine is closer to saturation with villiaumite than any other sample considered here (see the next section). Groundwaters in the area show variable saturation indices. Samples from sites 242 (Mr Theledi's Farm) and 335 (Saltpan artesian borehole) are undersaturated with respect to fluorite, and show decreasing saturation with halite and natron, indicative of either mixing with fresh water or a shorter residence time. The Stinkwater sample (243) is undersaturated with fluorite.

6.3.5 Modelling Villiaumite solubility

Villiaumite is restricted to silica- and calcium- poor rocks, such as peralkaline nepheline syenites and phonolites. Pilanesberg rocks in general conform to these criteria, having mean SiO_2 and CaO of 52.4 and 2.9 wt%, respectively (n=23, calculated from Lurie,

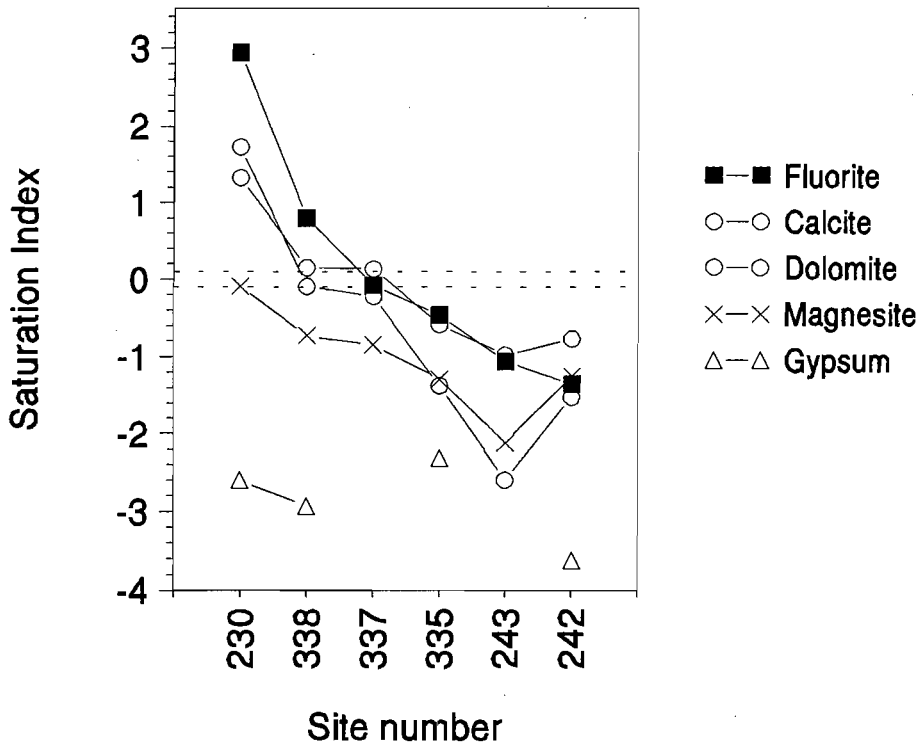

Figure 6.17 Saturation indices for selected minerals for groundwaters from the vicinity of the Pretoria Saltpan crater (hosted in Nebo Granite), calculated using MINTEQA2.

1974). The phonolite of the Pilanesberg is a prime candidate to host villiaumite, as is the carbonatitic fluorite ore described in Chapter 4 and Appendix B4. Given that this ore has large amounts of fluorite, its SiO_2 concentration is only 10% and the plagioclase composition is close to 100% albite, villiaumite is very likely to occur in this rock.

It has been shown that some of the groundwaters in the study area are supersaturated with respect to fluorite. It is postulated that in some of these cases the F^- concentration is being controlled by a more soluble fluoride salt. The most likely mineral is villiaumite, NaF. Stormer and Carmichael (1970) reviewed the occurrence of villiaumite and related minerals in igneous rocks. They stated that villiaumite may be controlled by the reactions represented in the following equations:

$$2NaF + 4SiO_2 + CaAl_2Si_2O_8 \rightleftharpoons 2NaAlSi_3O_8 + CaF_2 \qquad \textbf{eq. (6.1)}$$

$$villiaumite + silica + anorthite \rightleftharpoons albite + fluorite \qquad \textbf{eq. (6.2)}$$

The thermodynamic databases which are included with the computer package MINTEQA2 do not include villiaumite as a mineral species, and so the relevant thermodynamic data had to be collated, calculated and inserted in the correct format. Woods and Garrels (1987) compiled a list of thermodynamic values which includes the enthalpy of formation, ΔH°_{f}, of inorganic compounds from free elements. This parameter is also known as the enthalpy of reaction. MINTEQA2 makes use of the enthalpy of formation calculated from aqueous species, and so a new ΔH°_{f} had to be calculated. The values used are shown in Table 6.3. Woods and Garrels (1987) stated that although the absolute enthalpy values may change between researchers, the enthalpy of formation resulting from the use of values from a single source is often similar. In other words, the enthalpy values are internally consistent. Table 6.3 illustrates this effect; the enthalpy of F^- varies by 6.3 kJ/mol between sources, whereas the resulting enthalpy of formation values vary by only 0.7 kJ/mol. The Rossini *et al.* (1952) value is clearly an outlier, whilst the two most recent compilations yield a calculated ΔH°_{f} of -0.9 kJ/mol, the value used in the MINTEQA2 database. Since the temperature of all the groundwaters to be modelled was very close to 25°C, the temperature corrections based on the calculated ΔH°_{f} at 25°C are not large.

Table 6.3 Enthalpy values used in the calculation of ΔH°_{f} (enthalpy of formation) used in MINTEQA2, kJ/mol.

Source	Na^+	F^-	NaF	ΔH°_{f}
Rossini *et al.* (1952)	-239.6	-329.1	-569.0	-0.3
Naumov *et al.* (1974)	-240.4	-333.8	-575.2	-1.0
Robie *et al.* (1978)	-240.3	-335.4	-576.6	-0.9
Wagman *et al.* (1982)	-240.1	-332.6	-573.6	-0.9
Babushkin *et al.* (1985)	-240.4	-333.8	n/a	n/a
Mean	-240.2	-332.9	-573.6	-

Application of Villiaumite saturation index. A plot of the saturation indices for villiaumite *vs.* those of calcite, natron, fluorite and halite shows that groundwaters have contrasting indices of saturation with respect to these minerals (Figure 6.18). All groundwaters are undersaturated with respect to villiaumite, but Pilanesberg groundwaters show less undersaturation than others. Pilanesberg and Lebowa groundwaters are generally saturated to supersaturated with respect to fluorite but have a range of undersaturated values with respect to NaF; Nebo groundwater is mostly undersaturated with respect to

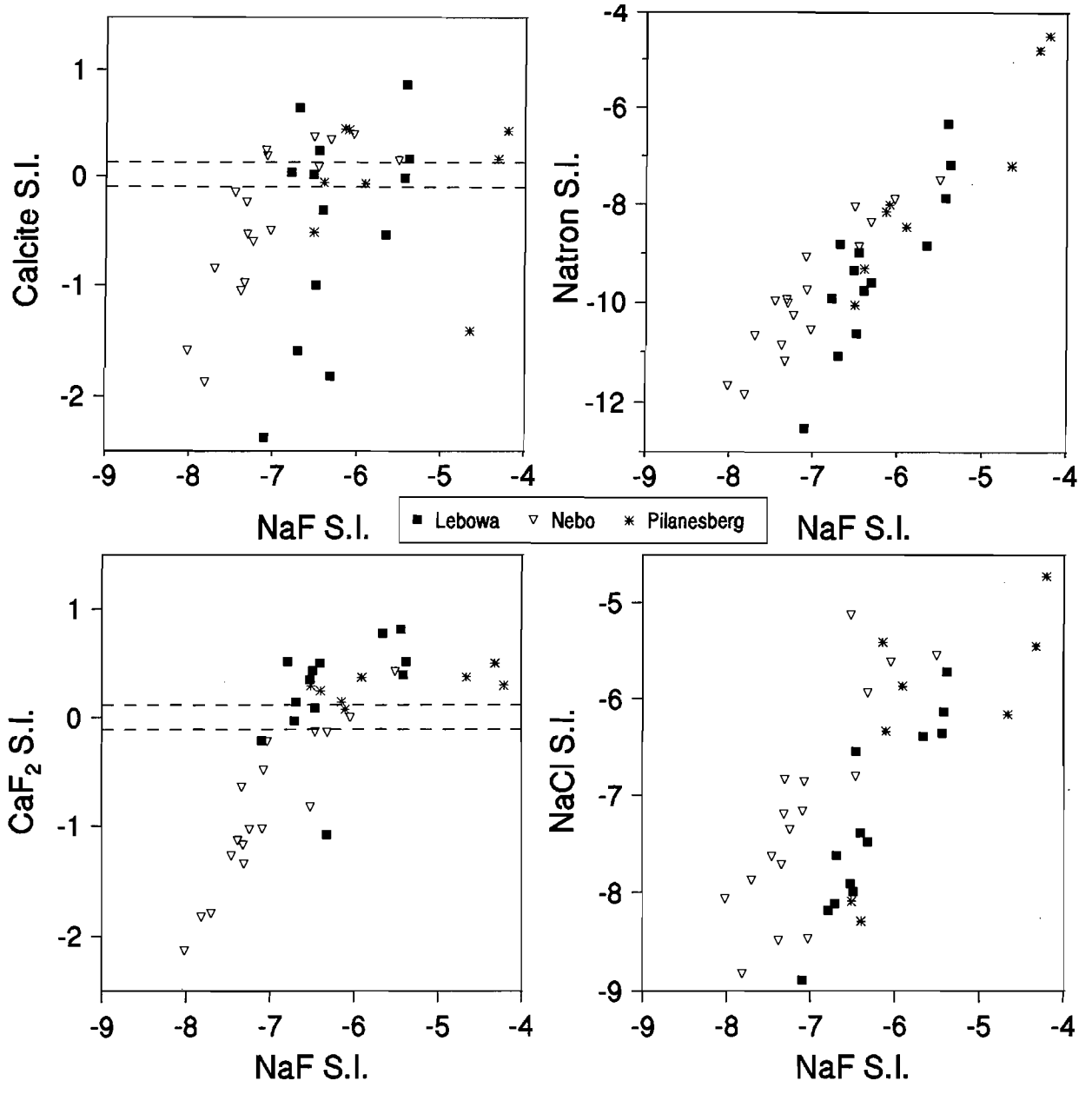

Figure 6.18 Plots of villiaumite (NaF) saturation index (S.I.) *vs.* saturation of calcite, natron, fluorite and halite for groundwaters from the Lebowa and Nebo Granites and from the Pilanesberg. Dashed lines are limits of saturation.

fluorite. The plots can be misleading as all the Na could come from albite and the F from CaF_2 or mica. Consequently the plots give no definite indication that NaF exists as a discreet mineral phase in the rock.

Comparison of MINTEQA2 and JESS. The results of two speciation modelling programmes have been compared in this study to determine the degree of agreement. The public-domain software package MINTEQA2 (Allison *et al.*, 1991) uses 'best estimate' formation constants and enthalpy values in its database, and it is claimed that the thermodynamic data often lacks internal consistency (Dr P. Wade, Centre for Scientific and

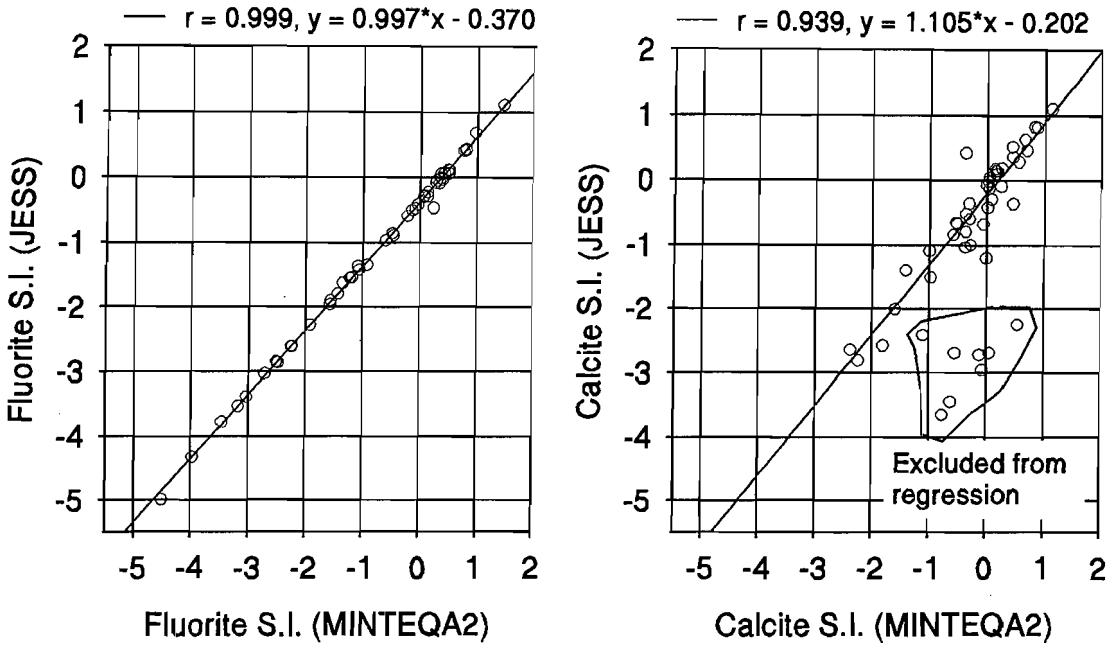

Figure 6.19 Comparison of saturation indices calculated by MINTEQA2 and JESS for fluorite and calcite, for selected groundwater analyses from the western Bushveld.

Industrial Research, Pretoria, *pers. comm*). A more sophisticated speciation modelling program named JESS (Joint Expert Speciation System) has been implemented by the CSIR and Murdoch University of Western Australia (May and Murray, 1991a, 1991b). JESS features a very large thermodynamic database which has been produced by the systematic collation of data from the literature. Thermodynamic values are checked for internal consistency before addition; all values are retained, but are weighted for validity - inconsistent data being given a weighting of zero. Because the computer code for JESS is not in the public domain, Dr Peter Wade of the CSIR was commissioned to model a subset of the water analyses produced in this study. Specifically, the saturation indices for major minerals were required for comparative purposes with the MINTEQA2 results.

JESS produced very similar results to MINTEQA2 for minerals not containing carbonate (e.g. fluorite; Figure 6.19). The main difference is a small systematic bias of -0.37; this is the result of the two databases having different estimates of the solubility product of fluorite.

The estimation of saturation indices for minerals containing carbonate at times differed considerably between the two modelling methods. The discrepancy is likely to stem from the use of slightly different alkalinity values in the two modelling runs. For MINTEQA2 modelling, the alkalinity as measured in the field was used as a measure of carbonate

concentration. For the JESS modelling, carbonate concentration was estimated iteratively from the measured alkalinity. In most cases the alkalinity and the estimated carbonate concentration were within 0.1% relative to one another, but in several cases (groundwater analyses from sites 13, 17, 18, 59, 243, 311, 312 and notably, 230) the JESS carbonate concentrations were much higher. This may have caused JESS to calculate different saturation indices for carbonate minerals for these analyses (e.g. calcite, Figure 6.19). In general, however, MINTEQA2 provided similar values to JESS and this created confidence in the MINTEQA2 calculations.

6.3.6 Aqueous chemical controls on F^- concentration

It is apparent that dissolution of fluorite provides much of the F^- in groundwater of the western Bushveld region. If this is the case, why are so many groundwaters either supersaturated with respect to fluorite, or far from simple stoichiometric dissolution of fluorite? The possibility that other, more soluble F compounds are responsible for high F concentrations has already been discussed. Other reactions, apart from mineral dissolution, can also affect F^- concentrations. These include displacement of F^- by OH^- on clay surfaces at high pH (anion exchange), precipitation of $CaCO_3$, cation exchange on clays, and precipitation of ions upon evaporation.

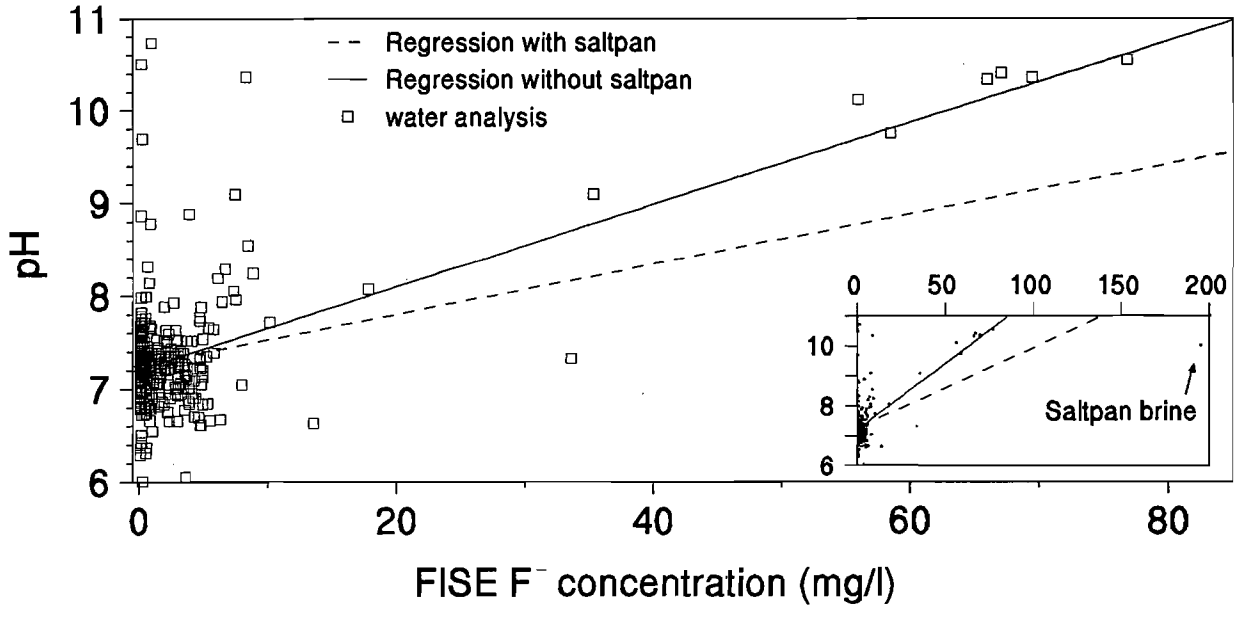

Figure 6.20 Fluoride concentration plotted against pH for groundwater. Two regression lines are given: one does not include the Saltpan datum. Both are significant at the 99.9% confidence level, but this is due entirely to outliers.

pH. In general, the pH of the groundwater does not correlate with F^- concentration (Figure 6.20). No clear trend is seen at near neutral pH (pH>6, <8). The regression lines

shown in Figure 6.20, whilst being statistically significant, are clearly influenced by a small number of high pH and high F^- outliers (see next section). From this data it must be concluded that F^- is not correlated with pH at near-neutral pH. Little work has been done on the solubility of F-bearing minerals at high pH, and it seems possible that increased OH^- activity might displace F^- from adsorbed sites in clay minerals and from structural sites in micas and amphiboles. The good correlation in the groundwaters with high pH and high F^- supports the suggestion that anion exchange (OH^- for F^-) may have occurred.

$CaCO_3$ precipitation. It can be argued that F^- concentrations in groundwater increase due to precipitation of $CaCO_3$, which may occur at high pH. For an aqueous system in equilibrium with the atmosphere and fluorite, the equations governing equilibrium reactions can be written:

$$H_2O + CO_2 \rightleftharpoons HCO_3^- + H^+ \qquad \textbf{eq. (6.3)}$$

$$HCO_3^- \rightleftharpoons CO_3^{2-} + H^+ \qquad \textbf{eq. (6.4)}$$

$$CaF_2 \rightleftharpoons Ca^{2+} + 2F^- \qquad \textbf{eq. (6.5)}$$

$$Ca^{2+} + HCO_3^- \rightleftharpoons CaCO_3 + H^+ \qquad \textbf{eq. (6.6)}$$

$$Ca^{2+} + CO_3^{2-} \rightleftharpoons CaCO_3 \qquad \textbf{eq. (6.7)}$$

The ΔG°_f of equations 6.6 and 6.7 are +12.6 and -46.36 kJ/mol, respectively, and therefore, the formation of $CaCO_3$ from Ca^+ and CO_3^{2-} occurs spontaneously, whilst from Ca^{2+} and HCO_3^- it does not. When pH is increased to above 8, CO_3^{2-} combines with Ca^{2+} ions from the dissolution of fluorite to form $CaCO_3$ which then precipitates. The lowered activity of Ca^{2+} means that more CaF_2 can then dissolve, thereby increasing the F/Ca ratio of the solution. At neutral pH the concentration of CO_3^{2-} is negligible, and $CaCO_3$ precipitation can be ignored; at low pH, precipitation of $CaCO_3$ does not occur and F^- concentration is not affected by the stripping of Ca^{2+} ions from solution.

However, the groundwater with high pH and F^- concentrations shown in Figure 6.20 do *not* have low CO_3^{2-} concentrations, the lowest being 258 mg/ℓ. All of these groundwaters (from sites 12, 15, 74, 75 and 287) are from the perimeter of the Pilanesberg, previously noted for its high pH and high F^- concentrations. All of these groundwaters have high Na concentrations and low Ca^{2+} and Mg^+ concentrations, indicative of cation exchange. The

depletion of Ca^{2+} by coprecipitation with CO_3^{2-} is, therefore, thought to be of little importance in the process of increasing F^- concentrations in the field area.

Ion Exchange. Boyle (1992) showed that very high levels of F^- in groundwater (up to 25 mg/ℓ) were the result of base exchange softening of groundwater in a sedimentary basin. Cation (or 'base') exchange of Ca^{2+} (and Mg^{2+}, Sr^{2+}) for Na^+ and K^+ on clays reduces the Ca^{2+} concentration in solution, thus promoting dissolution of CaF_2. Unlike the studies of Cederstrom (1946) and Foster (1950), Boyle (1992) showed that base exchange could take place at a shallow depth (as little as 15m below the surface) and without a long apparent residence time or flow path. However, Freeze and Cherry (1979) stated that, depending on conditions, several million years may pass before the exchange medium is in *equilibrium* with inflowing groundwater. Boyle (1992) found that with progressive softening of the waters, pH increased up to 9.8 and Ca and Mg concentrations decreased to less than 1 mg/ℓ. He ascribed this to the exchange of Ca^{2+} and Mg^{2+} on 'solid phases' for Na^+, and the involvement of H^+ in satisfying the exchange capacity of the sediments towards the end of the exchange process.

The evidence for the action of ion exchange in the field area is good. The groundwaters of the Pilanesberg Complex with very high F^- contents have very low Ca^{2+} (Figure 6.9) and Mg^{2+}, high Na^+ and pH, and moderately high HCO_3^-. Such a composition is characteristic of groundwater which has undergone cation and anion exchange (e.g. Gascoyne and Kamineni, 1994). Water-bearing fractures in the Pilanesberg Complex are known to be often lined with clays, and flow paths in the order of 5 kilometres are possible (McCaffrey, 1994). The conceptual model of the geohydrology of the area (outlined previously) does not indicate long flow paths or high porosity in the rest of the Bushveld Complex, which would limit the action of cation exchange. The probability of cation exchange is highest in the vicinity of the Karoo basin. Groundwaters of the Lebowa and Nebo Granites, saturated with respect to fluorite, would flow from the granitic highlands into the porous and clayey sediments of the Irrigasie and Ecca formations of the low-lying Karoo basin.

When plotted on a trilinear diagram ('Piper diagrams'; Piper, 1944) hydrochemical processes can be more clearly seen (Lloyd and Heathcote, 1985). Figure 6.21 shows simple divisions into which the groundwaters can be divided. To plot all the data points would result in a confusing and cluttered graph, so only the mean analyses have been plotted. Figure 6.22 shows mean groundwater analyses of the 8 major lithologies of the field area. Most of the groundwaters fall in the 'No Dominant Type' area. Mean groundwater from the RLS is of the $Ca+Mg+Cl+SO_4$ type. Mean Pilanesberg groundwater has no dominant

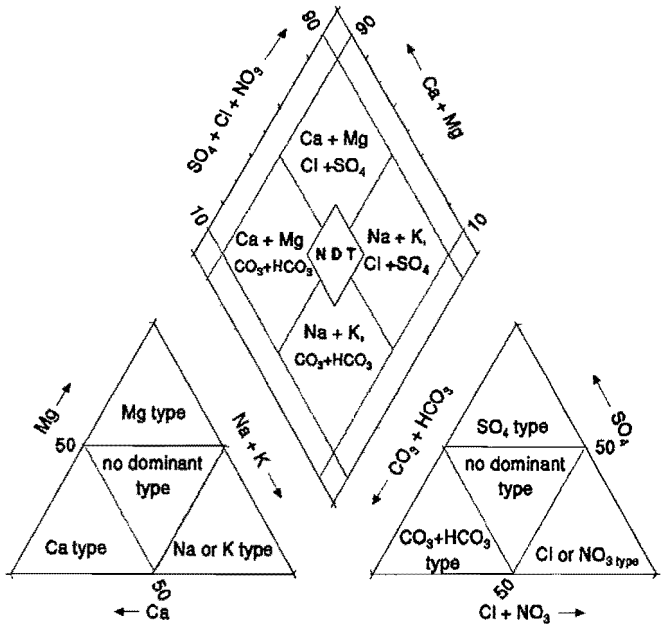

Figure 6.21 Piper diagram divided into descriptive groundwater types. 'NDT' is no dominant type.

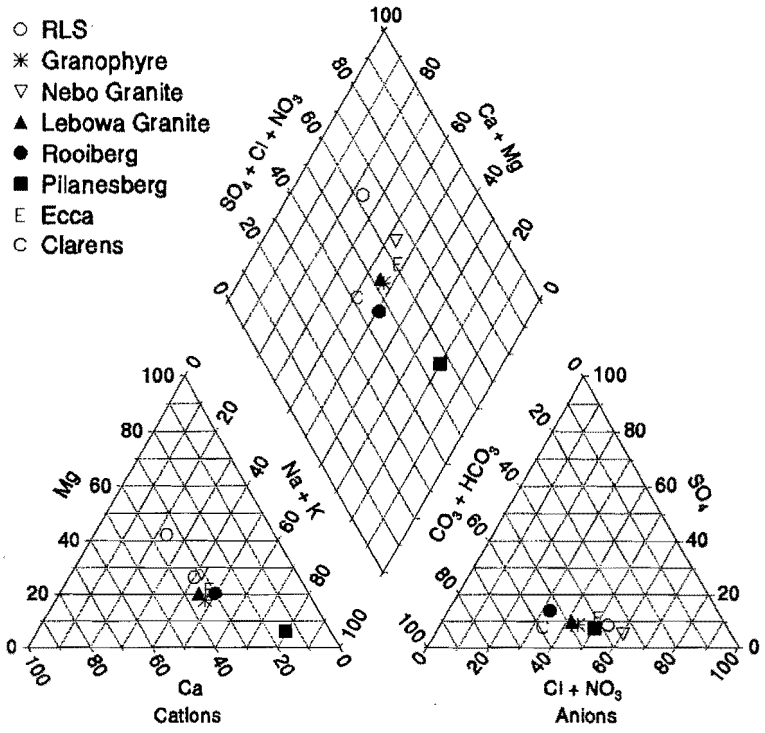

Figure 6.22 Mean groundwater analyses for 8 lithologies plotted on a Piper diagram.

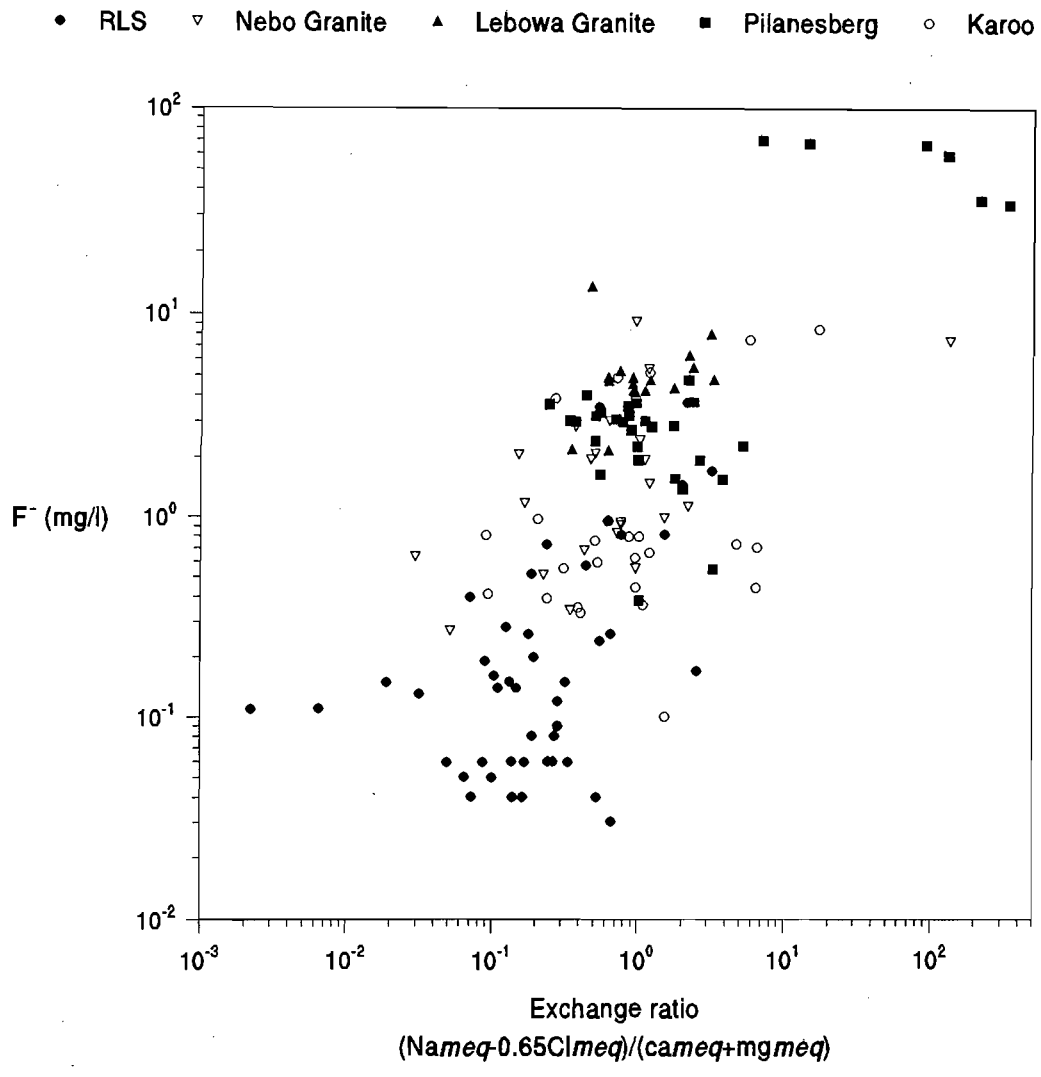

Figure 6.23 Exchange ratio (from Boyle and Chagnon, 1995) against F^- concentration. See text for discussion.

anion, but the cations are dominated by Na+K. This is not in itself evidence that Pilanesberg groundwaters have been subject to ion exchange (the sodium rich, calcium poor rocks of the complex may be the cause), although it is suggestive.

Boyle and Chagnon (1995) used a plot of the ratios of exchangeable cations in water against F^- concentration to demonstrate the variation of exchange capacity of differing aquifers. Figure 6.23 is such a plot with data from this study. The data for the study area as a whole have only a weak covariation ($r=0.517$ at $p<0.001$). However, it is apparent that the very high F^- groundwaters from the Pilanesberg Complex also have very high exchange ratios, strongly suggesting that they have been subject to ion exchange. Conversely, the low F^- groundwaters of the RLS have low exchange ratios, indicating that they have not undergone ion exchange. From this plot, therefore, it seems likely that base exchange is occurring in parts of the Pilanesberg Complex, if not in other parts of the study area.

Evaporation. Evaporation of groundwater with Ca^{2+}, Na^+ and F^- in solution results in precipitation of relatively insoluble calcium minerals, whilst Na^+ forms a highly soluble ion-pair with F^- (since NaF_2 solubility is 3 orders of magnitude greater than that for CaF_2). The reaction can be written thus:

$$Ca^{2+}_{(aq)} + 2F^-_{(aq)} + 2Na^+_{(aq)} + M^{2-}_{(aq)} \Rightarrow CaM\downarrow + 2F^-_{(aq)} + 2Na^+_{(aq)} \qquad \textbf{eq. (6.8)}$$

where M is a product of chemical weathering such as sulphate, SO_4^{2-}. This reaction would result in the precipitation of gypsum and an increase in F^- and Na^+ in solution. Groundwaters around the perimeter of the Pilanesberg have high concentrations of F^-, Cl^- and Na^+, and low Ca^{2+} concentrations, somewhat strengthening the argument for evaporative or evapotranspirative concentration, given the absence of sedimentary evaporitic rocks in the area.

A plot of F^-/Cl^- ratio against TDS (Figure 6.24) shows some minor differences between groundwaters when classified according to their host rocks. The large overlap of the data set of each aquifer indicates that only minor differences exist in the F^-/Cl^- compositions of the source rocks, the only significantly separated F^-/Cl^- ratios being groundwaters from the Lebowa Granite and the Karoo rocks. Groundwaters from the RLS, Nebo and Lebowa Granites have significant positive covariation of F^-/Cl^- with TDS ($r=0.975$, 0.740 and 0.829 respectively), whereas those from the Pilanesberg Complex and the Karoo rocks do not ($r<0.5$). Thus it is suggested that the groundwaters of the RLS, Nebo and Lebowa Granites become enriched in F^- during processes which increase TDS (such as evaporation, evapotranspiration and dissolution of minerals), whilst the Pilanesberg and Karoo groundwaters maintain their F^-/Cl^- ratios. If the reaction represented in equation 6.8 is the dominant F^--increasing reaction in the Pilanesberg Complex or Karoo rocks, the F^-/Cl^- ratio in these groundwaters would increase with TDS. As the ratios do not increase significantly with increasing TDS, evaporation (and more particularly, the reaction represented in equation 6.8) has to be seen as a questionable cause of high F^- concentrations in these groundwaters.

6.3.7 Other factors controlling F^- concentration in groundwater

Most studies have shown that the source of F^- in groundwater is the dissolution of F-bearing minerals. However, some studies have shown fluorosis to occur in areas of volcanic exhalations (e.g. Vasak, 1992; Fridriksson, 1983), fluorite dust production from mining (Davies, 1994) and industrial sites such as aluminium smelters. These sources will

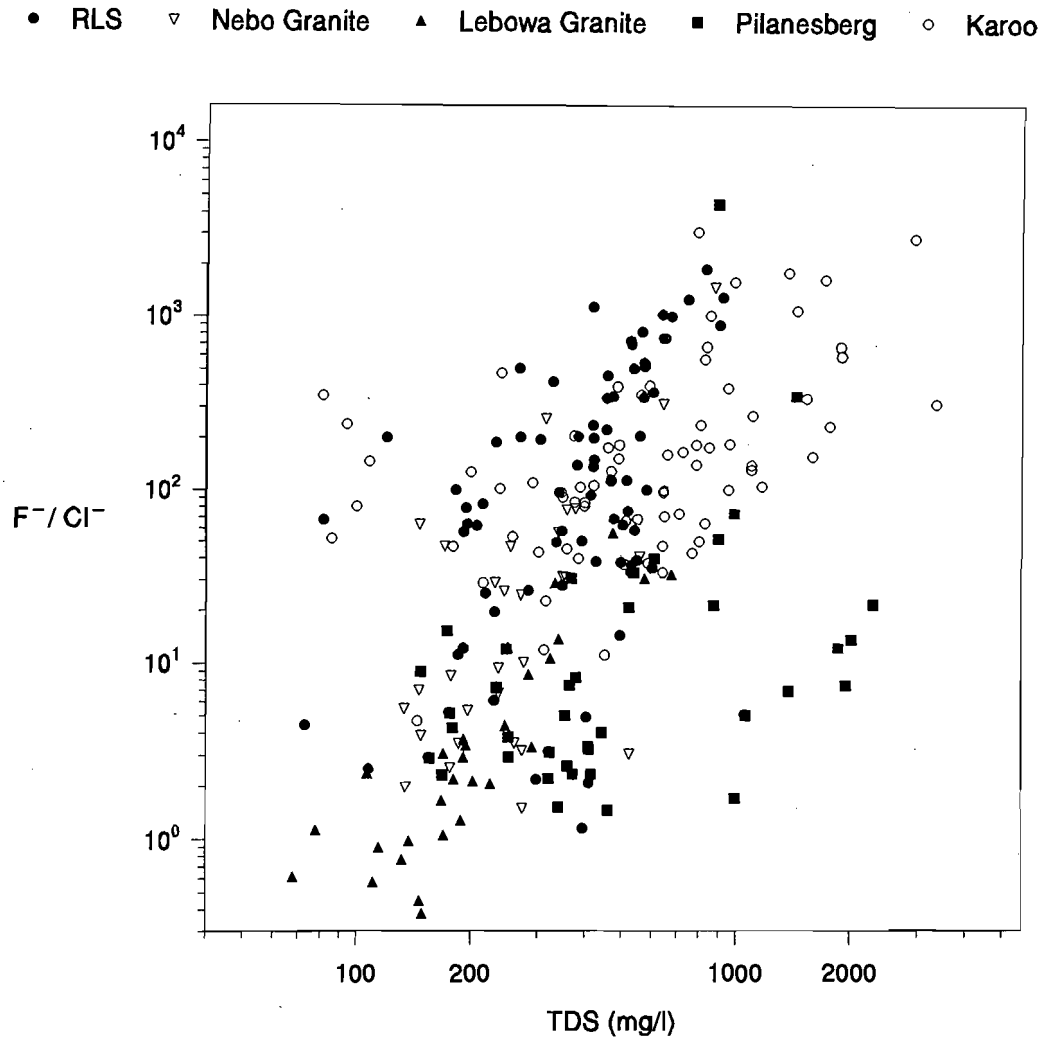

Figure 6.24 TDS plotted against the ratio of F^- to Cl^- for 5 major aquifers from the study area.

now be briefly discussed.

Volcanic exhalation. No volcanic activity currently exists in South Africa, and so HF from volcanic exhalations can be discounted as a source of F^- in groundwater.

Industrial emissions. Although many fluorite prospects occur in the Lebowa Granite Suite and Rooiberg felsite (Crocker and Martini, 1976), few large working fluorite mines still exist. Major fluorite mines are still active in the Malmani Dolomite of the Chuniespoort Group, on the edge of the study area. The impact of dust generated by blasting and processing the ore is likely to be local, and no gaseous emissions are generated.

Two other large F-handling industries exist in the study area, namely the Atomic Energy Corporation's uranium enrichment plant at Pelindaba in the south, and a major ore smelter in the centre of the area. At Pelindaba, uranium oxide is converted to uranium hexafluoride, which is then enriched by a diffusion process. Much activity occurred at the

plant in the 1960's and 70's, but production has since been scaled down. A request for information on the magnitude of fluoride emission from the plant has remained unanswered. Use of hydrofluoric acid (commercial grade, 31-32% HF by mass) by one of the metal smelters (which provided information on condition of anonymity) amounts to about 2.5 m^3 per year. Ninety five percent of this is deposited in an evaporative plastic lined dam, and no leakage to groundwater from this dam has yet been found. According to the reply, gases emitted from the smelter stacks are F free. Five percent of the total remains unaccounted for, equivalent to 125 ℓ HF per year.

To put this in perspective, a rapid calculation can be made using estimated parameters. It might be assumed that all the HF not accounted for reaches the groundwater table; that groundwater is being affected to a depth of 10 m within a radius of 10 km from the smelter; and that the rock has a porosity of 0.5%. If it is further assumed that the smelter has 'lost' 125 ℓ HF per year for the last 50 years, then groundwater F^- concentration would have been increased by less than 0.1 mg/ℓ. Clearly, this amount is negligible. If the same assumptions are made with the exception that the radius of affected groundwater is reduced to 1 km, groundwater concentrations are increased by 6.4 mg/ℓ. Lateral groundwater flow rates in the Rustenburg Layered Suite probably do not exceed 1 m/year (Xu Yongxin, Department of Water Affairs, Pretoria, *pers. comm.*) and so it is possible that localised F^- contamination could occur around such a smelter.

Fluoride in rainwater. Fluoride occurs in rainwater at very low concentrations, between 2 and 20 µg/ℓ (Barnard and Nordstrom, 1982a). The origin of F^- in rainwater has been the subject of some controversy. Carpenter (1969) found that F^- originated from the ocean and is injected into the atmosphere at the air-sea interface. The studies of Wilkniss and Bressan (1971 and 1972) totally contradicted this result. Barnard and Nordstrom (1982b) found that the majority of F^- in precipitation in the United States is anthropogenic in origin and that F^- is not injected at the air-sea interface.

No rainwater samples suitable for F^- analysis were taken for this study. However, it is likely that, given the distance from the ocean and the absence of major F-handling industries in the area, F^- concentration in rainfall would be near the background concentrations of 8 µg/ℓ found by Barnard and Nordstrom (1982a).

Dissolution of atmospheric fluorine compounds. Fluorine exists in the atmosphere in the form of F_2 at concentrations between <0.01 and 0.4 µg/m^3 (Bowen, 1966). Concentrations near industrial plants increase markedly (e.g. Machoy *et al.*, 1991). In South African coal, up to 90% of the F is volatilised upon combustion, often combining with boron to form BF_3; these coals have F concentrations between 75 and 200 ppm (Kunstmann *et al.*,

1963). It is possible that F emitted into the atmosphere by the burning of South African coals could affect groundwater concentrations significantly. Values given in DMEA (1995) indicate that in 1993, 130 million tonnes of coal were burnt each year in South Africa. This corresponds to between 8.775×10^9 and 2.34×10^{10} g F released into the atmosphere each year. However, most of this coal is burnt on the Transvaal Highveld (approximately 300 km to the east of the study area), and with the prevailing wind systems coming from the southwest, is very unlikely to influence groundwater F^- in the study area (Prof. H. Annegarn, Schonland Centre for Nuclear Research, University of the Witwatersrand, *pers. comm.*).

Temporal factors. Chemical analysis of repeat samples taken from boreholes over almost 2 years show great variation for most major ions, but comparatively little variation in F^- (previous Chapter). This indicates that F^- concentration is effectively buffered by mineral-water equilibria during short term fluctuations in climate.

Hydrological factors. Infiltrating rainwater is undersaturated with respect to CaF_2, and so actively recharging groundwater will not to be in equilibrium with the mineral. Infiltrating fresh water should reach equilibrium with fluorite-containing rocks within days of reaching the water table. Groundwater with a residence time of less than 30 days is unlikely to have been sampled, since all sampling took place several months after the wet season.

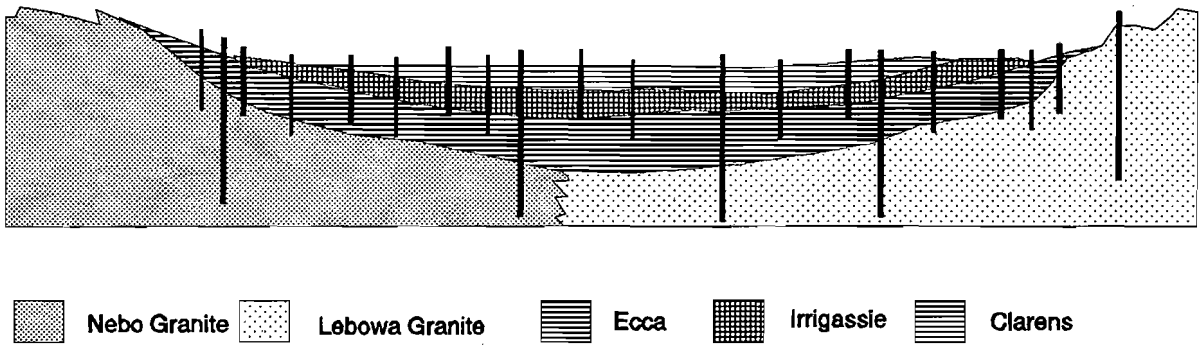

Figure 6.25 Schematic cross section of the Karoo basin, with boreholes of varying depths reaching the high fluoride groundwater of the underlying granites.

Borehole depth. It was noted in Chapter 5 that high F^- concentrations in groundwater from boreholes located in the outcrop area of the Karoo sediments had a varied spatial distribution. It is suggested that this is due to the possibility that some boreholes penetrate the low F^- Ecca shales and tap water from the underlying high F^- Nebo and Lebowa granites (shown schematically in Figure 6.25). The groundwater in Karoo sediments in the

central part of the basin, namely the Irrigasie and Clarens Formations, have lower mean F^- concentrations, at 1.0 and 0.9 mg/ℓ F^- respectively, than the Ecca formation (2.3 mg/ℓ F^-; Chapter 5) and have fewer high F^- outliers. This suggests that boreholes in these areas of increased sediment thickness are not deep enough to penetrate to the underlying granites.

The absence of depth information associated with any of the groundwater samples is a major disadvantage of the current data set. The deficiency all but prevents any speculation of the variation of F^- concentration with depth. Whilst the data of Boyle (1992) appears to show little or no correlation of F^- concentration with depth, Hitchon (1995) found that F^- concentrations increased in deeper groundwaters. Salinisation is known to occur in most crystalline basement massifs at depths between 500 and 1000 m below the earth's surface (e.g. Smalley *et al.*, 1988; Gascoyne and Kamineni, 1994). If depth data could be supplemented to the current data set it would be reasonable to expect higher F^- concentrations with depth.

Leakage of fluid inclusions. Waber and Nordstrom (1992) proposed that deep granitic groundwaters were geochemically influenced by the release of fluid from fluid inclusions. In saline, high pH waters with high F^- concentrations, they found that up to 3.8% of ions may have been derived from fluid inclusions. However, their method of calculating the composition of fluid inclusions is flawed, being based on a circular argument involving fluid inclusion contribution to groundwater, and fluid inclusion composition based on groundwater chemistry (Waber and Nordstrom (1992), p 244, paragraph 4).

The possibility that fluid inclusions contribute significant amounts of dissolved ionic species to Bushveld groundwater cannot be ruled out. Most of the samples collected during this investigation had inclusion trails, most notably in quartz grains (Chapter 4 and Appendix B1). However, no data on F^- concentrations in fluid inclusions exist for the area. Although F^- concentrations in fluid inclusions in the field area have not been established, the contribution of F^- from inclusions to the overall groundwater F^- content is likely to be minor compared to that from fluorite and other F-bearing minerals. Given the retrograde solubility of CaF_2 above 100°C (Strübel, 1965), it is predicted that the medium to high temperature fluid inclusions found in the study area are not likely to contain more than about 5 mg/ℓ F^-. To actually measure the F^- concentration of fluid inclusions would be difficult and was not attempted in this project.

Soil. The leaching experiments described in Chapters 3 and 4 have confirmed that soil is a source of F^-, but that it contains an order of magnitude less soluble-F than associated fresh rock. Soil as a source of F^- is therefore of proportionately less significance than the fresh rock of the host aquifer. However, if soil water is partially evaporated whilst in contact

with F salts, higher concentrations of F^-, as well as distinct stable isotope ratios, in groundwater may result.

6.4 Hydrogen and Oxygen Isotopes

The previous discussion has shown that evaporation is a potentially important process in increasing F^- concentrations in groundwater. The study of the stable isotopes of H and O allows an estimation of the extent of any evaporation. The expense of isotope analysis constrained the number of samples which could be analysed. The following discussions are based on a limited sample set, and additional analyses would clarify the relationships found here.

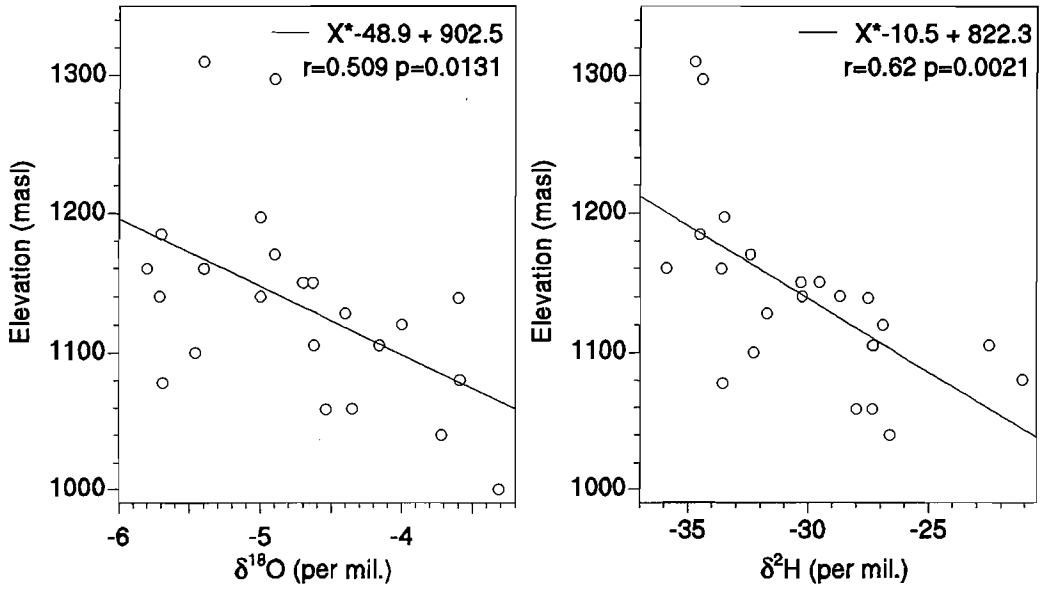

Figure 6.26 $\delta^{18}O$ and δ^2H plotted against elevation of *sampling point*. Some of the scatter may be explained by flow away from the point of recharge.

6.4.1 Correlation with elevation and temperature

The δ^2H and $\delta^{18}O$ values found in groundwater in this study are weakly correlated to sampling point elevation (Figure 6.26), with considerable scatter around the calculated regression line. The correlation of $\delta^{18}O$ with elevation is significant at the 95% confidence level, whilst for δ^2H it is significant at the 99% level. The scatter may be due to variable

vertical flow away from the recharge area, which cannot as yet be quantified because of uncertainty about the location and elevation of the recharge areas of these groundwaters. The regression shows that there is a decrease in $\delta^{18}O$ of 0.2‰ per 100 m increase in elevation. With a typical lapse rate in summer of 1°C per 100 m, the resultant relationship for $\delta^{18}O$ of 0.2‰/°C is comparable to the value of 0.4‰/°C found by Heaton *et al.* (1986) for groundwater along the southern coast of South Africa. The relationship of $\delta^{2}H$ to temperature for this area is 3.6‰/°C. The isotope results for hail and rain are discussed in Appendix G.

6.4.2 Isotopic signature of rock types

The rock type with which groundwaters interact may control the oxygen and hydrogen stable isotope signature of the water. A summary diagram, plotting H and O isotopes in groups according to their host rock is shown in Figure 6.27. The Pilanesberg perimeter groundwaters and those of the Nebo Granite have very different $\delta^{2}H$ and $\delta^{18}O$ values. It should be possible to identify the Pilanesberg Perimeter groundwater type, if encountered in boreholes in the surrounding RLS or Nebo Granite, based on its 'light' isotopic signature. The Nebo granite samples are tightly grouped around -4.4‰ $\delta^{18}O$ and -27‰ $\delta^{2}H$, and deviations from these values are considered significant. Central Pilanesberg groundwater has a much larger spread and shows evidence of having been subjected to evaporation (McCaffrey, 1993).

The Pretoria Saltpan brine is isotopically very much heavier than the precipitation falling in the area and has been subjected to large amounts of evaporation. One groundwater sample, taken from a borehole situated in Nebo Granite 1 km west of the Pretoria Saltpan, has a significantly heavier isotopic signature than other Nebo Granite water, and lies on a mixing line between Saltpan brine and either Nebo Granite groundwater or rainwater. This is taken as evidence that the Saltpan brines are somehow leaving the crater environs and mixing with local groundwater.

Warmbaths spring water. Mazor and Verhagen (1983) investigated many geochemical parameters in thermal springs in South Africa, including the spring hosted in Nebo Granite at Warmbaths. Their isotopic results are shown in Table 6.4 and are also plotted in Figure 6.27. The $\delta^{18}O$ of Warmbaths spring water is appreciably lighter than that of the Nebo Granite in the field area. No change in $\delta^{18}O$ with age has been found for the Nebo Granite groundwaters in this study (see later section), and since the water from the Warmbaths spring is of a comparable model age to several of the samples in this study, no palaeoclimatic effect can be invoked to explain the difference.

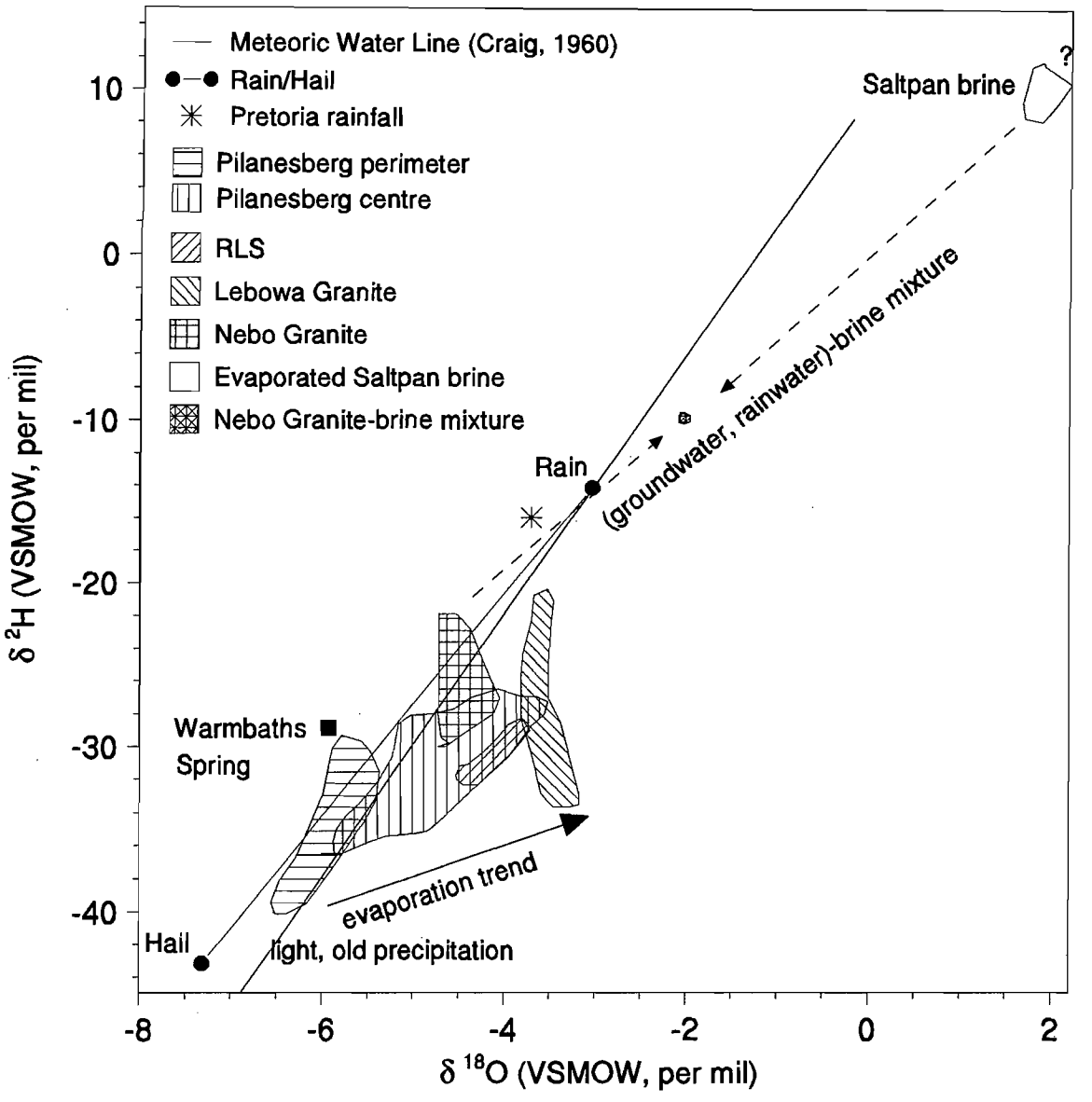

Figure 6.27 Interpretive diagram of hydrogen and oxygen isotopes. Some groundwaters may be the result of mixing between freshly recharged groundwater and evaporated brines. Central Pilanesberg data from McCaffrey (1993).

Table 6.4 Isotopic data for Warmbaths spring from Mazor and Verhagen (1983).

Isotope	$\delta^{2}H$ (‰)	$\delta^{18}O$ (‰)	Tritium (TU)	^{14}C (pmc)	$\delta^{13}C$ (‰)
Measured	-28.9	-5.9	0.2	8.6	-6.8
Error (±)	2.0	0.2	0.2	0.4	0.2

Two explanations are conceivable. It is quite possible that the recharge area for the Warmbaths spring is in the high Waterberg, which with elevations up to 2000 m, would readily account for the difference in $\delta^{18}O$. Alternatively, equilibration of meteoric water with alkali feldspar in granitic rocks, which have $\delta^{18}O$ values between +7 and +10‰ (Faure, 1987), would tend to shift the water to lower values. This is because of the large $\delta^{18}O$ fractionation factor of alkali feldspar and water at 25°C (in the order of -20 ‰; O'Neil and Taylor, 1967).

6.5 Radiogenic isotopes

This section attempts firstly to use radiocarbon to gauge the mean residence time of groundwater, and thus the rate of reactions which affect groundwater composition. Secondly, the section includes an attempt to characterise groundwater from the field area using Sr isotopes.

6.5.1 Radiocarbon - ^{14}C

Mean Residence Time. The ^{14}C results presented in Chapter 5 may be used simplistically as a chemical parameter to indicate a groundwater type (A. Issar, Ben-Gurion University, *pers. comm.*, 1995). More productively, ^{14}C may be used to calculate the mean residence time (T) of a groundwater flow unit.

Where the recharge area of a confined aquifer is of a similar cross sectional area to the flow path, and where ^{14}C is not depleted by interaction with ^{14}C-free aquifer material, or augmented by ongoing recharge along the flow path, the mean residence time can be modelled with the equation:

$$C_s = C_o(t - t_u - T)e^{-\lambda(t_u+T)} \qquad \textit{equ. (6.9)}$$

where C_s is the ^{14}C activity at the time of sampling, C_o is the input concentration (initial ^{14}C activity), λ the decay constant, T the mean residence time, t the time of sampling and t_u is the delay time in the unsaturated zone (Verhagen *et al.*, 1991). Mook (1980) and others use A_o to denote the original specific radioactivity of the sample, but the notation of Verhagen *et al.* (1991) is used here. The model is known as the 'piston flow' model. Equation 6.9 can be rearranged and simplified to:

$$T = 8267 \ln\left(\frac{C_o}{C_s}\right) \qquad \textit{equ. (6.10)}$$

This simplified equation is valid when the delay time in the unsaturated zone is small (Verhagen *et al.*, 1991). In the field area 'piston flow' conditions are probably only strictly fulfilled in the tuff bands of the Pilanesberg, which are confined on either side by impermeable syenite.

The open fracture system of the granitic rocks of the field area suggests that a discrete recharge area does not exist for these rocks. Rather, rainwater infiltrates over the entire outcrop, and much of the subcrop of the granite, mixing with groundwater on its way to the discharge area. This behaviour can be approximated using the 'exponential mixing' model (Geyh, 1972; Fritz *et al.*, 1979; Verhagen *et al.*, 1991), and the mean residence time of a groundwater flow unit in this system can be calculated using:

$$C_s = \frac{e^{-\lambda t_u}}{T}\int_0^\infty C_o(t-t_u-t^*)e^{-(\lambda+1/T)t^*}dt^* \qquad \textit{equ. (6.11)}$$

where t^* is the transit time of a ground water volume element (Verhagen, *pers. comm.*). This equation can be re-arranged and simplified to:

$$T = \frac{C_o - C_s}{C_s\lambda} \qquad \textit{equ. (6.12)}$$

where λ is the decay constant of ^{14}C, equal to 0.000121 and calculated from

$$\lambda = \frac{ln2}{T_h} \qquad \textit{equ. (6.13)}$$

The half life (T_h) of radiocarbon used here is therefore 5730 years (Faure, 1987).

Estimation of C_o. Equations 6.9 to 6.12 assume that C_o is known. In most hydrologic studies of ^{14}C, soils derived from aquifer material contain appreciable quantities of fossil C (^{12}C), diluting the ^{14}C activity of infiltrating rainwater. This reduces C_o from 100 pmc to as low as to 50 pmc. However, most igneous rocks and the soil derived from them are comparatively free of carbonate. Therefore, at a first approximation it might be assumed that C_o is between 90 and 100 pmc; McCaffrey (1993) assumed that C_o was 90 pmc for Pilanesberg groundwater. Although this study has shown for the first time (Chapter 4, Appendix B4) that carbonate minerals occur in the Pilanesberg, their distribution is likely to be very limited and their importance in terms of their affect on ^{14}C is therefore minimal. Several samples from the Pilanesberg have ^{14}C above 90 pmc. McCaffrey (1993) explained

this as due either to an absence of carbonate in the soils of the complex or to the influence of the increased atmospheric ^{14}C since the nuclear weapons tests of the 1960's.

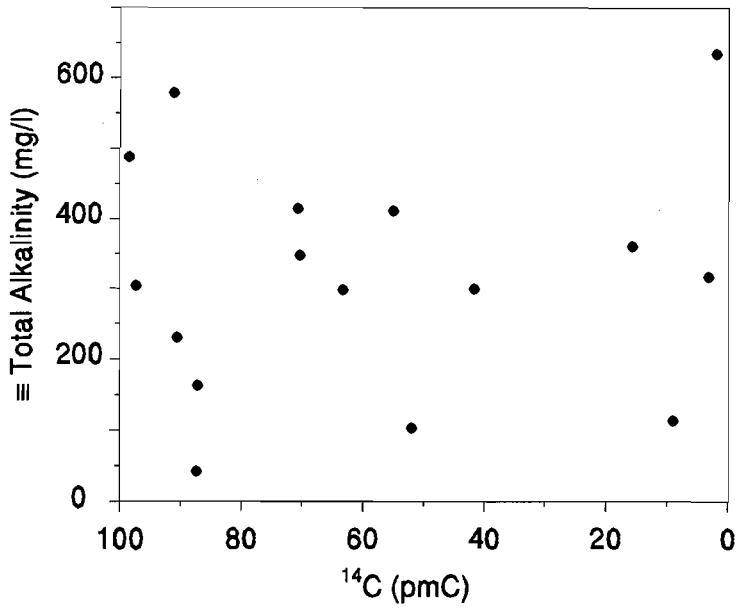

Figure 6.28 Plot of total alkalinity against ^{14}C, showing no significant trend in the data. This confirms that ^{14}C can be used to estimate residence time.

To use the radiocarbon method as a means of dating groundwater, it must be possible to affirm that ^{14}C has not been reduced by an increase in inorganic carbon content resulting from the dissolution of carbonates contained within the aquifer, as opposed to within soil derived from aquifer material. Figure 6.28 shows that the total alkalinity of the sample is not correlated to ^{14}C activity. This observation suggests that the assumption implicit in equations 6.9 to 6.12, that ^{14}C activity is reduced only by radioactive decay, is correct, and suggests that ^{14}C can be used to estimate mean residence time.

A method which has been used to gauge the initial activity of radiocarbon, C_o, is that of isotope dilution correction (Mook, 1980). The quantitative use of ^{13}C to gauge radiocarbon dilution is fraught with difficulties, and indeed its quantitative use is considered to be suspect when the hydrological parameters of a system are poorly known (Prof. B. Th. Verhagen, Schonland Centre for Nuclear Research, University of the Witwatersrand, *pers. comm.*). Typically, the extra parameters involved in the isotope dilution correction equations introduce extra uncertainty and errors into calculations of residence time, errors possibly greater than the actual correction. Isotope dilution corrections also sometimes produce apparent negative residence times, which are obviously impossible. It is with these limitations in mind that an isotope dilution correction is attempted here. In this method the $\delta^{13}C$ value of the groundwater is used to gauge the degree to which the original ^{14}C has been diluted after infiltration. The dilution factor $^{14}C_\Sigma/^{14}C_o$ is equivalent to

$$\frac{^{14}C_{\Sigma}}{^{14}C_{o}} = \frac{(\delta^{13}_{\Sigma} - \delta^{13}_{l})}{(\delta^{13}_{o} - \delta^{13}_{l})} \qquad \textit{equ. (6.14)}$$

where δ^{13}_{Σ} is the $\delta^{13}C$ value of carbonate in solution in the groundwater, δ^{13}_{l} is the $\delta^{13}C$ value in aquifer carbonate and δ^{13}_{o} is the $\delta^{13}C$ of soil CO_2. The $\delta^{13}C$ value for groundwaters (δ^{13}_{Σ}) is shown in Table 6.5. The table also includes the data of McCaffrey (1993). The value of δ^{13}_{l} is set at -2.7‰, the $\delta^{13}C$ value for carbonate in the Pilanesberg (Appendix B4). Difficulties ensue when estimating the value of δ^{13}_{o} (the $\delta^{13}C$ of soil CO_2). No direct measurements of this value have been made in any Bushveld soils (Prof. W. Stock, Department of Botany, University of Cape Town, *pers. comm.*). However, as the Bushveld is a semi-arid area of open grassland and Acacia trees, the resulting soil CO_2 $\delta^{13}C$ values are likely to be between -17 and -12‰ (Mook, 1980). The uncertainty in δ^{13}_{o} propagates into an uncertainty in the dilution factor, and thus C_o.

Table 6.5 shows that several groundwaters apparently have, after the ^{13}C correction described above, initial radiocarbon activities above 100 pmc. Although this seems to confirm that they contain bomb-generated ^{14}C, the lack of hydrological information and the current poor understanding of Bushveld groundwaters makes this a questionable interpretation.

Variation of F with residence time. Figure 6.29 shows residence times of groundwaters, estimated from equations 6.10 and 6.12 and the ^{14}C data, plotted against F^- concentration. The assumptions and drawbacks of radiocarbon dating and isotope dilution corrections should be remembered when attempting to interpret these graphs. Notably, the graphs show 'negative' residence times (obviously impossible), resulting from the application of the isotope dilution equation, and have error bars which reflect the likely range of initial radiocarbon values (C_o).

The upper plot in Figure 6.29 clearly shows that two trends are present; a high F^- and a low F^- trend. When ^{14}C activity is used to estimate a mean residence time, it is possible to interpret the two trends as two different rates for reactions which release F^- into solution.

For piston type flow, the equations for the regression lines indicate that the slower reaction releases 7.4×10^{-4} mg/ℓ/yr, whilst the faster reaction releases 2.6×10^{-3} mg/ℓ/yr F^- into solution. The intercept on the y axis of 3.4 mg/ℓ is interpreted as the result of the dissolution of rapidly dissolving, relatively soluble F-bearing minerals. In the context of the long time period under consideration, this may represent the dissolution of fluorite. The *p*K calculated from the intercept of the lower trend is very close to the *p*K of -10.4 calculated

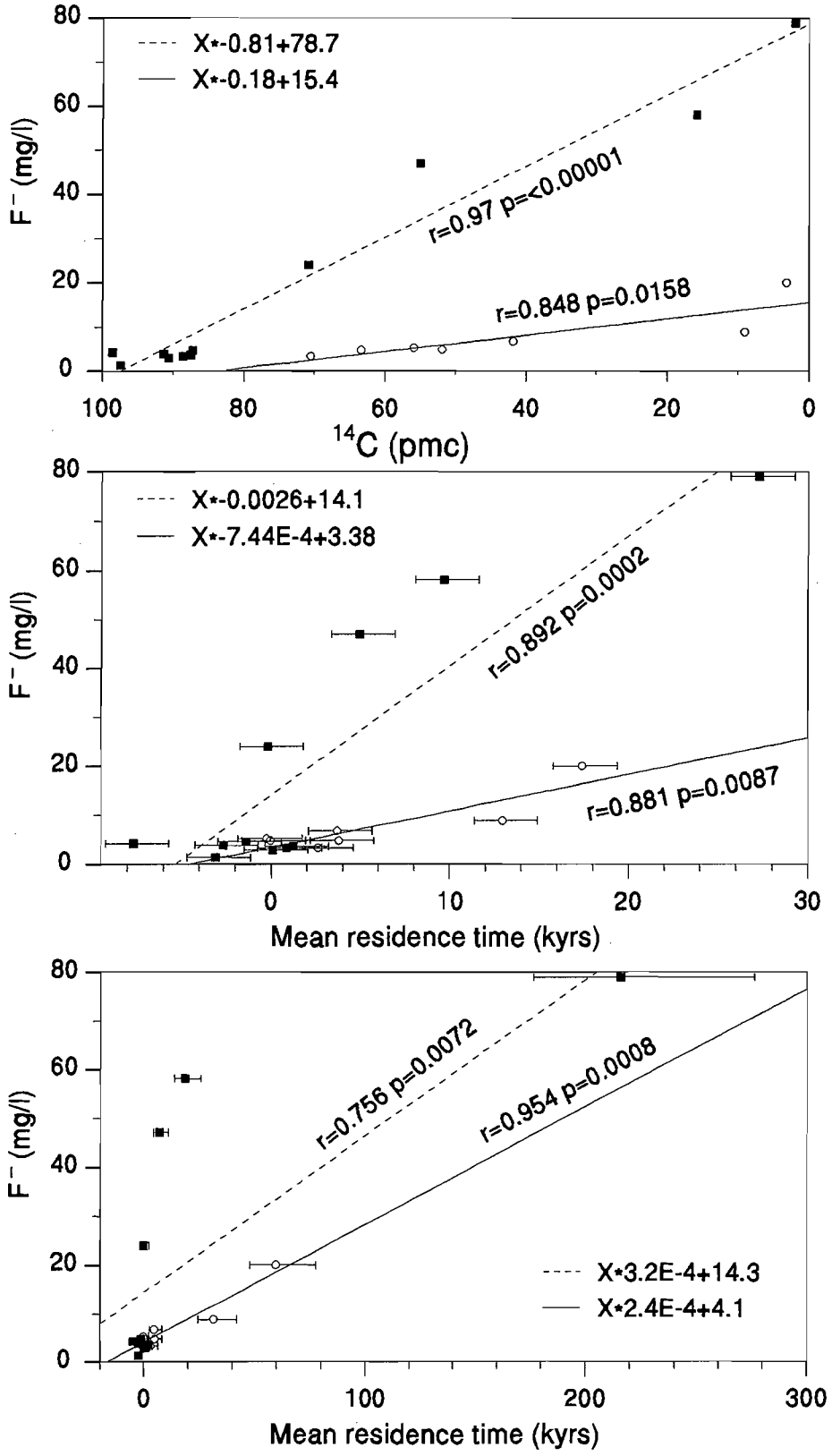

Figure 6.29 Correlation of F^- with ^{14}C and with mean residence time ('age') estimated using the 'Piston Flow' and 'Exponential' equations. '●' is upper trend, 'o' is lower trend.

for fluorite by Gill (1996), while the *p*K for the upper trend is an order of magnitude higher. When the 'exponential' equation is used to model residence time, the *p*K calculated for both trends is similar to those calculated using 'piston flow' conditions.

Variation of other ions with residence time. Several other chemical parameters (Na, pH, Ca and Mg) are correlated with ^{14}C and mean residence time, and these are shown in Figures 6.30 and 6.31. It has previously been noted that Na, pH and Ca are involved in reactions which increase F^- above the concentrations expected from the simple stoichiometric dissolution of CaF_2. These reactions are either ion exchange reactions, where Ca in solution is removed by exchange with Na on clay, and the release of F^- from clay surfaces at high pH, or reactions which precipitate $CaCO_3$ or gypsum. The regression equations shown in Figures 6.30 and 6.31 show that Na^+ in these groundwaters increases with residence time ten times faster than Ca^{2+} is removed, suggesting that a simple two-for-one swap of Na^+ for Ca^{2+} on ion-exchanging clays is not the only mechanism for hydrochemical change in these groundwaters. In each case, the reaction or exchange rate calculated using the piston flow model is generally an order of magnitude faster than that calculated from the exponential flow model.

Compared to the dissolution of fluorite, which in this time frame reaches equilibrium quickly, the processes operating here are very slow. Regressions calculated for these parameters are always more significant for the piston flow model than for the exponential flow model. The cation data is generally poorly correlated with residence time.

6.5.2 $^{87}Sr/^{86}Sr$ isotope ratios

The geohydrology of the Bushveld area is not known in any detail (Chapter 1), and the migration of F^- bearing groundwaters from one aquifer to another cannot be ruled out. The likeliest places where this may have occurred are from the Nebo and Lebowa Granites into the low lying Karoo sediments of the Springbok Flats, and from the Pilanesberg into the surrounding Nebo Granite and RLS. This study has attempted to characterise groundwater hosted in different rock types by their Sr isotope ratios, and to use these ratios to study hypothetical groundwater flow and provenance. Unfortunately the number of groundwater $^{87}Sr/^{86}Sr$ samples per rock type is very small, limiting the veracity of the conclusions. The samples were chosen for their geographic isolation from other rock types, so that the resulting Sr isotope values can be treated as a typical signature. Future workers will be able to use these signatures in studies on the provenance of groundwater along flow paths.

Dissolution of Sr-bearing minerals is the main source of Sr in groundwater. Modelling

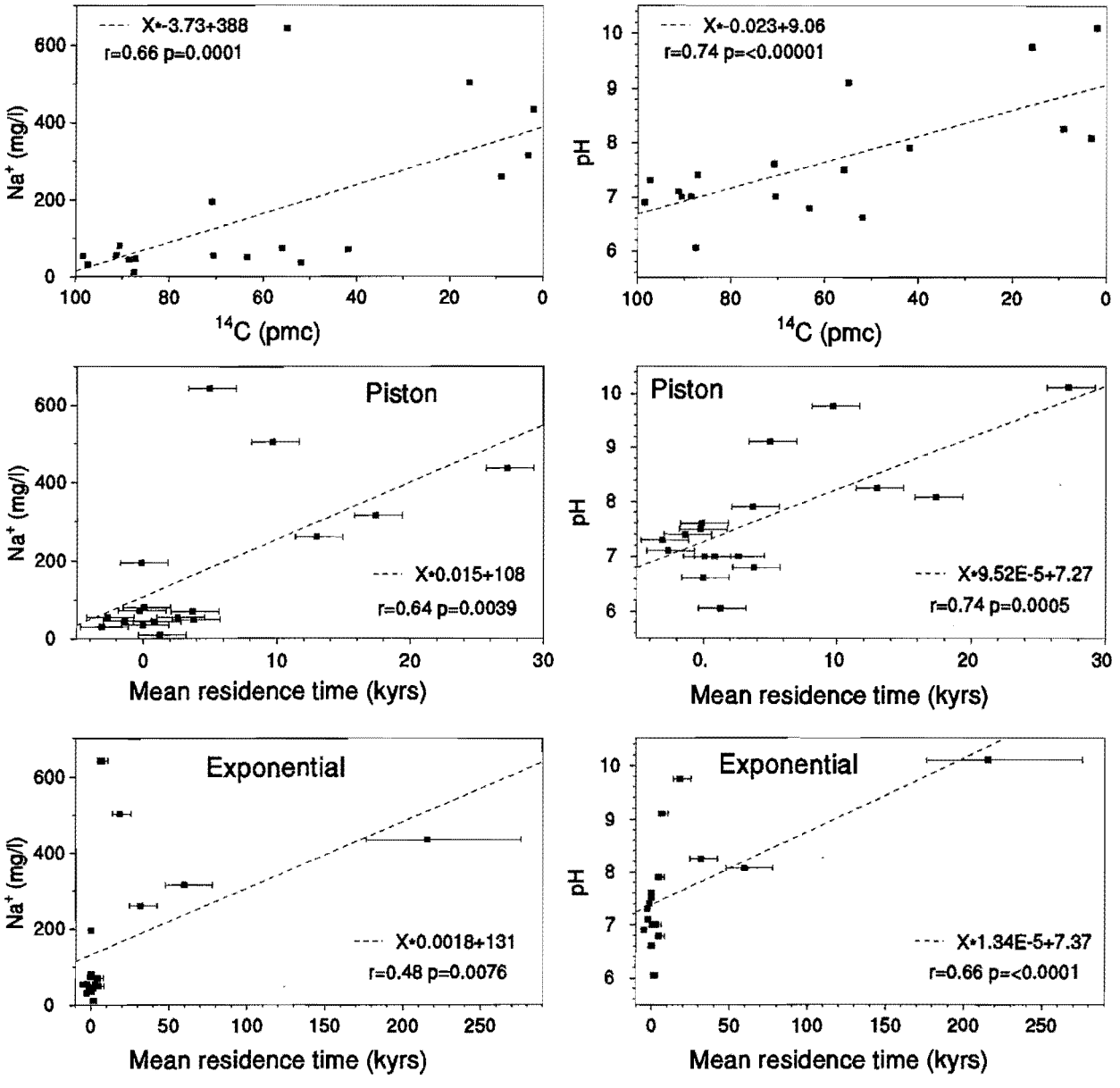

Figure 6.30 Correlation of Na and pH with ^{14}C and with mean residence time, calculated using the 'Piston Flow' and 'Exponential' models.

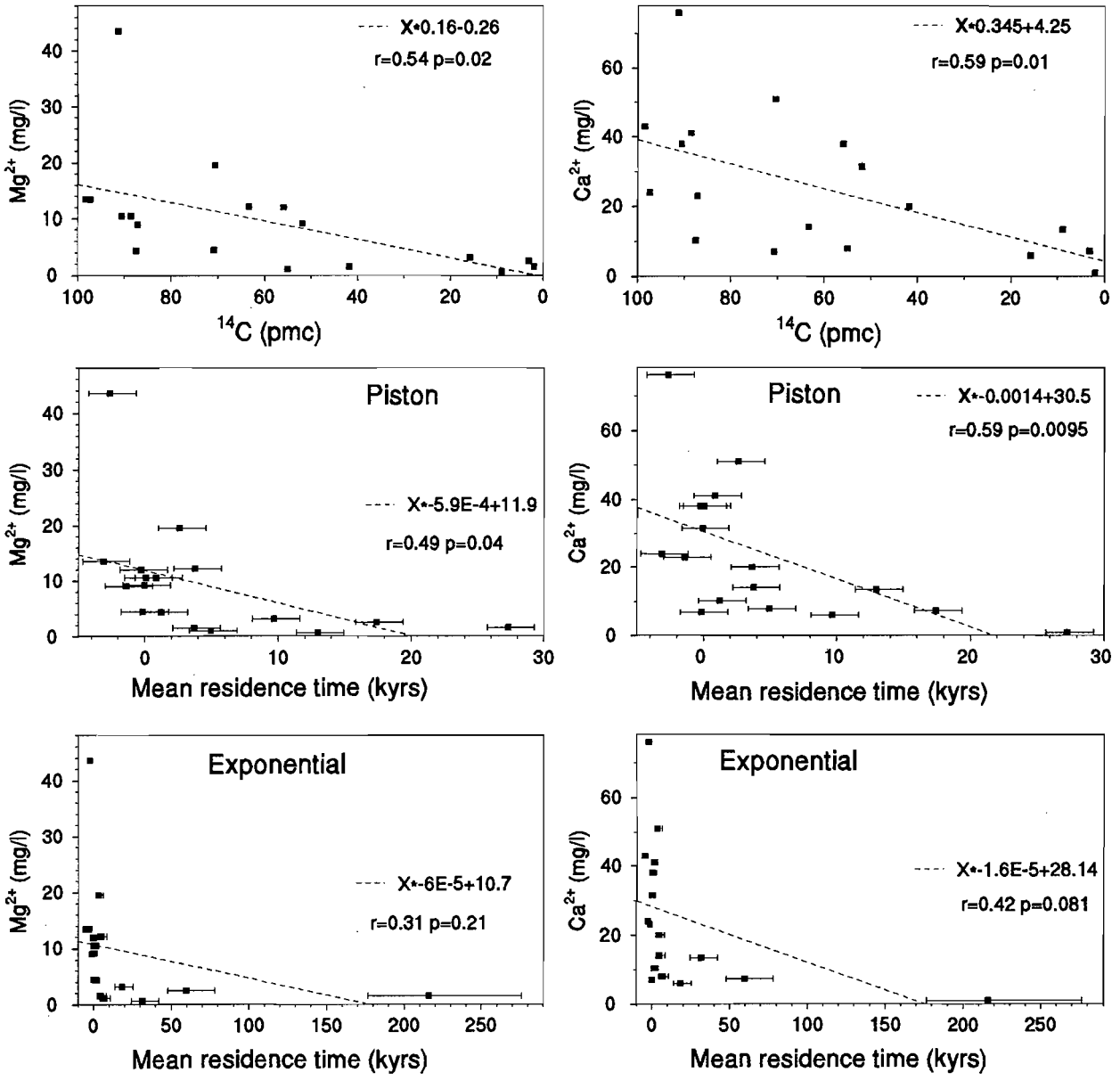

Figure 6.31 Inverse correlation of Ca and Mg with ^{14}C and mean residence time, calculated from 'Piston Flow' and 'Exponential' equations.

Table 6.5 Data used in the calculation of initial ^{14}C activity (C_o), the minimum and maximum value of C_o (min C_o and max C_o, respectively), and groundwater residence times for the Piston Flow and Exponential models. Sites in italics are from McCaffrey (1993). The superscripts ^{l,u} indicate which trend (lower and upper, respectively) in Figure 6.29 the groundwater belongs to. No $\delta^{13}C$ was measured for Stinkwater or Tswaaneng groundwaters, and the value of -14.5‰ is a best estimate, being the middle of the range for semi-arid Hache-Slack type vegetation. Minimum and maximum errors for Piston flow model is 1588 and 1968 years respectively for all groundwaters.

Site: site no.	^{14}C	$\delta^{13}C$	C_o	min C_o	max C_o	Piston	Expon-ential	Min error	Max error
Units:	pmc	‰	pmc			Years			
Klipvoor: 299^{u}	87.5	-14.7	102	84	129	1243	1341	1679	2582
Stinkwater: 243^{l}	63.3	(-14.5)	100	83	127	3780	4792	2283	3510
Tswaaneng: 286^{u}	55	(-14.5)	100	83	127	4942	6762	2627	4039
Slipfontein: 300^{l}	51.9	-8.8	52	43	66	-33	-33	1439	2213
Makoropeja: 292^{l}	9	-7.8	43	36	55	12972	31424	6938	10669
Mr Theledi's Farm:242^{l}	3.2	-5.8	26	22	33	17405	59585	11862	18239
Quarantine Camp: 287^{u}	2	-9.1	54	45	69	27283	215857	39182	60248
Mankwe Camp^{u}	98.5	-7.3	39	32	49	-7663	-4994	572	879
Gravel Pit^{u}	97.4	-10.6	67	55	85	-3099	-2584	993	1527
Bagkatla Gate^{u}	91.3	-10.5	66	55	84	-2670	-2281	1046	1608
Ruighoek Staff Acc.^{u}	90.6	-13.5	92	76	116	84	84	1460	2244
Bakubung Gate^{u}	88.6	-14.3	98	81	125	859	905	1603	2465
Tshukudu Camp^{u}	87.2	-11.4	74	61	94	-1387	-1277	1222	1878
Nkakana Int.^{u}	70.8	-10.9	69	57	88	-154	-153	1418	2181
FOP^{l}	70.5	-14.1	97	80	123	2605	3061	1980	3044
Mankwe Dam H/P^{l}	55.9	-9.1	54	45	69	-250	-246	1402	2156
Kololo Camp^{l}	41.8	-10.4	65	54	83	3682	4637	2256	3468
Ruighoek ELC: 35^{u}	15.8	-8.7	51	42	65	9663	18332	4650	7150

of the dissolution of such minerals can indicate the evolution of Sr isotope ratios over time (e.g. Fritz *et al.*, 1992). These workers indicated that groundwater Sr isotope ratios reach equilibrium with their host rocks within days to months, so that groundwaters (with residence times of centuries to millenia) can be regarded as in equilibrium with the aquifer. The first influence on groundwater Sr is the Sr content of rain water and this will be briefly discussed.

Rainwater Sr. No rainwater $^{87}Sr/^{86}Sr$ ratios are available for the study area and it is therefore not possible to calculate input into the groundwater system from that source. The $^{87}Sr/^{86}Sr$ ratio of modern seawater is 0.70906 (Faure, 1987); rainwater from New Mexico and Scotland had similar ratios, between 0.70917 and 0.71042 (Graustein and Armstrong, 1983; Bacon and Bain, 1995). However, Sr occurs at very low concentrations in rainwater (e.g. Bacon and Bain (1995) found between 2 and 210 Sr μg/ℓ in Scottish rainwater). Because of the very low Sr concentration in rainwater, the $^{87}Sr/^{86}Sr$ ratio of the solution rapidly changes upon dissolution of Sr-bearing minerals in rock and soil, and so the rainwater $^{87}Sr/^{86}Sr$ input into groundwater can effectively be ignored.

Mixing of groundwaters with differing $^{87}Sr/^{86}Sr$ and Sr concentrations. The $^{87}Sr/^{86}Sr$ ratio of a mixture of two groundwaters A and B ($^{87}Sr/^{86}Sr_M$) having Sr concentrations Sr_A and Sr_B and Sr isotope ratios of $^{87}Sr/^{86}Sr_A$ and $^{87}Sr/^{86}Sr_B$ is equivalent to

$$\left(\frac{^{87}Sr}{^{86}Sr}\right)_M = \frac{Sr_A Sr_B \left[\left(\frac{^{87}Sr}{^{86}Sr}\right)_B - \left(\frac{^{87}Sr}{^{86}Sr}\right)_A\right]}{Sr_M\,(Sr_A - Sr_B)} + \frac{Sr_A \left(\frac{^{87}Sr}{^{86}Sr}\right)_A - Sr_B \left(\frac{^{87}Sr}{^{86}Sr}\right)_B}{Sr_A - Sr_B} \qquad \textit{equ. (6.15)}$$

(Faure, 1987). The parameter Sr_M (concentration of Sr in the mixture) is calculated from

$$Sr_M = Sr_A f + Sr_B(1-f) \qquad \textit{equ. (6.16)}$$

where f is equivalent to

$$f = \frac{V_A}{V_A + V_B} \qquad \textit{equ. (6.17)}$$

The parameters V_A and V_B are the volumes of each groundwater in a given mixture. Figure 6.32 shows the application of these equations to the results presented at the end of Chapter 5, Table 5.4. It should be stressed that the values for $^{87}Sr/^{86}Sr$ in groundwater from each lithology in Figure 6.32 are probably members of a continuum. Without further sampling and analysis it will not be possible to assert whether the values analysed in the current study are 'end-members' or perhaps more central to that continuum. In Figure 6.32, Pilanesberg

groundwater, with high Sr concentration and low $^{87}Sr/^{86}Sr$ ratio, retains a low Sr isotope ratio in mixtures with Nebo Granite groundwaters, because of the relatively low Sr concentration of Nebo Granite groundwater. In contrast, saline groundwater from the perimeter of the Pilanesberg Complex (from a site known as the Quarantine Camp) readily loses its Sr isotope signature when mixed with Nebo Granite groundwater, because of the low Sr concentration in Quarantine Camp groundwater. It is apparent from Figure 6.32a that Quarantine Camp groundwater does not result from the simple mixing of Nebo Granite and Pilanesberg groundwaters. Figure 6.32b shows that, although the Lebowa Granite groundwater has the highest $^{87}Sr/^{86}Sr$ ratios of any groundwater in the study area, the low Sr concentration of this water means that it easily loses its Sr isotope signature when mixed with small quantities of a groundwater with moderate Sr concentration and lower $^{87}Sr/^{86}Sr$ ratio, such as that which occurs in the Irrigasie Formation of the Karoo.

The low-lying Karoo basin is surrounded to the north, west and south by elevated outcrops of the Nebo and Lebowa Granites, and it is probable that groundwater moves from these granites into the sediments of the Karoo basin. The groundwater will have equilibrated with the granites and will have the Sr isotope signatures described in the previous sections. Figure 6.33 shows a hypothetical mixing diagram for groundwaters from the Nebo and Lebowa Granites, and from the Irrigasie Formation of the Karoo basin. The diagram is plotted in coordinates of $^{87}Sr/^{86}Sr$ and 1/Sr concentration to give straight mixing lines. The diagram shows that, using just these 3 selected analyses, these groundwaters can be distinguished from each other quite readily using $^{87}Sr/^{86}Sr$ and Sr concentration.

However, when the full range of $^{87}Sr/^{86}Sr$ ratios and Sr concentrations are plotted, it becomes clear that large ranges of strontium concentration make this method inapplicable (Figure 6.34). The area on this graph where, for instance, Karoo and Lebowa groundwaters mix also includes the two analyses of Nebo Granite groundwater, producing ambiguous mixing relationships. The same problem occurs for Pilanesberg and Nebo Granite groundwater mixtures, which, when taking into account the 'end-members', encloses the analysis of Rustenburg Layered Suite groundwater. With only two analyses of $^{87}Sr/^{86}Sr$ for groundwater from each rock type, it is very unlikely that the full range of variability has been sampled. With further sampling, the ranges of Sr concentration and isotope value are likely to become larger, making the exercise futile. It is concluded that, even given the small number of samples, Sr isotope and Sr concentration characterisation of groundwater is unlikely to be of use in the Bushveld area.

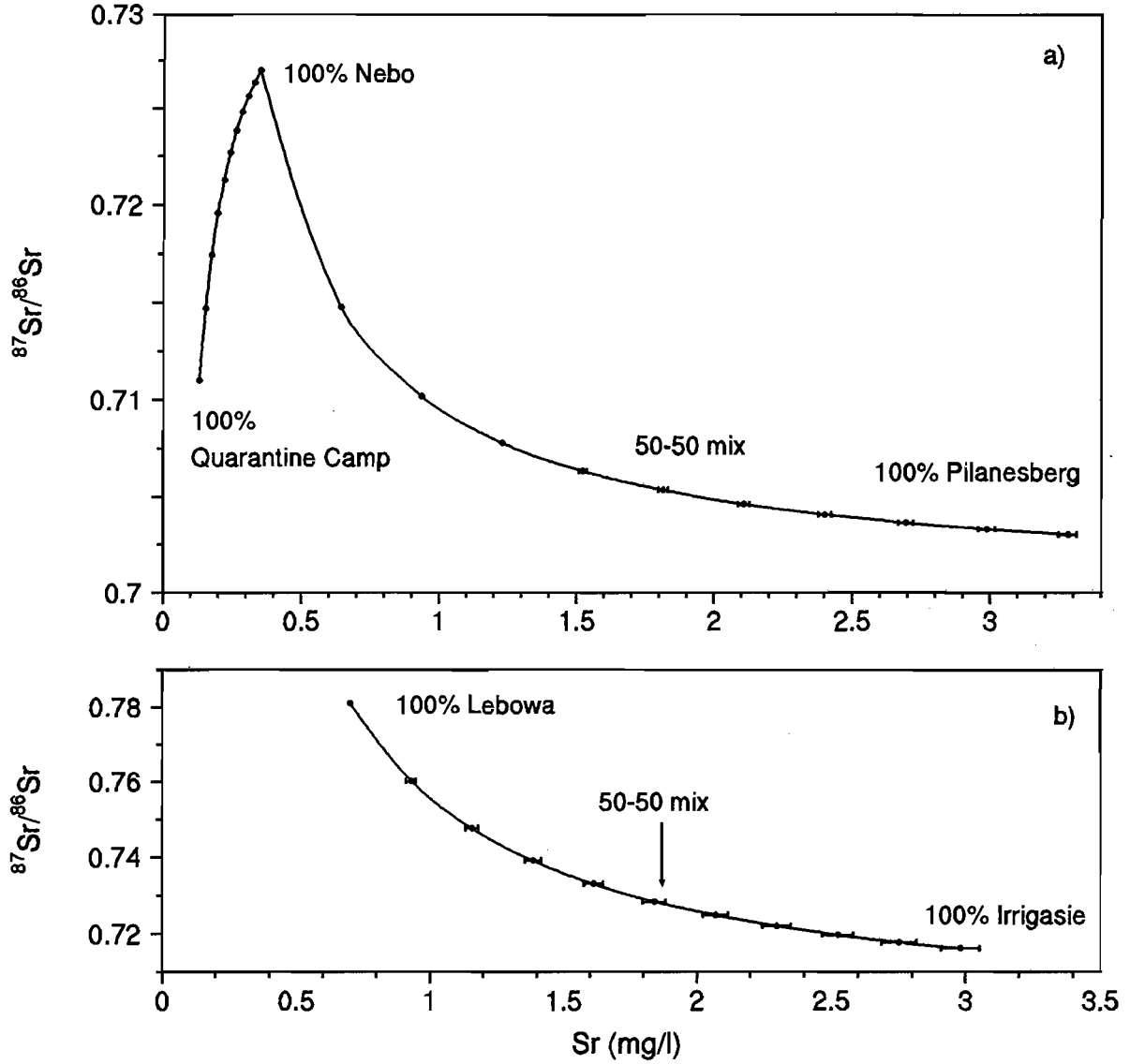

Figure 6.32 $^{87}Sr/^{86}Sr$ ratios in mixtures of various groundwater types. Points represent admixtures of 10 vol% and 90 vol%, 20 vol% and 80 vol%, etc. Error bars are ±1 s.d. Errors smaller than symbols are not shown.

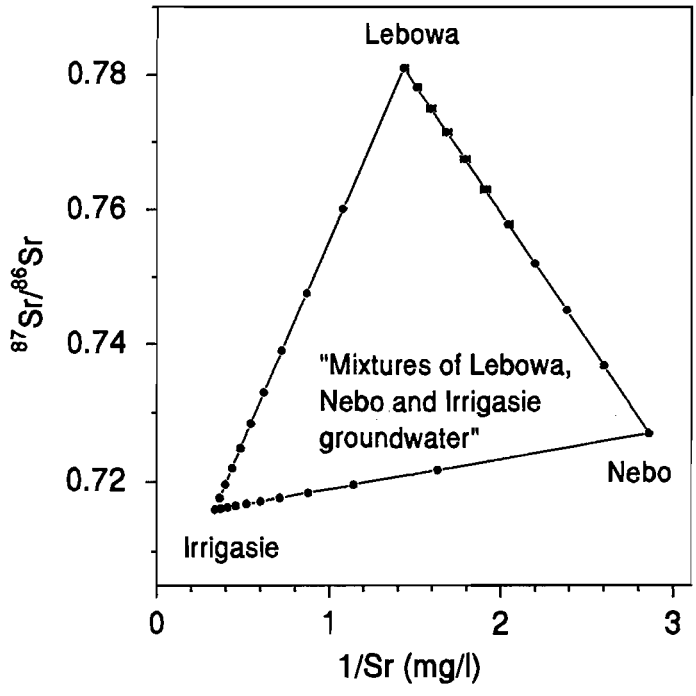

Figure 6.33 Hypothetical mixing diagram for 3 groundwater samples from the Nebo and Lebowa Granites, and from the Irrigasie Formation of the Karoo, based on Sr isotope ratios and Sr concentration.

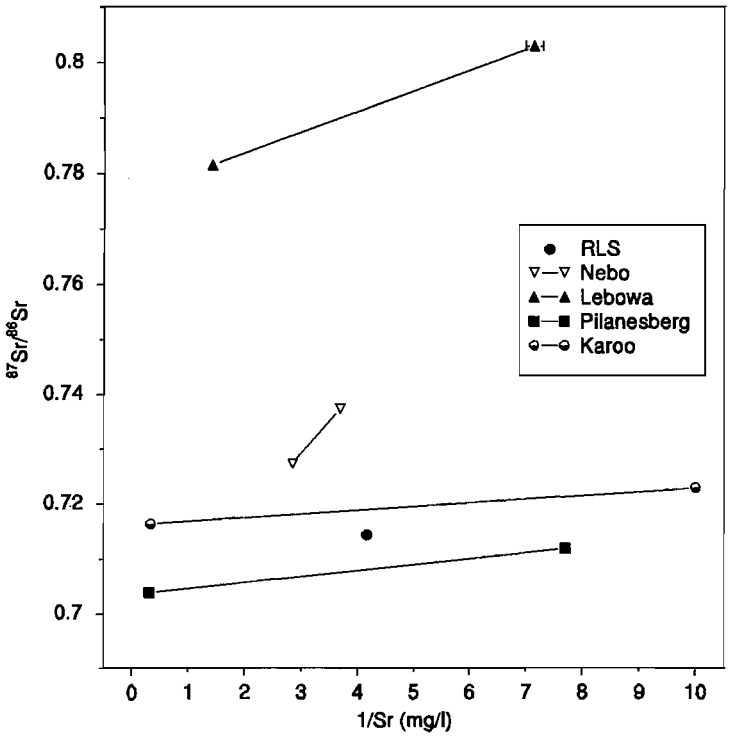

Figure 6.34 The range of $^{87}Sr/^{86}Sr$ ratios and Sr concentrations for groundwater from specific rock types of the area.

7 CONCLUSIONS

This chapter has two sections: a synthesis of the findings of previous chapters; and suggestions for further research. Groundwater data acquisition and data quality is summarised followed by a discussion of the results. The distribution of F in soils, rocks and minerals is linked to the distribution of F^- in groundwater, and other causes of high F^- groundwater are reviewed. An evaluation of the impact on human health of the ubiquity of high F^- groundwater in the Bushveld is reiterated. The main conjectures of this thesis are then presented, and finally a series of suggestions are made for further research which would answer questions arising from the current body of work.

7.1 Synthesis

This section summarises the findings of previous chapters. The most important conclusions are presented schematically in Figure 7.1.

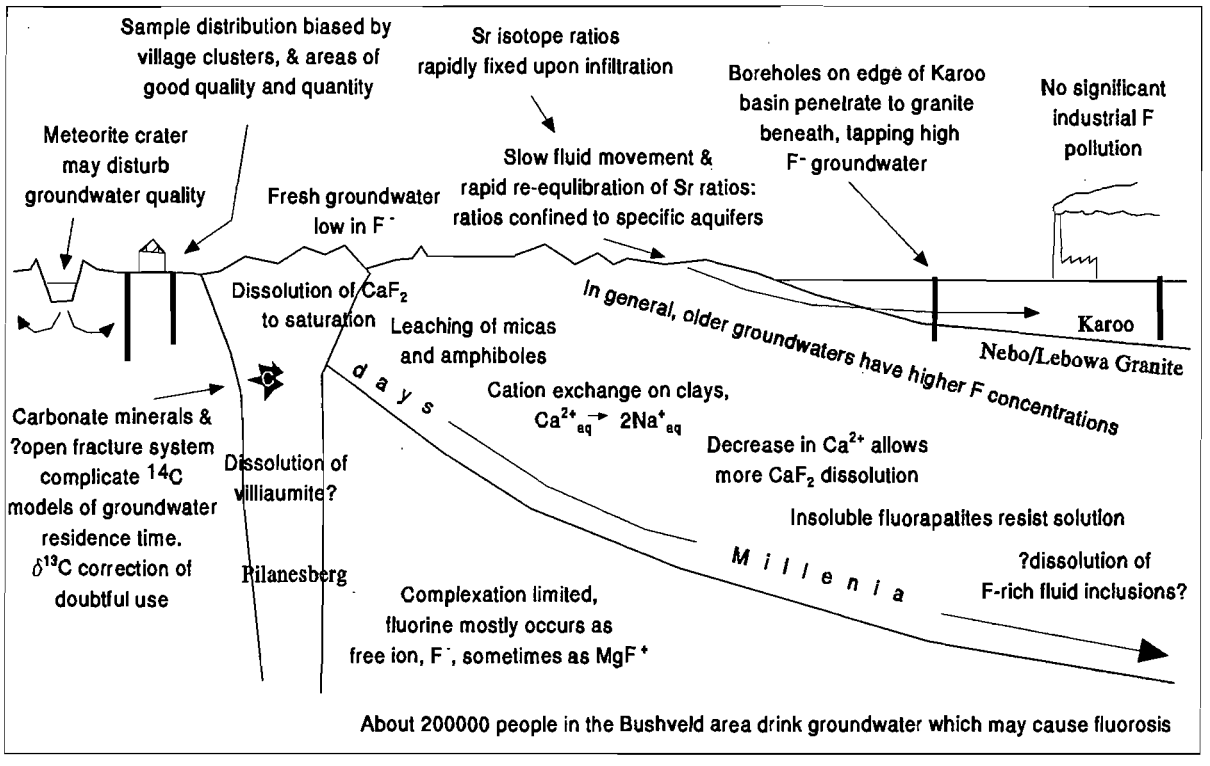

Figure 7.1 A sketch of the major conclusions arising from this thesis.

7.1.1 Groundwater

It was shown that analysis of F^- in groundwater using FISE with a standard buffer solution provided satisfactory analyses of typical Bushveld groundwaters, with no significant interference from Al. However, using a carbonate/bicarbonate eluent with HPIC often over-estimates the concentration of F^- relative to FISE. The presence of a water dip in the carbonate/bicarbonate chromatogram generally complicates the process of determining a baseline for the fluoride peak and is the probable cause of the overestimation, which is removed completely when a sodium tetraborate eluent is used. However, although using sodium tetraborate as an eluent gives an accurate and precise determination of fluoride in solution, the method is slower and other anions cannot be determined in the same run.

Two pre-existing data sets were combined with the author's; each had distinct differences in ion balance error. The combined data set is the largest available for F^- in the Bushveld.

Several factors affect the spatial quality of the data, namely humanity, availability, quality and rivers. Firstly, there is a clustering of the data since boreholes are most common in villages. Secondly, a low data density in some areas occurs because of the absence of boreholes, such as in the granite areas to the northeast of the Pilanesberg. Boreholes in these areas have low success rates and low yields - they are either abandoned after drilling or fall into disrepair after being equipped. Thirdly, boreholes with 'good' quality water are maintained and more boreholes are drilled in the area. Boreholes with 'poor' quality water tend to be abandoned after drilling, or are equipped but fall into disrepair, and naturally act as a disincentive for further drilling in the area. Finally, few boreholes exist in the vicinity of the perennial rivers, such as the Apies, since water is usually available from the river all year round.

Any data concerning groundwater chemistry collected from rural areas anywhere in the world might be affected in these ways. The current data set is, therefore, highly biased towards clustered boreholes with high yields and good water quality. In this instance, 'good' quality water is measured solely by palatability, as many of the boreholes drilled by local people undergo no other quality test than taste. The results from this study are of the 'best scenario' type.

The median concentration of F^- in groundwater of the western Bushveld is 0.3 mg/ℓ, whilst the mean is 1.43 mg/ℓ; the population is highly skewed towards low concentrations. Fluoride is found at low concentrations in most groundwaters from the RLS (mean of 0.4 mg/ℓ F^-). Groundwater F^- concentrations are high in the acid intrusive phases of the

BIC. Nebo Granite groundwater has a mean concentration of 2.0 mg/ℓ F^-, whilst that from the Lebowa Granite has a higher mean value of 5.0 mg/ℓ with a maximum over 10 mg/ℓ.

The Pilanesberg complex has the highest mean groundwater F^- concentration (15 mg/ℓ). Concentrations around the perimeter of the Complex reach 80 mg/ℓ, although values for the perimeter are generally in the range of 30 to 60 mg/ℓ. Fluoride concentrations of groundwater within the geographic boundaries of the Complex range from 2 to 7 mg/ℓ.

Bushveld groundwaters have concentrations of several trace elements often in excess of South African drinking water guidelines. Of these trace elements, Zn and Al are the likeliest to interact with F^-. Zinc occurs in surprisingly high concentrations in these groundwaters, with the highest concentrations in those of the Pilanesberg Complex. At pH 3.0 and 37°C, representative of conditions in the human stomach, all Zn is likely to be in the form Zn^{2+}, which is likely to be readily metabolised. No significant zinc-fluoride complexes are likely to form at the concentrations reported in these groundwaters, and complexation of F^- by Al is of little biological significance in the field area. In most groundwaters, less than 5% of F^- is complexed by Al, Ca or Mg, but Mg is the usual complexing ion. The majority of F exists in the form of the free fluoride ion, F^-.

7.1.2 F in rock, soil and minerals

High F concentrations occur in the Lebowa granite and Pilanesberg Complex, whilst the Nebo granite has scattered high values. The RLS is uniformly low in fluorine and the sedimentary rocks of the area generally have F concentrations well below 1000 ppm. The distribution of F in rock and soil is very similar to the distribution of high F concentrations in groundwater.

Fluorine was determined in paired rock and topsoil samples which showed that fluorine concentrations in soils are generally lower than parental rock fluorine concentrations by up to an order of magnitude. High F concentrations in soil have a similar distribution to high F in rock. Some contamination of soil by tailings has occurred in the vicinity of fluorite mines.

The rocks of the RLS and the Pretoria Group generally contain no major fluoride-bearing minerals. The granophyres, granites and alkaline complexes all contain fluorite (CaF_2) which can have a major effect on groundwater at very low volume percentages. Fluorapatite should occur in the granitic rocks but microscopic examination failed to reveal its presence. Fluorapatites in fluorite ore from the Pilanesberg were shown to have an unusually high Sr concentration, up to 6.8 wt%.

All F concentrations in micas analysed from the Pilanesberg complex and Lebowa Granite were below the detection limit (0.17 wt%), and are presumably hydroxy-micas. Fluorine in amphibole ranged from below the detection limit of 0.17 wt% in Lebowa Granite to 2.69 wt% in the Pilanesberg Complex. Much of the F in the Lebowa Granite is contained in fluorite.

Leaching experiments were conducted on all rock and soil samples. The highest concentrations of F^- in the leachate came from rocks and soils with the highest fluorine concentrations. In the rock leaching experiment, several of the samples had leachate with very high F^- concentrations (>30 mg/ℓ), but concentrations in leachate derived from soil samples was generally below ≈5 mg/ℓ. Soluble F was approximately 1% of the total F in rocks but only 0.1% of the total in soils, indicating that the soils had been effectively leached of soluble F^-.

7.1.3 Origins of high F^- groundwaters

There are three main reasons why fluorite is of prime importance in controlling fluoride solubilities in natural waters: fluorite is the most ubiquitous and abundant fluoride containing mineral; it is sparingly soluble; and Ca is generally always present in natural waters. These three factors also show why fluorapatite is not frequently cited as a controlling factor in fluoride concentration - fluorapatites are relatively uncommon, they are insoluble and phosphate is found at very low concentrations in natural waters. The possibility that other, more soluble fluorine minerals (such as villiaumite - NaF) are responsible for very high fluoride concentrations (>30 mg/ℓ) is strongly suggested by dissolution experiments on powdered rock samples. Pilanesberg and Lebowa groundwaters are generally saturated to supersaturated with respect to fluorite, while Nebo Granite groundwater is generally less saturated. All groundwaters are undersaturated with respect to NaF.

Speciation and saturation index calculations were undertaken using the thermodynamic modelling package JESS, designed and operated by the CSIR. The package produced very similar results to MINTEQA2, produced by the US EPA, for minerals not containing carbonate. Confidence is expressed in the results of modelling by MINTEQA2.

Other reactions, apart from mineral dissolution, can also affect F^- concentrations. These include: anion exchange of F^- by OH^- on clay surfaces at high pH; precipitation of $CaCO_3$; cation exchange on clays (replacing Ca^{2+} with Na^+), and precipitation of gypsum upon evaporation. The latter three processes remove Ca^{2+} from solution and allow CaF_2 to dissolve further, beyond stoichiometric dissolution. Strong evidence was found for the operation of ion exchange processes in some of the groundwaters.

There is little anthropogenic addition of F to groundwater in the area. Few large working fluorite mines still exist in the Lebowa Granite Suite and Rooiberg felsite, but major fluorite mines are still active in the Malmani Dolomite of the Chuniespoort Group, on the edge of the study area. The impact of dust generated by blasting and processing the ore is likely to be local, and no gaseous emissions are generated. Two other large fluorine-handling industries exist in the study area; a uranium enrichment plant in the south, and a major platinum ore smelter in the centre of the area. Neither of these facilities are likely to add significant F^- concentrations to groundwaters of the region.

Fluoride concentration in rainfall should be near the background concentrations of 8 μg/ℓ, insignificant in terms of fluorosis risk. Infiltrating rainwater is undersaturated with respect to CaF_2, and so recharging groundwater will actively dissolve the mineral. Groundwater should reach equilibrium with fluorite within one month of infiltration.

Some workers have suggested an influence on groundwater compositions from the dissolution of fluid inclusions. Given the retrograde solubility of CaF_2 above 100°C, it is predicted that medium to high temperature fluid inclusions are not likely to contain more than about 5 mg/ℓ F^- and the contribution from weathering fluid inclusions is expected to be negligible.

The Pilanesberg perimeter groundwaters and those of the Nebo Granite have very different δ^2H and $\delta^{18}O$ values, and it should be possible to identify the Pilanesberg perimeter groundwater type, if encountered in boreholes in the RLS or Nebo Granite near the Pilanesberg, based on its 'light' isotopic signature. Nebo granite groundwaters are tightly grouped isotopically, and deviations are considered significant. Central Pilanesberg groundwater has a much larger spread and shows evidence of being subjected to evaporation. The Pretoria Saltpan brine is isotopically much heavier than the precipitation falling in the area and has been subject to large amounts of evaporation. One groundwater sampled in the vicinity has a significantly heavier isotopic signature than other Nebo Granite waters, and lies on a mixing line between Saltpan brine and Nebo Granite groundwater. This is taken as evidence that the Saltpan brines are somehow leaving the crater environs and mixing with local groundwater.

Radiocarbon (^{14}C) activity was used to estimate mean residence times for groundwaters, after correction for variation in initial activities using an isotope dilution correction method. It is possible to interpret the associated groundwater composition data as evidence for different rates for various water-mineral reactions. These reactions appear to increase F^- concentrations in groundwater at two different reaction rates. If piston type flow is assumed, the slowest reaction releases 7.4×10^{-4} mg/ℓ/yr F^-, whilst the faster reaction

liberates 2.6×10^{-3} mg/ℓ/yr F^- into solution. An implied solubility of at least 3.4 mg/ℓ is interpreted as the dissolution of a rapidly dissolving, relatively soluble F-bearing mineral. In the context of the long time period under consideration, this probably represents the dissolution of fluorite. Two values of *p*K may be calculated from the data, one of which is very close to the *p*K of -10.4 calculated for fluorite by other workers.

The large range in Sr isotope ratios and Sr concentrations found in the few samples analysed suggests that natural variability will complicate further use of Sr in tracing groundwater provenance in the Bushveld area. Based on the current Sr isotope data, groundwater from the Quarantine Camp, on the perimeter of the Pilanesberg, with a F^- concentration of 80 mg/ℓ, does not result from a mixture of 'typical' Nebo Granite and Pilanesberg Complex groundwaters.

7.1.4 The possible extent of fluorosis

The optimal F^- concentration in drinking water for several of the towns within the field area was estimated using an equation which related the optimal F^- concentration to the maximum mean temperature. The variation in the value between towns is only 0.07 mg/ℓ, and the mean optimum concentration of 0.65 mg/ℓ is almost identical to the maximum safe concentration of 0.7 mg/ℓ calculated by Du Plessis (1995) for the Free State goldfields.

Spatial analysis by GIS shows that groundwater underlying 17000 km^2 of the western Bushveld has a F^- concentration >0.7 mg/ℓ, the optimum fluoride concentration in drinking water for the area. Over 540 of the 3000 groundwater samples have a F^- concentration >0.7 mg/ℓ. Since between 150 and 200 people are supplied by each borehole, between 82 000 and 109 000 people are drinking groundwater which may induce fluorosis in the long term.

Using a Thiessen polygon method, three hundred areas have been delineated where there is a medium or higher risk of dental fluorosis. The resulting 'fluorosis risk map' will be of use to water supply planners.

7.2 Recommendations for further work

7.2.1 Groundwater studies

Spatial gaps still exist in the data base, especially in the areas underlain by Archaean Granite. Further groundwater sampling in these areas could be undertaken to improve data

density. However, the cost-benefit relationship of further sampling would have to be carefully considered. Silica was not determined in this study, and the absence of silica data meant that saturation indices for silicate minerals could not be calculated. The analysis of a sub-set of samples for silica would improve understanding of mineral-water interaction in the area. The extension of the study to include the rest of the South African groundwater database, which holds ≈45 000 groundwater analyses, would enable further high F^- areas to be delineated. The translation from the chinese of the potentially important text by Fuhong *et al.* (1996) should be undertaken by a specialist.

7.2.2 Analysis of rock, soil and minerals

The lack of analyses for F in rocks from the field area is apparent, and the fact that the Regional Geochemical Mapping Programme (RGMP) of the Council for Geoscience does not include the analysis of F is regrettable. The analysis of F in just 1 % of the thousands of soil samples taken by the RGMP, which coincidentally covers most of the high groundwater fluoride areas shown in Figure 2.2, would provide a very valuable data set.

The Moepo Fluorite mine in the Pilanesberg has been shown to contain an unusual assemblage of minerals and rare mineral types (high-Sr calcite and high Sr-apatite) which have not been reported previously in South Africa. Additional mineralogical and geochemical investigation may produce further interesting results.

The characterisation of clays and/or zeolites lining fractures in Bushveld Igneous Complex and Pilanesberg Complex rocks would help to define possible cation exchange processes taking place in the groundwater regime. The use of XRD to identify the clays and the determination of cation exchange capacities would be of use in delimiting ion exchange processes in the area.

An investigation into the presence of NaF in rocks of the Pilanesberg Complex and Lebowa Granite would test the theory that groundwater F^- concentrations have been influenced by dissolution of this mineral.

7.2.3 Groundwater isotopes

The geohydrology of the hard rock aquifers of the western Bushveld has been comparatively poorly researched. The area is, therefore, a prime target for the large scale application of isotope hydrology. The wide range of radiocarbon activities in the Pilanesberg and Lebowa Granite Suite is still a conundrum, and the accurate estimation of groundwater residence time requires more accurate knowledge of the local geohydrology. Given the relative cheapness of oxygen and hydrogen isotope analyses, these parameters should be

measured on the whole sample set to show regional trends, and possibly recharge/discharge areas. The uncertainty in recharge areas and groundwater movement in the study area might be solved by the analysis of such stable isotope data. Sr isotope analyses of a greater number of samples from groundwaters from the western Bushveld would help to show the range of natural variation in this parameter.

7.2.4 Geohydrology of the western Bushveld

The lack of water level and borehole depth data has been one of the major limitations of this study. An analysis of all available water-table elevation data should delineate flow directions. The glimpse of the hydrological systems existing around a recent meteorite crater should be followed up with a total hydro-census of the area, intensive sampling for major and trace elements, and stable isotopes, and computer modelling of the results.

8 REFERENCES

Acker, JG and Bricker OP (1992) The influence of pH on biotite dissolution and alteration kinetics at low temperature. *Geochim. Cosmochim. Acta*, **56**, 3073-3092.

Ahrens, LH (1952) The use of ionization potentials, Part 1: Ionic radii of the elements. *Geochim. Cosmochim. Acta*, **2**, 155-169.

Al-Aasm, IS, Taylor, BE and South, B (1990) Stable isotope analysis of multiple carbonate samples using selective acid extraction. *Chemical Geology*, **80**, 119-125.

Allison, JD, Brown, DS and Novo-Gradac, KJ (1991) *MINTEQA2/PRODEFA2, a geochemical assessment model for environmental systems, version 3.0 users manual.* US Environmental Protection Agency, Athens, Georgia. 106pp.

Anderson, C (1991) Fluoride given the all clear. *Nature*, **349**, 732.

APHA [American Public Health Association] (1995) *Standard methods for the examination of water and wastewater, 19th edition.* American Public Health Association, American Water Works Association and Water Environment Federation, Washington D.C.

Arnold, FA, Dean, HT and Knutson, JW (1953) Effect of fluoridated public water supplies on dental caries prevalence: results of the seventh year of study at Grand Rapids and Muskegon, Michigan. *Public Health Report*, **68**, 141-148.

Ashley, RP and Burley, MJ (1994) Controls on the occurrence of fluoride in groundwater in the Rift Valley of Ethiopia. 45-54 *In:* Nash, H and McCall, GJH (*eds.*) *Groundwater Quality 17th Special Report.* Chapman and Hall, London. 204pp.

Ashton, PJ and Schoeman, FR (1983) Limnological studies on the Pretoria Salt Pan, a hypersaline maar lake. *Hydrobiologia*, **99**, 61-73.

Auméras, M (1927) Etude de l'equilibre fluorure de calciu-acide chlorhydrique etendu - contribution a l'étude des équilibres ioniques. *J. Chim. Phys.*, **24**, 548-571.

Babushkin, VI, Matveyev, GM and Mchedlov-Petrossyan, OP (1985) *Thermodynamics of silicates*. Springer Verlag, Berlin. 459pp.

Backer Dirks, O (1992) Biokinetics of fluoride in relation to dental and skeletal fluorosis. *In:* Frencken, JE (*ed.*) *Endemic fluorosis in developing countries*. Report of a symposium held in Delft, the Netherlands, April 27th, 1990, 20-30.

Bacon, JR and Bain, DC (1995) Characterization of environmental water samples using strontium and lead stable isotope compositions. *Environmental Geochemistry and Health*, **17**, 39-49.

Bailey, JC (1977) Fluorine in granitic rocks and melts: a review. *Chem. Geol.*, **19**, 1-42.

Banner, JL, Musgrove, M and Capo, RC (1994) Tracing ground-water evolution in a limestone aquifer using Sr isotopes: effects of multiple sources of dissolved ions and

mineral-solution reactions. *Geology*, **22**, 687-690.

Barker, DS (1989) Field relations of carbonatites. *In:* Bell, K (*ed.*) *Carbonatites: Genesis and Evolution*. Unwin Hyman, 38-69.

Barker, DS (1993) Diagnostic magmatic features in carbonatites: implications for the origins of dolomite- and ankerite-rich carbonatites. *S Afr. J. Geol.*, **96**, 131-138.

Barnard, WR and Nordstrom, DK (1982a) Fluoride in precipitation - 1. Methodology with the fluoride-selective electrode. *Atmospheric Environment*, **16**, 99-103.

Barnard, WR and Nordstrom, DK (1982b) Flouride [*sic*] in precipitation - 2. Implications for the geochemical cycling of fluorine. *Atmospheric Environment*, **16**, 105-111.

BDWA, [Bophuthatswana Department of Water Affairs] (1992) *Moretele Water Plan.* Unpubl. Report.

Birch, GF (1981). The Karbonat-Bombe: a precise, rapid and cheap instrument for determining calcium carbonate in sediments and rocks. *S Afr. J. Geol.*, **84**, 199-203.

Blavoux, B and Letolle, R (1995) Apports des techniques isotopiques a la connaissance des eaux souterraines. *Géochronique*, **54**, 12-15.

Blum, JD, Erel, Y and Brown, K (1994) $^{87}Sr/^{86}Sr$ ratios of Sierra Nevada stream waters: Implication for relative mineral weathering rates. *Geochim. Cosmochim. Acta.*, **58**, 5019-5025.

Bond, GW (1947) A Geochemical Survey of the Underground Water Supplies of the Union of South Africa. *Department of Mines, Geological Survey Memoir*, **41**. 203pp.

Botchway, CA, Ansa-Asare, OD and Antwi, LA (1996) Natural fluoride and trace metal levels of ground and surface waters in the greater Accra region of Ghana. *West Afr. J. Med.*, **15**, 204-209.

Botha, CJ, Naude, TW, Minnaar, PP, Van Amstel, SR and Janse van Rensburg, SD. (1993) Two outbreaks of fluorosis in cattle and sheep. *J.S.Afr. Vet. Assoc.*, **64**, 165-168.

Boudreau, AE, Mathez, EA and McCallum, IS (1986) Halogen geochemistry of the Stillwater and Bushveld Complexes: evidence for transport of the platinum-group elements by Cl-rich fluids. *J. Petrology*, **27**, 967-986.

Bowen, HJM (1966) *Trace elements in biochemistry*. Academic Press, London.

Boyle, DR (1976) *The geochemistry of fluorine and its applications in mineral exploration.* PhD Thesis, Imperial College, University of London. 386pp.

Boyle, DR (1992) Effects of base exchange softening on fluoride uptake in groundwaters of the Moncton Sub-Basin, New Brunswick, Canada. *In:* Kharaka, YK and Maest, AS (*eds.*) *Symposium on Water-Rock interaction*, Volume 1. Balkema, Rotterdam. 771-774.

Boyle, DR and Chagnon, M (1995) An incidence of skeletal fluorosis associated with groundwaters of the maritime carboniferous basin, Gaspé region, Quebec, Canada. *Environmental Geochemistry and Health*, **17**, 5-12.

Brandt, D and Reimold, WU (1995) The geology of the Pretoria Saltpan impact structure and the surrounding area. *S Afr. J. Geol.*, **98**, 287-303.

Brantley, SL and Chen, Y (1995) Chemical weathering rates of pyroxenes and amphiboles. *In:* White, AF and Brantley, SL (*eds.*) Chemical weathering rates in silicate minerals. *Reviews in Mineralogy*, **31**, 119-172.

Broecker, WS (1995) Cooling the tropics. *Nature*, **376**, 212-213.

Brouwer, ID, Backer Dirks, O, De Bruin, A and Hautvast, JGAJ (1988) Unsuitability of World Health Organisation guidelines for fluoride concentrations in drinking water in Senegal. *The Lancet*, **1 (8579)**, 223-225.

Brown, DW, and Roberson, CE (1977) Solubility of natural fluorite at 25°C *J. Res. US Geol. Surv.*, **5**, 509-518.

Cameron, EN (1980) Evolution of the lower Critical Zone, central sector, eastern Bushveld Complex, and its chromite deposits. *Econ. Geol.*, **75**, 845-871.

Campbell, AD (1987) Determination of fluoride in various matrices. *Pure and Appl. Chem.*, **59(5)**, 695-702.

Campbell, IH, Naldrett, AJ and Barnes, SJ (1983) A model for the origin of the platinum-rich sulfide horizons in the Bushveld and Stillwater complexes. *J. Pet.*, **24**, 133-165.

Cao, J, Bai, X, Zhao, Y, Liu, J, Zhou, D, Fang, S, Jia, M and Wu, J (1996) The relationship of fluorosis and brick tea drinking in Chinese Tibetans. *Environ. Health Perspect.*, **104**, 1340-1343.

Carpenter, R (1969) Factors controlling the marine geochemistry of fluorine. *Geochim. Cosmochim. Acta*, **33**, 1153-1167.

Carstens, IL, Louw, AJ and Kruger, E. (1995) Dental status of rural school children in a sub-optimal fluoride area. *J. Dent. Assoc. S. Afr.*, **50**, 405-411.

Cawthorn, RG (1988) *The Geology of the Pilanesberg.* National Parks Board of Bophuthatswana, Mafikeng. 24pp.

Cederstrom, DJ (1946) Genesis of groundwaters in the coastal plain of Virginia. *Economic Geology*, **41**, 218-245.

Charter, RH (1928) Solubilities of some inorganic fluorides in water at 25°C. *Ind. Engng. Chem.*, **20**, 1195. *In:* Strübel, G (1965) Quantitative Untersuchungen über die hydrothermale Löslichkeit van flußspat (CaF_2). *Neues Jahr. Miner.*, **3**, 83-95.

Chaumba, JB (*in prep.*) *A stable isotope study of the northern limb of the Bushveld Complex.* Unpubl. PhD thesis, University of Cape Town.

Collerson, KD, Ullman, WJ and Torgersen, T (1988) Ground waters with unradiogenic $^{87}Sr/^{86}Sr$ ratios in the Great Artesian Basin, Australia. *Geology*, **16**, 59-63.

Coplen, TB (1995) Discontinuance of SMOW and PDB. *Nature*, **375**, 285.

Corbett, RG and Manner, BM (1984) Fluoride in the ground water of northeastern Ohio. *Ground Water*, **22**, 13-17.

Correns, CW (1956) Geochemistry of the Halogens. *Phys. Chem. Earth*, **1**, 181-233.

Craig, H (1961) Isotopic variations in meteoric waters. *Science*, **133**, 1702-1703.

Crocker, IT and Martini, JEJ (1976) Fluorspar. *In:* Coetzee, CB (*ed.*) *Mineral resources of the Republic of South Africa.* The Government printer, Pretoria, 357-363.

CSIR [Centre for Scientific and Industrial Research] (1991) *Recommendations to the Department of Water Affairs, Bophuthatswana on criteria for drinking water quality.* Internal report **10/8/4/3/32508**, CSIR, Pretoria, 9pp.

Dansgaard, W (1964) Stable isotopes in precipitation. *Tellus*, **16**, 436-468.

Datta, PS, Deb, DL and Tyagi, SK (1996) Stable isotope (^{18}O) investigations on the processes controlling fluoride contamintaion of groundwater. *J. Contaminant Hydrol.*, **24**, 85-96.

Davies, RD, Allsop, HL, Erlank, AJ and Manton, WI (1970) Sr-isotopic studies on various layered mafic intrusions in Southern Africa. *Geol. Soc. S Afr., Special publication*, **1**, 576-593.

Davies, TC (1994) Water quality characteristics associated with fluorite mining in the Kerio Valley area of western Kenya. *Int. J. Env. Health Res.*, **4**, 165-175.

Dawson, JB and Fuge, R (1980) Halogen content of some African primary carbonatites. *Lithos*, **13**, 139-143.

Day, TK and Powell-Jackson, PR (1972) Fluoride, water hardness, and endemic goitre. *The Lancet,* **1 (7763)**, 1135-1138.

Dean, HT, Arnold FA and Elvove, E (1942) Domestic water and dental caries. V. Additional studies of the relation of fluoride domestic waters to dental caries experience in 4,425 white children aged 12-14 years, of 13 cities in 4 states. *Public Health Reports*, **57**, 1115-1179.

Dean, HT (1954) Fluorine in the control of dental caries: some aspects of the epidemiology of the fluorine-dental caries relationship. *Int. Dent. J*, **4**, 311-326.

Deer, WA, Howie, RA and Zussman, J (1977). *An introduction to the rock forming minerals.*

Longman, London. 528pp.

Dia, AN, Castrec, M, Boulègue, J, and Boudou, JP (1995) Major and trace element and Sr isotope constraints on fluid circulations in the Barbados accretionary complex. Part 1: Fluid origin. *Earth and Planetary Science Letters*, **134**, 69-85.

Dissanayake, CB (1996) Water quality and dental health in the Dry Zone of Sri Lanka. *In:* Appleton, JD, Fuge, R and McCall, GJH (*eds.*) Environmental geochemistry and health. *Geol. Soc. Spec. Publ.*, **113**, 131-140.

DMEA, [Department of Mineral and Energy Affairs, Eskom Marketing Intelligence] (1995) *South African energy statistics 1950-1993, no. 2.* Department of Mineral and Energy Affairs, Pretoria. 101pp.

Dodd, NF, Levy, DW, Jackson, WPU and Traut, ML (1960) Environmental bone disease of hitherto undescribed type. *S.A. Med. J*, 606-611.

Driscoll, WS, Heifetz, SB, Horowitz, HS, Kingman, A, Meyers, RJ and Zimmerman, ER (1983) Prevalence of dental caries and dental fluorosis in areas with optimal and above-optimal water fluoride concentrations. *J. Am. Dental Assoc.*, **107**, 42-47.

Duncan, AR, Erlank, AJ and Betton, PJ (1984) Appendix 1: Analytical techniques and database descriptions. 389-395. *In:* Erlank, AJ (*ed.*) *Petrogenesis of the volcanic rocks of the Karoo Province*. Geol. Soc. S Afr., Spec. Publ., **13**, 395pp.

Du Plessis, JB (1995) What would be the maximum concentration of fluoride in water that will not cause dental fluorosis. p4. *In:* McCaffrey, LP (*ed.*) *Fluoride and fluorosis: the status of South African research*. Abstract volume of a Workshop held on 10th August 1995 in the Pilanesberg National Park, South Africa. 11pp.

Du Plessis JB, van Rooyen JJ, Naude DA and van der Merwe CA (1995) Water fluoridation in South Africa: will it be effective? *J. Dent. Assoc. S. Afr.*, **50**, 545-549.

DWAF, [Department of Water Affairs and Forestry] (1996) *Draft of South African Water Quality Guidelines, Volume 1: Domestic Use (second edition)*. The Government Printer, Pretoria. 37pp.

Eales, HV, Botha, WJ, Hattingh, PJ, de Klerk, WJ, Maier, WD and Odgers, ATR (1993) The mafic rocks of the Bushveld Complex: a review of emplacement and crystallization history, and mineralization, in the light of recent data. *J. Afr. Earth Sci.*, **16**, 121-142.

Edgar, AD (1989) Barium- and strontium-enriched apatites in lamproites from West Kimberley, Western Austrlia. *Am. Miner.*, **74**, 889-895.

Ehhalt, D (1967) Deuterium and tritium content of hailstones: additional information their growth. *Trans. Am. Geophys Union.*

Elfimov, AS, Kravchenko, SM and Vasih'eva, ZV (1962) Strontium apatite: a new mineral. *Akademiya Nauk SSSR Doklady*, **142**, 439-442.

Ellis, AJ and Mahon, WAJ (1977) *Chemistry and Geothermal Systems*. Academic Press, New York. 375pp.

Elrashidi, MA and Lindsay, WL (1986) Chemical equilibria of fluorine in soils: a theoretical development. *Soil Science*, **141**, 274-280.

Eriksson, PG, Hattingh, PJ and Altermann, W (1995) An overview of the geology of the Transvaal Sequence and Bushveld Complex, South Africa. *Mineralium Deposita*, **30**, 98-111.

Fanning, DS and Keramidas, VZ (1977) Micas. *In:* Dixon, JB and Weed, SB (*eds.*) *Minerals in Soil Environments*. Soil Science Society of America, Wisconsin. 195-258.

Faure, G (1987). *Principles of isotope geology*. John Wiley and sons, New York. 589pp.

Fayazi, M (1995) Distribution of fluoride in groundwater of the northern Springblok Flats. p1. *In:* McCaffrey, LP (*ed.*) *Fluoride and fluorosis: the status of South African research*. Abstract volume of a Workshop held on 10th August 1995 in the Pilanesberg National Park, South Africa. 11pp.

Fejerskov, O, Manji, F, Baelum, V and Moller, IJ (1988) *Dental fluorosis - a handbook for health workers*. Munksgaard, Copenhage. 123pp.

Felsenfeld, AJ and Roberts, MA (1991) A report of fluorosis in the United States secondary to drinking well water. *J. Am. Med. Assoc.*, **265**, 486-488.

Ferguson, J (1973). The Pilanesberg Alkaline Igneous Complex. *S Afr. J. Geol.*, **76**, 249-270.

Feuchtwanger, T (1973) *Zoutpan: carbonatite-alkaline volcano*. Unpubl. Honours Thesis, Uni. Witwatersrand, 41pp.

Filippov, LV, Savimova, YN, Kapitonova, TA and Andreyeva, TP (1974) Fluorine in Mg-Fe micas from granitoids of various magmatic formations in the folded belt of Central Asia. *Geochem Int.*, **11**, 185-194.

Fluhler, H, Polomski, J and Balser, P (1982) Retention and movement of fluoride in soils. *J. Environ. Qual.*, **11**, 461-468.

Foss, PJ and Pittman, JM (1986) Efficacy of fluoride on dental caries reduction by means of a community water supply. *J. Dent. Child.*, **53**, 219-222.

Foster, MD (1950) The origin of high sodium bicarbonate waters in the Atlantic and Gulf Coastal Plains. *Geochim. Cosmo. Acta*, **1**, 32-48.

Fourie, N, Basson, AT, Basson, KM, Ferreira, GC, van der Berg, H, Smith, JC and Labuschagne, L (1996) Poisoning of wildlife in South Africa. *J. S. Afr. Vet. Assoc.* **50**, 467-471.

Franke, J, Runge, H and Fengler, F (1978) Endemic and industrial fluorosis *In:* Courvoisier, B, Donath, A and Baud, CA (*eds.*) *Fluoride and Bone*. Hans Huber, Bern. 129-143.

Frant, MS and Ross, JW (1966) Electrode for sensing fluoride ion activity in solution. *Science*, **154**, 1553-1554.

Freeze, RA and Cherry, JA (1979) *Groundwater*. Prentice-Hall, New Jersey. 604pp.

French, BM (1990) Absence of shock-metamorphic effects in the Bushveld Complex, South Africa: Results of an intensive search. *Tectonophysics*, **171**, 287-301.

Freni, SC and Gaylor, DW (1992) International trends in the incidence of bone cancer are not related to drinking water fluoridation. *Cancer*, **70**, 611-618.

Fridriksson, S (1983) Fluoride problems following volcanic eruptions. *In:* Sharpe, JL, Peterson, HB and Leone, NC (*eds.*) *Fluorides - effects on vegetation, animals and humans*. Paragon Press, Salt Lake City. 339-344.

Friedman, I and O'Neil, JR (1977) Compilation of stable isotope fractionation factors of geochemical interest. *In*: *Data of Geochemistry*. US Geol. Surv. Prof. Paper 440-KK, 6th ed.

Fritz, B, Richard, L and McNutt, RH (1992) Geochemical modelling of Sr isotopic signatures in the interaction between granitic rocks and natural solutions. *In:* Kharaka, YK and Maest, AS (*eds.*) *Symposium on Water-Rock interaction*, Volume 1. Balkema, Rotterdam. 927-930.

Fritz, P, Gale, JE and Reardon, EJ (1979) Comments on Carbon-14 dating of groundwaters from crystalline environments. *Geoscience Canada*, **6**, 10-15.

Frommurze, HF (1937) The water bearing properties of the more important geological formations in the Union of South Africa. *Department of Mines, Geological Survey Memoir*, **34**. 252pp.

Fudali, RF, Gold, DP and Gurney, JJ (1973) The Pretoria Salt Pan: astrobleme or cryptovolcano? *J. Geol.*, **81**, 495-507.

Fuge, R (1988) Sources of halogens in the environment, influences on human and animal health. *Env. Geochem. and Health*, **10**, 51-61.

Fuge, R (1989) Iodine in waters: possible links with endemic gotre. *Applied Geochemistry*, **4**, 203-208.

Fuge, R (1996) Geochemistry of iodine in relation to iodine deficiency diseases. *In:* Appleton, JD, Fuge, R and McCall, GJH (*eds.*) Environmental geochemistry and health. *Geol. Soc. Spec. Publ.*, **113**, 201-211.

Fuhong, R, Jianhui, Z, Wensheng, L and Cuiyun, Z (1996) Hydrogeochemical environment of high fluorine groundwater and the relation between the speciation of fluorine and the diseased ratio of endemic fluorosis - a case study of the North China Plain. *Acta Geoscientia Sinica*, **17**, 85-97.

Gaciri, SJ and Davies, TC (1993) The occurrence and geochemistry of fluoride in some

natural waters of Kenya. *Journal of Hydrology*, **143**, 395-412.

Galagan, DJ and Lamson, GG (1953) Climate and endemic fluorosis. *Publ. Health Report*, **68**, 497-508.

Galvin, RM (1996) Occurrence of metals in waters: an overview. *Water SA*, **22**, 7-18.

Garven, G (1995) Continental-scale groundwater flow and geological processes. *Annu. Rev. Earth Planet. Sci.*, **23**, 89-117.

Gascoyne, M and Kamineni, DC (1994) The hydrogeochsmistry of fractured plutonic rocks in the Canadian Shield. *Applied Hydrogeology*, **2**, 43-49.

Gat, JR (1980) The isotopes of hydrogen and oxygen in precipitation. 21-45 *In:* Fritz, P and Fontes, JCh (*eds.*) *Handbook of environmental isotope geochemistry*. Volume 1A. Elsevier, Amsterdam.

Gelberg, KH, Fitzgerald, EF, Hwang, S and Dubrow, R (1995) Fluoride exposure and childhood osteosarcoma: a case-control study. *Am. J. Public Health*, **85**, 1678-1683.

Gessner, BD, Beller, M, Middaugh, JP and Whitford, GM (1994) Acute fluoride poisoning from a public water system. *New Eng. J. Med.*, **330**, 95-99.

Geyh, MA (1972) Basic studies in hydrology and ^{14}C and ^{3}H measurements. *Proc. 24th Internatl. Geol. Conf., Montreal*, **11**, 227-234.

Gill, R (1996) *Chemical fundamentals of geology*. Chapman and Hall, London. 290pp.

Ginster, M and Fey, MV (1995) Soil and plant responses to irrigation with a fluoride-rich wate water. *In:* McCaffrey, LP (*ed.*) *Fluoride and fluorosis: the status of South African research*. Abstract volume of a Workshop held on 10th August 1995 in the Pilanesberg National Park, South Africa. 11pp.

Gíslason, SR, Andrésdóttir, A, Andrésdóttir, ÁE, Óskarsson, N, Thordarson, Th, Torssander, P, Novâk, M and Zâk, K (1992) Local effects of volcanoes on the hydrosphere: example from Hekla, southern Iceland. *In:* Kharaka, YK and Maest, AS (*eds.*) *Symposium on Water-Rock Interaction*, Volume 1. Balkema, Rotterdam. 477-481.

Gizaw, B (1996) The origin of high bicarbonate and fluoride concentrations in the waters of the Main Ethiopian Rift Valley, East African Rift system. *J. Afr. Earth Sci.*, **22**, 391-402.

Goldman, SM, Sievers, ML and Templin, DW (1971) Radiculomyopathy in a southwestern Indian due to skeletal fluorosis. *Arizona Medicine*, **28**, 32-48.

Graustein, WC and Armstrong, RL (1983) The use of $^{87}Sr/^{86}Sr$ ratios to measure atmospheric transport into forested watersheds. *Science*, **219**, 289-292.

Grobler, SR and Dreyer, AG (1988) Variations in the fluoride levels of drinking water in South Africa - implications for fluoride supplemantation. *S. Afr. Med. J.*, **73**, 217-219.

Guidotti, CV (1984) Micas in metamophic rocks. *In:* Bailey, SW (*eds*) Micas. *Reviews in Mineralogy*, **13**, 357-468.

Guntz, M (1884) Recherches thermiques sur les combinaisons du fluor. Ann. Chim. Phys. **6**, p38. *In:* Strübel, G (1965) Quantitative Untersuchungen über die hydrothermale Löslichkeit van flußspat (CaF_2). *Neues Jahrbuch Mineralogie*, **3**, 83-95

Gupta, RK, Chhabra, R and Abrol, IP (1982) Fluorine adsorption behaviour in alkaline soils: relative roles of pH and sodicity. *Soil Sci.*, **133**, 364-368.

Gupta, SK and Sharma, P (1995) An approach to tackling fluoride problem [*sic*] in drinking water. *Current Science*, **68**, 774.

Hamamoto, E (1957) On bone changes observed in in residents of a high fluorine zone. *In:* Utzino, S (*ed.*) *Medico-Dental researches on fluorides*, Japanese Society for Promotion of Science, Tokyo. 118-130.

Hamilton, PJ (1977) Sr isotope and trace element studies of the Great Dyke and Bushveld mafic phase and their relation to early Proterozoic magma genesis in southern Africa. *J. Petrology*, **18**, 24-52.

Hamilton, W (1970) Bushveld Complex - product of impacts? *Geol. Soc. S. Afr. Spec. Publ.*, **1**, 3667-379.

Hamza SM and Hamdona, SK (1991) Kinetics of dissolution of calcium fluoride crystals in sodium chloride solutions: influence of additives. *J. Phys. Chem.*, **95**, 3149-3152.

Harmer, RE (1985) A Sr isotope study of Transvaal carbonatites. *Trans. Geol. Soc. S Afr.*, **88**, 471-472.

Harmer, RE (1992) *The geochemistry of Spitskop and related alkaline intrusions*. Unpubl. PhD thesis, Uni. Cape Town. 332pp.

Harmer, RE and Farrow, D (1995) An isotopic study on the volcanics of the Rooiberg Group: age implications and a potential exploration. *Mineralium Deposita*, **30**, 188-195.

Harwood, JE (1969) The use of an ion-selective electrode for routine fluoride analyses on water samples. *Water Research*, **3**, 273-280.

Heaton, THE, Talma, AS and Vogel, JC (1986) Dissolved gas paleotemperatures and ^{18}O variations derived from groundwater near Uitenhage, South Africa. *Quaternary Research*, **79**, 79-88.

Henderson, P (1986) *Inorganic Geochemistry*. Pergamon Press, Oxford. 353pp.

Hill, M, Barker, F, Hunter, D, Knight, R (1996) Geochemical characteristics and origin of the Lebowa Granite Suite, Bushveld Complex. *Int. Geol. Rev.*, **38**, 195-227.

Hitchon, B (1995) Fluorine in formation waters, Alberta Basin, Canada. *Applied*

Geochemistry, **10**, 357-367.

Hrudey, SE, Soskolne, CL, Berkel, J and Fincham, S (1990) Drinking water fluoridation and osteosarcoma. *Can. J. Public Health*, **81**, 415-416.

Hübner, M (1969) Geochemische Interpretation von Fluorid/Hydroxid-Austauschversuchen an Ton-mineralen. *Freiberger Forschungsheft*, **C244**.

Hudson, TD (1977) Stable isotopes and limestone lithification. *J. Geol. Soc. Lond.*, **133**, 637-660.

Humphrey, WA (1913) The Volcanic Rocks of the Pilanesberg. *Trans. Geol. Soc. S.A.*, **15**, 100-106.

Hunter, DR and Hamilton, PJ (1978) The Bushveld Complex. *In:* Tarling, DH (*ed.*) *Evolution of the Earth's Crust*. Academic Press, London, 107-173.

Ibrahim, YE, Affan, AA and Bjorvatn, K (1995) Prevalence of fental fluorosis in Sudanese children from two villages with 0.25 and 2.56 ppm fluoride in the drinking water. *Int. J. Paediatr. Dent.*, **5**, 223-229.

Jago, BC and Gittins, J (1991) The role of fluorine in carbonatite magma evolution. *Nature*, **349**, 56-58.

Jakosky, BM and Jones, JH (1994) Evolution of water on Mars. *Nature*, **370**, 328-329.

Jenkins, GN (1990) The metabolism and effects of fluoride. *In:* Preist, ND and Van De Vyver, FL (*eds*) *Trace metals and fluoride in bones and teeth*. CRC press, Boca Raton. 142-173.

Jinadasa, KBPN, Dissanayake, CB, Weerasooriya, SVR and Senaratne, A (1993) Adsorption of fluoride on goethite surfaces - implications on dental epidemiology. *Environ. Geol.*, **21**, 251-255.

Kalk, WJ, Sitas, F and Patterson, AC (1997) Thyroid cancer in South Africa - an indicator of regional iodine deficiency. *S. Afr. Med. J.*, **87**, 735-738.

Kazakov, AV and Sokolova, EE (1950) Conditions of formation of fluorite in sedimentary rocks (the fluorite system). *Akad. Nauk SSSR Inst. Geol. Nauk Tr.*, **114**, 22-64. *In:* Nordstrom, DK and Jenne, EA (1977) Fluorite solubility equilibria in selected geothermal waters. *Geochim. Cosmochim. Acta*, **41**, 175-188.

Kilborn, LG, Outerbridge, TS and Lei, HP (1950) Fluorosis with a report of an advanced case. *Can. Med. Ass. J.*, **62**, 135-141.

Kinlen, L (1975) Cancer incidence in relation to fluoride level in water supplies. *Br. Dent. J.*, **138**, 221-224.

Kleeman, GJ and Twist, D (1989) The compositionally-zoned sheet-like granite pluton of the Bushveld Complex: evidence bearing on the nature of A-type magmatism. *J. Petr.*,

30, 1383-1414.

Kogarko, LN, Krigman, LD and Sharudilo, NS (1968) Experimental investigations of the effect of alkalinity of silicate melts on the separation of fluorine into the gas phase. *Geochem. Int.*, **5**, 782-790.

Kohlrausch, GG (1908) Über gesättigte wäßrige lösungen schwerlöslicher salze II: Die gelösten mengen mit ihrem temperaturgang. *Z Phys. Chem.*, **64**, 129-169. *In:* Strübel, G (1965) Quantitative Untersuchungen über die hydrothermale Löslichkeit van flußspat (CaF_2) *Neues Jahrbuch Mineralogie*, **3**, 83-95.

Koritnig, S (1951) Ein Beitrag zur Geochemie des Fluor. *Geochim. Cosmochim. Acta*, **1**, 89-100.

Koritnig, S (1974) *Fluorine. In:* Wedepohl, KH (*ed.*) *Handbook of Geochemistry Vol. II/1.* Springer-Verlag, Berlin.

Kraynov, SR, Mer'kov, AN, Petrova, NG, Baturinskaya, IV and Zharikova, VM (1969) Highly alkaline (pH 12) fluorosilicate waters in the deeper zones of the Lovozero Massif. *Geochemistry International*, **6**, 635-640.

Kunstmann, FH, Harris, JF, Bodenstein, LB and van den Berg, AM (1963) The occurrence of boron and fluorine in South African coals and their behaviour during combustion. *Bull. Fuel Res. Inst.*, **63**, 45pp.

Lane, SJ and Dalton, JA (1994). Electron microprobe analysis of geological carbonates. *American Mineralogist*, **79**, 745-749.

Langmuir, D (1971) The geochemistry of some carbonate ground waters in central Pennsylvania. *Geochim. Cosmochim. Acta*, **35**, 1023-1045.

Lasaga, AC (1984) Chemical kinetics of water-rock interactions. *J. Geophys. Res.*, **B89**, 4009-4025.

Launay, L (1913) Traité de Métallogenie: Gites minéraux et métallifères, Paris et Siège. Unknown publisher. *In:* Strübel, G (1965) Quantitative Untersuchungen über die hydrothermale Löslichkeit van flußspat (CaF_2). *Neues Jahrbuch Mineralogie*, **3**, 83-95.

Le Maitre, RW (1989). *A classification of igneous rocks and glossary of terms. Recommendations of the International Union of Geological Sciences Subcommission on the systematics of Igneous Rocks.* Blackwell, London, 193pp.

Leung, AKC (1988) Water standards for fluoride. *The Lancet*, **1 (8591)**, 935.

Lewis HA and Chikte UM (1995) Prevalence and severity of fluorosis in the primary and permanent dentition using the TSIF. *J. Dent. Assoc. S. Afr.*, **50**, 467-471.

Libby, WF (1955) *Radiocarbon Dating.* University of Chicago Press, Chicago. 175pp.

Lloyd, JW and Heathcote, JA (1985) *Natural inorganic hydrochemistry in relation to ground*

water. Clarendon Press, Oxford. 294pp.

Lombaard, BV (1932) The felsites and their relations in the Bushveld Complex. *Trans. Geol. Soc. S. Afr.*, **35**, 165-169.

Lurie, J (1974) *The Pilanesberg: Geology, Rare Element Geochemistry and Economic Potential*. Unpublished PhD thesis, Rhodes Univ.

Lyth, O (1946) Endemic fluorosis in Kweichow, China. *Lancet*, **1**, 233.

Machoy, Z, Dabkowska, E and Nowicka, W (1991) Increased fluoride content in mandibular bones of deer living in industrialised regions of Poland. *Env. Geochem. and Health*, **13**, 161-163.

Mahoney, MC, Nasca, PC, Burnett, WS, Melius, JM (1991) Bone cancer incidence rates in New York State: time trends and fluoridated drinking water. *Am. J. Public Health*, **81**, 475-479.

Manji, F, Baelum, V and Fejerskov, O (1986) Dental fluorosis in an area of Kenya with 2 ppm fluoride in the drinking water. *J. Dent. Res.*, **65**, 659-662.

Mason, B and Moore, CB (1966) *Principles of Geochemistry*. John Wiley & Sons, New York. 344pp.

Mathez, EA, Agrinier, P and Hutchinson, R (1994) Hydrogen isotope composition of the Merensky Reef and related rocks, Atok Section, Bushveld Complex. *Econ. Geol.*, **89**, 791-802.

Matthess, G (1982) *The properties of Groundwater*. John Wiley & Sons, New York.

May, PM and Murray, K (1991a) JESS, a joint expert speciation system - I: Raison d'être. *Talanta*, **38**, 1409-1417.

May, PM and Murray, K (1991b) JESS, a joint expert speciation system - II: the thermodynamic database. Talanta, **38**, 1419-1426.

Mazor, E and Verhagen, B Th. (1983) Dissolved ions, stable and radioactive isotopes and noble gases in thermal waters of South Africa. *J. Hydrology*, **63**, 315-329.

McCaffrey, LP (1993) *The Geohydrology of the Pilanesberg*. Unpubl. MSc. dissertation, Univ. Witwatersrand, Johannesburg. 130pp.

McCaffrey, LP (1994) Fluoride electrode versus ion chromatograpic analyses of groundwater. *Abstract volume*, Analitika 94, Stellenbosch, 8-13 December 1994. 87pp.

McCaffrey, LP, Harris, C and Willis, JP (1996) An occurrence of calcite, stontianite and ankerite in the Pilanesberg Complex, North West Province, South Africa. *S. Afr. J. Geol*, **99**, 33-36.

McCrea, JM, (1950). On the isotopic chemistry of carbonates and palaeo-temperature scale.

Journal of Chemical Physics, **18**, 849-857.

McInnes, PM, Richardson, BD and Cleaton-Jones, PE (1982) Comparison of dental fluorosis and caries in primary teeth of preschool-children living in arid high and low fluoride villages. *Community Dentistry and Oral Epidemiology*, **10**, 182-186.

McKay FS and Black, GV (1916) An investigation of mottled teeth. *Dental Cosmos*, **58**, 477-484.

McKenzie, WJ, Becker, BJP, Dreyer, CJ, du Toit, J, Dowdle, EBD, de Graad, JW and van Deventer, BJS (1966) *Report of the commission of enquiry into fluoridation.* The Government Printe, Pretoria. 174pp.

McNutt, RH, Frape, SK, Fritz, P, Jones, MG and MacDonald, IM (1990) The $^{87}Sr/^{86}Sr$ values of Candian Shield brines and fracture minerals with applications to groundwater mixing, fracture history, and geochronology. *Geochimica et Cosmochimica Acta*, **54**, 205-215.

Meeussen, JCL, van Riemsdijk, WH, de Wilde, PGM, Aalbers, Th.G (1994) Modeling [*sic*] fluoride transport in soils using ion binding models for oxides. *Transactions of the 15th World Congress of Soil Science, Acapulco, Mexico, July 10-16, 1994*, **3a**, 170-180.

Meunier, PJ, Femenias, M, Duboeuf, F, Chapuy, MC and Delmas, PD (1989) Increased vertebral bone density in heavy drinkers of mineral water rich in fluoride. *The Lancet*, **1 (8630)**, p 152.

Meyer, R and de Beer, JH (1987) Structure of the Bushveld Complex from resisitivity measurements. *Nature*, **352**, 610-612.

Molengraaff, GAF (1905) Preliminary Note on the Geology of the Pilandsberg and a Portion of the Rustenburg District. *Trans. Geol. Soc. S.A.*, **8**, 108-115.

Moller, PF and Gudjonsson, SV (1932) Massive fluorosis of bones and ligaments. *Acta Radiol.*, **13**, 269-304.

Mook, WG (1980) Carbon-14 in hydrogeological studies. *In:* Fritz, P and Fontes, J Ch (*eds.*) *Handbook of environmental isotope geochemistry: Volume 1, The Terrestrial environment.* Elsevier, Amsterdam. 49-74.

Moola, MH (1996) Fluoridation in South Africa. *Community and Dent. Health*, **13**, 51-55.

Mougnard, P (1931) Sur le dosage du fluor. Compt. Rend. **192**, 1733-1735. *In* Nordstrom, DK and Jenne, EA (1977) Fluorite solubility equilibria in selected geothermal waters. *Geochim. Cosmochim. Acta*, **41**, 175-188.

Munoz, JL and Ludington, SD (1974) Fluoride-hydroxyl exchange in biotite. *Am. J. Sci.*, **274**, 396-413.

Nagy, KL (1995) Dissolution and precipitation kinetics of sheet silicates. *In:* White, AF and Brantley, SL (*eds.*) Chemical weathering rates in silicate minerals. *Reviews in*

Mineralogy, **31**, 173-234.

Nash, WP (1976) Fluorine, chlorine and OH-bearing minerals in the Skaergaard Intrusion. *Am. J. Sci.*, **276**, 546-57.

Naumov, GB, Ryzhenko, BN and Khodakovsky, IL (1974) *Handbook of thermodynamic data.* Nat. Tech. Inf. Serv., **Pb-226, 722/7GA**, US Dept. Commerce, 328pp.

Newbrun, E (1989) Effectiveness of water fluoridation. *J. Public Health Dentistry*, **49**, 279-289.

Ng'ang'a, PM and Valderhaug, J (1993) Prevalence and severity of dental fluorosis in primary schoolchildren in Nairobi, Kenya. *Community Dentistry and Oral Epidemiology*, **21**, 15-18.

Nicholson, K and Pasquier, C (1993) The determination of fluoride in water in the presence of organic acids and iron using a fluoride-selective electrode. *Env. Geochem. and Health*, **15**, 185-186.

Nordstrom, DK and Jenne, EA (1977) Fluorite solubility equilibria in selected geothermal waters. *Geochim. Cosmochim. Acta*, **41**, 175-188.

Norrish, K and Hutton, JT (1969) An accurate X-ray spectrometric method for the analyses of a wide range of geological samples. *Geochim. Cosmochim. Acta.*, **33**, 431-453.

NPRL, [National Physical Research Laboratory] (1984) *Annual report.* **FIS 350**, 71.

Ockerse, T (1941) Endemic fluorosis in the Pretoria district. *S.A. Med. J.*, **15**, 261-266.

Ockerse, T and Meyer, HP (1941) Endemic fluorosis in the Pilandsberg area. *S.A. Dent. J*, **15**, 62-72.

Ockerse, T (943) *Endemic fluorosis in South Africa.* Department of Public Health, Pretoria. 93pp.

Odenthal, H and Wieneke, HL (1959) Chronische fluorvergiftung und osteomyelosklerose. *Deutsche Medizinische Wochenschrift*, **84**, 725-728.

Oldham, PD and Newell, DJ (1977) Fluoridation of water supplies and cancer - a possible association? *Appl. Stat.*, **26**, 125-135.

O'Neil, JR, Clayton, RN and Mayeda, TK (1969) Oxygen isotope fractionation in divalent metal carbonates. *J. Chem. Phys.*, **51**, 5547-5558.

O'Neil, JR and Taylor, HP (1967) The oxygen isotope and cation exchange chemistry of the feldspars. *Am. Mineral.*, **52**, 1414-1437.

Pakalns, P and Farrar, YJ (1976) Effects of surfactants on the determination of fluoride in waters. *Water Research*, **10**, 1087-1092.

Pekdeger, A, Özgür, N and Schneider, HJ (1992) Hydrogeochemistry of fluorine in shallow aqueous systems of the Gölcük area, SW Turkey. *In:* Kharaka, YK and Maest, AS (*eds.*) *Symposium on Water-Rock Interaction*, Volume 1. Balkema, Rotterdam. 821-824.

Pelpola, KU, Pienaar, P and Xu, Y (1992) Development of groundwater resources in Bophuthatswana. *In:* Proceedings of the 18th WEDC Conference, Kathmandu, Nepal, 30 August - 3 September 1992.

Pendrys, DG (1995) Risk of fluorosis in a fluoridated population. *J. Am. Dent. Ass.*, **126**, 1617-1624.

Peng, C, Qi, J and Rubin, AJ (1996) Use of fluorspar in water fluoridation. *J. Env. Eng.*, **122**, 132-140.

Petersen, E (1889) Neutralisationswärme der fluoride. *Z Phys. Chem.*, **4**, 384-412. *In:* Strübel, G (1965) Quantitative Untersuchungen über die hydrothermale Löslichkeit van flußspat (CaF_2). *Neues Jahrbuch Mineralogie*, **3**, 83-95.

Pettifor, JM, Schnitzler, CM, Ross, FP and Moodley, GP (1989) Endemic skeletal fluorosis in children: hypocalcemia and the presence of renal resistance to parathyroid hormone. *Bone Miner.*, **7**, 275-288.

Pickering, WF (1985) The mobility of soluble fluoride in soils. *Environ. Pollut.*, **B9**, 281-308.

Piper, AM (1944) A graphic procedure in the geochemical interpretion of water analyses. *Trans. Am. Geophys. Union*, **25**, 914-923.

Plankey, BJ and Patterson, HH (1986) Kinetics of aluminium fluoride complexation in acidic waters. *Environ. Sci. Technol.*, **20**, 160-165.

Pokrovskii, VA and Helgeson, HC (1995) Thermodynamic properties of aqueous species and the solubilities of minerals at high pressures and temperatures: the system Al_2O_3-H_2O-NaCl. *Am. J. Science*, **295**, 1255-1342.

Preston-Whyte, RA and Tyson, PD (1988) *The Atmosphere and Weather of Southern Africa.* Oxford University Press, Cape Town. 374pp.

Prins, P (1981) The geochemical evolution of the alkaline and carbonatite complexes of the Damaraland Igneous Province, South West Africa. *Annall Uni. Stellenbosch*, series A1, **3**, 145-278.

Qi, J and Knaebel, KS (1989) Dissolution equilibria and kinetics of fluorite and calcite mixtures. *Am. Inst. Chem. Engin. J*, **35**, 1293-1303.

Raubenheimer, EJ, Okonska, ET, Dauth, J, Dreyer, MJ, Lourens, C, Bruwer, CA and de Vos, V (1990) Fluoride concentrations in the rivers of the Kruger National Park: a five year survey. *S. Afr. J. Wildlife Res.*, **20**, 127-129.

Reimold, WU, Koeberl, C, Kerr, SJ and Partridge, TC (1991) The Pretoria Saltpan - the

first firm evidence for an origin by impact. *Lunar Planet. Sci.*, **22**, 1117-1118.

Reimold, WU, Koeberl, C, Partridge, TC and Kerr, SJ (1992) Pretoria Saltpan crater: impact origin confirmed. *Geology*, **20**, 1079-1082.

Retief, DH, Bradley, EL, Barbakow, FH, Friedman, M, van der Merwe, EH and Bischoff, JI (1979) Relationships among fluoride concentration in enamel, degree of fluorosis and caries incidence in a community residing in a high fluoride area. *J. Oral Pathol.*, **8**, 224-236.

Retief, EA (1962) Preliminary observations on the feldspars from the Pilanesberg alkaline complex, Transvaal, South Africa. *Norsk. geol. Tidskr.*, **42** (Feldspar-volume), 493-513.

Retief, EA (1963) *Petrological and mineralogical studies in the southern part of the Pilanesberg alkaline complex, Transvaal, South Africa*. Unpub. PhD thesis, Univ. of Oxford.

Riggs, RL, Hodgson, SF, O'Fallon, WM, Chao, EYS, Wahner, HW, Muhs, JM, Cedel, SL and Melton, LJ (1990) Effect of fluoride treatment on the fracture rate in postmenopausal women with osteoporosis. *New England J. Med.*, **332**, 802-809.

Roberson, CE and Hem, JD (1969) Solubility of aluminum in the presence of hydroxide, fluoride, and sulfate. *U.S. Geol. Surv. Water Supply Paper*, **1827**, C1-C37.

Robie, RA, Hemingway, BS and Fisher, JR (1978) Thermodynamic properties of minerals and related substances at 298.15 K and 1 bar (10^5 Pascals) pressure and at higher temperatures. *US Geol Surv. Bull.*, **1452**, 456pp.

Robinson, JBD (1978) Fluorine: its occurrence, analysis, effects on plants, diagnosis and control. *Commonwealth Bureau of Soils Spec. Publ.*, **6**.

Roedder, E (1972) Composition of fluid inclusions. *In: Data of Geochemistry, 6th edition,* U.S. Geol. Surv., Prof. Pap. **440-JJ, Ch.JJ**, 164pp.

Rossini, FD, Wagman, DD, Evans, WH, Levine, S and Jaffe, I (1952) *Selected values of chemical thermodynamic properties.* Nat. Bureau Standards Circ. **500**, US Dept. Commerce, Washington DC.

Rozendaal, A, Toros, MS and Anderson, JR (1986) The Rooiberg tin deposits, West-Central Transvaal. 1307-1327. *In:* Anhaeusser, CR and Maske, S (*eds.*) *The mineral deposits of Southern Africa Volume II* Geol Soc. S Afr., Johannesburg. 2335pp.

Rudolph, MJ, Molefe, M, and Chikte, UME (1995) Dental fluorosis with varying levels of fluoride in drinking water. Abstract, *J. Dental Research*, **74**, 1012.

SACS, [South African Council for Stratigraphy] (1980) Stratigraphy of South Africa, Part 1 (Comp. L.E. Kent), Lithostratigraphy of the Republic of South Africa, South West Africa/Namibia, and the Republics of Bophuthatswana, Transkei and Venda. *Handb. Geol. Surv. S. Afr.*, **8**, 690pp.

Schidlowski, M, Hayes, JM and Kaplan, IR (1983). Isotopic inferences of ancient

biochemistries: Carbon, sulfur, hydrogen, and nitrogen. *In:* Schopf, JW (*ed.*) *Earth's earliest biosphere*. Princeton University Press, Princeton. 543pp.

Schlatter, Ch (1978) Metabolism and toxicology of fluorides. *In:* Courvoisier, B, Donath, A and Baud, CA (*eds*) *Fluoride and Bone*. Hans Huber, Bern. 1-21.

Schloemann, H (1995) *The Geochemistry of some Western Cape soils (South Africa) with emphasis on toxic and essential elements.* Unpubl. PhD Thesis, Uni. Cape Town, 300pp.

Schreiner, GDL (1958) Comparison of the ^{87}Rb-^{86}Sr ages of the red granite of the Bushveld Complex from measurements on the total rock and seperated mineral fractions. *Proc. Roy. Soc.*, **A245**, 112-117.

Schulz, EE, Libanati, CR and Farley, SM (1984) Skeletal scinitigraphic changes in osteoporosis treated with sodium fluoride: concise communication. *J. Nucl. Med.*, **25**, 651-655.

Schweitzer, JK, Hatton, CJ and de Waal, SA (1995) Regional lithochemical stratigraphy of the Rooiberg Group, upper Transvaal Supergroup: a proposed new subdivision. *S Afr. J. Geol*, **98**, 245-255.

Seemann, F (1905) Studien über die quantitative bestimmung und trennung der Kieselsäure und des fluors. *Z Anal. Chem.*, **44**, 343-387. *In:* Strübel, G (1965) Quantitative Untersuchungen über die hydrothermale Löslichkeit van flußspat (CaF_2) *Neues Jahrbuch Mineralogie*, **3**, 83-95.

Senewiratne, B, Senewiratne, K, Hettiarachchi, J and Thambipillai, S (1973) Assessment of the fluoride content of water in wells selected randomly and after examining schoolchildren for dental fluorosis. *Bull. WH.O.*, **49**, 419-422.

Shand, SJ (1928) The Geology of Pilansberg (Pilaan's Berg) in the Western Transvaal; A Study of Alkaline Rocks and Ring-Intrusions. *Trans. Geol. Soc. S.A.*, **31**, 97-156.

Sharpe, MR (1985) Strontium isotope evidence for preserved density stratification in the Main Zone of the Bushveld Complex, South Africa. *Nature*, **316**, 119-126.

Shcherba, GN (1970) Greisens. *Int. Geol. Rev.*, **12**, 239-255.

Shortt, HE, McRobert, GR, Barnard, and Mannadi Nayar, AS (1937) Endemic Fluorosis in the Madras Presidency. *Ind. J. Med. Res.*, **25**, 553-568.

Smalley, PC, Blomqvist, R and Råheim, A (1988) Sr isotopic evidence for discrete saline components in stratified ground waters from crystalline bedrock, Outokumpu, Finland. *Geology*, **16**, 345-357.

Smet, J (1992) Fluoride in drinking water. *In:* Frencken, JE (*ed.*) *Endemic fluorosis in developing countries*. Report of a symposium held in Delft, the Netherlands, April 27th 1990. 98pp.

Smyshlyaev, SI and Edeleva, NP (1962) Determination of solubility of minerals I: The solubility product of fluorite. *Izv. Vysshikh Uchebn. Zavedenii Khim. Teknol.*, **5**, 871. *In:* Nordstrom, DK and Jenne, EA (1977) Fluorite solubility equilibria in selected geothermal waters. *Geochim. Cosmochim. Acta*, **41**, 175-188.

Socki, RA, Karlsson, HR and Gibson, EK (1992) Extraction Technique for the determination of Oxygen-18 in water using preevacuated glass vials. *Anal. Chem.*, **64**, 829-931.

Sonnet, CP and Finney, SA (1990) The spectrum of radiocarbon. *In:* Pecker, J and Runcorn, SK (*eds.*) *The Earth's climate and variability of the sun over recent millennia.* Royal Society, London. 692pp.

Speer, JA (1984) Micas in igneous rocks. *In:* Bailey, SW (*eds*) Micas. *Reviews in Mineralogy*, **13**, 299-356.

Stauffer, RE (1982) Fluorapatite and fluorite solubility controls on geothermal waters in Yellowstone National Park. *Geochim. Cosmochim. Acta*, **46**, 465-474.

Stormer, JC and Carmichael, ISE (1970) Villiaumite and the occurrence of fluoride minerals in igneous rocks. *Am. Mineralogist*, **55**, 126-134.

Strübel, G (1965) Quantitative Untersuchungen über die hydrothermale Löslichkeit van flußspat (CaF_2). *Neues Jahrbuch Mineralogie*, **3**, 83-95.

Stuckless, JS, Peterman, ZE and Muhs, DR (1991) U and Sr isotopes in ground water and calcite, Yucca Mountain, Nevada: evidence against upwelling water. *Science*, **254**, 551-554.

Stumm, W, Wehrli, B and Wieland, E (1987) Surface complexation and its impact on geochemical kinetics. *Croatica Chemica Acta*, **60**, 429-456.

Suwa, K, Oana, S, Wada, H and Osaki, S (1975) Isotope geochemistry and petrology of African carbonatites. *Phys. and Chem. of the Earth*, **9**, 735-745.

Suzuki, K and Endo, Y (1995) Relation of Na^+ concentration and $\delta^{18}O$ in winter precipitation with weather conditions. *Gephys. Res. Lett.*, **22**, 591-594.

Sverdrup, HU (1990) *The kinetics of base cation release due to chemical weathering.* Lund Univ. Press.

Taylor, HP (1974) The application of oxygen and hydrogen isotope studies to problems of hydrothermal alteration and ore deposition. *Econ. Geol.*, **69**, 843-883.

Taylor, HP, Frechen, J and Degens, ET (1967) Oxygen and carbon isotope studies of carbonatites from the Laacher See district, West Germany, and the Alno district, Sweden. *Geochim. Cosmochim. Acta*, **31**, 407-430.

Thiessen, AH (1911) Precipitation averages for large areas. *Monthly Weather Rev.*, **39**, 1082-1084.

Thorsden, JJ, Kharaka, YK, Mariner, RH and White, LD (1992) Controls on the distribution of stable isotopes of meteoric water and snow in the greater Yellowstone National Park region, USA. *In:* Kharaka, YK and Maest, AS (*eds.*) *Symposium on Water-Rock Interaction*, Volume 1. Balkema, Rotterdam. 591-595.

Thylstrup, A and Fejerskov, O (1978) Clinical appearance of dental fluorosis in permanent teeth in relation to histologic changes. *Community Dentistry and Oral Epidemiology*, **6**, 315-328.

Tobayiwa, C, Musiyambiri, M, Chironga, L, Mazorodze, O and Sapahla, S (1991) Fluoride levels and dental fluorosis in two districts in Zimbabwe. *Central African J. Medicine*, **37**, 355-361.

Torino, M, Rognini, M and Fornaciari, G (1995) Dental fluorosis in ancient Herculaneum. *The Lancet*, **345**, 1306.

Treadwell, FP and Koch, AA (1904) Über die bestimmung von fluor in wein und bier. *Z Anal. Chem.*, **43**, 114-115. *In:* Strübel, G (1965) Quantitative Untersuchungen über die hydrothermale Löslichkeit van flußspat (CaF_2) *Neues Jahrbuch Mineralogie*, **3**, 83-95.

Trotignon, L and Turpault, MP (1992) The dissolution kinetics of biotite in dilute HNO_3 at 24°C *In:* Kharaka, YK and Maest, AS (*eds.*) *Symposium on Water-Rock interaction*, Volume 1. Balkema, Rotterdam. 123-125.

US Dept of Health and Human Services (1991) *Review of fluoride: benefits and risks*. Report of the Ad Hoc Subcommittee on fluoride of the Committee to Coordinate Environmental Health and Related Programs. Washington DC.

Van der Merwe, EH, Bischoff, JI, Fatti, LP, Retief, DH, Barbakow, FH and Friedman, M. (1977) Relationships between fluoride in enamel, DMFT index and fluorosis in high- and low-fluoride areas in South Africa. *Community Dent. Oral Epidemiol.*, **5**, 61-64.

Van Wyk, PJ, Louw, AJ and Snyman, WD (1983) Dental fluorosis in two communities in S.W.A. (namibia). *J. Dental Res.*, **62**, 508.

Vasak, L (1992) Primary sources of fluoride. *In:* Frencken, JE (*ed.*) *Endemic fluorosis in developing countries*. Report of a symposium held in Delft, the Netherlands, April 27th, 1990. 98pp.

Verdoux, P, Lancelot, J and Faillat, J (1995) Traçage de l'origine des eaux karstiques en bordure d'un massif cristallin à l'aide des isotopes du strontium: Exemple des causses lozériens (France). *CR Acad. Sci. Paris*, **320**, 387-394.

Verhagen, B Th., Geyh MA, Fröhlich, K and Wirth, K (1991) *Isotope hydrological methods for the quantitative evaluation of ground water resources in arid and semi-arid areas - Development of a methodology*. Federal Ministry for Economic Co-operation, Bonn. 164pp.

Verhagen, B Th., Mazor, E and Sellschop, JPF (1974) Radiocarbon and tritium evidence

for direct rain recharge to ground waters in the northern Kalahari. *Nature*, **249**, 643-644.

Verwoerd, WJ (1967) The carbonatites of South Africa and South West Africa. *Department of Mines, Geological Survey Handbook*, **6**.

Verwoerd, WJ (1993). Update on carbonatites of South Africa and Namibia. *S Afr. J. Geol.*, **96**, 75-95.

Von Gruenewaldt, G, Hatton, CJ, Merkle, CJ and Gain, SB (1986) Platinum-group element - chromitite associations in the Bushveld Complex. *Econ. Geol.*, **81**, 1067-1079.

Waber, N and Nordstrom, DK (1992) Geochemical modeling of granitic ground waters at the Stripa site (Sweden) using a mass balance approach. 243-246. *In:* Kharaka, YK and Maest, AS (*eds.*) *Water-Rock interaction*, Volume 1. Balkema, Rotterdam.

Wager, LR and Brown, GM (1968) *Layered Igneous Rocks*. Oliver and Boyd, Edinburgh. 588pp.

Wagman, DD, Evans, WH, Parker, VB, Schumm, RH, Halow, I, Bailey, SM, Churney, KL and Nutall, RL (1982) The NBS tables of chemical thermodynamic properties: selected values for inorganic and C_1 and C_2 organic substances in SI units. *J. Phys. and Chem. Ref. data*, **11**, Supplement No. 2, 392pp.

Wagner, PA (1920) Note on the volcanic origin of the Salt Pan on the farm Zoutpan, No.467. *Trans. Geol. Soc. S.A.*, **23**, 52-58.

Wagner, PA (1922) *The Pretoria Salt-Pan, a soda caldera*. Geol. Surv. S.A. Memoir 20.

Walraven, F (1976) Notes on the late-stage history of the western Bushveld Complex. Trans. *Geol. Soc. S Afr.*, **79**, 13-21.

Walraven, F (1981) *The Geology of the Rustenburg area, explanation of sheet 2526*. Geological Survey of South Africa, Pretoria. 37pp.

Walraven, F (1987) Geochronological and isotopic studies of Bushveld Complex rocks from the Fairfield borehole at Moloto, northeast of Pretoria. *S Afr. J. Geol.*, **90**, 352-360.

Walraven, F and Hattingh, E (1993) Geochronology of the Nebo Granite, Bushveld Complex. *S Afr. J. Geol.*, **96**, 31-41.

Warner, TB (1971) Electrode determination of fluoride in ill-characterized natural waters. *Water Research*, **5**, 459-465.

Weast, RC (1975) *Handbook of Chemistry and Physics, 56th Edition*. CRC Press. Cleveland, Ohio.

White, SL (1988) Water standards for fluoride. *The Lancet*, **1 (8583)**, p475.

White, DE and Waring, GA (1963) Volcanic emanations *In: Data of Geochemistry, 6th*

edition, U.S. Geol. Surv., Prof. Pap. **440-K, Ch.K**, K1-K29.

Whitford, GM (1996) *The metabolism and toxicity of fluoride.* Karger, Basel. 156pp.

WHO (1984) *Guidelines for drinking water quality, volume 1: Recommendations.* World health Organisation, Geneva.

WHO (1993) *Guidelines for drinking water quality, volume 1: Recommendations.* 2nd edition, volume 1. World health Organisation, Geneva.

Wilkniss, PE and Bressan, DJ (1971) Chemical processes at the air-sea interface: the behaviour of fluorine. *J. Geophys. Res.*, **76**, 736-741.

Wilkniss, PE and Bressan, DJ (1972) Fractionation of the elements F, Cl, Na and K at the air-sea interface. *J. Geophys. Res.*, **77**, 5307-5315.

Willis, JP (1995) *Instrumental parameters and data quality for routine major and trace element determinations by WDXRFS.* Department of Geological Sciences, University of Cape Town, information circular **14**, 7pp.

Woods, TL and Garrels, RM (1987) *Thermodynamic values at low temperature for natural inorganic materials: an uncritical summary.* Oxford University Press, New York. 242pp.

Yang, Y, Wang, X and Guo, X (1994) Effects of high iodine and high fluorine on childrens intelligence and the metabolism of iodine and fluorine [Chinese]. *Chung Hua Liu Hsing Ping Hsueh Tsa Chih*, **15**, 296-298.

Yong, L and Hua, ZW (1991) Environmental characteristics of regional groundwater in relation to fluoride poisoning in North China. *Environ. Geol. and Water Sci.*, **18**, 3-10.

Yurtsever, Y and Gat, JR (1981) Atmospheric Waters. *In:* Stable Isotope Hydrology, technical report series, **210**. IAEA, Vienna.

Zhang, H, Bloom, PR and Nater, EA (1993) Change in surface area and dissolution rates during hornblende dissolution at pH 4.0. *Geochim. Cosmochim. Acta*, **57**, 1681-1689.

Zhu, C (1991) Biotite ((Mg,FE^{2+},Al^{VI}) (F,Cl,OH) reciprocal mixing properties: evidence from the partitioning of F-Cl-OH between biotite and apatite. *Abstract 5133, Geol. Soc. Amer.*

Zhu, C and Sverjensky, DA (1992) F-Cl-OH partitioning between biotite and apatite. *Geochim. Cosmochim. Acta*, **56**, 3435-3467.

Zietsman, S (1985) *Die verband tussen sekere fisies-geografiese veranderlikes en die voorkoms van tandfluorose in die Odi 1 gebied.* Unpubl. M.Sc. diss., Uni. S. Africa. 327pp.

Zietsman, S (1989) The relationship between the geological variation, the F^- of the water and the spatial variation in the occurrence of dental fluorosis in an endemic area. *S. Afr. Geog. J.*, **71**, 102-108.

Zietsman, S (1991) Spatial variation of fluorosis and fluoride content of water in an endemic area in Bophuthatswana. *J. Dent. Ass. S. Afr.*, **46**, 11-15.

Zipkin, I, McClure, FJ, Leone, NC and Lee, WA (1958) Fluoride deposition in human bones after prolonged ingestion of fluoride in drinking water. *Public Health Report*, **73**, 732-740.

APPENDICES

Appendix A: Site Locations

Appendix A.1 Groundwater sample site information. "B/H No." (borehole number) has the following codes; "n/n" is no number; "unk./n" is a borehole with a number but is unclear. Site type has the following codes; "B" for borehole, "F" for spring, "P" for pan or dam, "R" for river or stream, "O" for seepage from opencast mine and "Z" for other. Site equipment has the following codes; "H" for handpump, "M" for mono-type pump, "N" for no equipment, "S" for submersible pump, "W" for windpump, "Z" for other and blank for no information. Unconsecutive site numbers result from either errors in the field maps or duplication of previous sites.

B/H No.	Site Number: Location, Description	Long. E	Lat. S	Type	Equip
n/n	Site 1: Bapong, self help garden	26.84806	25.30934	B	H
n/n	Site 2: Bapong, southern end	26.84110	25.31384	B	Z
n/n	Site 3: Bapong, northern end	26.84807	25.30121	B	H
06-65005	Site 7: Mabeeskraal, middle of village	26.79908	25.20140	B	H
06-65184	Site 8: Mabeeskraal, Marula Park	26.81794	25.19555	B	H
n/n	Site 9: Maneeskraal, Mami's house, zone 4	26.81300	25.18291	B	H
n/n	Site 10: Maologane	26.94143	25.26697	B	Z
n/n	Site 11: Maologane, Joyce's yard	26.94540	25.27059	B	S
n/n	Site 12: Maologane, Private Yard	26.94441	25.27149	B	H
n/n	Site 13: Maologane, Private yard	26.94639	25.27194	B	H
n/n	Site 14: Maologane, private yard	26.94589	25.27284	B	H
n/n	Site 15: Maologane, Private yard	26.94689	25.27329	B	H
06-65307	Site 16: Maologane, Dikeme middle school	26.94242	25.27555	B	H
n/n	Site 17: Raborife, Mr Raborife's yard	26.90721	25.22407	B	H
n/n	Site 18: Raborife, private	26.90970	25.21911	B	S
n/n	Site 19: Mmorogong (Tlhatlhaganyane)	26.94045	25.23610	B	Z
n/n	Site 20: Mmorogong, Christoff's yard	26.94055	25.23718	B	H
n/n	Site 21: Mmorogong, Tapson's yard	26.94045	25.23808	B	H
n/n	Site 22: Mmorogong, Johanna's yard	26.94169	25.23899	B	H
n/n	Site 23: Mmorogong, Witness' yard	26.94144	25.23989	B	H
n/n	Site 24: Mmorogong, animal gear	26.94144	25.24124	B	Z
n/n	Site 25: Mmorogong, owner absent	26.94144	25.24260	B	H
n/n	Site 26: Mmorogong, Joseph's yard	26.94144	25.24328	B	H
n/n	Site 27: Mmorogong, Mthembu's yard	26.94045	25.24395	B	H
n/n	Site 28: Mmorogong, Sekgwelea's yard	26.94065	25.24418	B	H

B/H No.	Site Number: Location, Description	Long. E	Lat. S	Type	Equip
n/n	Site 29: Mmorogong, Master's yard	26.94065	25.24485	B	H
n/n	Site 30: Mmorogong, Public H/P	26.94065	25.24576	B	H
T6234	Site 31: Tlhatlhaganyane, Animal gear east	26.93996	25.21822	B	Z
n/n	Site 32: Tlhatlhaganyane	26.92061	25.22047	B	H
06-65436	Site 33: Tlhatlhaganyane	26.91367	25.20963	B	H
06-65192	Site 34: Tlhatlhaganyane, Early learning	26.94344	25.22138	B	H
n/n	Site 35: Ledig, Lena's yard	27.06607	25.36853	B	H
n/n	Site 36: Ledig, Lydia's yard	27.07899	25.36943	B	H
n/n	Site 37: Ledig, Pilanesberg seepage spring	27.08245	25.35002	F	
n/n	Site 38: Ledig, Esky's yard	27.07749	25.35408	B	H
06-65324	Site 39: Ledig, public	27.07451	25.36356	B	H
n/n	Site 40: Ledig, Nicholas's yard	27.06755	25.35228	B	H
n/n	Site 41: Ledig, Joan's yard	27.06756	25.36311	B	H
n/n	Site 42: Ledig, Phineas's yard	27.05812	25.35860	B	H
n/n	Site 43: Ledig, Jacob's yard	27.05464	25.35454	B	H
n/n	Site 44: Ledig, Alexander's yard	27.05116	25.35319	B	H
06-65302	Site 45: Ledig, Zulu section	27.04520	25.35274	B	Z
06-65304	Site 46: Ledig, public borehole	27.03626	25.34958	B	H
n/n	Site 47: Ledig, Onika's yard	27.03079	25.34733	B	H
n/n	Site 48: Ledig, Katherine's yard	27.02483	25.34733	B	H
n/n	Site 49: Ledig, Moses' yard	27.03427	25.35365	B	H
n/n	Site 50: Ledig, Dorothy's yard	27.04769	25.35680	B	H
BB 2035	Site 51: Makoshong, northern end	26.84369	25.23666	B	H
BB 2033	Site 52: Makoshong	26.84418	25.23937	B	H
BB 2031	Site 53: Makoshong, next to shop	26.84120	25.24162	B	H
N 204	Site 54: Makoshong	26.83971	25.23801	B	H
n/n	Site 55: Mahobieskraal	26.96672	25.34642	B	
06-40709	Site 56: Mahobieskraal, vegetable garden	26.97268	25.34327	B	H
n/n	Site 57: Motlhabe, south east	26.95837	25.07830	B	S
06-65532	Site 58: Motlhabe	26.95391	25.06656	B	H
06-65301	Site 59: Motlhabe	26.94846	25.06475	B	H
06-65387	Site 60: Motlhabe	26.93905	25.06701	B	H
n/n	Site 61: Motlhabe	26.95243	25.06295	Z	Z

B/H No.	Site Number: Location, Description	Long. E	Lat. S	Type	Equip
06-65084B	Site 62: Ntswana le Metsing	26.96878	25.05347	B	H
06-65347	Site 63: Motlhabe	26.97423	25.05573	B	H
n/n	Site 65: Makgope Mine	26.92564	25.11891	B	S
n/n	Site 66: Makgope mine, domestic supply	26.93853	25.11530	B	S
n/n	Site 67: Witkleifontein grazing	26.95043	25.10041	B	W
T6768	Site 69: Southeast of Pilanesberg	27.21503	25.32912	B	W
T41731	Site 70: Southeast of Pilanesberg	27.22542	25.30608	B	W
T141900	Site 71: Sefikile	27.20554	24.99917	B	W
T7693	Site 72: Sefikile	27.18276	25.00416	B	W
T6292	Site 73: Tsweneng, south	27.01237	24.92437	B	W
n/n	Site 74: Leswaaneng spring	27.12398	25.15454	F	
n/n	Site 75: Salty spring	27.12595	25.15002	F	
n/n	Site 76: Lesetlheng, outside chief's house	27.09917	25.14553	B	H
n/n	Site 77: Ramatshaba	27.05206	25.13427	B	H
n/n	Site 78: Ramatshaba	27.02975	25.14104	B	H
06-65284	Site 79: Ramatshaba	27.04757	25.06114	B	W
n/n	Site 80: Ramatshaba	27.05103	25.04534	B	W
n/n	Site 81: north of Pilanesberg	27.04954	25.02548	B	W
n/n	Site 82: north of Pilanesberg	27.17792	25.07910	B	W
06-65547	Site 83: north of Pilanesberg	27.08179	25.10040	B	W
n/n	Site 84: Chaneng, next to Agricor	27.12920	25.40776	B	H
n/n	Site 87: Robega A (Boshkoppie farm)	27.14909	25.41677	B	W
?2861	Site 88: Tsitsing	27.33801	25.44083	B	Z
05-62054	Site 89: Maile (Rooikraal farm)	27.24546	25.39768	B	H
T6921	Site 90: Rietspruit	27.28714	25.37052	B	W
T6869	Site 91: Monnakato	27.27118	25.34302	B	W
05-62041	Site 92: Tsitsing	27.32024	25.48871	B	W
05-62162	Site 93: KwaSeretube	27.29348	25.52714	B	H
05-62163	Site 94: KwaSeretube	27.30591	25.52666	B	H
n/n	Site 95: Bospoort Dam	27.34232	25.55953	P	
n/n	Site 95: Marikana	27.48562	25.68415	B	S
n/n	Site 97: Swartkoppies, Engelbrechts farm	27.47953	25.65528	B	S
05-62167	Site 98: Tlapa, grazing lands	27.43562	25.63195	B	H

B/H No.	Site Number: Location, Description	Long. E	Lat. S	Type	Equip
T6918	Site 99: Tlapa, grazing lands	27.40419	25.61218	B	W
RB067	Site 100: Tlapa, arable field	27.43957	25.62291	B	H
05-62120	Site 101: Tlapa	27.43555	25.61299	B	H
05-62121	Site 102: Tlapa	27.43329	25.60623	B	H
n/n	Site 103: Maumong	27.45337	25.58586	B	H
05-62180	Site 104: Lekgalong	27.40941	25.53724	B	H
T6227	Site 105: Rankelanyane	27.40926	25.56635	B	Z
05-62013	Site 106: Lekjaneng	27.39308	25.56346	B	H
05-62012	Site 107: Malejaneng	27.37325	25.58789	B	H
24400	Site 108: Thekwane, kraal	27.35490	25.60892	B	
n/n	Site 109: Bapong oustad	27.70630	25.69137	B	H
n/n	Site 110: Bapong, roberts yard	27.67851	25.71001	B	H
n/n	Site 111: Bapong	27.67409	25.72041	B	Z
n/n	Site 112: Bapong	27.66659	25.71548	B	H
n/n	Site 113: Bapong, Legalawong sub village	27.66255	25.70602	B	H
04-56110	Site 114: Modderspruit	27.65220	25.72592	B	H
BB 130	Site 115: Modderspruit	27.64769	25.72098	B	H
n/n	Site 116: Seqwelane	27.60255	25.66250	B	H
n/n	Site 117: Makolokwe, western end	27.61234	25.62770	B	H
T6955	Site 118: Bethanie farm	27.56013	25.53471	B	W
BB 1284	Site 119: Bethanie cattle post	27.61475	25.51644	B	W
BB1292	Site 120: Wilgevonden east cattle post	27.61360	25.48462	B	W
BB 1282	Site 121: Bethanie, south east	27.59910	25.56908	B	W
04-59958	Site 122: Bethanie, outside church	27.60701	25.55912	B	H
T6231	Site 123: Waaikraal farm	27.57705	25.53577	B	W
04-59162	Site 124: Modikwe	27.53721	25.52599	B	H
T49020	Site 125: Modikwe, south	27.53476	25.53526	B	H
04-57078	Site 126: Modikwe	27.53774	25.53479	B	H
n/n	Site 127: Gwatlhe River	27.53675	25.53592	R	
n/n	Site 128: Modikwe, school	27.53519	25.51968	B	H
T49064	Site 130: Modikwe, west	27.50606	25.51121	B	W
04-59080	Site 131: Berseba	27.52937	25.55265	B	H
04-59053	Site 132: Bethanie	27.61648	25.56134	B	H

B/H No.	Site Number: Location, Description	Long. E	Lat. S	Type	Equip
n/n	Site 133: Krokodile Riv, Hartebeespoort fm.	27.67961	25.50690	R	
T4397	Site 134: Maboloka, Bafokeng section	27.84883	25.41981	B	H
03-56174	Site 135: Maboloka, Taung section	27.86042	25.44321	B	H
03-56370	Site 136: Maboloka, Solomon middle school	27.86493	25.44815	B	H
BB 1266	Site 137: Maboloka, Phuthanang Primry schl	27.85881	25.42652	B	H
03-56177	Site 138: Maboloka grazing	27.86774	25.42421	B	W
n/n	Site 139: Maboloka, Tumo primary school	27.85803	25.42156	B	H
03-56595	Site 140: Maboloka	27.85526	25.41661	B	H
n/n	Site 141: Letlhakaneng	27.81882	25.39109	B	H
03-65150	Site 142: Letlhakaneng	27.82181	25.39378	B	H
n/n	Site 143: Letlhakaneng	27.82826	25.39104	B	H
T4	Site 144: Rietgat grazing	27.80553	25.40990	B	W
T4305	Site 145: Rietgat grazing	27.80492	25.39343	B	W
4308	Site 146: Rietgat grazing	27.79690	25.38309	B	W
unk./n	Site 147: Waterval grazing	27.73031	25.37892	B	W
n/n	Site 148: Waterval grazing	27.73809	25.35180	B	W
03-56145	Site 149: Waterval (Tsogwe)	27.74907	25.36077	B	H
T4860	Site 150: Tsogwe	27.75108	25.36460	B	H
03-56143	Site 151: Tsogwe, Tsogwe School	27.75356	25.36301	B	H
n/n	Site 152: Kgomokgomo (Rooiwal)	27.76121	25.31557	B	H
n/n	Site 153: Kgomokgomo	27.75476	25.31696	B	H
03-56383	Site 154: Legonyane	27.77133	25.26813	B	H
T46033	Site 155: Legonyane	27.77532	25.27082	B	H
03-57331	Site 156: Legonyane, outskirts	27.77532	25.27082	B	H
unk./n	Site 157: Leganyane, lethabong prmry sch.	27.77929	25.27034	B	H
03-56331	Site 158: Legonyane	27.79021	25.27119	B	H
T46009	Site 159: Legonyane	27.78929	25.28248	B	H
T46039	Site 161: GaTsefoqe	27.71680	25.10997	B	H
03-56017	Site 162: Jericho	27.82928	25.32288	B	
03-56415	Site 163: Madinyane, Ramogatla	27.88097	25.39750	B	H
03-56327	Site 164: Madinyane	27.87745	25.39166	B	H
n/n	Site 165: Fafung	27.78182	25.20037	B	H
n/n	Site 166: Bultfontein grazing	27.71097	25.21517	B	W

B/H No.	Site Number: Location, Description	Long. E	Lat. S	Type	Equip
03-56409	Site 167: Jonathan, next to cemetary	27.86970	25.21207	B	H
T4237	Site 168: GaHabedi grazing	27.89137	25.18937	B	W
T4876	Site 169: Zoutpansleegte grazing	27.88281	25.17182	B	W
unk./n	Site 170: GaHabedi	27.90113	25.16855	B	H
n/n	Site 171: Sephai grazing	27.82227	25.24122	B	W
n/n	Site 172: Sephai	27.80543	25.24606	B	H
n/n	Site 173: Sephai	27.80572	25.25170	B	H
03-56356	Site 174: Sephai	27.80170	25.24404	B	H
T46022	Site 175: Mmakau, Tshwara section	27.93212	25.62015	B	H
0036	Site 176: Tshwara	27.93486	25.62058	B	Z
n/n	Site 177: Mmakau, Mongopeng section	27.95675	25.61954	B	H
n/n	Site 178: Mmakau, Polonia Section	27.96071	25.61680	B	H
n/n	Site 179: Mmakau	27.93408	25.61607	B	H
n/n	Site 180: Mmakau, Tetele subvillage	27.89594	25.60728	B	H
BB1273	Site 181: Mmakau, Switch subvillage	27.88837	25.59424	B	H
0032	Site 182: Mothuthlung	27.89585	25.59623	B	H
BB1021	Site 183: Mothuthlung, Switch subvillage	27.88962	25.59423	B	H
n/n	Site 184: btwn Rankotia and Ntswaphelong	27.84688	25.56696	B	S
NO. 2	Site 185: Vametco mine	27.89972	25.58154	B	N
n/n	Site 186: Lerulaneng	27.89874	25.51655	B	H
T4072	Site 187: Lerulaneng	27.90003	25.52196	B	H
n/n	Site 188: Lerulaneng	27.90377	25.52419	B	H
BB1226	Site 189: Paarlkraal farm	27.79225	24.97147	B	W
BB1313	Site 190: Paarlkraal grazing	27.78049	24.99049	B	W
T4636	Site 191: Doornfontein grazing	27.76074	25.00052	B	W
BB1204	Site 192: Doornfontein grazing	27.73561	25.02186	B	W
BB1264	Site 193: Blokspruit grazing	27.74268	25.04485	B	W
n/n	Site 194: Goudkoppie Veldspaatmyn	27.77187	25.03748	O	
BB1222	Site 195: Ruigterpoort grazing	27.78375	25.03651	B	W
n/n	Site 196: Blokspruit grazing	27.76188	25.06416	B	W
BB11	Site 197: Blokspruit grazing	27.81223	25.07292	B	W
BB1172	Site 198: Die mont van Blokspruit	27.74285	25.11436	B	W
BB1193	Site 199: Die mont van Blokspruit	27.74549	25.09900	B	W

B/H No.	Site Number: Location, Description	Long. E	Lat. S	Type	Equip
T4742A	Site 200: Kenkelbos	27.70064	25.05679	B	W
T4852	Site 201: Kwarriekraal	27.65559	25.06467	B	W
n/n	Site 202: Tolwane River	27.82832	25.32830	R	
n/n	Site 203: Shakung	27.91981	25.34310	B	H
T4903	Site 204: Shakung	27.90934	25.33866	B	H
03-56404	Site 205: Shakung	27.90831	25.33279	B	H
03-65121	Site 206: Shakung	27.90037	25.33465	B	H
03-56372	Site 207: Moiletswane	27.92207	25.37965	B	H
03-56195	Site 208: Moiletswane	27.92703	25.37826	B	H
03-56371	Site 209: Moiletswane	27.92458	25.38370	B	H
03-56398	Site 210: Dipompong	27.94675	25.39168	B	H
03-56397	Site 211: Dipompong	27.94599	25.38898	B	H
n/n	Site 212: Makgabetlwane	27.94607	25.27253	B	H
03-56395	Site 213: Makgabetlwane	27.92966	25.26812	B	H
BB1064	Site 214: Rabosula, Kalkbank prmry sch.	27.97570	25.37660	B	H
BB1065	Site 215: Rabosula	27.98264	25.37519	B	H
03-56382	Site 216: Rabosula	27.98293	25.28808	B	H
n/n	Site 217: Botshabelo (Vyeboschlaagte no.1)	27.99854	25.31506	B	S
03-56274	Site 218: Klippan	28.04664	25.44173	B	H
03-56269	Site 219: Winterveld	27.99238	25.41214	B	H
T4066	Site 220: Winterveld	27.96519	25.39833	B	H
T4064	Site 221: Winterveld, Palatselenyae mdl sch	28.01992	25.36573	B	H
BB1315	Site 222: Winterveld, Matlwareng prmry sch	28.05601	25.45172	B	H
BB?	Site 223: Kgabaletsane	27.95010	25.53270	B	H
BB1084	Site 224: Kgabaletsane	27.96532	25.53914	B	H
BB1086	Site 225: Kgabaletsane	27.96776	25.53371	B	H
n/n	Site 226: Hebron	28.00850	25.54687	B	H
n/n	Site 227: Hebron	28.02344	25.54494	B	H
BB1080	Site 228: Hebron	28.02615	25.54811	B	H
n/n	Site 229: Hebron	28.03060	25.55243	B	H
n/n	Site 230: Pretoria Saltpan, surface	28.08316	25.41082	P	
n/n	Site 231: Pretoria Saltpan, artesian b/h	28.08170	25.40720	Z	
T4894	Site 232: Tamootielaagte	27.87859	25.06667	B	W

B/H No.	Site Number: Location, Description	Long. E	Lat. S	Type	Equip
T4997	Site 233: Tambootielaagte	27.85554	25.06636	B	M
02-53055	Site 234: Tambootielaagte	27.82861	25.07780	B	W
n/n	Site 235: Tambootielaagte	27.86907	25.05229	B	M
BB0103	Site 236: Waterval	27.87611	24.99673	B	W
T49020	Site 237: Waterval	27.84197	25.00189	B	M
n/n	Site 238: Witpoortje	27.91725	25.00190	B	M
n/n	Site 239: Lebitloane	27.92414	25.06234	B	H
02-53591	Site 240: Lebitloane	27.92721	25.07496	B	H
n/n	Site 242: Stinkwater, Mr Teledi's farm	28.16481	25.38784	B	M
n/n	Site 243: Stinkwater, next to Namo Prm Scl	28.16281	25.39009	B	H
n/n	Site 244: Stinkwater	28.16228	25.39460	B	H
02-53324	Site 245: Mogogelo	28.13668	25.36105	B	H
n/n	Site 246: Dilopye	28.19292	25.38190	B	H
T442?8	Site 247: Suurman	28.21601	25.38361	B	H
T4032	Site 248: Makekeng (Syferkuil)	28.22560	25.08531	B	
T4207B	Site 249: Syferkuil	28.24378	25.07141	B	
T4376	Site 250: Syferkuil A grazing	28.22900	25.05689	B	W
n/n	Site 251: Syferkuil grazing	28.19286	25.05264	B	W
n/n	Site 252: Mathiebiestad, Senteng Prm schl	28.16915	25.26104	B	H
02-53251A27	Site 253: Mathiebiestad, Lepomo Prm sch	28.15674	25.26187	B	
01-53385	Site 254: Mathiebiestad, Regodile ELC	28.15321	25.26952	B	H
02-53384	Site 255: Mathiebiestad, south	28.15267	25.27584	B	H
n/n	Site 256: Mathiebiestad	28.16899	25.28586	B	H
02-5330?	Site 257: Mathiebiestad, Ramogoga ELC	28.19832	25.27880	B	H
02-00093	Site 258: Mathiebiestad, Mahobotle prm sch	28.20082	25.27565	B	
n/n	Site 259: Mathiebiestad	28.17754	25.26830	B	H
n/n	Site 260: Mathiebiestad	28.16263	25.27183	B	H
n/n	Site 261: Potoane (Goedgewacht)	28.15839	25.23841	B	H
n/n	Site 262: Mathiebiestad, Geodgewaagd 2	28.17772	25.24213	B	H
T4991	Site 263: Slagboom grazing	28.00950	25.12013	B	H
02-53455	Site 264: Slagboom	28.00230	25.12144	B	H
n/n	Site 265: Bollantlokwe	27.97968	25.06785	B	H
n/n	Site 266: Bedwang grazing	28.02492	25.11256	B	

B/H No.	Site Number: Location, Description	Long. E	Lat. S	Type	Equip
4689	Site 267: Tholwe	27.91266	25.11838	B	H
T4546	Site 268: De Grens trust	27.93028	25.08848	B	H
02-53581	Site 269: De Grens private	27.91682	25.07773	B	H
n/n	Site 270: Lefiswane	28.86383	24.96765	B	H
01-50099	Site 271: Lefiso	28.88763	24.93878	B	H
01-50098	Site 272: Lefiso	28.90100	24.93066	B	H
01-5277?	Site 275: Rooikoppies grazing	28.73087	25.09025	B	H
n/n	Site 276: Ramantsho, primary school	28.76712	25.05329	B	H
n/n	Site 277: Rooifontein grazing	28.67043	25.07839	B	M
01-50771?	Site 278: Semohlase	28.70660	25.08208	B	H
T4269	Site 279: Semohlase grazing camp	28.68158	24.98317	B	W
T42600	Site 280: Goedviralles	28.66474	24.98313	B	M
T4507	Site 281: Bultfontein grazing	28.52865	25.08839	B	W
T4710	Site 282: Bultfontein grazing	28.59841	25.12877	B	W
n/n	Site 283: Bultfontein grazing	28.51458	25.13754	B	W
n/n	Site 284: Klippan grazing	28.49735	25.10860	B	M
n/n	Site 286: Tswaaneng Spring west	27.00893	25.14917	F	
n/n	Site 287: Quarantine Camp	27.02233	25.23448	B	
n/n	Site 288: Letswaaneng spring auger hole	27.11058	25.14778	F	
BB2088	Site 289: Mabele a Podi	27.20353	25.28039	B	H
NO. 2	Site 290: Main Camp borehole, Borakalalo	27.80978	25.15328	B	M
n/n	Site 291: Jonathan Camp, Borakalalo Park	27.84812	25.17518	B	S
n/n	Site 292: Makoropeja	27.83629	25.11431	B	H
n/n	Site 293: Tlolwe Base, Borakalalo	27.88743	25.12530	B	M
n/n	Site 294: Blokspruit base, Borakalalo	27.73717	25.11710	B	M
n/n	Site 295: Moretele Camp, Borakalalo Park	27.79122	25.12043	B	M
n/n	Site 298: Bultfontein	27.81142	25.17539	B	H
n/n	Site 299: Klipvoor Primary school	27.80541	25.09192	B	H
n/n	Site 300: Slipfontein fluorite mine	27.68452	25.00992	B	M
n/n	Site 302: Mankwe river at Mankwe bridge	27.10969	25.25566	R	
n/n	Site 303: Blinkwater, Pilanesberg	27.11063	25.20104	R	
unk./n	Site 304: Pilanesberg centre	27.10372	25.24754	B	
unk./n	Site 306: Pilanesberg, Green Tweed	26.98510	25.33559		

B/H No.	Site Number: Location, Description	Long. E	Lat. S	Type	Equip
n/n	Site 307:Nooitgedacht farm	27.51583	25.05800	B	S
n/n	Site 308: Nooitgedacht, Wolvaardts	27.51091	25.06659	B	S
n/n	Site 309: Nooitgedacht, cattle	27.49156	25.06169	B	
n/n	Site 310: Nooitgedacht, Van niekerk	27.51227	25.03770	B	
n/n	Site 311: Nooitgedacht, Eloff's	27.53149	25.01416	B	
n/n	Site 312: Bakgat Farm	27.52718	25.04803	B	
n/n	Site 313: Pienaars river, Buffelspoort	27.62518	25.12664	R	
n/n	Site 314: Buffelspoort, Fred de la poorts'	27.63448	25.10313	B	
n/n	Site 315: Buffelspoort, Standers	27.61618	25.11178	B	
n/n	Site 316: Kwarriekraal	27.64165	25.05254	B	H
n/n	Site 317: Mooimeisjiesfontein	27.64588	25.00874	B	
n/n	Site 318: Slipfontein, fanigalo	27.65632	25.01592	B	
n/n	Site 319: Mooimeisjiesfontein, spruit	27.62446	24.98400	R	
n/n	Site 320: Rietfontein	27.59249	24.92636	B	M
n/n	Site 321: Weihoek	27.62808	24.91628	B	
n/n	Site 322: Driefontein game farm	27.68708	24.93588	B	
n/n	Site 323: Koperfontein, Shikari game camp	27.64367	24.96496	B	
n/n	Site 324: Driefontein	27.71312	24.98722	B	
n/n	Site 325: Hartbeesfontein	27.81150	24.96234	B	
n/n	Site 326: Rietdal	27.76547	24.96484	B	
n/n	Site 327: Morgenzon	27.85164	24.89531	B	
n/n	Site 328: Kromdraai	27.90670	24.91349	B	S
n/n	Site 329: Kromdraai, plot 142	27.84262	24.95133	B	
n/n	Site 330: Kromdraai, plot 304	27.87693	24.97280	B	
n/n	Site 331: Kromdraai, plot 48	27.87115	24.92589	B	
n/n	Site 332: Hardekoolbult	27.56136	24.93731	B	
n/n	Site 333: Kruidfontein, dam draining hills	27.51617	25.14015	P	
n/n	Site 334: Kruidfontein	27.51620	25.14782	B	
n/n	Site 335: Pretoria Saltpan, old artesian	28.08122	25.41081	B	N
n/n	Site 337: Soutpan	28.07802	25.43291	B	M
n/n	Site 338: Soutpan, Mr Mon's	28.09856	25.41137	B	

Appendix A2 Rock and soil sample locations. "N" = Nebo Granite, "L" = Lebowa Granite.

No.	Site Name	Rock Type	Long. E.	Lat. S.
1	Bapong	Quartzite	26.8337	25.3035
2	Moreteletsi	Monzonite	26.7895	25.2860
3	Green Tweed	Syenite	26.9841	25.3473
4	Thabayadiotsa	Syenite	27.1677	25.2574
5	Kubu drive Quarry	Syenite	27.0998	25.2837
6	Moepo	Fluorite ore	27.0799	25.2968
7	N of Pilanesberg	Norite	27.1537	25.1324
8	Mabele a podi	Alkali granite	27.1961	25.2854
9	Lesung	Norite	27.3667	25.5166
10	Lesung	Magnetite ore	27.3667	25.5000
11	Modikwe	Alkali granite (N)	27.5242	25.5125
12	Sun city-Lesung	Norite	27.2355	25.3900
13	Smaldale Farm	Dolomitic limestone	26.6043	24.8385
14	Tamboetieshoek Fm	Ironstone	26.5943	24.8692
15	Dwarsberg	Sandstone	26.6683	24.9561
16	Rampapaanspoort	Norite	26.6811	24.9931
17	Holfontein	Garnet-biotite hornfels	26.7361	25.1837
18	Leboaneng	Ironstone	27.4149	25.0989
19	GaRamolorengpoort	Dolomite	27.4183	25.0958
20	Makoropeja	Granite (L)	27.8343	25.1206
21	North block 7	Granite (L)	27.8626	25.1264
22	North block 10	Granite (L)	27.8959	25.1352
23	Slipfontein	Quartz pegmatite	27.6845	25.0108
24	Kwarriekraal	Granophyre	27.6531	25.0561
25	Kenkelbos	Alkali granite (L)	27.6837	25.0465
26	Blokspruit	Alkali granite (L)	27.7467	25.0471
27	Blokspruit	Alkali granite (L)	27.7324	25.0724
28	Borakalalo	Sandstone	27.7998	25.1484
29	Sephai	Limestone	27.7938	25.2418
30	GaTsogwe	Granite (N)	27.7595	25.3607
31	Rashoop	Granophyre	27.7660	25.5327

No.	Site Name	Rock Type	Long. E.	Lat. S.
32	Mpatsetlha	Sandstone	27.7213	25.1136
33	Mpatsetlha	Mudstone	27.7193	25.1154
34	Leeupoort Tin	Felsite	27.7048	24.9141
35	Tooyspruit	Feldspathic sandstone	27.8764	24.8220
36	Kwaggafontein	Greenschist	27.8409	24.8385
37	Rietfontein	Alkali granite (N)	27.5652	24.9192
38	Rietfontein	Alkali granite (N)	27.5860	24.9110
39	Sutelong	Quartzite	27.9500	25.1000
40	Dikebu	Granite (L)	27.9666	25.2000
41	Pretoria Saltpan	Granite (N)	28.0822	25.4063
42	Pretoria Saltpan	Granite (N)	28.0792	25.4054

Appendix B: Thin Section Studies and analysis of Pilanesberg Fluorite Ore

Appendix B1. Petrographic description of rock sample from thin section. All samples are hollocrystalline. The composition of some carbonate minerals is known from microprobe and XRF analysis. Abbreviations: plag = plagiocalse feldspar, alk fldspr = alkali feldspar, cpx = clinopyroxene, opx = orthopyroxene, hrnblnd = hornblende, RLS = Rustenburg Layered Suite. Numbers after main minerals are estimated modal mineral percentages.

Sample	Formation	Lithology	Main Minerals	Accessory	Description
RO1	Pretoria Seq.	Quartzite	Quartz		Coarse Grained. Consertal contacts, many fluid inclusions.
RO2	RLS	Monzonite	Plag 30, alk fldspr 30, cpx 30, biotite 10	Opaques	Medium grained. Euhedral biotite, embayed by fldspr & cpx. Euhedral fldspr laths, occasionally variolitic. Skeletal anhedral cpx. Poikilitic, subophitic alk fldspr enclosing plag.
RO3	Pilanesberg	Syenite	Alk fldspr 80, hrnblnd 10, biotite 5, cpx 5	Quartz, opaques	Coarse grained. Coarse subhedral fldspr, enclosing fine hrnblnd. Brown hrnblnd also coarse twinned & zoned, altered green around edges and smaller crystals. Subhedral biotite with opaque lamellae, associated with clumps of hrnblnd.
RO4	Pilanesberg	Nepheline syenite	Alk fldspr 60, cancrinite 30, nepheline 10, Ca-amphibole 10	Fluorite	Medium grained, porphyritic, altered. Euhedral nepheline, occasionally fresh, more often altered around edges or entirely replaced by fine grained cancrinite. Anhedral colourless to purple fluorite, often interstitial. Groundmass of nepheline, amphibole and fldspr.
RO5	Pilanesberg	Syenite	Alk fldspr 80, plag 10, opaque 9	Fluorite	Coarse to medium grained. Euhedral to subhedral, cloudy alkali fldspr, rare simple twinning. Partially replaced by microcrystalline alteration products and opaques. Fluorite and opaques interstitial to alk fldspr. Fluorite is anhedral, usually colourless with faint purple tinges.
RO6	Pilanesberg	Fluorite ore	Calcite 30, apatite 20, fluorite 15, strontianite 10, ankerite 10, opaques 10	Sphene, cancrinite	Coarse. Interlocking coarse crystals of apatite with abundant fine anhedral inclusions of carbonate and medium anhedral colourless to purple fluorite. Large subhedral plag, more often patches of fine interdigitating crystals. Medium fluorite enclosed by anhedral carbonate and partially enclosed by apatite. Carbonate has remnant euhedral to subhedral crystal shapes, rimmed by opaques. Rock cut by fine carbonate veins.

Sample	Formation	Lithology	Main Minerals	Accessory	Description
RO7	RLS	Norite	Plag 50, opx & cpx 50	quartz	Coarse grained. Anhedral interlocking plag. Anhedral opx & cpx, lamellar inclusions of cpx in opx. Patches of symplectic and graphitic plag and quartz.
RO8	Granophyres	Alkali granite	Alk fldspr 60, quartz 20, Hrnblnd 10	plag, opaques	Medium grained. Subhedral, dusty alk fldspr, occasionally with radial arrangement. Skeletal anhedral hrnblnd, larger examples with simple twinning. Fine grained anhedral quartz, sometimes crack filling. Opaques interstitial to other crystals.
RO9	RLS	Norite	Plag 70, cpx 20, opx 10	Hrnblnd, quartz	Coarse to medium grained. Fresh, subhedral plag with anhedral pyroxenes in interstices. Some opx interstitial to cpx.
RO10	RLS	Magnetite ore	Magnetite 95	Biotite, quartz, feldspar	Medium to fine grained. Magnetite has some rounded grains, most contact straight or angular. Interstitial, distorted biotite, occasionally skeletal filled with microcrystalline feldspar. Quartz fills interstitial gaps and cracks.
RO11	Nebo Granite	Alkali granite	Quartz 50, alk fldspr 40	Biotite, cpx, opaques, plag	Medium grained. Anhedral consertal quartz. Microperthitic subhedral tabular alk fldspr with biotite and sparse, irregular, blebby quartz inclusions. Anhedral skeletal biotite, embayed by quartz and plag. Sparse cpx, embayed by quartz, alk fldspr lamellae.
RO12	RLS	Norite	Plag 50, cpx 25, opx 25.	Biotite, opaques, quartz	Medium to coarse grained. Euhedral to subhedral plag, sometimes bent around opx. Opx encloses plag and is patchily rimmed by fine cubic opaque minerals.
RO13	Chuniespoort	Dolomitic limestone	Carbonate 90, quartz 10	Opaques	Fine grained. Microcrystalline dusty interlocking grains of carbonate. Quartz as fine subrounded clasts and medium grained subangular conglomerations of interlocking grains. Cracks filled with carbonate and opaques.
RO14	Chuniespoort	Banded ironstone	Fe oxide 60, quartz 30, garnet 10		Fine grained. Quartz and Fe oxide as fine crystals in very fine alternating bands. Occasional medium grained polygrain conglomerations of quartz. Garnets have dusty cores, red-brown cracks.
RO15	Pretoria	Sandstone	Quartz 95, muscovite 5	Opaques	Medium grained. Consertal quartz with quartz overgrowth rims. Rare lithic fragments. Microcrystalline muscovite patches interstitial to quartz.

Sample	Formation	Lithology	Main Minerals	Accessory	Description
RO16	RLS	Norite	Opx 50, plag 40	Biotite, opaques	Medium to fine grained. Euhedral to subhedral opx, occasionally in large clumps, encloses fine cubic opaques. Some cruciform and penetration twinning of opx. Laths and stumpy equant crystals of plag, some bent around opx. Biotite interstitial to opx.
RO17	RLS	Garnet-biotite hornfels	Quartz 50, biotite 25, garnet 25	Opaques, fluorite	Medium grained. Seriate, anhedral consertal and rounded quartz, embaying biotite. Anhedral to subhedral equant skeletal biotites with radiation damage haloes, embayed by quartz. Coarse garnet, many quartz inclusions, some biotite inclusions, increased number of hexagonal opaque minerals. Fine euhedral colourless fluorite.
RO18	Chuniespoort	Banded ironstone	Quartz 50, Fe Oxide 50		Fine grained. Fine quartz and Fe oxides in layers <1 mm wide of varying proportions. Microfaults offsetting banding filled with quartz and opaques.
RO19	Chuniespoort	Dolomite	Dolomite 98	Opaques	Fine consertal dolomite, occasionally coarser subhedral crystals. Opaques fill cracks.
RO20	Lebowa Granite	Granite	Quartz 50, alk fldspr 40, plag 5	Biotite, opaques	Medium to coarse grained. Quartz as medium grained, rounded, anhedral and consertal crystals, containing fluid inclusions. Weathered fldspr, infilled with serricite, microperthitic in places, simple twinning occasionally. Weather interstitial medium sized biotite.
RO21	Lebowa Granite	Granite	Quartz 40, alk fldspr 40, Biotite 5, plag 5	Fluorite, opaques	Coarse to medium grained. Consertal quartz with many fluid inclusion trails. Microperthitic alk fldspr, occasionally with simple twinning. Fine biotite in clumps, anhedral, embayed by quartz and fluorite. Fluorite is fine and colourless, rounded to anhedral.
RO22	Lebowa Granite	Granite	Quartz 60, alk fldspr 30, plag 5, biotite 5	Fluorite	Fine grained, porphyritic. Fine subhedral to anhedral consertal quartz, also porphyritic anhedral quartz with fluid inclusion trails. Intergranular, dusty, anhedral alk fldspr, also as coarse porphyritic euhedral crystals enclosing plag, quartz and skeletal biotite. Blebs of fluorite.
RO23	Lebowa Granite	Quartz pegmatite	Quartz 100		Very coarse grained quartz pegmatite.

Sample	Formation	Lithology	Main Minerals	Accessory	Description
RO24	Lebowa Granite	Granophyre	Quartz 50, Alk fldspr 45, Biotite 5	Fluorite	Coarse grained. Quartz as subhedral to anhedral equant to hexagonal crystals with many fluid inclusions. Symplectic and granophyric intergrowths of Quartz and alk fldspr. Microperthitic alk fldspr, occasionally with simple twinning. Skeletal biotite, lenses of quartz along cleavage. Fluorite as scarce anhedral dusty crystals and crack infilling.
RO25	Lebowa Granite	Alkali granite	Alk fldspr 50, quartz 40, biotite 10	Fluorite	Coarse grained. Subhedral quartz with many fluid inclusions, enclosing alk fldspr. Coarse, anhedral, dusty alk fldspr in turn encloses quartz blebs. Interstitial skeletal fine grained biotite.
RO26	Lebowa Granite	Alkali granite	Alk fldspr 50, quartz 25, opaques 25		Fine grained, altered. Quartz as elongate to equant coarse crystals, many fluid inclusions, rimmed by alk fldspr. Fine to medium grained very anhedral alk fldspr. Opaques visually dominate the rock, anhedral, occur in conglomerations with interstitial very fine fldspr.
RO27	Lebowa Granite	Alkali granite	Alk fldspr 40, quartz 45	Muscovite, hrnblnd, fluorite	Medium grained. Anhedral, seriate fine to coarse quartz enclosing alk fldspr and muscovite. Many fluid inclusions. Alk fldspr subhedral to anhedral, rare simple twinning, often with fine rounded quartz inclusions. Microcrystalline muscovite aggregates occur interstitially, rarely as fine inclusions in quartz. Altered remnant hrnblnd, cleavages filled with elongate opaques, surrounded by fine muscovite. Anhedral, fine, colourless fluorite, rarely purple.
RO28	Croc. River Fragment	Sandstone	Quartz 80, clay 20	Muscovite, opaques	Fine grained. Angular grain supported quartz clasts, consertal contacts, fluid inclusion trails. Fine muscovite and clay interstitially. Scattered rounded opaques.
RO29	Karoo	Limestone	Calcite 95, quartz 5		Microcrystalline calcite with some druzy fillings. Subrounded fine quartz clasts. Cracks filled by quartz.
RO30	Nebo Granite	Granite	Quartz 45, Alk fldspr 40, plag 5, biotite 5, hrnblnd 5		Coarse grained. Very coarse quartz with consertal contacts. Anhedral microperthitic alk fldspr. Subhedral plag, very fine multiple twinning. Subhedral medium grained books of biotite. Coarse anhedral hrnblnd enclosing biotite and fine quartz.

Sample	Formation	Lithology	Main Minerals	Accessory	Description
RO31	Granophyre	Granophyre	Quartz 45, alk fldspr 40, biotite 5	Hrnblnd	Medium to coarse grained. Anhedral coarse quartz, usually in spectacular granophyric, symplectic, graphitic and graphic intergrowth with alk fldspr. Quartz has large randomly oriented fluid inclusions. Biotite as fine grained interstitial aggregates of randomly oriented weathered crystals. Skeletal hrnblnd, filled by alk fldspr.
RO32	Croc. River Fragment	Fine sandstone	Quartz 98	Clay, muscovite	Fine grained. Interlocking quartz grains, very fine grained interstitial clay and muscovite. No bedding.
RO33	Croc. River Fragment	Mudstone	Clay 90, quartz 10	Opaques	Very fine grained subrounded quartz clasts, matrix supported. Fining up cycles present. Very fine anhedral opaques.
RO34	Rooiberg	Felsite	Quartz 50, alk fldspr 20, carbonate 15, plag 10, muscovite 5	Opaques	Fine grained. Fine subrounded to angular quartz grains, some consertal contacts. Occasional well rounded grains are matrix supported by fine muscovite. Alk fldspr subrounded with consertal contacts. Angular, fresh anhedral plag. Carbonate as medium grained patches, enclosing fine quartz and alk fldspr. Fine grained interstitial muscovite. Fine euhedral hexagonal opaques. Rock has both igneous and sedimentary textures.
RO35	Croc. River Fragment	Feldspathic sandstone	Quartz 85, alk fldspr 10, biotite 5	Plag	Fine grained. Very fine interlocking quartz grains. Fine anhedral alk fldspr. Fresh, medium grained, skeletal subhedral biotite.
RO36	Rooiberg	Greenschist	Actinolite 50, epidote 50	Opaques	Medium grained, altered rock. Anhedral actinolite as clumps replacing prismatic mineral. fine epidote?, pale pink in plain light, often completely obscured by cryptocrystalline dark alteration product, pseudomorphing prismatic mineral.
RO37	Nebo Granite	Alkali granite	Alk fldspr 50, quartz 45	Fluorite, biotite, opaques	Coarse grained. Coarse consertal and subhedral quartz, some distinctly rounded and embaying into fldspr. Many fluid inclusions. Anhedral alk fldspr encloses quartz, cracks filled with quartz and fluorite. Fluorite as colourless crack filling and medium anhedral colourless and purple crystals. Fine altered biotite. Scattered clumps of anhedral opaques.

Sample	Formation	Lithology	Main Minerals	Accessory	Description
RO38	Nebo Granite	Alkali granite	Alk fldspr 75, quartz 20	Fluorite, biotite, plag, amph, opx, muscovite	Coarse grained. Very coarse subhedral microperthitic alk fldspr, some medium grained euhedral zoned crystals. Much simple twinning, encloses quartz, biotite and plag. Consertal quartz, fine biotite along contacts and interstitially. Biotite also as medium euhedral crystals surrounded by plag; as radiating fine acicular needles from larger biotites; and as randomly oriented very fine clumps. Medium subhedral colourless fluorite, interstitial to quartz. Medium acicular plag. Opx as fine euhedral to subhedral crystals associated with biotite and biotite.Muscovite as fine radiating green crystals from clumps of biotite.
RO39	Karoo	Quartzite	Quartz 100		Medium grained. Grain supported rounded quartz, some pressure solution contacts, many fluid inclusions. Fine angular quartz interstitially.
RO40	Lebowa Granite	Granite	Quartz 50, alk fldspr 40, plag 10	Opaques	Medium grained. Quartz with straight contacts. Anhedral dusty alk fldspr, occasionally euhedral and columnar. Plag anhedral, consertal contacts with quartz.
RO41	Nebo Granite	Granite	Alk fldspr 55, quartz 35, plag 10	Biotite, opaques	Medium grained. Seriate quartz with 3-way contacts. Interstitial alk fldspr with rounded quartz inclusions. Subhedral plag encloses quartz. Anhedral interstitial biotite with opaques along the cleavage. Large cracks filled with fine opaques.
RO42	Nebo Granite	Granite	Alk fldspr 50, quartz 30, plag 10, hrnblnd 10	Biotite	Coarse grained. Anhedral quartz with straight contacts with alk fldspr. Anhedral alk fldspr with plag patches. Plag as subhedral medium crystals. Medium grained fresh subhedral biotite. Large skeletal hrnblnd, embaying and including quartz.

Appendix B2. Fluorine bearing minerals in thin section. The percentage of the four main fluorine-bearing mineral groups was estimated in thin section using an optical microscope. Calculating the maximum F content of each mineral from the chemical formulae in Deer *et al.* (1977) gives the maximum F concentration in the whole rock after multiplication by the appropriate estimated percentages. The actual F concentration is shown for comparison.

No.	Rock Type	%flrt	%apa	%mica	%hrnbld	F section (F ppm)	F XRF ppm
1	Quartzite	0	0	0	0	0	40
2	Monzonite	0	0	5	0	7000	162
3	Syenite	1	0.1	5	1	12328	5310
4	Syenite	1	0	0	5	7150	16431
5	Syenite	1	0	0.1	0	4940	6958
6	Fluorite ore	10	0.1	0	0	48058	80514
7	Norite	0	0	0	0	0	183
8	Alkali granite	0	0	0	10	4700	1061
9	Norite	0	0	0	0	0	153
10	Magnetite ore	0	0	0	0	0	-320
11	Alkali granite	0	0	2	0.1	2847	489
12	Norite	0	0	0	0	0	221
13	Dolomitic limestone	0	0	0	0	0	400
14	Ironstone	0	0	0	0	0	168
15	Sandstone	0	0	0	0	0	24
16	Norite	0	0	0	0	0	205
17	Garnet-biotite hornfels	0	0	20	0	28000	774
18	Ironstone	0	0	0	0	0	-318
19	Dolomite	0	0	0	0	0	509
20	Granite	0	0		0	0	216
21	Granite	0	0	2	0	2800	2849
22	Granite	0	0	5	0	7000	1924
23	Quartz	0	0	0	0	0	39
24	Granophyre	0	0	2	0	2800	949
25	Alkali granite	0.1	0	1	0	1880	2527
26	Alkali granite	0	0	0	0	0	1260
27	Alkali granite	1	0.1	0	0	4858	3351

No.	Rock Type	%flrt	%apa	%mica	%hrnbld	F section (F ppm)	F XRF ppm
28	Sandstone	0	0	0	0	0	735
29	Limestone	0	0	0	0	0	858
30	Granite	0	0	0.1	3	1550	480
31	Granophyre	0	0	0.1	2	1080	127
32	Sandstone	0	0	0	0	0	119
33	Mudstone	10	0	0	0	48000	464
34	Felsite	0	0	0	0	0	2171
35	Feldspathic sandstone	0	0	0.1	0	140	373
36	Greenschist	0	0	0	0	0	4981
37	Alkali granite	1	0	0.1	0	4940	2570
38	Alkali granite	1	0	0	0	4800	2284
39	Sandstone	0	0	0	0	0	132
40	Granite	0	0	0	0	0	520
41	Granite	0	0	0.1	0	140	410
42	Granite	0.1	0	1	3	3290	437

Appendix B3. Electron Microprobe analyses of minerals from rock types in the study area. Concentrations in weight percent, LLD is the mean lower limit of detection, *n/d* is not detected and K-flsp is potassium feldspar.

Table B3.1 Analyses of mica and amphiboles from miscellaneous rock types in the field area.

Sample No.	Mineral	F	Na_2O	K_2O	SiO_2	TiO_2	Al_2O_3	Cr_2O_3	FeO	MnO	MgO	CaO	Total
	LLD:	0.17	0.04	0.03	0.06	0.04	0.05	0.05	0.09	0.08	0.03	0.03	
RO3	Amph	2.69	4.11	1.32	45.39	2.79	6.46	*n/d*	14.04	1.02	12.82	10.10	100.74
RO3	Amph	2.38	4.24	1.39	45.66	2.55	6.16	*n/d*	15.71	1.06	12.10	9.62	100.87
RO3	Amph	*n/d*	11.65	*n/d*	51.65	3.04	0.98	*n/d*	27.12	0.46	0.60	2.98	98.48
RO3	Amph	1.33	8.71	2.28	50.72	1.30	1.12	*n/d*	24.69	4.00	4.65	0.36	99.16
RO3	Amph	2.47	3.95	1.36	44.47	3.09	6.85	*n/d*	13.74	1.01	12.47	10.33	99.74
RO4	Amph	*n/d*	3.92	*n/d*	47.67	0.58	1.35	*n/d*	25.67	1.71	2.05	16.61	99.56
RO4	Mica	*n/d*	12.97	5.76	43.55	*n/d*	32.83	*n/d*	1.82	*n/d*	*n/d*	0.30	97.23
RO4	Amph	*n/d*	4.56	*n/d*	50.23	0.22	0.45	*n/d*	23.43	1.60	3.10	16.10	99.69
RO8	K-Flsp	*n/d*	0.30	15.79	65.19	*n/d*	17.05	*n/d*	1.22	0.35	*n/d*	0.53	100.43
RO11	Mica	*n/d*	0.10	8.62	33.14	3.33	13.15	*n/d*	35.76	0.36	0.32	*n/d*	94.78
RO11	Mica	*n/d*	0.10	8.10	32.83	3.42	13.72	*n/d*	35.97	0.30	0.38	0.06	94.88
RO11	Mica	*n/d*	0.10	8.25	33.43	3.59	12.96	*n/d*	35.71	0.33	0.55	0.23	95.15
RO11	Mica	*n/d*	0.11	6.43	33.94	2.57	14.01	*n/d*	34.71	0.20	0.77	0.18	92.92
RO11	Mica	*n/d*	*n/d*	7.93	33.73	3.16	12.69	*n/d*	36.90	0.36	0.67	0.2	95.64
RO11	Mica	*n/d*	0.07	8.04	32.76	3.35	13.24	*n/d*	36.59	0.21	0.20	0.06	94.52

Sample No.	Mineral	F	Na_2O	K_2O	SiO_2	TiO_2	Al_2O_3	Cr_2O_3	FeO	MnO	MgO	CaO	Total
	LLD:	0.17	0.04	0.03	0.06	0.04	0.05	0.05	0.09	0.08	0.03	0.03	
RO11	Amph	0.45	2.01	1.41	38.79	1.55	8.92	*n/d*	33.25	0.55	0.50	10.46	97.89
RO11	Amph	0.65	2.01	1.45	39.27	1.69	8.80	*n/d*	33.63	0.58	0.55	10.61	99.24
RO11	Amph	0.72	2.07	1.36	39.41	1.66	8.48	*n/d*	34.19	0.46	0.54	10.41	99.30
RO11	Mica	*n/d*	0.30	7.05	32.81	2.68	12.97	*n/d*	35.27	0.26	1.10	0.15	92.59
RO11	Mica	*n/d*	*n/d*	7.99	33.15	3.22	12.50	*n/d*	35.21	0.25	0.76	0.72	93.80
RO22	Amph	0.30	0.17	3.20	37.95	0.30	23.07	*n/d*	20.71	0.14	4.07	0.19	90.10
RO24	Mica?	1.27	0.05	*n/d*	44.14	*n/d*	38.45	*n/d*	1.48	*n/d*	0.05	0.30	85.74
RO24	Mica?	1.36	0.06	*n/d*	43.36	*n/d*	39.31	*n/d*	0.74	*n/d*	0.04	0.31	85.18
RO24	Mica?	*n/d*	*n/d*	*n/d*	42.20	*n/d*	23.63	0.84	7.27	0.28	18.76	4.10	97.08
RO25	Amph	*n/d*	0.13	3.64	23.98	*n/d*	13.60	*n/d*	42.77	*n/d*	0.84	0.15	85.11
RO25	Mica	*n/d*	0.12	4.83	29.89	*n/d*	14.78	*n/d*	33.1	*n/d*	1.11	0.15	83.98
RO25	Amph	0.19	0.17	2.92	20.80	0.29	15.96	*n/d*	46.23	*n/d*	0.91	0.17	87.64
RO25	Mica	*n/d*	0.13	3.73	32.48	0.20	18.93	*n/d*	32.13	*n/d*	0.98	0.17	88.75
RO30	Mica	*n/d*	*n/d*	8.33	33.44	2.51	11.63	*n/d*	38.58	*n/d*	1.22	*n/d*	95.71
RO30	Mica	*n/d*	*n/d*	8.12	34.14	2.50	11.40	*n/d*	37.19	0.14	1.17	*n/d*	94.66
RO30	Mica	*n/d*	0.10	7.45	33.68	2.02	12.01	*n/d*	36.47	*n/d*	1.22	0.11	93.06
RO30	Mica	*n/d*	0.13	7.40	33.26	2.02	11.66	*n/d*	36.75	*n/d*	1.24	0.16	92.62
RO30	Mica	*n/d*	0.08	7.91	34.09	2.01	12.03	*n/d*	36.81	0.14	1.26	0.08	94.41

Sample No.	Mineral	F	Na_2O	K_2O	SiO_2	TiO_2	Al_2O_3	Cr_2O_3	FeO	MnO	MgO	CaO	Total
	LLD:	0.17	0.04	0.03	0.06	0.04	0.05	0.05	0.09	0.08	0.03	0.03	
RO30	Mica	*n/d*	*n/d*	7.95	34.03	1.44	11.43	*n/d*	39.53	*n/d*	0.83	*n/d*	95.21
RO30	Mica	*n/d*	*n/d*	7.87	35.11	1.39	13.37	*n/d*	35.56	*n/d*	0.67	0.06	94.03
RO30	Mica	*n/d*	0.11	7.64	35.73	2.54	12.78	*n/d*	33.95	*n/d*	0.6	0.05	93.4
RO42	Mica	*n/d*	0.1	6.89	31.94	0.7	12.86	*n/d*	36.42	*n/d*	0.56	0.06	89.53
RO42	Mica	*n/d*	0.22	4.97	35.54	0.29	15.57	*n/d*	30.28	*n/d*	0.57	0.11	87.55

Table B3.2 Analyses of Mica in sample RO17, including the analysis of Cl.

	F	Cl	Na	K	Si	Ti	Al	Cr	Fe	Mn	Mg	Ca	Total
LLD:	0.17		0.04	0.02	0.06	0.04	0.05	0.05	0.09	0.08	0.03	0.03	
	n/d	0.16	0.16	9.24	35.33	4.62	17.72	0.14	22.71	*n/d*	8.00	*n/d*	98.08
	n/d	0.13	0.12	9.19	35.29	4.55	18.08	0.14	22.66	*n/d*	8.13	*n/d*	98.29
	n/d	0.15	0.12	9.25	34.73	4.76	17.84	0.12	22.39	*n/d*	7.94	*n/d*	97.3
	0.35	0.16	0.08	9.53	35.25	4.32	18.66	0.14	21.7	*n/d*	7.98	*n/d*	98.17

Table B3.3 Analyses of carbonate minerals in sample RO6 (Pilanesberg).

Mineral	$CaCO_3$	$FeCO_3$	$MgCO_3$	$MnCO_3$	$SiCO_3$	$SrCO_3$	$BaCO_3$	Total
LLD:	0.01	0.22	0.20	0.20	0.13	0.16	0.14	
Cal	93.61	*n/d*	*n/d*	*n/d*	*n/d*	4.29	*n/d*	97.9
Cal	95.24	1.37	*n/d*	1.26	*n/d*	0.64	*n/d*	98.51
Cal	91.95	*n/d*	*n/d*	*n/d*	*n/d*	6.00	*n/d*	97.95
Cal	91.46	*n/d*	*n/d*	*n/d*	*n/d*	7.28	*n/d*	98.74
Cl	90.64	*n/d*	*n/d*	*n/d*	*n/d*	8.01	*n/d*	98.65
Cal	91.85	*n/d*	*n/d*	*n/d*	*n/d*	7.49	*n/d*	99.34
Cal	91.63	*n/d*	*n/d*	*n/d*	*n/d*	7.07	*n/d*	98.7
Cal	91.99	*n/d*	*n/d*	*n/d*	*n/d*	7.24	*n/d*	99.23
Cal	86.80	*n/d*	*n/d*	*n/d*	*n/d*	11.10	*n/d*	97.9
Cal	99.10	1.15	*n/d*	1.28	*n/d*	0.28	*n/d*	101.81
Cal	95.67	1.40	*n/d*	2.06	*n/d*	0.51	*n/d*	99.64
Cal	94.97	1.25	*n/d*	1.94	*n/d*	0.60	*n/d*	98.76
Cal	95.94	1.58	*n/d*	1.99	*n/d*	0.51	*n/d*	100.02
Mean	**93.14**	**0.52**	**0.0**	**0.66**	**0.0**	**4.69**	**0.0**	**99.01**
Stron	14.60	*n/d*	*n/d*	*n/d*	*n/d*	87.58	*n/d*	102.18
Stron	14.53	*n/d*	*n/d*	*n/d*	*n/d*	87.27	*n/d*	101.8
Stron	7.15	*n/d*	*n/d*	*n/d*	*n/d*	95.12	*n/d*	102.27

Mineral	$CaCO_3$	$FeCO_3$	$MgCO_3$	$MnCO_3$	$SiCO_3$	$SrCO_3$	$BaCO_3$	Total
LLD:	0.01	0.22	0.20	0.20	0.13	0.16	0.14	
Mean	**12.09**	**0.00**	**0.00**	**0.00**	**0.00**	**89.99**	**0.00**	**102.08**
Mixed	56.83	19.59	13.28	7.56	0.70	0.93	*n/d*	98.89
Mixed	54.34	27.06	11.9	7.06	0.27	0.32	*n/d*	100.95
Mixed	51.82	17.21	17.79	9.90	1.69	0.60	*n/d*	99.01
Mean	**54.33**	**21.29**	**14.32**	**8.17**	**0.89**	**0.62**	**0.00**	**99.62**

Table B3.4 Analysis of apatites from sample RO6 (Pilanesberg). Cl, FeO, MnO and MgO were not present above the detection limit (0.026 wt% for Cl and approximately 0.08 wt% for the others). H_2O estimated assuming F + OH = 2.0 in structural formula.

P_2O_5	CaO	SrO	F	Subtotal	O=F	H_2O	Total
39.91	51.72	2.94	3.35	97.92	1.41	0.11	96.62
39.93	50.54	4.55	3.08	98.10	1.30	0.23	97.03
39.21	49.70	6.78	3.60	99.29	1.52	0	99.29
39.89	51.47	3.94	2.60	97.90	1.09	0.47	97.28
40.02	49.64	6.76	2.64	97.82	1.11	0.45	98.40
40.07	51.61	2.59	3.55	97.82	1.49	0.01	96.34
39.82	51.13	5.77	2.67	99.39	1.12	0.44	98.71
39.72	50.87	4.71	2.93	98.23	1.23	0.31	97.31
40.40	51.46	3.63	2.45	97.94	1.03	0.55	97.46
40.18	50.68	5.30	2.47	98.63	1.04	0.54	98.13

Table B3.5 Analysis of plagioclase from sample RO6 (Pilanesberg).

Na_2O	K_2O	SiO_2	Al_2O_3	Total
11.4	0.12	68.97	19.40	99.93
11.11	0.08	68.52	19.40	99.11
11.55	0.08	68.89	19.24	99.76
11.39	0.05	68.37	19.39	99.20

Appendix B4. Composition, origin and significance of Pilanesberg fluorite ore.

Introduction

Of some relevance to this thesis is the occurrence of carbonates in the igneous rocks, which has implications for ^{14}C dating of groundwater and for hydrogeochemistry. Sample RO6, a fluorite ore from the Pilanesberg Complex, was found to have an unusual abundance of carbonate for Pilanesberg rocks. The sample was selected for the presence of visible fluorite and collected from an ore dump at the abandoned Moepo fluorite mine in the southwest of the Pilanesberg Complex (Figure B4.1). The sample bears no chemical or petrographic resemblance to the nepheline syenite of the surrounding Pilanesberg Complex (c.f. sample RO5, Table 4.3). Calcium carbonate is the dominant carbonate phase, and together with strontianite and manganoan ankerite makes up approximately 24.4 wt% of the sample. The carbonate content of the rock is not sufficient (i.e. <50% carbonate) for it to be classified as a carbonatite (Le Maitre, 1989). The high F and Sr contents further complicate classification of the rock. The results presented here show for the first time the presence of carbonate-bearing rocks in the Pilanesberg (McCaffrey *et al.*, 1996). The methods of analysis are described in Chapter 3.

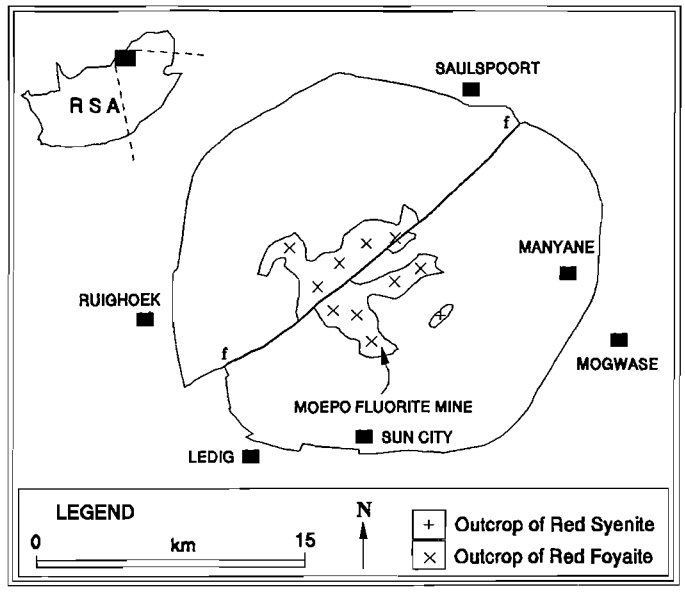

Figure B4.1 Location of the Moepo fluorite mine within the Pilanesberg Complex.

Results

Compared to the nepheline syenites which dominate the geology of the Pilanesberg (Lurie, 1974; this volume, Table 4.3), RO6 has a significantly greater content of calcium (31.6 wt% CaO) and strontium (6.22 wt% SrO; Table B4.1). The sample has a Ba concentration of less than 10 ppm. A rock chip moistened with dilute hydrochloric acid and inserted into a bunsen flame produced a vivid red flame, indicative of strontianite (Deer *et al.*, 1977). Initial X-Ray Diffraction (XRD) analysis on the whole-rock powder confirmed the presence of apatite, plagioclase and fluorite but failed to show the presence of calcite and produced a poor fit for dolomite. After heavy mineral enrichment, where plagioclase and calcite were separated from the denser phases, the powder was analysed again and strontianite was identified as the only carbonate phase, although the fit was poor.

Selected microprobe analyses of carbonate minerals in RO6 are presented in Table B4.2. Of 20 carbonate grains analysed, 14 were calcium carbonate, 3 were strontianite and the remainder were manganoan ankerite. The calcium carbonate crystals contain as much as 11% $SrCO_3$ and occur either as inclusions in apatite or within the medium-grained carbonate groundmass. The strontium content of this calcium carbonate is much higher than that reported for other magmatic calcium carbonates. Strontianite is present both as a vein-filling mineral and in the carbonate groundmass.

Carbon and oxygen isotope analyses of the total carbonate present in RO6 and comparative data from the literature are presented in Table B4.3. Sample RO6 has a $\delta^{13}C$ value intermediate between the mean for sedimentary carbonates and the mean for fresh continental carbonatites. The $\delta^{18}O$ value of RO6 is lower than those of the Transvaal sedimentary carbonates and quite close to the measured range for carbonatites.

Discussion

The lack of identification of calcite and the poor fit of strontianite in the XRD spectra can be ascribed to the ubiquitous solid solution of strontium and calcium respectively, which would alter the d-spacing of the mineral and give poor peak matching from the JCPDS database. However, the analytical results leave no doubt that carbonate does exist as a mineral phase in the Pilanesberg Complex.

Table B4.1 Major element analyses for sample RO6 and a comparative sample of sövite from Harmer (1992). Total Fe as Fe_2O_3. *n/r* is not reported. See Table 4.3 for analyses of typical Pilanesberg syenites.

Comp. (wt%)	RO6	Spitskop sövite
SiO_2	10.62	2.51
TiO_2	1.29	0.04
Al_2O_3	2.57	0.07
Fe_2O_3	13.55	2.47
MnO	1.09	0.69
MgO	1.00	2.29
CaO	31.60	50.94
Na_2O	1.28	0.63
K_2O	0.07	0.00
P_2O_5	6.94	1.76
CO_2	13.37	39.32
H_2O^-	0.52	0.01
LOI - CO_2	0.70	*n/r*
SrO	6.22	*n/r*
F	8.05	*n/r*
Subtotal	98.87	100.73
O≡F	3.39	-
TOTAL	95.48	100.73

Table B4.2 Mean analyses of carbonate minerals in sample RO6 (Pilanesberg). All concentrations in wt%. LLD is lower limit of detection, *n/d* is not detected.

Mineral	$CaCO_3$	$FeCO_3$	$MgCO_3$	$MnCO_3$	SiO_2	$SrCO_3$	$BaCO_3$	Total
LLD:	0.01	0.22	0.20	0.20	0.13	0.16	0.14	
Calcium carbonate (n=14)	93.14	0.52	*n/d*	0.66	*n/d*	4.69	*n/d*	99.01
Strontianite (n=3)	12.09	*n/d*	*n/d*	*n/d*	*n/d*	89.99	*n/d*	102.08
Manganoan ankerite (n=3)	54.33	21.29	14.32	8.17	0.89	0.62	*n/d*	99.62

Table B4.3 Bulk carbonate isotopic data for sample RO6, Moepo fluorite mine, Pilanesberg Complex. (a) Recalculated from Schidlowski *et al.* (1983) (b) Recalculated from Hudson (1977) using the PDB-SMOW conversion equation of Friedman and O'Neil (1977) (c) Taylor *et al.* (1967).

sample(s)	$\delta^{13}C_{PDB}$‰	$\delta^{18}O_{SMOW}$‰
Pilanesberg RO6 carbonate	-2.7	+12.1
Transvaal Supergroup (mean) and range[a]	(-0.8) -0.5 to -1.4	(+22.0) +20.0 to +24.9
Average marine limestones (range)[b]	-2.0 to +2.0	+20.6 to +29.3
Carbonatites (range)[c]	-4 to -8	+6 to +10

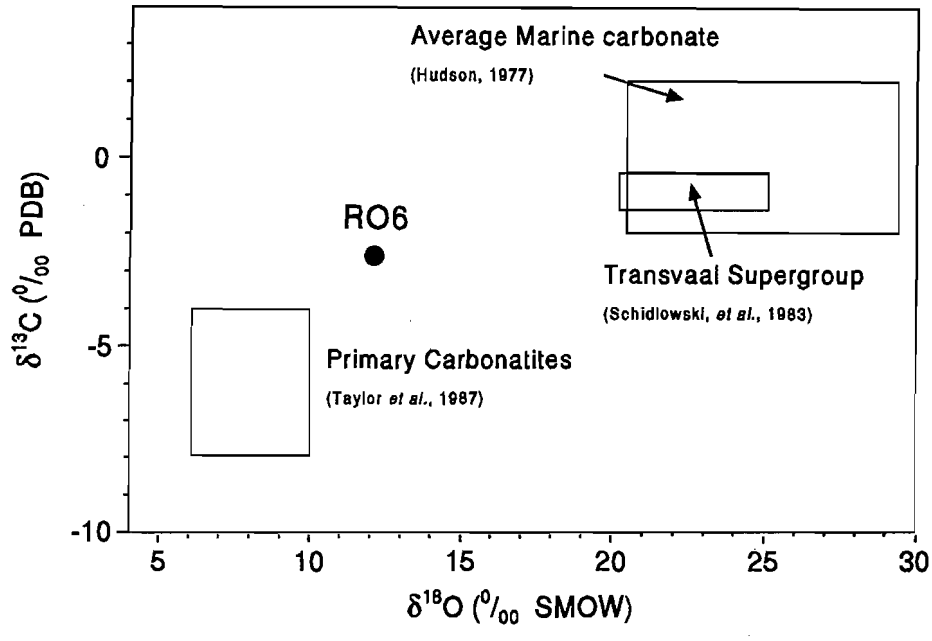

Figure B4.2 Oxygen and carbon isotope values of magmatic carbonate and marine limestone compared to that of sample RO6. Typical values for the Transvaal Supergroup, through which the Pilanesberg is intruded, are also shown.

The high strontium content of the whole-rock and of the calcium carbonate indicate that the carbonate minerals in RO6 are magmatic in origin (Barker, 1993), although the negligible barium concentration is unusual (Barker, D.S., University of Texas, *pers. comm.*). The high strontium to calcium ratio of the minerals and high whole-rock strontium content of RO6 make the Transvaal Group dolomites an unlikely source. The mineral assemblage in RO6 is similar to that for late stage, low temperature and hydrothermally altered carbonatites (Barker, 1989). The $\delta^{13}C$ value of carbonate in RO6, which is just outside the range for fresh continental carbonatites (Taylor *et al.*, 1967), may be interpreted as having a large mantle component (Figure B4.2), modified by late-stage fluids (Suwa *et al.*, 1975).

The $\delta^{18}O$ value of the carbonate in RO6 of 12.1‰ is consistent with precipitation from magmatic fluids at elevated temperatures. At 500°C the fractionation factor (Δ) between calcite and water is 1.8‰ (O'Neil *et al.*, 1969), which would be consistent with a fluid with a $\delta^{18}O$ value of 10.3‰. However, ambient meteoric water in the Johannesburg area has a $\delta^{18}O$ of around -6‰ (NPRL, 1984) and calcite with a value of 12.1‰ would have precipitated from such a fluid at about 90°C (calculated from the

equation for $\Delta_{calcite\text{-}water}$ of O'Neil *et al.*, 1969):

$$\Delta_{calcite\text{-}water} \approx 10^3 \ln\alpha = 2.78 \cdot 10^6 T^{-2} - 2.89 \quad (1)$$

As a temperature of 90°C seems too high for precipitation from groundwater, a late-stage magmatic origin modified by a hydrothermal system remains the most likely possibility.

Dawson and Fuge (1980) reported on halogen concentrations in primary, unweathered carbonatites from Africa. They reported a wide range of F and Cl concentrations and F/Cl ratios. The carbonatite with the closest halogen composition to RO6, from samples collected from all over Africa, interestingly comes from the Goudini carbonatite, located less than 100 km to the west of the Pilanesberg. The carbonatitic lavas of Oldoinyo Lengai in Tanzania also have F above 1 wt%, but these lavas are extremely rich in Cl, up to 3.6 wt%.

The occurrence of RO6 at a fluorite rich location is of interest as several other fluorite prospects exist in the Pilanesberg (J. Lurie, *pers. comm.*, 1991) and it is possible that carbonate may also exist at these locations. Carbonatites are associated with fluorite deposits at other undersaturated igneous complexes in southern Africa, for instance Okorusu in Namibia (Prins, 1981). Large amounts of carbonate in the Pilanesberg would have important hydrogeochemical and groundwater dating implications (McCaffrey, 1993), because the dissolution of essentially ^{14}C-free carbonate would dilute the ^{14}C content of modern groundwater and would result in an overestimate of residence time below ground. However, the abundance, and therefore importance, of carbonate in the Pilanesberg cannot be properly estimated until further investigations have taken place.

Appendix C. Whole rock major element analyses. Concentrations are in weight %, apart from F which is in parts per million. '*n/a*' is not available. (N) is Nebo Granite, (L) is Lebowa Granite. The total for RO6 include 6.22 wt% SrO.

No.	Site Name	Rock Type	SiO_2	TiO_2	Al_2O_3	Fe_2O_3	MnO	MgO	CaO	Na_2O	K_2O	P_2O_5	H_2O-	LOI	F	Total
RO1	Bapong	Quartzite	96.85	0.06	0.17	1.15	0.01	0.01	0.14	0.02	0.06	0.10	0.07	0.10	*n/d*	98.7
RO2	Moreteletsi	Monzonite	60.86	0.42	15.05	9.69	0.16	5.88	7.28	1.07	0.28	0.09	0.10	*n/d*	216	100.9
RO3	Green Tweed	Syenite	58.44	1.09	17.17	5.42	0.31	0.73	1.37	8.28	5.52	0.10	0.25	1.36	5310	100.6
RO4	Thabayadiotsa	Syenite	47.76	0.77	15.79	6.25	0.80	0.44	7.03	8.9	5.06	0.06	0.18	4.35	16431	99.0
RO5	Kubu drive Quarry	Syenite	57.31	0.22	16.72	10.38	0.47	0.10	1.15	6.08	4.59	0.04	0.64	1.36	6958	99.8
RO6	Moepo	Fluorite ore	10.67	1.29	2.57	13.55	1.09	1.00	31.60	1.28	0.07	6.94	0.52	14.07	80514	98.9
RO7	N of Pilanesberg	Norite	53.34	0.15	18.58	7.55	0.15	6.91	11.79	2.67	0.22	*n/d*	0.05	0.11	183	101.5
RO8	Mabeleapodi	Alkali granite	59.16	1.06	14.03	8.64	0.56	0.70	1.95	2.8	7.76	0.10	0.67	1.33	1061	98.9
RO9	Lesung	Norite	52.43	0.22	17.24	7.65	0.16	7.45	13.10	2.38	0.23	0.01	0.08	0.08	153	101.0
RO10	Lesung	Magnetite ore	1.53	14.22	4.10	78.87	0.20	0.07	0.03	*n/d*	0.03	*n/d*	0.34	1.18	*n/d*	100.6
RO11	Modike	Alkali granite (N)	73.88	0.18	12.25	3.33	0.04	0.07	0.62	3.33	5.54	0.04	0.18	0.36	489	99.9
RO12	Suncity-Lesung	Norite	51.99	0.18	18.74	7.37	0.14	6.92	12.93	2.4	0.18	*n/d*	0.12	0.06	221	101.1
RO13	Smaldale Farm	Dolomitic limestone	9.09	*n/d*	0.08	0.75	0.27	19.09	27.65	*n/d*	0.01	*n/d*	0.17	42.38	400	99.5
RO14	Tamboetieshoek	Ironstone	31.91	0.22	4.83	57.46	2.66	0.21	0.91	*n/d*	0.08	0.5	0.13	1.07	168	100.0
RO15	Dwarsberg	Sandstone	94.69	0.10	2.16	1.29	0.01	0.04	0.03	0.08	0.54	*n/d*	0.11	0.49	*n/d*	99.5
RO16	Rampapaanspoort	Norite	53.12	0.32	10.62	11.30	0.18	16.13	7.11	1.65	0.41	0.05	0.05	*n/d*	205	101.0
RO17	Holfontein	Garnet-biotite hornfels	61.26	0.86	17.98	10.54	0.12	3.59	0.78	1.74	2.88	0.07	0.09	0.63	774	100.6
RO18	Leboaneng	Ironstone	42.98	0.01	0.11	55.58	0.06	*n/d*	0.04	*n/d*	0.03	0.04	0.13	1.39	*n/d*	100.4
RO19	GaRamoloreng-	Dolomite	0.32	0.01	0.13	1.96	0.87	19.47	30.16	*n/d*	*n/d*	0.13	0.15	45.39	509	98.6
RO20	Makoropeja	Granite (L)	76.21	0.12	11.85	3.43	0.02	0.14	0.24	5.27	1.92	0.07	0.22	0.94	163	100.4

No.	Site Name	Rock Type	SiO_2	TiO_2	Al_2O_3	Fe_2O_3	MnO	MgO	CaO	Na_2O	K_2O	P_2O_5	H_2O-	LOI	F	Total
RO21	Northblock 7	Granite (L)	74.78	0.13	11.91	2.85	0.02	0.03	0.45	3.43	5.78	*n/d*	0.14	0.62	2849	100.4
RO22	Northblock 10	Granite (L)	74.6	0.16	12.33	3.01	0.01	0.2	0.34	3.52	5.34	*n/d*	0.40	0.57	1924	100.7
RO23	Slipfontein	Quartz pegmatite	98.49	*n/d*	0.04	1.19	0.01	*n/d*	*n/d*	0.05	0.01	*n/d*	0.06	*n/d*	*n/d*	99.9
RO24	Kwarriekraal	Granophyre					0.02	0.06	0.34	3.25	6.76	0.02			950	
RO25	Kenkelbos	Alkali granite (L)	75.32	0.17	11.45	3.33	0.02	0.09	0.81	3.59	4.31	*n/d*	0.24	1.07	2527	100.7
RO26	Blokspruit	Alkali granite (L)	77.58	0.40	4.38	12.95	0.21	0.26	0.14	0.03	1.46	0.03	0.33	0.56	1260	98.5
RO27	Blokspruit	Alkali granite (L)	76.58	0.06	12.00	1.59	0.01	0.08	0.49	2.92	6.00	*n/d*	0.33	0.56	3351	101.0
RO28	Borakalalo	Sandstone	89.23	0.17	6.17	1.08	0.01	0.19	0.03	0.05	1.93	0.02	0.21	0.78	735	99.9
RO29	Sephai	Limestone	6.02	0.05	0.74	0.42	0.03	2.84	47.87	*n/d*	0.08	*n/d*	1.52	39.79	858	99.4
RO30	GaTsogwe	Granite (N)	75.81	0.21	11.35	3.29	0.04	0.10	0.72	3.49	4.95	0.02	0.16	0.32	480	100.5
RO31	Rashoop	Granophyre	74.99	0.22	11.56	3.77	0.04	0.19	0.11	2.91	4.99	0.01	0.48	0.80	127	100.1
RO32	Mpatsetlha	Sandstone	95.76	0.05	1.68	1.34	0.01	0.05	0.03	0.04	0.54	0.01	0.11	0.19	119	99.8
RO33	Mpatsetlha	Mudstone	59.27	0.57	11.99	4.43	0.16	1.55	15.15	1.62	4.29	0.12	0.18	0.81	464	100.2
RO34	Leeupoort Tin	Felsite	73.40	0.48	13.05	2.15	0.04	0.88	0.61	5.44	2.06	0.04	0.18	1.48	2171	100.0
RO35	Tooyspruit	Feldspathic sandstone	89.97	0.05	4.58	0.77	0.01	0.12	0.04	0.10	3.99	0.02	0.17	0.05	373	99.9
RO36	Kwaggafontein	Greenschist	65.81	0.38	10.70	7.48	0.07	5.52	4.55	1.79	2.01	0.08	0.22	1.55	4981	100.7
RO37	Rietfontein	Alkali granite (N)	75.78	0.21	12.19	1.54	0.01	0.05	0.38	3.88	5.62	0.02	0.29	0.39	2570	100.6
RO38	Rietfontein	Alkali granite (N)	73.89	0.19	12.19	3.09	0.04	0.09	0.94	4.01	5.30	0.01	0.09	0.28	2284	100.3
RO39	Sutelong	Quartzite	96.77	0.06	0.88	1.10	0.01	0.01	0.10	0.40	0.37	*n/d*	0.08	0.10	132	99.9
RO40	Dikebu	Granite (L)	76.45	0.20	12.36	1.35	0.01	0.05	0.15	3.56	5.83	0.01	0.23	0.46	520	100.7
RO41	Pretoria Saltpan	Granite (N)	74.15	0.26	12.37	2.25	0.02	0.11	0.19	2.53	6.57	0.01	0.31	1.08	410	99.9
RO42	Pretoria Saltpan	Granite (N)	73.99	0.22	12.05	3.58	0.05	0.13	0.78	3.56	5.30	0.03	0.11	0.48	437	100.3

Appendix D: Analyses of groundwaters

Appendix D1. Major ion analyses of groundwaters. Concentrations in mg/ℓ. Abbreviations: "TDS" = total dissolved solids; "T.alk" = total alkalinity, in mg/ℓ $CaCO_3$. Site i.d. is derived from the 1:50 000 map reference, followed by a sequential number, stating at 10001.

Site id	Site no., name, description	pH	TDS	Ca^{2+}	Mg^{2+}	K^+	Na^+	NO_3^-	Cl^-	F^-	SO_4^{2-}	T.Alk
2526BD10001	1: Bapong, self help garden	6.80	108	8	20	0.7	2	2	1	0.4	4.0	96
2526BD10002	2: Bapong, southern end	6.29	268	31	99	1.5	9	195	35	0.07	6.0	49
2526BD10003	3: Bapong, northern end	5.34	120	11	33	1.4	4	9	6	0.03	4.0	85
2526BB10001	7: Mabeeskraal, middle of village	7.00	82	9	8	1.5	9	2	2	0.03	4.0	66
2526BB10002	8: Mabeeskraal, Marula Park	7.39	270	31	44	2.3	14	50	8	0.04	7.0	168
2526BB10003	9: Mabeeskraal, Mami's house, zone 4	7.15	183	19	23	1.7	17	15	4	0.04	5.0	131
2526BD10004	10: Maologane	7.31	540	74	38	1.8	125	53	99	3.02	14.3	259
2526BD10005	11: Maologane, Joyce's yard	6.93	901	138	50	8.2	204	140	152	2.97	27.6	409
2526BD10006	12: Maologane, Private Yard	9.09	2300	2	2	18.6	1205	2	748	35.3	103.8	775
2526BD10007	13: Maologane, Private yard	6.77	991	87	49	6.0	218	147	256	3.55	39.8	329
2526BD10008	14: Maologane, private yard	6.86	1440	288	111	4.8	289	91	601	1.75	67.0	342
2526BD10009	15: Maologane, Private yard	7.33	*n/a*	1	1	6.9	380	0	72	33.6	18.6	451
2526BD10010	16: Maologane, Dikeme middle school	7.35	612	66	39	1.8	172	17	107	2.72	31.2	354
2526BB10004	17: Raborife, Mr Raborife's yard	6.78	878	31	670	0.4	3	230	114	5.39	66.6	348
2526BB10005	18: Raborife, private	7.47	891	31	652	2.0	4	306	132	0.03	61.0	312
2526BB10006	19: Mmorogong (Tlhatlhaganyane)	7.26	411	60	85	0.7	52	19	7	3.51	3.7	318

Site id	Site no., name, description	pH	TDS	Ca^{2+}	Mg^{2+}	K^{+}	Na^{+}	NO_3^-	Cl^-	F^-	SO_4^{2-}	T.Alk
2526BB10007	20: Mmorogong, Christoff's yard	7.31	411	67	80	0.5	59	21	11	3.3	22.7	323
2526BB10008	21: Mmorogong, Tapson's yard	7.24	417	51	75	0.7	58	8	7	3.07	20.5	311
2526BB10009	22: Mmorogong, Johanna's yard	7.09	789	89	44	0.4	258	81	136	3.84	49.2	384
2526BB10010	23: Mmorogong, Witness' yard	7.35	409	73	69	0.6	53	18	8	2.39	4.7	305
2526BB10011	24: Mmorogong, animal gear	7.14	444	61	30	0.0	83	12	12	2.99	7.2	311
2526BB10012	25: Mmorogong, owner absent	7.02	361	75	22	0.5	65	18	8	2.98	22.6	256
2526BB10013	26: Mmorogong, Joseph's yard	7.14	324	51	19	0.0	60	6	11	3.68	4.9	219
2526BB10014	27: Mmorogong, Mthembu's yard	7.15	321	50	18	0.0	51	18	8	3.54	9.7	213
2526BB10015	28: Mmorogong, Sekgwelea's yard	7.10	342	10	2	0.0	8	8	6	3.62	4.7	262
2526BB10016	29: Mmorogong, Master's yard	7.05	373	70	20	0.0	66	1	7	3.2	23.3	274
2526BB10017	30: Mmorogong, Public H/P	7.06	381	72	21	0.6	62	13	26	3.18	12.2	244
2526BB10018	31: Tlhatlhaganyane, Animal gear east	6.95	461	83	74	0.8	49	6	6	4.02	5.7	342
2526BB10019	32: Tlhatlhaganyane	7.38	550	21	265	1.4	8	87	13	0.33	33.2	342
2526BB10020	33: Tlhatlhaganyane	7.20	429	23	172	0.6	5	2	8	0.2	4.8	359
2526BB10021	34: Tlhatlhaganyane, Early learning C	9.75	1060	1	3	5.6	504	16	290	58.4	98.8	360
2527AC10001	35: Ledig, Lena's yard	7.59	253	36	18	2.3	46	28	7	1.93	2.9	146
2527AC10002	36: Ledig, Lydia's yard	7.52	252	11	4	1.5	60	8	22	2.05	4.3	85
2527AC10003	37: Ledig, Pilanesberg seepage spring	7.63	135	60	8	7.6	80	98	50	1.63	10.1	158
2527AC10004	38: Ledig, Esky's yard	7.12	369	46	17	3.0	35	17	6	0.95	2.6	158

Site id	Site no., name, description	pH	TDS	Ca^{2+}	Mg^{2+}	K^{+}	Na^{+}	NO_3^{-}	Cl^{-}	F^{-}	SO_4^{2-}	T.Alk
2527AC10005	39: Ledig, public	7.29	231	26	5	3.2	71	2	8	2.93	4.6	158
2527AC10006	40: Ledig, Nicholas's yard	6.94	235	30	17	2.5	76	14	8	3.68	2.8	207
2527AC10007	41: Ledig, Joan's yard	7.24	298	15	4	1.8	57	17	9	1.7	6.5	91
2527AC10008	42: Ledig, Phineas's yard	7.20	176	28	5	1.9	66	44	18	1.55	7.6	128
2527AC10009	43: Ledig, Jacob's yard	7.02	249	14	2	3.5	56	1	7	1.54	2.9	122
2527AC10010	44: Ledig, Alexander's yard	7.28	179	15	5	3.3	46	5	6	1.92	3.2	109
2527AC10011	45: Ledig, Zulu section	7.30	156	9	2	2.1	53	4	5	2.26	2.5	109
2527AC10012	46: Ledig, public	7.05	169	26	6	1.1	31	4	6	0.38	5.1	128
2527AC10013	47: Ledig, Onika's yard	6.84	174	11	3	2.3	41	7	5	0.55	3.3	103
2527AC10014	48: Ledig, Katherine's yard	7.12	148	22	5	3.1	57	62	21	2.84	5.4	115
2527AC10015	49: Ledig, Moses' yard	7.16	234	16	4	1.2	38	16	7	1.37	3.1	109
2527AC10016	50: Ledig, Dorothy's yard	7.05	177	40	16	1.1	30	36	18	2.39	10.7	103
2526BB10022	51: Makoshong, northern	7.27	231	21	34	0.7	9	29	6	0.28	7.3	207
2526BB10023	52: Makoshong	7.29	415	38	48	0.8	13	45	30	0.32	16.6	237
2526BB10024	53: Makoshong, next to shop	7.44	285	13	23	0.2	7	13	9	0.35	8.3	189
2526BB10025	54: Makoshong	7.63	192	14	26	0.8	15	21	3	0.24	5.5	128
2526BD10011	55: Mahobieskraal	6.87	48	6	7	0.8	2	1	2	0.08	0.5	33
2526BD10012	56: Mahobieskraal, vegetable garden	7.59	131	16	18	1.5	10	2	3	0.11	2.3	97
2526BB10026	57: Motlhabe, south east	8.14	495	22	143	1.2	27	24	10	0.73	9.2	342

Site id	Site no., name, description	pH	TDS	Ca^{2+}	Mg^{2+}	K^{+}	Na^{+}	NO_3^{-}	Cl^{-}	F^{-}	SO_4^{2-}	T.Alk
2526BB10027	58: Motlhabe	7.28	515	3	114	1.6	22	79	27	0.24	16.6	280
2526BB10028	59: Motlhabe	7.13	384	52	79	3.5	15	129	24	0.12	19.1	178
2526BB10029	60: Motlhabe	7.09	196	39	15	1.6	15	20	10	0.15	8.4	122
2526BB10030	61: Motlhabe	7.78	470	33	118	2.1	13	26	13	0.11	6.7	329
2526BB10031	62: Ntswana le Metsing	7.72	581	10	171	0.3	14	25	18	0.18	9.8	408
2526BB10032	63: Motlhabe	7.60	542	0	165	0.3	15	32	8	0.14	24.9	408
2427CC10001	64: Sefikile	7.53	571	88	53	1.4	78	32	78	0.23	30.0	329
2526BB10033	65: Makgope Mine	7.82	520	3	145	0.0	12	7	10	0.13	2.1	402
2526BB10034	66: Makgope mine, domestic supply	7.81	499	4	174	0.5	13	10	6	0.16	2.6	360
2526BB10035	67: Witkleifontein grazing	7.71	478	14	155	0.6	18	29	23	0.34	*n/a*	364
2527AC10017	69: Southeast of Pilanesberg	6.90	248	17	8	0.9	23	2	4	1.93	0.8	73
2527AC10018	70: Southeast of Pilanesberg	7.22	135	53	53	0.8	29	6	7	0.15	9.6	250
2427CC10002	71: Sefikile	6.72	382	11	47	3.1	29	6	26	0.19	22.7	244
2527AA10001	72: Sefikile	6.79	505	423	308	0.0	423	34	50	0.81	32.7	299
2427CC10003	73: Tsweneng, south	7.15	396	60	60	0.8	14	1	0	0.26	0.0	292
2527AA10002	74: Leswaaneng spring	10.36	2010	15	7	25.1	1038	1	928	69.4	167.2	262
2527AA10003	75: Salty spring	10.41	1860	4	2	24.0	870	1	803	67	148.3	286
2527AA10004	76: Lesetlheng, outside chief's house	7.88	356	36	5	3.7	96	45	24	4.77	3.4	195
2527AA10005	77: Ramatshaba	7.63	524	336	197	0.4	511	111	58	2.82	37.0	262

Site id	Site no., name, description	pH	TDS	Ca^{2+}	Mg^{2+}	K^{+}	Na^{+}	NO_3^{-}	Cl^{-}	F^{-}	SO_4^{2-}	T.Alk
2527AA10006	78: Ramatshaba	7.52	366	26	13	3.8	94	99	28	3.71	1.2	238
2527AA10007	79: Ramatshaba	8.88	219	5	2	1.1	83	0	96	3.85	9.6	49
2527AA10008	80: Ramatshaba	7.66	604	71	56	2.6	153	108	28	0.81	71.2	323
2527AA10009	81: north of Pilanesberg	7.44	404	26	39	1.5	81	32	7	1.45	15.7	268
2527AA10010	82: north of Pilanesberg	7.99	186	37	12	1.7	13	16	6	0.52	2.0	128
2527AA10011	83: north of Pilanesberg	8.78	305	17	3	1.5	93	0	162	0.83	30.9	43
2527AC10019	84: Chaneng, next to Agricor	7.36	337	0	88	2.7	87	32	6	0.17	9.0	384
2527AC10020	87: Robega A (Boshkoppie farm)	7.29	530	15	2	3.2	9	10	10	2.23	22.6	64
2527AD10001	88: Tsitsing	7.07	261	40	13	1.5	90	0	61	5.8	3.9	250
2527AD10004	92: Tsitsing	7.22	532	7	1	4.7	14	0	3	5.51	1.8	37
2527CB10001	93: KwaSeretube	7.23	605	1632	693	121.5	134	5459	1460	0.09	1745	268
2527CB10002	94: KwaSeretube	7.35	474	31	38	0.1	5	7	3	0.06	3.6	158
2527CB10003	95: Bospoort Dam	10.50	419	88	53	1.4	78	32	78	0.23	30.0	329
2527CB10005	97: Swartkoppies, Mev Engelbrechts fa	7.40	456	26	43	0.7	6	27	3	0.05	2.5	140
2527CB10006	98: Tlapa, grazing lands	7.35	456	31	48	0.4	7	19	3	0.04	3.8	238
2527CB10007	99: Tlapa, grazing lands	7.39	423	129	63	1.1	30	21	8	0.04	9.6	244
2527CB10008	100: Tlapa, arable field	7.46	642	138	91	0.0	48	164	74	0.1	91.7	305
2527CB10010	102: Tlapa	7.11	460	31	6	1.8	70	0	36	5.37	9.6	152
2527CB10011	103: Maumong	7.44	833	79	41	0.7	63	30	47	0.2	54.1	232

Site id	Site no., name, description	pH	TDS	Ca^{2+}	Mg^{2+}	K^{+}	Na^{+}	NO_3^{-}	Cl^{-}	F^{-}	SO_4^{2-}	T.Alk
2527CB10012	104: Lekgalong	7.42	233	21	3	1.6	50	0	31	9.1	24.8	73
2527CB10013	105: Rankelanyane	7.48	537	30	4	0.7	25	3	4	0.91	2.4	104
2527CB10014	106: Lekjaneng	7.52	329	43	9	0.8	54	7	28	3	7.0	170
2527CB10015	107: Malejaneng	7.42	392	40	30	1.3	36	53	16	0.57	32.4	195
2527CB10016	108: Thekwane, kraal	7.37	348	70	32	1.0	45	0	68	0.5	66.1	195
2527DA10001	109: Bapong oustad	6.79	5530	84	72	9.2	155	2	271	0.22	385.1	49
2527DA10002	110: Bapong, roberts yard	7.58	192	85	60	0.0	59	30	24	2.82	2.8	85
2527DA10003	111: Bapong	7.53	571	60	13	1.5	32	5	6	1.63	6.6	158
2527DA10005	113: Bapong, Legalawong sub village	7.50	159	162	67	1.8	87	580	219	0.15	77.4	104
2527DA10006	114: Modderspruit	7.41	208	94	53	12.8	113	3	142	0.46	343.7	152
2527DA10007	115: Modderspruit	7.38	216	81	49	0.2	32	112	30	0.15	13.6	232
2527DA10008	116: Seqwelane	7.22	561	63	61	0.7	43	227	51	0.1	38.8	232
2527DA10009	117: Makolokwe, western end	7.12	649	69	99	0.6	24	189	62	0.09	73.0	195
2527DA10010	118: Bethanie farm	7.13	197	105	80	0.1	32	242	81	0.08	137.8	274
2527DA10011	119: Bethanie cattle post	7.66	237	88	54	0.1	38	66	41	0.09	41.1	256
2527BC10001	120: Wilgevonden east cattle post	7.50	195	21	12	3.8	23	14	5	0.93	1.5	85
2527DA10012	121: Bethanie, south east	7.23	421	130	77	0.5	77	103	109	0.11	289.6	262
2527DA10013	122: Bethanie, outside church	8.29	186	72	61	0.1	23	8	81	0.1	154.6	287
2527DA10014	123: Waaikraal farm	6.94	148	118	107	1.1	75	257	177	0.2	392.6	268

Site id	Site no., name, description	pH	TDS	Ca^{2+}	Mg^{2+}	K^{+}	Na^{+}	NO_3^{-}	Cl^{-}	F^{-}	SO_4^{2-}	T.Alk
2527DA10015	124: Modikwe	7.38	237	147	125	0.0	23	38	70	0.13	160.0	280
2527DA10016	125: Modikwe, south	6.95	350	82	64	0.0	54	2	86	0.12	147.7	216
2527DA10017	126: Modikwe	7.18	421	72	90	0.0	130	182	179	0.14	521.2	250
2527DA10018	127: Gwatlhe River	9.69	747	37	9	1.9	22	0	17	0.66	3.3	116
2527DA10019	128: Modikwe, school	6.95	178	30	7	1.4	22	37	9	0.85	2.3	79
2527DA10020	130: Modikwe, west	7.27	237	11	4	3.3	23	0	4	1.57	1.1	79
2527DA10021	131: Berseba	6.97	343	34	8	2.2	71	49	38	1.94	12.7	91
2527DA10022	132: Bethanie	6.50	875	77	18	2.1	51	197	95	0.24	4.3	91
2527DA10023	133: Krokodile Riv, Hartebeespoort fm	7.76	644	14	10	2.3	46	11	3	0.15	2.5	122
2527BD10001	134: Maboloka, Bafokeng section	7.32	351	45	9	1.8	25	1	5	1.94	3.6	140
2527BD10002	135: Maboloka, Taung section	7.12	255	11	2	1.7	14	5	4	0.55	0.3	61
2527BD10003	136: Maboloka, Solomon middle school	7.30	341	62	5	1.9	24	122	29	1	3.0	67
2527BD10004	137: Maboloka, Phuthanang Primry schl	6.72	180	26	3	2.2	18	74	17	0.27	1.8	128
2527BD10005	138: Maboloka grazing	7.10	469	33	16	6.3	335	17	378	0.38	41.1	225
2527BD10006	139: Maboloka, Tumo primary school	6.87	350	55	12	2.2	52	0	42	0.97	9.6	171
2527BD10007	140: Maboloka	6.73	374	287	59	9.0	222	14	754	0.43	20.6	262
2527BD10008	141: Letlhakaneng	6.81	258	62	14	4.9	262	1	224	0.95	57.6	292
2527BD10009	142: Letlhakaneng	7.28	723	43	15	3.0	101	9	63	0.79	48.6	189
2527BD10010	143: Letlhakaneng	7.20	964	105	26	5.2	247	106	143	0.79	60.1	354

Site id	Site no., name, description	pH	TDS	Ca^{2+}	Mg^{2+}	K^{+}	Na^{+}	NO_3^{-}	Cl^{-}	F^{-}	SO_4^{2-}	T.Alk
2527BD10012	145: Rietgat grazing	6.90	378	114	28	7.3	197	15	318	0.57	22.9	244
2527BD10013	146: Rietgat grazing	7.34	274	43	11	3.7	49	20	48	0.63	43.8	231
2527BD10014	147: Waterval grazing	6.79	134	32	10	4.8	317	0	362	5.72	50.4	183
2527BD10015	148: Waterval grazing	6.83	177	241	60	11.0	343	3	970	0.6	37.2	171
2527BD10016	149: Waterval (Tsogwe)	6.37	147	35	12	18.6	102	14	68	0.62	64.2	213
2527BD10017	150: Tsogwe	6.54	232	149	79	12.2	177	2	162	0.41	14.8	281
2527BD10018	151: Tsogwe, Tsogwe School	6.00	147	30	56	12.2	249	8	275	0.09	40.3	274
2527BD10019	152: Kgomokgomo (Rooiwal)	7.71	854	90	43	7.5	137	0	46	0.44	19.9	341
2527BD10020	153: Kgomokgomo	7.31	302	97	69	8.3	138	0	141	0.36	10.7	207
2527BD10021	154: Legonyane	7.02	1370	81	50	3.3	110	41	64	0.76	47.7	189
2527BD10022	155: Legonyane	7.65	805	82	34	4.7	76	15	68	0.81	38.5	213
2527BD10023	156: Legonyane, outskirts	7.68	399	71	71	3.7	110	36	83	0.55	50.7	244
2527BD10024	157: Leganyane, lethabong primary scl	7.17	785	14	6	0.0	610	0	357	8.42	29.1	244
2527BD10025	158: Legonyane	7.22	460	106	37	14.8	369	0	242	5.19	29.0	250
2527BD10026	159: Legonyane	7.46	827	86	68	27.8	260	1	331	0.5	44.6	256
2527BD10027	162: Jericho	7.42	359	11	47	12.4	243	0	69	0.44	58.8	488
2527BD10028	163: Madinyane, Ramogatla	7.64	831	53	26	14.3	463	38	97	0.7	69.2	402
2527BD10029	164: Madinyane	7.12	1710	67	136	61.6	793	93	280	0.73	150.0	305
2527BB10003	166: Bultfontein grazing	7.52	1100	13	6	1.2	35	0	5	6.26	9.5	79

Site id	Site no., name, description	pH	TDS	Ca^{2+}	Mg^{2+}	K^{+}	Na^{+}	NO_3^-	Cl^-	F^-	SO_4^{2-}	T.Alk
2527BB10004	167: Jonathan, next to cemetary	7.21	1100	19	4	1.8	20	0	4	4.26	2.6	61
2527BB10005	168: GaHabedi grazing	7.73	588	32	6	2.8	21	0	2	4.91	4.3	85
2527BB10006	169: Zoutpansleegte grazing	7.01	650	15	9	2.3	68	0	17	7.95	11.5	122
2527BB10007	170: GaHabedi	6.84	313	33	6	3.5	55	1	17	4.76	5.2	122
2527BB10008	171: Sephai grazing	7.23	454	29	26	8.2	135	0	21	4.81	4.5	213
2527BB10009	172: Sephai	7.15	514	37	5	2.0	39	0	8	4.88	3.9	164
2527BB10010	173: Sephai	7.35	552	46	6	1.7	49	0	9	4.17	4.9	226
2527BB10011	174: Sephai	6.83	386	61	18	7.2	153	1	110	4.88	20.0	122
2527DB10001	175: Mmakau, Tshwara section	7.31	422	41	47	3.8	37	2	12	0.26	2.6	244
2527DB10002	176: Tshwara	7.30	573	172	122	16.2	223	12	563	0.53	282.2	378
2527DB10003	177: Mmakau, Mongopeng section	7.16	529	33	57	8.6	106	12	92	0.96	32.8	500
2527DB10004	178: Mmakau, Polonia Section	7.31	639	14	4	2.3	11	27	5	0.09	0.0	49
2527DB10005	179: Mmakau	7.24	459	13	5	3.3	14	41	5	0.06	0.0	43
2527DB10006	180: Mmakau, Tetele subvillage	7.39	674	33	10	2.9	308	0	301	6.08	111.8	189
2527DB10007	181: Mmakau, Switch subvillage	7.28	565	87	36	1.0	29	52	14	0.14	9.3	205
2527DB10008	182: Mothuthlung	7.31	904	139	22	4.7	83	3	63	2.04	15.1	183
2527DB10009	183: Mothuthlung, Switch subvillage	7.23	572	37	9	4.6	36	0	30	1.17	11.9	97
2527DB10010	184: btwn Rankotia and Ntswaphelong	7.61	527	7	3	2.8	315	0	54	17.8	27.6	317
2527DB10011	185: Vametco mine	7.26	920	14	12	7.1	49	6461	24	0.98	2.2	299

Site id	Site no., name, description	pH	TDS	Ca^{2+}	Mg^{2+}	K^{+}	Na^{+}	NO_3^{-}	Cl^{-}	F^{-}	SO_4^{2-}	T.Alk
2527DB10012	186: Lerulaneng	7.31	217	88	9	6.1	18	96	33	0.13	1.7	171
2527DB10013	187: Lerulaneng	7.04	153	13	22	3.7	164	0	121	3.01	17.4	268
2527DB10014	188: Lerulaneng	7.13	98	42	17	3.0	32	60	23	2.33	2.6	110
2427DD10001	189: Paarlkraal farm	7.09	138	23	7	1.3	29	1	4	4.22	4.1	85
2427DD10002	190: Paarlkraal grazing	6.69	111	22	4	1.6	22	1	3	4.58	4.9	73
2527BB10012	191: Doornfontein grazing	6.67	132	44	24	3.7	79	96	62	2.18	9.5	134
2527BA10001	192: Doornfontein grazing	6.84	149	45	14	1.4	93	0	66	4.89	4.7	180
2527BB10014	195: Ruigterpoort grazing	6.70	115	26	3	2.0	92	39	55	6.39	9.8	128
2527BB10015	196: Blokspruit grazing	6.83	147	19	3	2.0	21	5	7	2.92	1.9	171
2527BB10016	197: Blokspruit grazing	7.05	204	34	4	1.5	67	0	57	4.65	9.7	171
2527BA10003	198: Die mont van Blokspruit	7.22	145	20	5	1.9	69	104	318	1.08	112.0	420
2527BA10004	199: Die mont van Blokspruit	7.72	290	50	71	3.8	81	79	254	0.96	159.6	277
2527BA10005	200: Kenkelbos	7.00	189	25	26	3.4	149	26	206	2.06	185.9	225
2527BA10006	201: Kwarriekraal	6.66	68	62	164	6.5	209	142	1412	0.61	632.7	308
2527BD10030	202: Tolwane River	8.32	291	57	29	16.7	297	64	163	0.93	94.6	427
2527BD10031	203: Shakung	7.33	591	35	27	3.4	117	276	516	1.55	423.9	274
2527BD10032	204: Shakung	7.25	790	46	15	5.8	32	49	16	0.34	1.3	85
2527BD10033	205: Shakung	7.35	422	120	35	7.6	80	36	17	0.59	3.0	122
2527BD10034	206: Shakung	7.51	486	119	80	0.0	41	110	40	0.11	29.4	341

Site id	Site no., name, description	pH	TDS	Ca^{2+}	Mg^{2+}	K^{+}	Na^{+}	NO_3^{-}	Cl^{-}	F^{-}	SO_4^{2-}	T.Alk
2527BD10035	207: Moiletswane	6.93	400	64	47	0.0	45	35	21	0.06	46.7	274
2527BD10036	208: Moiletswane	7.29	376	3	3	0.7	8	3	156	0.14	107.0	92
2527BD10037	209: Moiletswane	7.00	492	97	68	0.3	36	39	49	0.08	43.0	268
2527BD10038	210: Dipompong	8.54	769	70	58	0.3	42	151	20	0.06	39.4	226
2527BD10039	211: Dipompong	7.35	644	64	62	0.0	27	0	12	0.08	13.0	311
2527BD10040	212: Makgabetlwane	7.25	837	122	155	5.8	59	186	45	0.06	86.7	403
2527BD10041	213: Makgabetlwane	7.19	660	58	70	1.0	42	23	20	0.09	0.0	317
2527BD10042	214: Rabosula, outside Kalkbank Pr.sc	7.39	785	101	89	0.0	49	281	150	0.08	63.5	262
2527BD10043	215: Rabosula	7.19	951	40	24	0.0	22	14	11	0.06	15.1	134
2527BD10044	216: Rabosula	7.39	850	101	70	0.0	46	85	30	0.06	35.7	305
2527BD10045	217: Botshabelo (Vyeboschlaagte no.1)	7.06	1530	74	44	0.0	27	99	29	0.07	52.4	250
2528AC10001	218: Klippan	7.39	356	152	170	28.4	317	1	1000	1.52	20.3	342
2527BD10046	219: Winterveld	6.72	171	95	53	0.0	22	30	7	0.14	*n/a*	311
2527BD10047	220: Winterveld	6.73	216	54	56	0.1	26	1	7	0.12	9.1	268
2528AC10003	222: Winterveld, Matlwareng primary s	6.84	245	57	90	20.5	230	1	273	2.11	1.6	329
2527DB10015	223: Kgabaletsane	7.88	212	36	14	1.6	45	0	5	3	3.0	183
2527DB10016	224: Kgabaletsane	7.23	403	40	54	6.0	35	56	31	0.17	8.2	305
2527DB10017	225: Kgabaletsane	7.19	95	67	36	3.1	37	2	16	0.17	3.8	305
2528CA10001	226: Hebron	10.36	227	*n/a*	*n/a*	*n/a*	*n/a*	*n/a*	*n/a*	8.24	*n/a*	128

Site id	Site no., name, description	pH	TDS	Ca^{2+}	Mg^{2+}	K^{+}	Na^{+}	NO_3^{-}	Cl^{-}	F^{-}	SO_4^{2-}	T.Alk
2528CA10002	227: Hebron	7.09	227	26	20	6.9	49	54	33	0.63	64.9	85
2528CA10003	228: Hebron	7.57	136	9	4	9.4	36	*n/a*	*n/a*	0.19	*n/a*	85
2528CA10004	229: Hebron	6.42	145	*n/a*	*n/a*	*n/a*	*n/a*	*n/a*	*n/a*	0.14	*n/a*	30
2527BB10017	232: Tamootielaagte	7.34	192	75	29	1.8	81	19	137	2.45	64.4	144
2527BB10018	233: Tambootielaagte	7.05	248	13	1	6.1	260	0	280	8.82	10.7	114
2527BB10019	234: Tambootielaagte	4.66	169	33	7	2.0	37	4	10	3.4	5.9	114
2427DD10003	236: Waterval	6.90	170	28	9	1.8	54	0	5	4.33	3.4	157
2527BB10021	237: Waterval	7.22	226	13	7	4.1	33	24	15	4.73	6.2	72
2527BB10023	239: Lebitloane	7.13	317	47	5	1.4	34	0	7	2.15	9.1	128
2527BB10024	240: Lebitloane	6.75	335	54	12	2.4	91	16	64	2.07	17.4	170
2528AC10006	242: Stinkwater, Mr Teledi's farm	8.07	527	26	15	5.5	114	28	141	1.94	26.9	187
2528AC10007	243: Stinkwater, next to Namo Prm Scl	6.79	272	56	128	21.4	643	0	803	1.38	386.9	421
2528AC10008	244: Stinkwater	6.81	315	17	24	4.2	190	1	215	2.97	42.4	256
2528AC10009	245: Mogogelo	7.24	560	25	20	4.4	6	57	52	0.11	5.5	91
2528AC10010	246: Dilopye	6.65	277	19	26	3.0	18	26	14	0.14	4.2	152
2528AC10011	247: Suurman	7.35	274	6	53	6.4	164	34	77	0.78	24.0	370
2528AA10001	248: Makekeng (Syferkuil)	7.35	359	12	5	2.6	26	11	15	0.1	0.4	91
2528AC10012	249: Syferkuil	7.07	493	19	44	1.6	95	51	137	0.39	11.8	262
2528AC10013	250: Syferkuil A grazing	7.62	347	13	7	2.4	5	0	4	0.79	0.3	287

Site id	Site no., name, description	pH	TDS	Ca^{2+}	Mg^{2+}	K^{+}	Na^{+}	NO_3^-	Cl^-	F^-	SO_4^{2-}	T.Alk
2528AC10014	251: Syferkuil grazing	6.80	108	26	20	6.9	49	54	33	0.63	64.9	85
2528AC10015	252: Mathiebiestad, Senteng Prm schl	6.86	3350	184	157	33.8	1450	279	1181	3.83	1955.6	433
2528AC10016	253: Mathiebiestad, Lepomo Prm schl	6.31	2940	43	48	21.5	348	36	1465	0.52	1066.1	280
2528AC10017	254: Mathiebiestad, Regodile ELC	7.12	1760	74	180	34.2	452	29	681	2.98	323.4	433
2528AC10018	255: Mathiebiestad, south	6.90	1590	57	100	10.3	415	87	644	4.2	76.8	402
2528AC10019	256: Mathiebiestad	7.32	1170	733	254	39.4	601	8	493	4.76	28.1	262
2528AC10020	257: Mathiebiestad, Ramogoga ELC	7.40	643	39	37	18.0	184	0	104	3.16	28.8	341
2528AC10021	258: Mathiebiestad, Mahobotle Prm sch	6.95	1880	152	170	28.4	317	1	1000	1.52	20.3	342
2528AC10022	259: Mathiebiestad	7.29	960	46	60	19.4	274	47	247	2.48	40.6	390
2528AC10023	260: Mathiebiestad	7.51	1100	57	90	20.5	230	1	273	2.11	1.6	329
2528AA10002	261: Potoane (Goedgewacht)	7.36	1440	184	157	33.8	1450	279	1181	3.83	1955.6	433
2528AA10003	262: Mathiebiestad, Geodgewaagd 2	7.21	646	43	48	21.5	348	36	1465	0.52	1066.1	280
2528AA10004	263: Slagboom grazing	7.56	86	74	180	34.2	452	29	681	2.98	323.4	433
2528AA10005	264: Slagboom	7.11	100	57	100	10.3	415	87	644	4.2	76.8	402
2527BB10025	265: Bollantlokwe	7.53	508	60	10	0.8	36	59	24	0.51	3.4	128
2528AA10006	266: Bedwang grazing	8.19	802	733	254	39.4	601	8	493	4.76	28.1	262
2527BB10026	267: Tholwe	7.94	284	66	17	1.1	66	15	39	0.68	19.5	213
2527BB10027	268: De Grens trust	6.65	107	35	8	2.5	30	43	16	0.35	1.7	98
2527BB10028	269: De Grens private	7.77	251	112	23	3.4	45	4	120	1.07	74.6	183

Site id	Site no., name, description	pH	TDS	Ca^{2+}	Mg^{2+}	K^{+}	Na^{+}	NO_3^-	Cl^-	F^-	SO_4^{2-}	T.Alk
2428DD10001	270: Lefiswane	6.85	94	8	3	5.0	13	27	19	0.08	0.2	92
2428DD10002	271: Lefiso	6.37	81	12	5	3.6	12	34	24	0.07	0.1	24
2428DD10003	272: Lefiso	7.75	200	19	7	2.5	26	6	9	0.07	1.3	134
2528BA10001	275: Rooikoppies grazing	7.16	1890	56	128	21.4	643	0	803	1.38	386.9	421
2528BB10001	276: Ramantsho, primary school	6.66	145	13	7	2.4	5	0	4	0.79	0.3	287
2528BA10002	277: Rooifontein grazing	7.27	711	17	24	4.2	190	1	215	2.97	42.4	256
2528BA10003	278: Semohlase	7.14	240	25	20	4.4	6	57	52	0.11	5.5	91
2428DC10001	279: Semohlase grazing?	7.17	470	69	39	2.4	74	153	40	0.31	34.1	207
2428DC10002	280: Goedviralles	6.95	986	92	106	3.5	103	144	313	0.2	135.6	274
2528BA10004	281: Bultfontein grazing	7.02	238	19	26	3.0	18	26	14	0.14	4.2	152
2528BA10005	282: Bultfontein grazing	7.29	647	6	53	6.4	164	34	77	0.78	24.0	370
2528BA10006	283: Bultfontein grazing	7.32	562	19	44	1.6	95	51	137	0.39	11.8	262
2528AB10001	284: Klippan grazing	7.08	389	39	37	18.0	184	0	104	3.16	28.8	341
2527AA10013	287: Quarantine Camp	10.55	997	6	0	16.9	807	4	481	65.9	246.2	258
2527AA10014	288: Letswaaneng spring auger hole, L	10.33	1950	14	5	3.3	14	7	9	0.44	15.5	53
2527BB10029	291: Jonathan Camp, Borakalalo Park	7.43	476	73	14	3.4	48	65	50	0.55	10.2	158
2527BB10031	292: Makoropeja	8.24	682	47	18	4.0	40	43	41	0.77	10.5	116
2527BB10032	293: Tlolwe Base, Borakalalo	7.38	192	105	26	5.1	169	0	276	1.69	50.8	201
2527BA10007	294: Blokspruit base, Borakalalo	7.54	342	28	11	6.4	44	0	83	0.35	49.3	94

Site id	Site no., name, description	pH	TDS	Ca^{2+}	Mg^{2+}	K^{+}	Na^{+}	NO_3^-	Cl^-	F^-	SO_4^{2-}	T.Alk
2527BB10033	295: Moretele Camp, Borakalalo Park	8.05	576	111	31	6.5	273	33	371	2.04	56.7	288
2527BB10034	298: Bultfontein	6.61	169	67	12	2.8	78	45	81	1.04	16.3	152
2527BB10035	299: Klipvoor Primary school	6.05	78	21	5	1.2	29	0	8	2.41	12.7	176
2527BA10008	300: Slipfontein fluorite mine	6.61	181	35	77	9.6	317	72	360	1.29	182.6	292
2527AC10023	302: Mankwe river at Mankwe bridge	7.87	73	29	5	2.6	22	0	2	5.28	2.1	91
2527AA10015	303: Blinkwater, Pilanesberg	7.49	72	35	5	2.5	41	4	7	3.88	8.0	123
2527AA10016	304: Pilanesberg centre	6.97	196	60	43	1.9	18	238	8	0.73	9.8	274
2526BD10013	306: Pilanesberg, Green Tweed	7.10	263	27	6	2.8	79	27	49	2.97	22.9	142
2527BA10009	307: Nooitgedacht farm	7.02	845	41	74	1.4	168	86	131	1.34	167.0	360
2527BA10010	308: Nooitgedacht, Wolvaardts	7.16	744	28	7	2.5	37	0	30	4.9	0.0	143
2527AB10001	309: Nooitgedacht, cattle	7.25	421	45	16	3.0	51	11	7	2.25	3.6	170
2527BA10011	310: Nooitgedacht, Van niekerk	7.66	545	20	4	1.8	50	5	22	3.11	92.3	173
2527BA10012	311: Nooitgedacht, Eloff's	7.26	2170	45	6	1.8	38	0	22	2.79	8.4	169
2527BA10014	313: Pienaars river, Buffelspoort	8.16	259	85	55	1.3	53	16	9	1.22	20.9	322
2527BA10015	314: Buffelspoort, Fred de la poorts'	7.18	1540	74	18	9.4	379	0	555	4.04	47.3	226
2527BA10016	315: Buffelspoort, Standers	7.22	974	160	57	13.4	156	2	577	2.18	139.3	330
2527BA10017	316: Kwarriekraal	7.25	241	37	10	3.8	171	0	173	4.67	147.7	153
2527BA10018	317: Mooimeisjiesfontein	7.35	326	66	12	3.9	138	16	237	3.38	113.1	209
2527BA10019	318: Slipfontein, fanigalo	7.99	280	49	10	4.4	59	88	46	3.88	11.5	113

Site id	Site no., name, description	pH	TDS	Ca^{2+}	Mg^{2+}	K^{+}	Na^{+}	NO_3^{-}	Cl^{-}	F^{-}	SO_4^{2-}	T.Alk
2427DC10001	319: Mooimeisjiesfontein, spruit	7.54	234	32	6	5.4	16	5	51	0.89	80.4	82
2427DC10002	320: Rietfontein	7.75	804	28	7	2.2	291	1	18	5.62	1.3	350
2427DC10003	321: Weihoek	7.83	517	16	3	2.4	175	0	94	11.2	12.5	143
2427DC10004	322: Driefontein game farm	7.11	457	24	9	1.5	133	4	117	8.99	20.3	143
2427DC10005	323: Koperfontein, Shikari game camp	9.41	504	6	2	3.7	178	0	153	11.6	15.4	131
2427DC10006	324: Driefontein	7.60	225	34	6	1.9	38	0	11	3.98	7.1	120
2427DD10004	325: Hartbeesfontein	6.54	135	13	3	1.4	24	11	11	4.01	2.8	71
2427DD10005	326: Rietdal	7.00	240	17	8	1.3	36	4	15	4.01	10.1	157
2427DD10006	327: Morgenzon	7.38	234	54	5	2.5	22	0	11	3.77	4.6	143
2427DD10007	328: Kromdraai	7.10	175	26	5	0.5	27	19	17	3.36	2.7	82
2427DD10008	329: Kromdraai, plot 142	6.91	558	50	13	1.8	49	0	31	4.34	13.2	184
2427DD10009	330: Kromdraai, plot 304	7.29	215	41	6	1.1	29	0	8	3.41	2.7	139
2427DD10010	331: Kromdraai, plot 48	7.29	253	54	7	0.6	39	1	8	3.83	3.9	165
2427DC10007	332: Hardekoolbult	7.21	454	58	13	2.0	104	21	73	4.11	18.2	172
2527BA10020	333: Kruidfontein, dam draining hills	7.04	168	115	47	7.2	32	4	4	0.39	10.8	330
2527BA10021	334: Kruidfontein	7.08	502	77	44	6.8	56	93	22	0.33	20.4	300
2528AC10024	335: Pretoria Saltpan, old artesian	8.21	2680	9	2	9.7	1052	0	1544	7.59	0.0	259
2528AC10025	337: Soutpan	7.02	200	17	3	2.7	31	14	6	1.11	0.0	75
2528AC10026	338: Soutpan, Mr Mon's	7.00	558	26	15	5.5	114	28	141	1.94	26.9	187

Appendix D.2 Trace element analyses of acidified groundwater samples. Performed by Dr. A. Bartha of the Bophuthatswana Geological Survey using ICP-AES. All concentrations are in mg/ℓ.

Site	As	Mo	Al	Sr	Ba	Ni	Cr	V	Zn	Cu	Li	Cd	Co	Pb
LLD:	**0.012**	**0.004**	**0.0015**	**0.00002**	**0.00007**	**0.006**	**0.004**	**0.004**	**0.009**	**0.002**	**0.0006**	**0.0015**	**0.005**	**0.014**
1	0.003	0.002	0.000	0.033	0.019	0.000	0.004	0.002	0.009	0.001	0.000	0.000	0.001	0.006
7	0.003	0.001	0.001	0.054	0.021	0.001	0.001	0.001	0.036	0.002	0.007	0.000	0.002	0.002
12	0.021	0.049	0.017	0.081	0.001	0.000	0.000	0.001	0.870	0.002	0.014	0.000	0.004	0.000
17	0.004	0.004	0.007	0.139	0.024	0.007	0.001	0.007	7.429	0.014	0.000	0.001	0.006	0.001
21	0.002	0.002	0.049	1.960	0.002	0.000	0.000	0.009	1.790	0.010	0.003	0.000	0.001	0.000
27	0.003	0.007	0.118	1.684	0.001	0.000	0.000	0.000	0.050	0.004	0.003	0.000	0.000	0.002
32	0.002	0.006	0.005	0.323	0.042	0.000	0.071	0.075	0.209	0.005	0.000	0.000	0.000	0.000
37	0.001	0.000	4.416	1.610	0.047	0.001	0.001	0.003	0.033	0.001	0.002	0.000	0.003	0.001
43	0.002	0.010	0.041	1.227	0.022	0.000	0.000	0.000	16.960	0.001	0.008	0.000	0.001	0.007
48	0.002	0.002	0.001	0.748	0.008	0.000	0.000	0.001	1.875	0.001	0.002	0.000	0.002	0.000
60	0.003	0.006	0.030	0.179	0.011	0.001	0.002	0.001	3.727	0.007	0.005	0.000	0.009	0.000
63	0.002	0.002	0.001	0.091	0.005	0.000	0.051	0.014	0.202	0.001	0.000	0.000	0.006	0.000
65	0.002	0.004	0.006	0.074	0.016	0.000	0.013	0.025	0.023	0.003	0.001	0.000	0.004	0.000
69	0.002	0.001	0.000	1.116	0.003	0.000	0.001	0.003	1.110	0.007	0.000	0.000	0.003	0.000
72	0.002	0.004	0.039	0.573	0.009	0.000	0.001	0.041	0.106	0.008	0.000	0.001	0.004	0.000
74	0.005	0.046	0.162	0.121	0.007	0.001	0.000	0.013	0.005	0.001	0.000	0.000	0.001	0.000

Site	As	Mo	Al	Sr	Ba	Ni	Cr	V	Zn	Cu	Li	Cd	Co	Pb
LLD:	**0.012**	**0.004**	**0.0015**	**0.00002**	**0.00007**	**0.006**	**0.004**	**0.004**	**0.009**	**0.002**	**0.0006**	**0.0015**	**0.005**	**0.014**
80	0.002	0.002	0.050	0.534	0.007	0.000	0.001	0.009	0.138	0.004	0.000	0.000	0.002	0.000
86	0.001	0.001	0.033	0.225	0.102	0.000	0.013	0.006	0.225	0.003	0.013	0.000	0.002	0.000
91	0.002	0.000	0.086	0.398	0.041	0.000	0.001	0.051	0.061	0.000	0.001	0.000	0.006	0.000
97	0.001	0.000	0.010	0.530	0.017	0.000	0.000	0.020	0.758	0.003	0.000	0.000	0.000	0.000
103	0.002	0.000	0.154	0.525	0.017	0.000	0.000	0.020	0.758	0.004	0.000	0.000	0.003	0.000
108	0.002	0.000	0.064	0.231	0.006	0.000	0.000	0.048	0.140	0.000	0.000	0.000	0.003	0.017
109	0.001	0.001	0.707	11.000	0.104	0.002	0.002	0.001	5.650	0.000	0.001	0.002	0.004	0.000
114	0.002	0.002	0.009	0.103	0.016	0.000	0.000	0.004	0.061	0.009	0.001	0.001	0.000	0.000
119	0.003	0.003	0.018	0.249	0.052	0.000	0.000	0.000	0.148	0.005	0.099	0.001	0.000	0.021
125	0.003	0.001	0.012	0.360	0.037	0.000	0.000	0.000	0.177	0.011	0.004	0.000	0.001	0.000
131	0.001	0.000	0.018	0.281	0.015	0.000	0.001	0.028	0.294	0.009	0.003	0.000	0.000	0.013
132	0.001	0.001	0.000	0.408	0.002	0.000	0.000	0.000	0.416	0.007	0.042	0.001	0.002	0.034
134	0.002	0.004	0.015	0.588	0.270	0.003	0.001	0.000	0.099	0.011	0.065	0.000	0.000	0.016
143	0.001	0.000	0.016	1.146	0.095	0.000	0.000	0.000	0.292	0.000	0.116	0.001	0.001	0.022
148	0.002	0.008	0.021	0.079	0.023	0.001	0.000	0.000	0.908	0.009	0.005	0.000	0.003	0.024
152	0.002	0.002	0.009	0.594	0.207	0.000	0.000	0.000	0.320	0.030	0.092	0.000	0.002	0.029
155	0.002	0.009	0.168	0.754	0.128	0.000	0.002	0.000	1.287	0.016	0.069	0.001	0.000	0.016
161	0.002	0.004	0.026	0.184	0.034	0.001	0.006	0.000	4.287	0.001	0.029	0.003	0.003	0.010

Site	As	Mo	Al	Sr	Ba	Ni	Cr	V	Zn	Cu	Li	Cd	Co	Pb
LLD:	**0.012**	**0.004**	**0.0015**	**0.00002**	**0.00007**	**0.006**	**0.004**	**0.004**	**0.009**	**0.002**	**0.0006**	**0.0015**	**0.005**	**0.014**
163	0.001	0.003	0.027	0.874	0.024	0.000	0.000	0.000	0.897	0.009	0.106	0.001	0.000	0.015
166	0.004	0.008	0.007	0.970	0.126	0.000	0.000	0.000	0.030	0.005	0.236	0.001	0.000	0.030
172	0.001	0.000	0.011	0.707	0.038	0.000	0.000	0.030	0.766	0.000	0.017	0.002	0.000	0.042
178	0.002	0.003	0.007	0.416	0.011	0.002	0.000	0.007	0.768	0.004	0.004	0.000	0.001	0.000
182	0.001	0.000	0.024	0.735	0.064	0.000	0.003	0.060	0.811	0.012	0.005	0.001	0.006	0.009
185	0.007	0.001	0.027	0.768	0.078	0.000	0.000	0.063	0.022	0.004	0.005	0.000	0.000	0.008
192	0.006	1.000	0.018	0.052	0.014	0.000	0.000	0.000	0.373	0.006	0.006	0.000	0.001	0.020
201	0.003	0.003	0.091	0.017	0.040	0.003	0.000	0.000	1.800	0.022	0.004	0.004	0.002	0.035
205	0.002	0.005	0.014	1.143	0.448	0.001	0.000	0.000	0.709	0.005	0.047	0.007	0.000	0.004
215	0.002	0.001	0.013	1.667	0.051	0.000	0.000	0.014	0.529	0.002	0.029	0.001	0.000	0.014
219	0.001	0.002	0.012	0.108	0.007	0.002	0.000	0.000	1.886	0.000	0.007	0.000	0.000	0.005
224	0.001	0.000	0.001	0.150	0.017	0.000	0.009	0.000	7.663	0.009	0.008	0.001	0.001	0.023
229	0.001	0.002	0.329	0.039	0.073	0.000	0.000	0.000	0.141	0.009	0.002	0.000	0.000	0.018
230	0.187	0.023	0.047	0.094	0.068	0.005	0.000	0.038	0.052	0.017	0.004	0.000	0.000	0.000
233	0.012	0.004	0.012	0.090	0.030	0.001	0.000	0.000	0.437	0.011	0.008	0.002	0.003	0.014
236	0.006	0.002	0.011	0.051	0.001	0.001	0.000	0.000	0.250	0.013	0.007	0.000	0.002	0.000
251	0.002	0.001	0.007	0.053	0.088	0.000	0.000	0.000	0.117	0.005	0.002	0.001	0.001	0.047
255	-0.001	0.000	0.001	1.903	0.133	0.001	0.002	0.000	0.187	0.006	0.090	0.002	0.006	0.013

Site	As	Mo	Al	Sr	Ba	Ni	Cr	V	Zn	Cu	Li	Cd	Co	Pb
LLD:	**0.012**	**0.004**	**0.0015**	**0.00002**	**0.00007**	**0.006**	**0.004**	**0.004**	**0.009**	**0.002**	**0.0006**	**0.0015**	**0.005**	**0.014**
262	0.001	0.000	0.025	0.991	0.128	0.002	0.004	0.001	3.248	0.005	0.031	0.001	0.000	0.005
271	0.002	0.000	0.045	0.053	0.231	0.000	0.005	0.000	6.809	0.003	0.002	0.002	0.006	0.021
275	0.002	0.000	0.024	3.851	0.103	0.001	0.002	0.000	2.819	0.000	0.133	0.002	0.001	0.029
280	0.002	0.000	0.000	0.605	0.028	0.000	0.001	0.051	0.089	0.006	0.005	0.000	0.000	0.000
282	0.002	0.000	0.025	1.004	0.152	0.002	0.000	0.003	0.134	0.006	0.054	0.001	0.000	0.021

Appendix D3. Iodide concentrations in selected groundwater.

Concentration in µg/l. For sample site details refer to appendix A. Iodide analysed by J. Paiker, South African Institute for Medical Research.

Site No.	Iodide	Site No.	Iodide	Site No.	Iodide
1	0	103	0	182	1.6
12	96	108	0	185	12.2
17	63	109	91	192	2.3
21	0	114	0	201	6.3
27	0	119	0	205	85
32	0	125	0	215	220
37	0	131	0	219	1.0
43	0	132	3.0	224	7.2
60	0	1?	63	229	3.2
63	0	142	83	230	641
65	61	152	0	236	2.5
69	0	155	95	251	0
72	0	161	15.0	255	188
74	70	163	82	262	64
80	0	166	94	271	0
91	58	172	4.2	275	86
97	185	178	2.2	280	0

Appendix E. Histograms of analyte concentrations in 16 major rock types in the field area.

E1 Electrical Conductivity

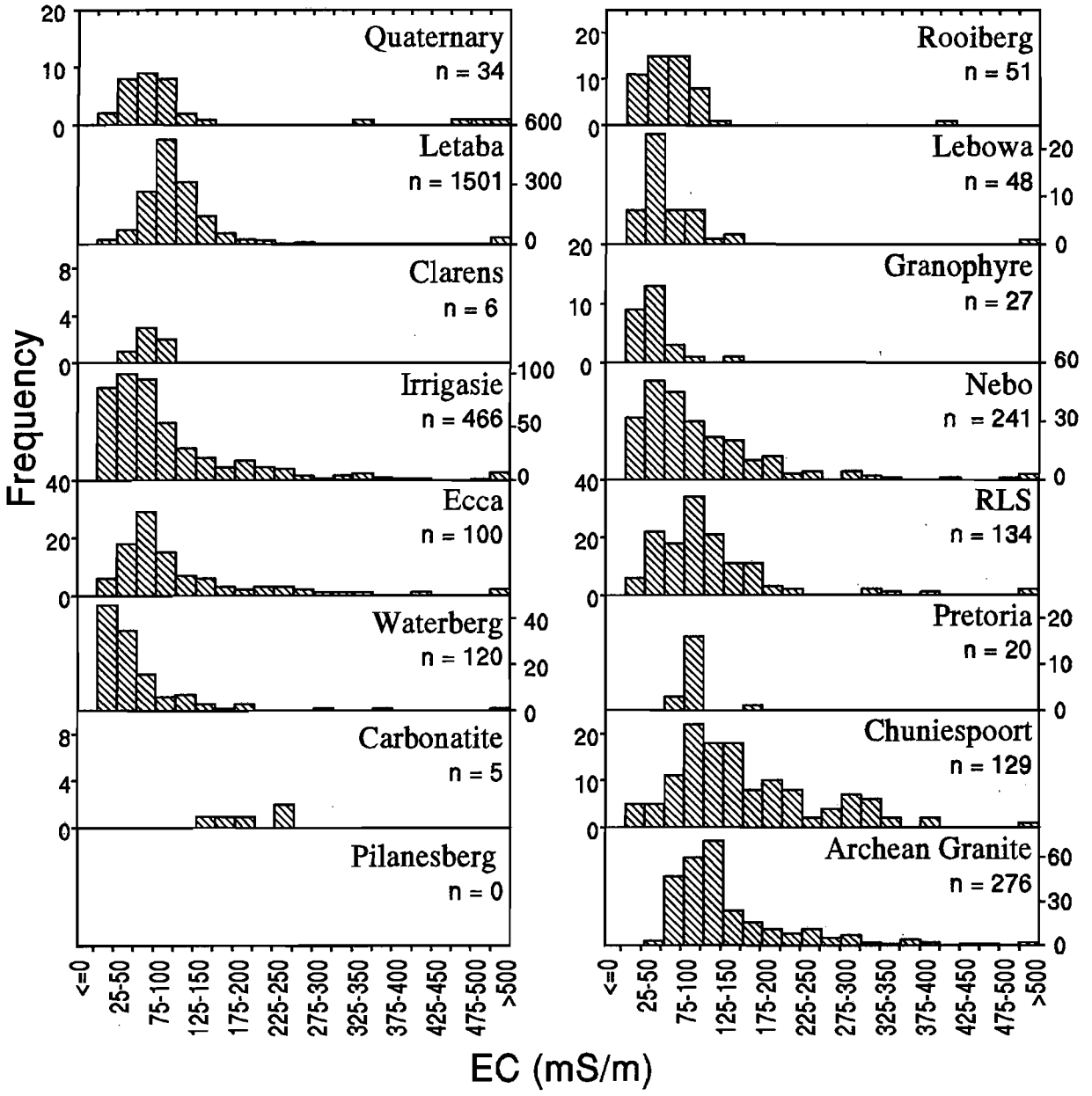

E2 Total Dissolved Solids

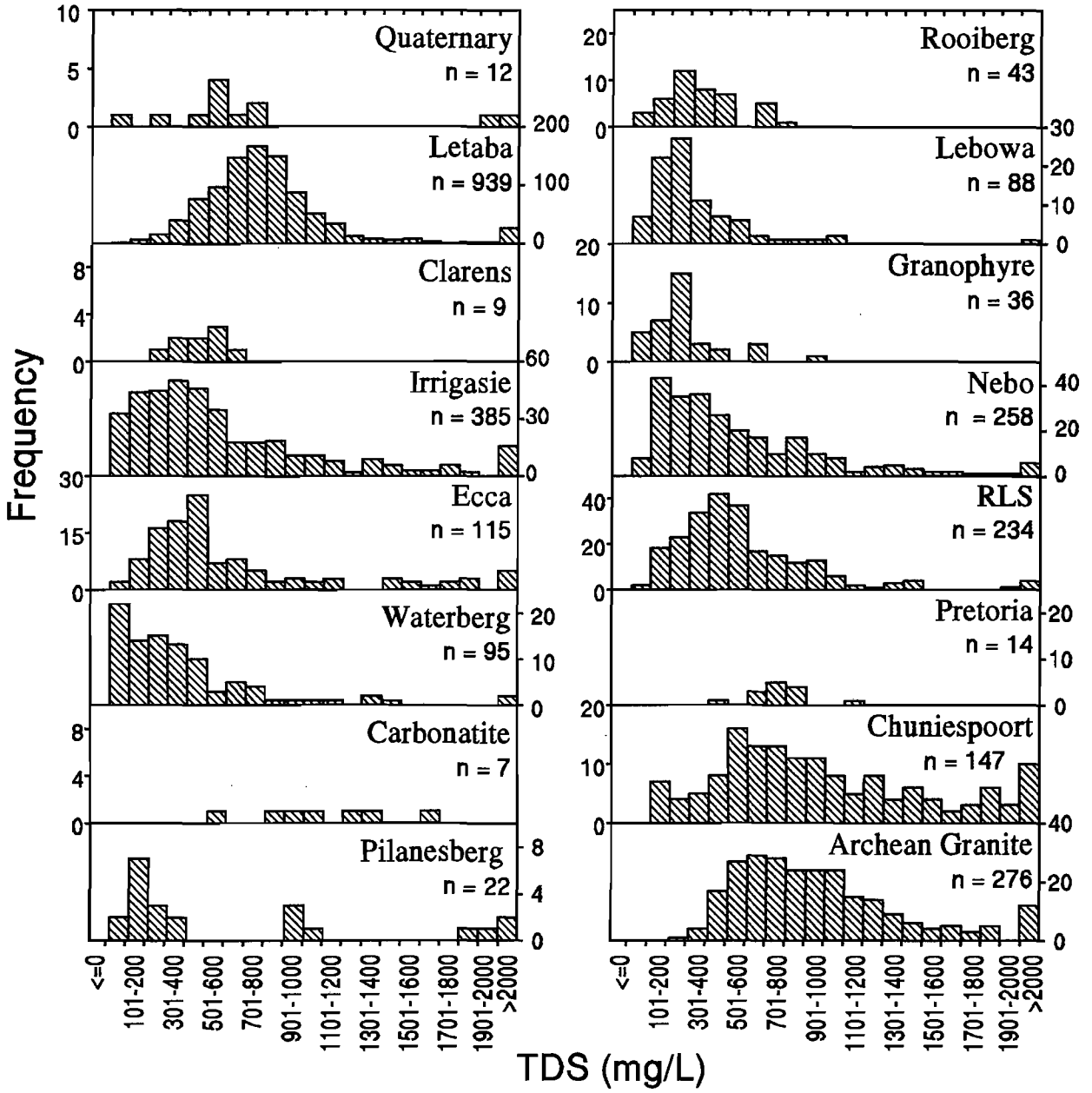

E3 pH

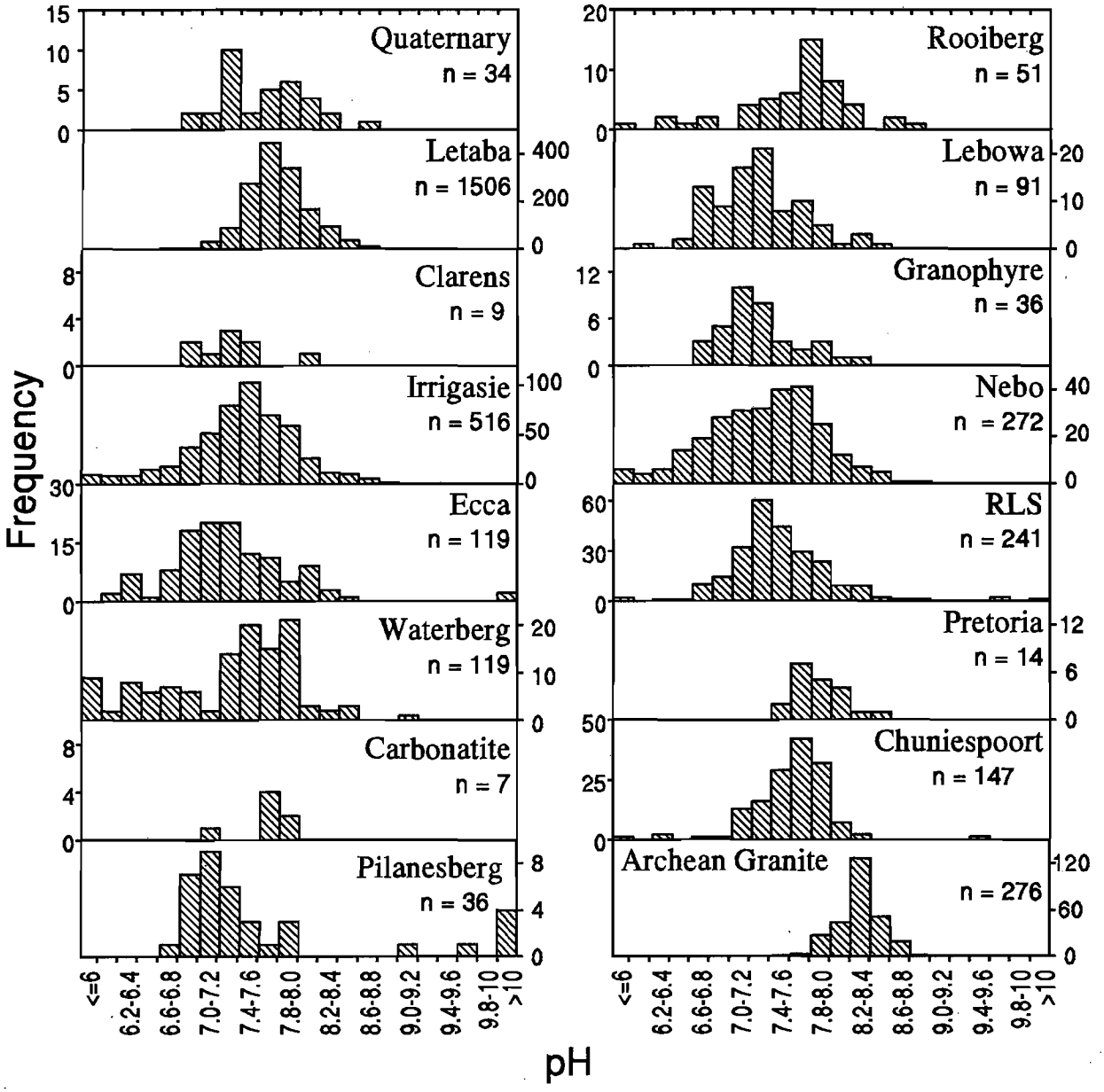
Quaternary
n = 34
Letaba
n = 1506
Clarens
n = 9
Irrigasie
n = 516
Ecca
n = 119
Waterberg
n = 119
Carbonatite
n = 7
Pilanesberg
n = 36
Rooiberg
n = 51
Lebowa
n = 91
Granophyre
n = 36
Nebo
n = 272
RLS
n = 241
Pretoria
n = 14
Chuniespoort
n = 147
Archean Granite
n = 276
Frequency
pH
<=6
6.2-6.4
6.6-6.8
7.0-7.2
7.4-7.6
7.8-8.0
8.2-8.4
8.6-8.8
9.0-9.2
9.4-9.6
9.8-10
>10

E4 Chloride

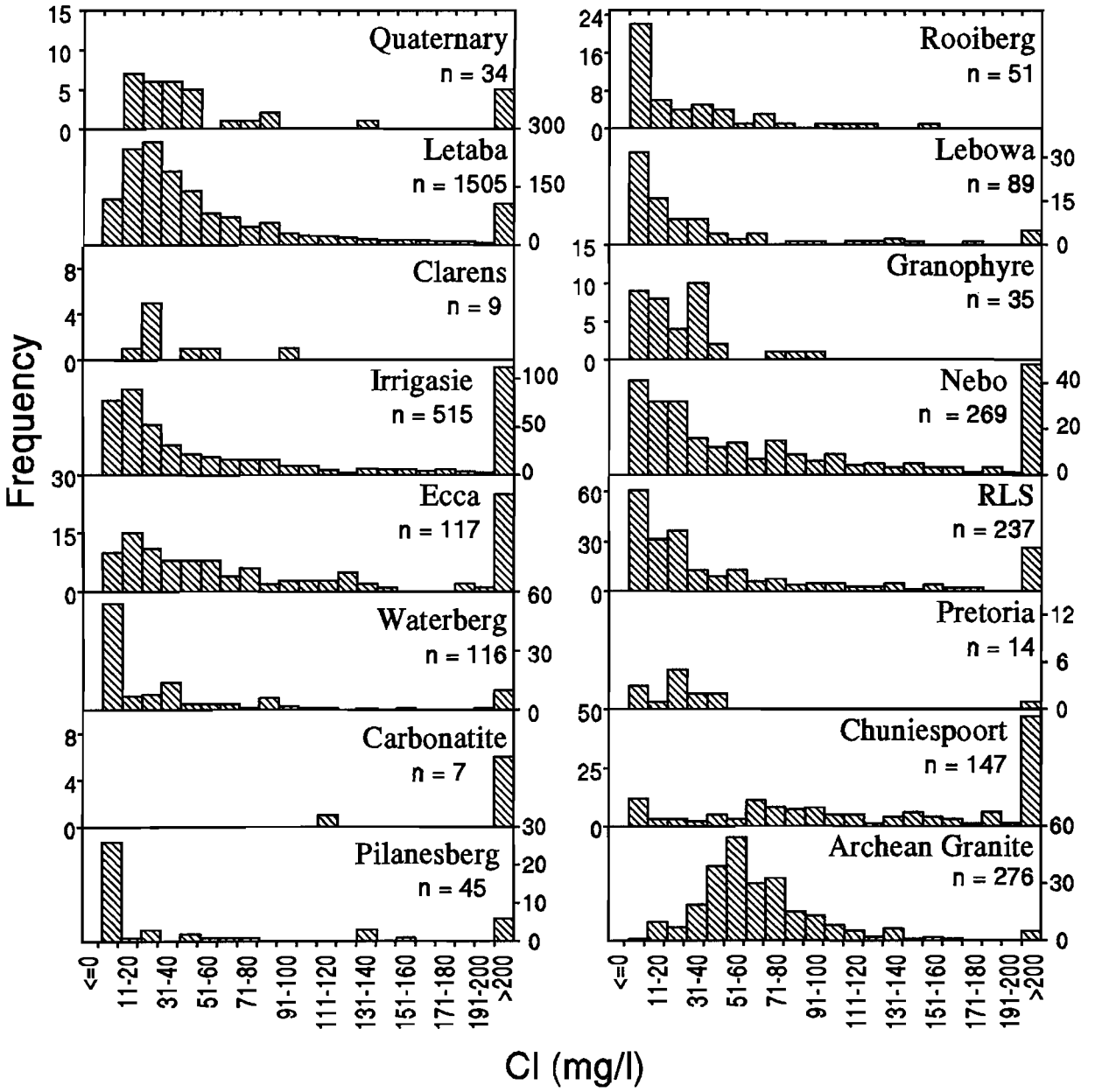
Quaternary
n = 34
Letaba
n = 1505
Clarens
n = 9
Irrigasie
n = 515
Ecca
n = 117
Waterberg
n = 116
Carbonatite
n = 7
Pilanesberg
n = 45
Rooiberg
n = 51
Lebowa
n = 89
Granophyre
n = 35
Nebo
n = 269
RLS
n = 237
Pretoria
n = 14
Chuniespoort
n = 147
Archean Granite
n = 276
Frequency
<=0
11-20
31-40
51-60
71-80
91-100
111-120
131-140
151-160
171-180
191-200
>200
Cl (mg/l)

E5 Nitrate

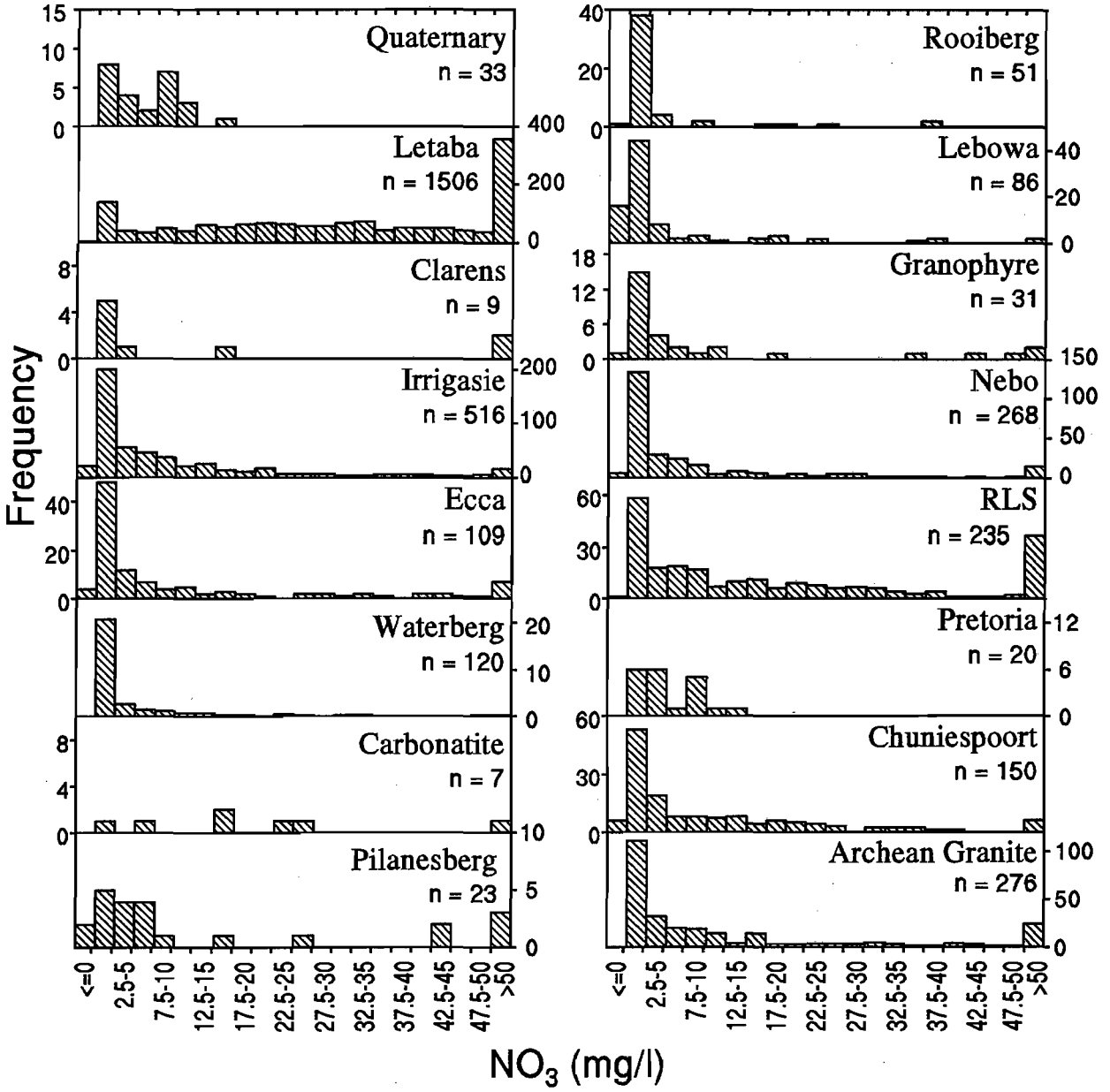
Quaternary
n = 33
Letaba
n = 1506
Clarens
n = 9
Irrigasie
n = 516
Ecca
n = 109
Waterberg
n = 120
Carbonatite
n = 7
Pilanesberg
n = 23
Rooiberg
n = 51
Lebowa
n = 86
Granophyre
n = 31
Nebo
n = 268
RLS
n = 235
Pretoria
n = 20
Chuniespoort
n = 150
Archean Granite
n = 276
Frequency
<=0
2.5-5
7.5-10
12.5-15
17.5-20
22.5-25
27.5-30
32.5-35
37.5-40
42.5-45
47.5-50
>50
NO3 (mg/l)

E6 Sulphate

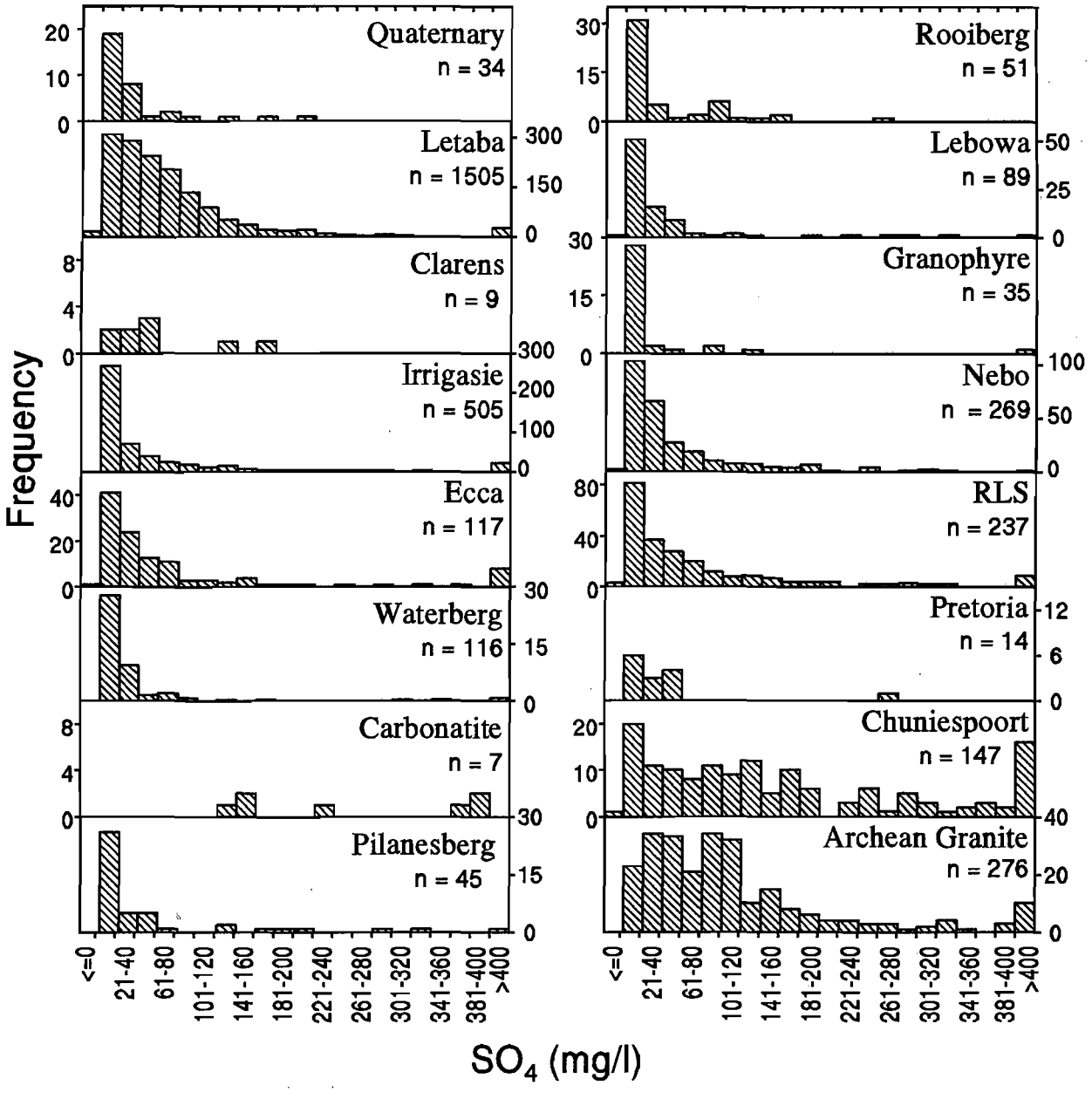
Quaternary
n = 34
Letaba
n = 1505
Clarens
n = 9
Irrigasie
n = 505
Ecca
n = 117
Waterberg
n = 116
Carbonatite
n = 7
Pilanesberg
n = 45
Rooiberg
n = 51
Lebowa
n = 89
Granophyre
n = 35
Nebo
n = 269
RLS
n = 237
Pretoria
n = 14
Chuniespoort
n = 147
Archean Granite
n = 276
Frequency
<=0
21-40
61-80
101-120
141-160
181-200
221-240
261-280
301-320
341-360
381-400
>400
SO4 (mg/l)

E7 Total Alkalinity

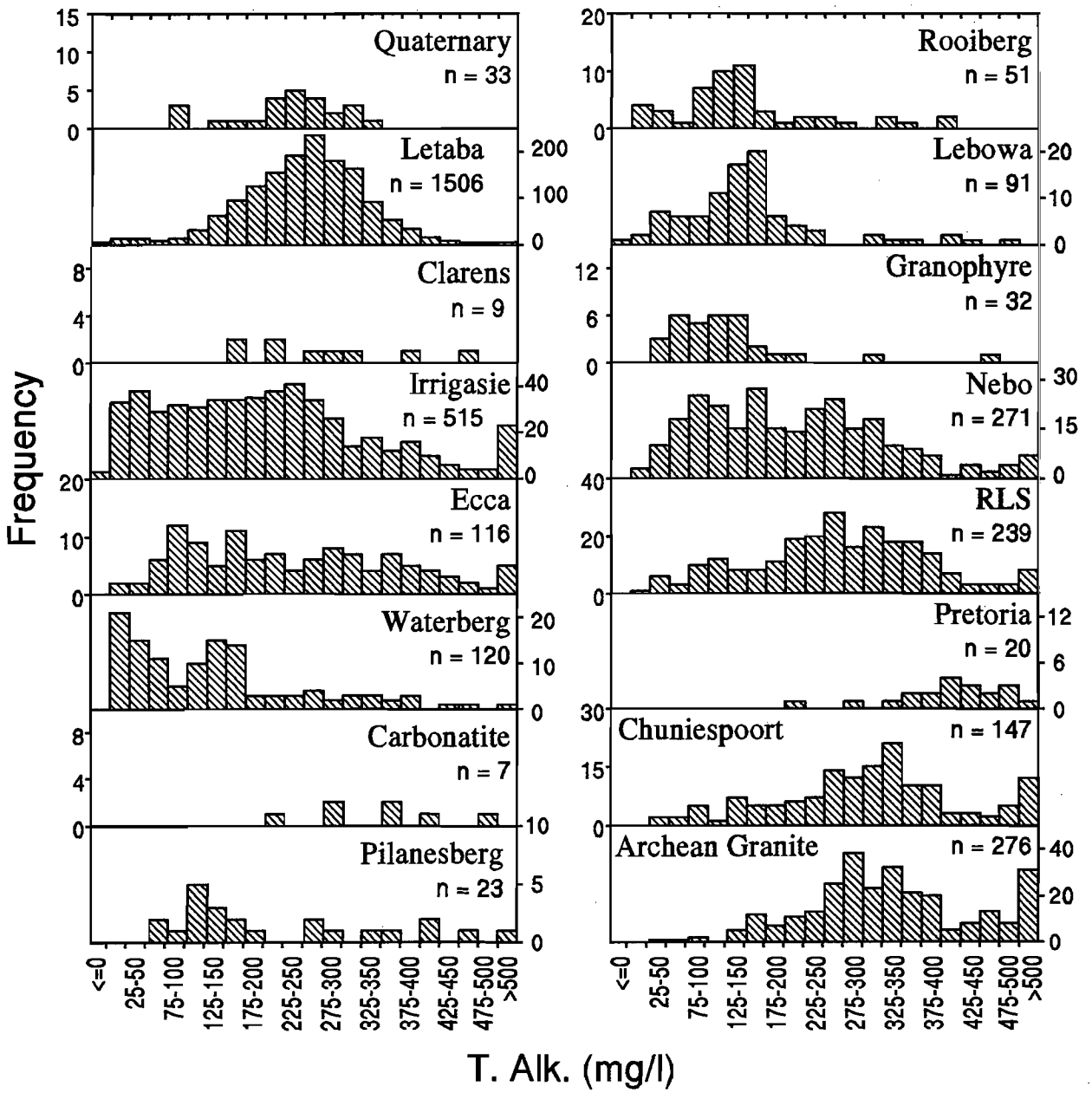

E8 Potassium

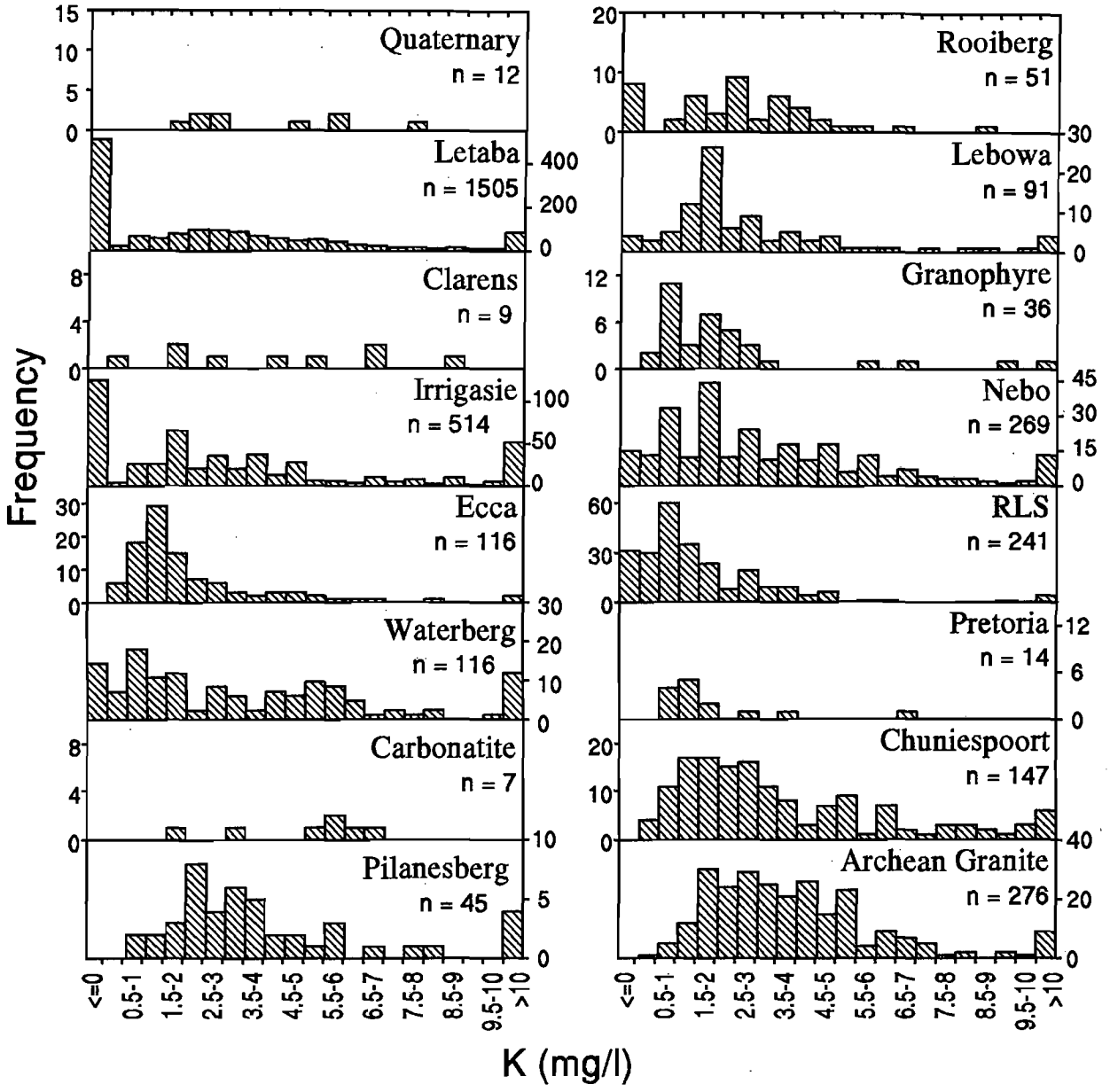

E9 Sodium

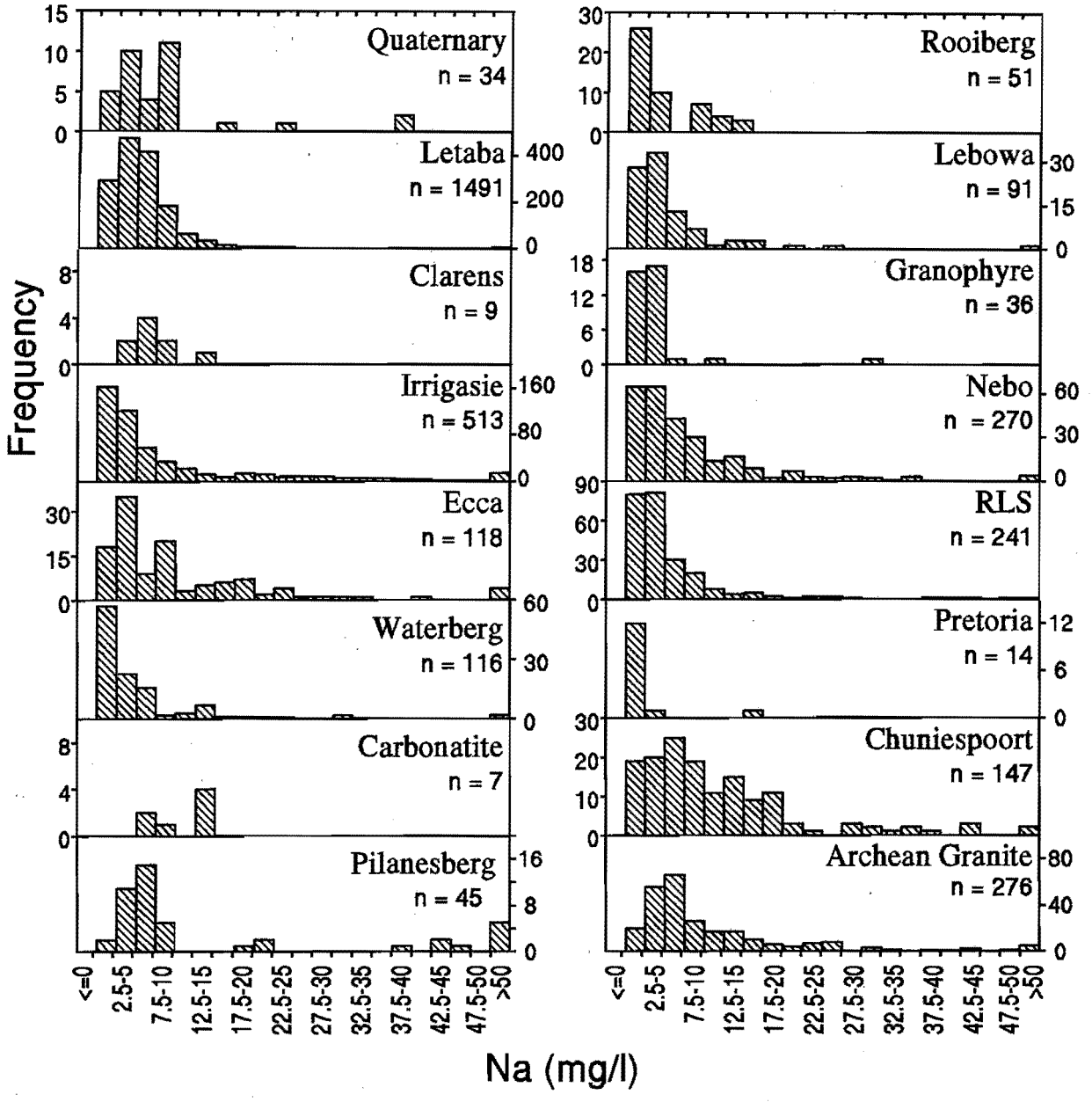
Frequency
Quaternary
n = 34
Letaba
n = 1491
Clarens
n = 9
Irrigasie
n = 513
Ecca
n = 118
Waterberg
n = 116
Carbonatite
n = 7
Pilanesberg
n = 45
Rooiberg
n = 51
Lebowa
n = 91
Granophyre
n = 36
Nebo
n = 270
RLS
n = 241
Pretoria
n = 14
Chuniespoort
n = 147
Archean Granite
n = 276
<=0
2.5-5
7.5-10
12.5-15
17.5-20
22.5-25
27.5-30
32.5-35
37.5-40
42.5-45
47.5-50
>50
Na (mg/l)

E10 Magnesium

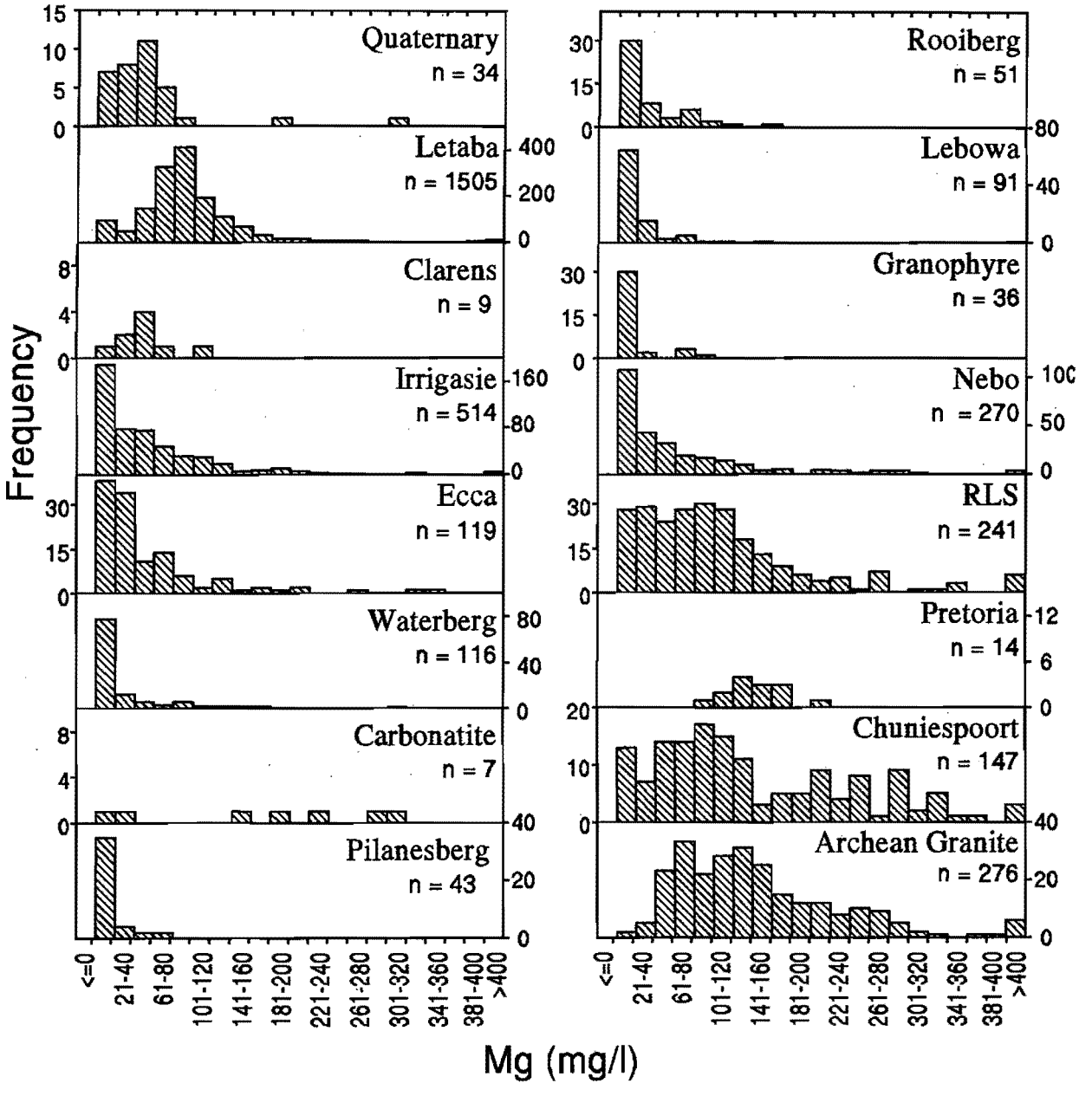

E11 Calcium

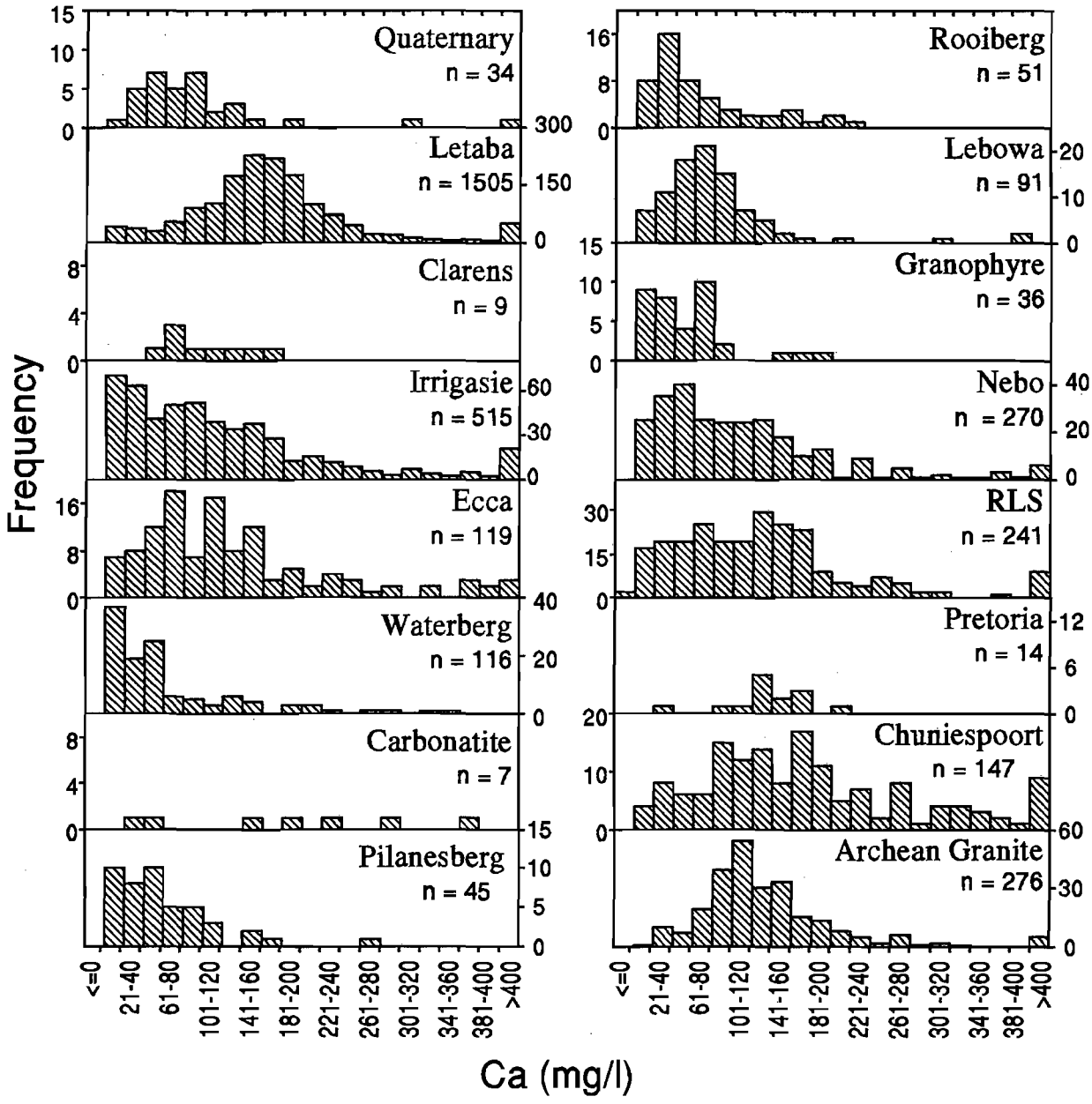
Frequency
Quaternary
n = 34
Letaba
n = 1505
Clarens
n = 9
Irrigasie
n = 515
Ecca
n = 119
Waterberg
n = 116
Carbonatite
n = 7
Pilanesberg
n = 45
Rooiberg
n = 51
Lebowa
n = 91
Granophyre
n = 36
Nebo
n = 270
RLS
n = 241
Pretoria
n = 14
Chuniespoort
n = 147
Archean Granite
n = 276
<=0
21-40
61-80
101-120
141-160
181-200
221-240
261-280
301-320
341-360
381-400
>400
Ca (mg/l)

Appendix F: The problems of calculating a mean for trace elements

Many of the trace element concentrations in groundwater presented in this thesis are below the lower limit of detection (LLD), and this gives rise to an awkward and common problem which is encountered when attempting to calculate a mean value for trace elements: what should be done with an analysis which is below the LLD? To throw away each value which is below the LLD is to increase the mean and throw away possibly important information. No discussion of this problem could be found in the literature, apart from Hitchon (1995), discussed at the end of this section. The trace element results from the present study are used as an example to clarify the reasons for the eventual selection of the method of treatment used in this thesis. The trace element results used in this study were supplied with values reported *below* the lower limit of detection, while most laboratories will simply report the value as 'below the detection limit'.

Several possibilities suggest themselves. The values might be used without alteration; all values reported below the LLD are ignored; replace any value below the LLD with a constant value which is half the LLD; or replace the value with a random number between zero and the LLD. For brevity these methods shall be called *as is, throw away, assumed and random*, respectively. If values below the LLD are used *as is*, are *assumed* or *randomised* when calculating the mean and standard deviation, an unknown error is introduced into the statistics which is undesirable. Each method has a different effect on the resultant statistics, and these are illustrated, using sample data from the trace element sample set, in Figure F.1.

To use the value *as is*, even when it is below the detection limit and is therefore analytically suspect, ignores the point of a detection limit. Furthermore, this method implies that the value has validity when calculating statistics, but that the value is invalid when considered in isolation.

To *throw away* the value when calculating statistics is to disregard important information (that this element is present in concentrations less than the LLD). This treatment also has the effect of increasing the mean to at least the LLD and generally reducing the standard deviation. In Figure F.1, some groundwater types have all V and Pb below the LLD, and consequently can have no statistics calculated.

If half the detection limit is *assumed*, then an arbitrary, unnatural distribution below the detection limit is produced. For instance, it is apparent from the *assumed* treatment of V (Figure F.1) that three of the groundwater types had all analyses of V below the LLD, and all then have the same mean and zero standard deviation. If the values are *randomised*,

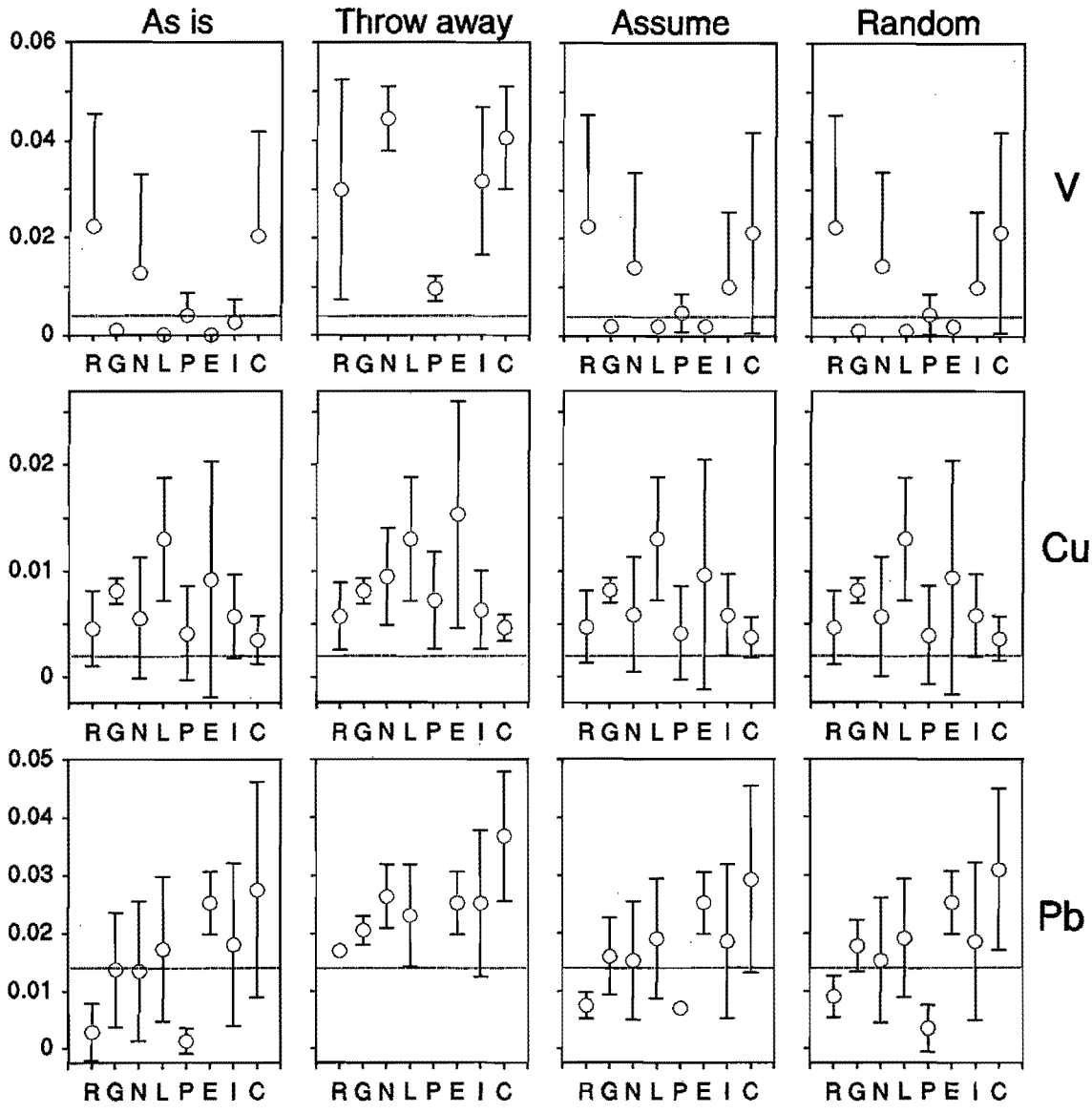

Figure F.1 Mean (circle) and standard deviation (bars) for trace element data (mg/ℓ) in groundwater from 8 rock types, using 4 methods of dealing with results below the LLD. See text for details.

this has the effect of exchanging arbitrary numbers produced by the analytical method with other arbitrary random numbers produced computationally.

From these examples it is clear that each method has disadvantages, and all are arbitrary to some extent. If a mean is to be calculated for any group of values where even one is below the lower limit of detection, then one of these methods has to be chosen. For

the purposes of this thesis, the *as is* treatment is used, since it is the least arbitrary method, retains important information about analyses below the LLD and is the simplest to calculate. The resultant mean and standard deviation have to be treated with caution, especially where most of the analyses are below the LLD.

It is concluded that although the analysis of F^- does not generally suffer from any such problem, since F^- concentrations in groundwater are invariably above the very low detection limit produced by FISE, it is important to understand the variation in the reported means of trace element concentrations which are produced by the different methods. Hitchon (1995), in his study of F, Al and V in groundwater from the Alberta Basin, used both the *throw away* and the *assume* methods when calculating means for V concentration. However, where an analysis fell below the detection limit, he assumed that the analysis was at the detection limit.

Appendix G. Isotope analysis of rain and hail.

The analysis of rain and hail from the same thunderstorm highlights the variability of O and H isotopes in precipitation. The difference in $\delta^{18}O$ and $\delta^{2}H$ between the rain and hail samples (see Chapter 5) is unlikely to influence groundwater isotope composition, since no conceivable mechanism exists which would allow recharge by rainwater and not melted hail, at least in the current climate. Hail melts within minutes or hours of falling to the ground, and so effectively becomes part of the rain recharge event. The slight delay in infiltration due to melting might conceivably lead to the layers of an infiltration front having different isotopic values, but they would be quickly mixed in the unsaturated zone.

The difference in $\delta^{18}O$ and $\delta^{2}H$ between rain and hail from the same thunderstorm, noted in Chapter 5, may be due to several processes. The ^{18}O fractionation factor (α) for ice in equilibrium with water is 1.002 at 0°C (Faure, 1987); if hail formed in a simple one-step equilibrium freezing process from a large volume of water droplets, then the hail would have a $\delta^{18}O$ of +2‰ relative to rain. The measured difference of +4.3‰ probably implies that, since the fractionation factors for ^{18}O and ^{2}H become greater at lower temperatures, the hail formed from supercooled water vapour. Supercooled water vapour does occur in thunderclouds (Preston-Whyte and Tyson, 1988). Alternatively, the hail stone has formed from heavy-isotope depleted water vapour, which occurs at the tops of clouds (Gat, 1980) as well as occurring later in a storms life, due to the 'rain-out' effect. Ehhalt (1967) showed that concentric zones in hailstones can have differing isotopic values which record the movement of the hailstone through the cloud column, and so the value presented here for hail is a composite value for the hailstone as a whole.